January 2017

Polycyclobutanes Constructed From Biomass-Based Building Blocks

Zhihan Wang

POLYCYCLOBUTANES CONSTRUCTED FROM BIOMASS-BASED BUILDING BLOCKS

By

Zhihan Wang
Bachelor of Science in Medicine, Jilin University, 2007
Master of Science in Medicine, Jilin University, 2009

A Dissertation
Submitted to the Graduate Faculty

of the

University of North Dakota

in partial fulfillment of the requirements

for the degree of

Doctor of Philosophy

Grand Forks, North Dakota

May
2017

This dissertation, submitted by Zhihan Wang in partial fulfillment of the requirements for the Degree of Doctor of Philosophy from the University of North Dakota, has been read by the Faculty Advisory Committee under whom the work has been done and is hereby approved.

Dr. Qianli (Rick) Chu (Chairperson)

Dr. Irina P. Smoliakova

Dr. Alexei Novikov

Dr. Guodong Du

Dr. Matthew Cavalli

This dissertation is being submitted by the appointed advisory committee as having met all of the requirements of the School of Graduate Studies at the University of North Dakota and is hereby approved.

Dr. Grant McGimpsey
Dean of the School of Graduate Studies

April 27, 2017
Date

PERMISSION

Title Polycyclobutanes Constructed from Biomass-Based Building Blocks

Department Chemistry

Degree Doctor of Philosophy

In presenting this dissertation in partial fulfillment of the requirements for a graduate degree from the University of North Dakota, I agree that the library of this University shall make it freely available for inspection. I further agree that permission for extensive copying for scholarly purposes may be granted by the professor who supervised my dissertation work or, in his absence, by the Chairperson of the department or the dean of the School of Graduate Studies. It is understood that any copying or publication or other use of this dissertation or part thereof for financial gain shall not be allowed without my written permission. It is also understood that due recognition shall be given to me and to the University of North Dakota in any scholarly use which may be made of any material in my dissertation.

Zhihan Wang

May 1st, 2017

TABLE OF CONTENTS

LIST OF FIGURES

LIST OF SCHEMES

LIST OF TABLES

LIST OF ABBREVIATIONS

2D	Two-dimensional
CBDA	Cyclobutane-1,3-dicarboxylic acid
CBDA-1	*trans*-2,4-Diphenylcyclobutane-1,3-dicarboxylic acid
PBAT	Poly(1,4-butylene-α-truxillate)
PCB	Polycyclobutane
PEAT	Poly(ethylene-α-truxillate)
PET	Polyethylene Terephthalate
PHAT	Poly(1,6-hexylene-α-truxillate)
PPAT3	Poly(propylene-α-truxillate)
PPAT5	Poly(1,5-pentylene-α-truxillate)
SCSC	Single-Crystal-to-Single-Crystal
SLIM	Strong and Lightweight Materials

ACKNOWLEDGEMENTS

This dissertation could not have been completed without the guidance of my committee members, support from my family and help from friends.

I wish to express my deepest appreciation to my advisor Dr. Qianli Rick Chu, who has been a tremendous mentor for me during my time in the doctoral program at the University of North Dakota. I would like to thank Dr. Chu for his contributions of time, ideas, and encouraging in my research. He encouraged me to have independent thinking and gave me more flexible working time. His help not only allows me growing as a research scientist but also as an independent thinker. His advice on both research as well as on my future life have been priceless.

I would also like to thank my committee members, Dr. Irina P. Smoliakova, Dr. Alexei Novikov, Dr. Guodong Du, and Dr. Matthew Cavalli for the friendly guidance, suggestions, and knowledge that each of them offered to me over the years. Thank Dr. Smoliakova for her guidance and support in my graduate study, especially in organic chemistry. Thank Dr. Novikov for providing me bunches of suggestions in my research. Thank Dr. Du for sharing his knowledge of inorganic chemistry and studying experience with me. I'd also like to thank Dr. Cavalli for being a committee member and his support in my doctoral program.

I want to take this opportunity to express my gratitude to department staffs Sandie Routier and Kim Myrum for their support in my graduate study. My gratitude also goes to

all faculty members in the chemistry department. They not only provided chemistry knowledge to me but also offered valuable suggestions.

I'm very grateful for the help from Dr. Chu's group former and current members. They helped me in research and English study. I also want to thank Dr. Angel Ugrinov for his help in crystallography.

Special thanks to my parents and my sister. Words cannot express how grateful I am to my parents and sister for supporting me to do what I want to in the past five years. Without their support, I cannot complete my graduate study. I would also like to thank all of my friends who supported me in free time, oral speaking, writing, and incented me to strive towards my goal.

ABSTRACT

A series of sustainable polycyclobutane (**PCB**) materials were prepared from biomass-based chemicals by [2 + 2] photocycloaddition reaction in sunlight/floodlight or conventional organic synthesis. At the beginning, a family of gemini monomers was synthesized from furfural, which can be obtained from corncobs. First, a photoreactive building block, 3-(2-furyl)acrylic acid also called (*E*)-3-(furan-2-yl)acrylic acid, was synthesized from furfural and malonic acid. Five photostable diols were used to connect two photoreactive building blocks to obtain the monomers. These synthesized monomers were characterized by NMR, UV-Vis and FT-IR spectroscopy, XRD, P-XRD, TGA, and DSC. The photoreaction was monitored by FT-IR spectroscopy and the results indicated that all of the monomers were photoreactive. XRD analysis suggested that these monomers can be used to synthesize polyladderanes and linear polyesters. Monomer (2*E*,2'*E*)-butane-1,4-diyl bis[3-(furan-2-yl)acrylate] formed a polyladderane. Two pieces of independent evidence were obtained, single-crystal-to-single-crystal (SCSC) and a dimer intermediate. Monomer (2*E*,2'*E*)-pentane-1,5-diyl bis[3-(furan-2-yl)acrylate] formed a linear polyester thermoplastic. Both the polyladderane and linear polyesters are amorphous. TGA and DSC showed they decomposed around 300 ºC.

Two-dimensional (2D) polymers were synthesized from cinnamic acid, which can be obtained from cinnamon and from a byproduct of biofuels manufacture. Four molecules of cinnamic acids were linked with a durene group through nuclear substitution reaction. This

four-armed monomer provided four reacting centers, which was the key forming a 2D polymer. The obtained 2D polymer was insoluble in most common organic solvents. The thin layered 2D polymer was observed under TEM and SEM after exfoliation in DMF and H_2O. The key hydrolysis product *trans*-2,4-diphenylcyclobutane-1,3-dicarboxylic acid or *alpha*-truxillic acid was captured, which proved the newly formed cyclobutane rings.

The *alpha*-truxillic acid has two carboxylic groups on the opposite sides of the cyclobutane rings which, provided a semi-rigid structure. This diacid is one of the family members of cyclobutane-diacids (**CBDA**). This class of diacid can be used to synthesize thermoplastics through conventional synthetic method. Four polyesters, PEAT, PBAT, PPAT5 and PHAT, were successfully prepared from *trans*-2,4-diphenylcyclobutane-1,3-dicarboxylic acid (**CBDA-1**) by coupling reactions. TGA showed a high thermostability of these polymers. DSC results showed glass transition temperature decreased as the carbon chains increasing, which may be due to the flexibility of the polymers.

CHAPTER I

SYNTHESIS OF GEMINI MONOMERS FROM BIOMASS-BASED FURFURAL

1.1. Introduction

Over the past three decades, more than 85% of the world's energy requirement was met by fossil fuels and the world depends more and more on petroleum as its main source of chemicals.[1-8] The strong growth of energy demand and irreversible consumption of fossil fuels require the development of new materials from sustainable sources.[9-13] Furfural, one of the top valued renewable chemicals, is present in a variety of agricultural byproducts such as wheat bran, corncobs, and sawdust.[14, 15] It provides a renewable platform for the synthesis of new materials and has widely attracted attention of academic and industrial researchers.[3-6, 13-23] A series of monomers can help scientists explore the properties of chemicals such as odd-even effect and new materials design.[24-26] In addition, the series synthesis of monomers will help researchers reveal the relationship between monomers and polymeric materials, which will benefit people working in crystal engineering field, materials field, etc.[27, 28]

Gemini monomers are a class of molecules with two reactive centers, each capable of forming multiple covalent bonds (Figure 1).[29-32] Polymerization of these compounds results in the formation of rigid or semi-rigid moieties in the polymer chain (Figure 1). With proper design, this feature could be exploited to yield durable polymers derived from renewable materials, with unique properties and applications.[2, 5, 6, 12, 22, 33, 34] Symmetrical

gemini monomers can be synthesized by connecting identical reactive units with a linker molecule of variable length and character. This simple, modular design allows multiple compounds to be synthesized by the same reaction method, which makes it convenient for comparative study.

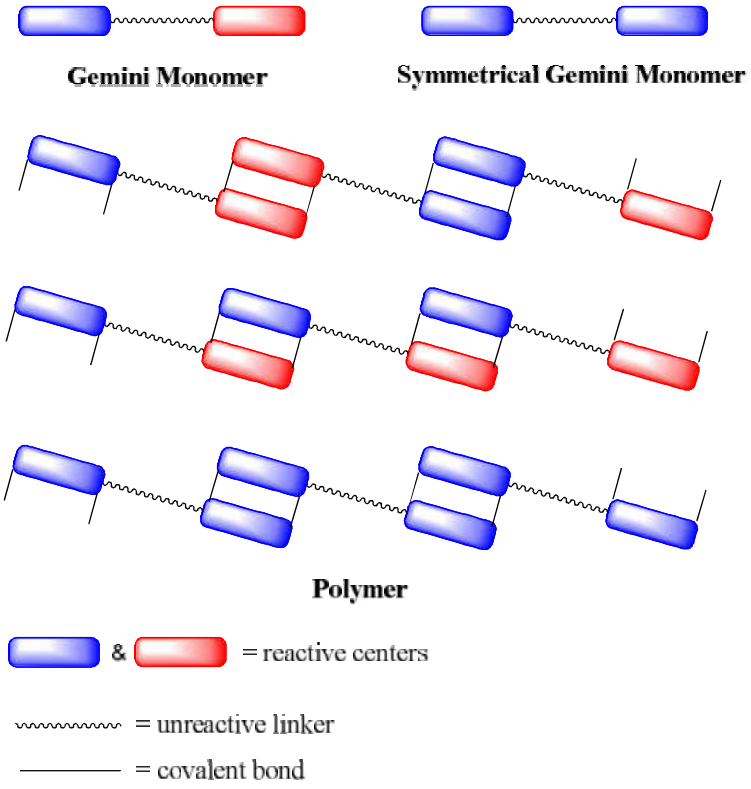

Figure 1. Diagrammatic sketch of gemini monomers used for synthesizing polymers in the solid-state. Energies used for polymerization can be heat, ultraviolet light, visible light, etc.

Synthesizing gemini monomers from biomass-based furfural is not only beneficial to material design but also beneficial to the sustainable future. In order to reduce the possibility for polymer cyclization and cross-linking, photopolymerization in the solid-state was chosen.[35-42] The crystal packing of the monomer units has a direct effect on their bonding pattern in a solid-state reaction, an integral property that determines the character

of the polymer product. Small alterations in the structure of monomer units can have dramatic effects on their crystal packing.[42-49] The simplicity and flexibility of symmetrical gemini monomer synthesis allow for careful manipulation of the monomers' chemical structure. For example, long linker molecules cause the properties of the reactive centers to be accentuated, encouraging head-to-tail packing. Using shorter linker makes the monomers more rigid.

1.2. Experimental Section

1.2.1. General Methods

All the reagents were purchased from Alfa Aesar, Sigma-Aldrich and used without further purification. The solution phase nuclear magnetic resonance (NMR) spectra were recorded with a Bruker AVANCE 500 MHz NMR Spectrometer (^{1}H: 500 MHz, ^{13}C: 125 MHz). All spectra were obtained in deuterated dimethyl sulfoxide (DMSO-d_6). Single crystal X-ray data were recorded on a Bruker Kappa Apex II Duo X-ray diffractometer with Mo $K\alpha$ (λ = 0.71073 Å) or Cu $K\alpha$ (λ = 1.54178 Å). Melting points were measured on a MEL-TEMP device without correction. Infrared (IR) spectra was recorded on a Thermo Scientific Nicolet iS5 FT-IR spectrometer. The mass spectrometric analyses were performed using a high-resolution time of flight G1969A mass spectrometer with electrospray (atmospheric pressure chemical) ionization (Agilent, Santa Clara, CA, USA) and reported as m/z. X-ray powder diffraction (P-XRD) analysis was performed on an X'PERT-PRO X-ray diffractometer (PANalytical, Netherlands) equipped with a 3 KW copper tube X-ray generator of λ = 0.1541 nm under 40 mA and 45 KV. Spectrum were collected at room temperature in a 2θ range of 3°~35° at a scanning rate of 3°/min. Thermogravimetric

analysis (TGA) was tested with a TA instrument SDT Q600 at a ramping rate 20 ºC/min under nitrogen protection. Accurate masses are reported for the molecular ion $[M+Na]^+$ or $[M]^+$.

1.2.2. Synthesis of (*E*)-3-(Furan-2-yl)acrylic Acid or 2-Furanacrylic Acid (**3**)

Furfural (**1**) (1.0 g, 10 mmol) and malonic acid (**2**) (1.6 g, 15 mmol) were added to pyridine (20 mL). The mixture was stirred at 100 ºC for 14 h. The mixture was poured into ice water (100 mL) and the aqueous was adjusted to pH value 2. The aqueous solution was extracted with ethyl acetate (100 mL × 3) and the combined organic layers were washed with brine, dried over sodium sulfate and concentrated to give product (*E*)-3-(furan-2-yl)acrylic acid (**3**) (1.1 g, 77%) as a white solid.[50, 51] ^{1}H-NMR (500 MHz, DMSO-d_6): δ 12.41 (s, 1H), 7.84 (s, 1H), 7.38 (d, J = 16 Hz, 1H), 6.93 (d, J = 3.5 Hz, 1H), 6.62-6.63 (dd, J = 1.5 Hz, J = 1.5 Hz, 1H), 6.15 (d, J = 16 Hz, 1H); ^{13}C-NMR (125 MHz, DMSO-*d6*): δ 167.7 (C), 150.7 (C), 146.1 (CH), 131.2 (CH), 116.3 (CH), 115.9 (CH), 113.1 (CH).

1.2.3. Synthesis of Monomer (2*E*,2'*E*)-Methylene bis[3-(furan-2-yl)acrylate] (**4**)

(2*E*,2'*E*)-Methylene bis[3-(furan-2-yl)acrylate] (**4**): (*E*)-3-(Furan-2-yl)acrylic acid (**3**) (1.8 g, 13 mmol), dibromomethane (1.0 g, 5 mmol) and CsF (4.4 g, 28 mmol) were added to dimethyl sulfoxide (40 mL). The mixture was stirred at 120 ºC for 3 hrs. Then the reaction solution was poured into water (100 mL) and the precipitate was filtered out to give monomer **4** (1.4 g, 84%) as a light yellow solid. M.p.: 116-117 °C; ^{1}H-NMR (500 MHz, DMSO-d_6): δ 7.89 (s, 2H), 7.56 (d, J = 15.5 Hz, 2H), 7.05 (d, J = 6.5 Hz, 2H), 6.67 (dd, J = 1.5 Hz, J = 1.5 Hz, 2H), 6.24 (d, J = 15.5 Hz, 2H), 5.93 (s, 2H); ^{13}C-NMR (125 MHz, DMSO-d_6): δ 165.1 (C), 150.3 (C), 146.9 (CH), 133.3 (CH), 117.6 (CH), 113.5 (CH), 113.4

(CH), 79.8 (CH_2); HRMS (m/z): $[M+Na]^+$ calcd. for $C_{15}H_{12}O_6Na$, 311.0531; found 311.0532.

1.2.4. General Procedure for Synthesis of Monomers **5**, **6**, **7**, **8**, and **9**

(2*E*,2'*E*)-Ethane-1,2-diyl bis[3-(furan-2-yl)acrylate] (**5**): (*E*)-3-(furan-2-yl)acrylic acid (2.8 g, 20 mmol), ethylene glycol (0.6 g, 9 mmol), DCC (4.4 g, 21 mmol) and DMAP (2.9 g, 24 mmol) were added into chloroform (20 mL). The mixture was stirred at room temperature for 12 h. Then the reaction mixture was concentrated. The residue was purified via column chromatography with ethyl acetate and hexane (5 : 1) to give monomer **5** (2.3 g, 78%) as a yellow solid. M.p.: 96-97 °C; ^{1}H-NMR (500 MHz, DMSO- d_6): δ 7.87 (s, 2H), 7.48 (d, J = 15.5 Hz, 2H), 7.00 (d, J = 3.5 Hz, 2H), 6.64-6.65 (dd, J = 1.5 Hz, J = 1.5 Hz, 2H), 6.27 (d, J = 16 Hz, 2H), 4.40 (s, 4H); ^{13}C-NMR (125 MHz, DMSO-d_6): δ 166.3 (C), 150.5 (C), 146.6 (CH), 132.1 (CH), 116.7 (CH), 114.6 (CH), 113.2 (CH), 62.6 (2CH_2); HRMS (m/z): $[M+Na]^+$ calcd. for $C_{16}H_{14}NaO_6$, 325.0688; found 325.0709.

(2*E*,2'*E*)-Propane-1,3-diylbis[3-(furan-2-yl)acrylate] (**6**): A yellow solid (1.7 g, 85%). M.p.: 78-79 °C; ^{1}H-NMR (500 MHz, DMSO-d_6): δ 7.84 (s, 2H), 7.46 (d, J = 15.5 Hz, 2H), 6.95 (d, J = 3.5 Hz, 2H), 6.62-6.63 (dd, J = 1.5 Hz, J = 1.5 Hz, 2H), 6.21 (d, J = 16 Hz, 2H), 4.24 (t, 4H), 2.00-2.03 (t, 2H); ^{13}C-NMR (125 MHz, DMSO-d_6): δ 166.3 (C), 150.5 (C), 146.4 (CH), 131.7 (CH), 116.5 (CH), 114.9 (CH), 113.2 (CH), 61.6 (2CH_2), 28.0 (CH_2); HRMS (m/z): $[M+Na]^+$ calcd. for $C_{17}H_{16}NaO_6$, 339.0844; found 339.0816.

(2*E*,2'*E*)-Butane-1,4-diyl bis[3-(furan-2-yl)acrylate] (**7**): A yellow solid (3.4 g, 93%). M.p.: 114-115 °C; ^{1}H-NMR (500 MHz, DMSO-d_6): δ 7.85 (s, 2H), 7.46 (d, J = 15.5 Hz, 2H), 6.97 (d, J = 3.5 Hz, 2H), 6.63-6.64 (dd, J = 1.5 Hz, J = 1.5 Hz, 2H), 6.22 (d, J = 15.5 Hz,

2H), 4.17 (t, J = 5 Hz, 4H), 1.72-1.73 (m, 4H); ^{13}C-NMR (125 MHz, DMSO-d_6): δ 166.4 (C), 150.5 (C), 146.4 (CH), 131.6 (CH), 116.5 (CH), 115.0 (CH), 113.2 (CH), 64.0 (2CH_2), 25.3 (2CH_2); HRMS (m/z): $[M+Na]^+$ calcd. for $C_{18}H_{18}NaO_6$, 353.1001; found 353.0924.

(2*E*,2'*E*)-Pentane-1,5-diyl bis[3-(furan-2-yl)acrylate] (**8**): A yellow solid (1.4 g, 84%). M.p.: 66-67 °C; ^{1}H-NMR (500 MHz, DMSO-d_6): δ 7.85 (s, 2H), 7.45 (d, J = 15.5 Hz, 2H), 6.97 (d, J = 3.5 Hz, 2H), 6.63-6.64 (dd, J = 1.5 Hz, J = 1.5 Hz, 2H), 6.21 (d, J = 15.5 Hz, 2H), 4.13-4.15 (m, 4H), 1.65-1.70 (m, 4H), 1.41-1.44 (m, 2H); ^{13}C-NMR (125 MHz, DMSO-d_6): δ 166.4 (C), 150.5 (C), 146.4 (CH), 131.5 (CH), 116.4 (CH), 115.1 (CH), 113.1 (CH), 64.2 (2CH_2), 28.2 (2CH_2), 22.3 (CH_2); HRMS (m/z): $[M+Na]^+$ calcd. for $C_{19}H_{20}O_6Na$, 367.1157; found 367.1119.

(2*E*,2'*E*)-Hexane-1,6-diyl bis[3-(furan-2-yl)acrylate] (**9**): A yellow solid (2.1 g, 87%). M.p.: 64-65 °C; ^{1}H-NMR (500 MHz, DMSO-d_6): δ 7.83 (s, 2H), 7.47 (d, J = 15.5 Hz, 2H), 6.96 (d, J = 3.5 Hz, 2H), 6.62-6.63 (dd, J = 1.5 Hz, J = 1.5 Hz, 2H), 6.21 (d, J = 15.5 Hz, 2H), 4.10 (t, J = 6.5 Hz, 4H), 1.61-1.64 (m, 4H), 1.37 (s, 4H); ^{13}C-NMR (125 MHz, DMSO-d_6): δ 166.4 (C), 150.5 (C), 146.3 (CH), 131.5 (CH), 116.3 (CH), 115.1 (CH), 113.1 (CH), 64.3 (2CH_2), 28.4 (2CH_2), 25.4 (2CH_2); HRMS (m/z): $[M+Na]^+$ calcd. for $C_{20}H_{22}O_6Na$, 381.1314; found 381.1314.

1.2.5. Crystallization

The crystals of **4-9** were obtained in ethyl acetate at room temperature. Monomers **4-9** (20 mg) were added to solvent ethyl acetate (20 mL) respectively. The suspended mixture was stirred in the vial for 10 min. Then the mixture was filtered into a 20 mL vial with filter

paper. The vial with clear solution was allowed to stay without cover until the crystals formed.

1.3. Results and Discussions

A series of diesters were prepared to investigate the properties of various bio-based monomers.[52-54] The photoreactive center 2-furanacrylic acid (also known as (*E*)-3-(furan-2-yl)acrylic acid) (**3**) was synthesized from furfural (**1**) and another biomass-based chemical, malonic acid (**2**), by Knoevenagel condensation.[2-6, 14, 19, 21, 23, 55-60] To avoid crosslinking and side reactions of polymerization, the linkers between the two reacting centers have to be photostable chemicals. In this case, alkyl diols are one of the promising candidates. To study the synthesis of monomers for sustainable polyesters, dibromomethane, 1,2-ethanediol (ethylene glycol), 1,3-propanediol, 1,4-butanediol, 1,5-petanediol, and 1,6-hexanediol were used to connect two 2-furancrylic acids (Scheme 1).[14, 57, 61-67] In fact, the initial synthesis of monomer **4** was started from 2-furanacrylic acid (**3**) and formaldehyde. [68, 69] However, the yield is not high and the formaldehyde has high toxicity to the nervous system which does not meet green chemistry rules.[70] An alternative synthetic method was applied to prepare monomer **4** which is based on the conjugated system of 2-furanacrylic acid. Due to the conjugation of the α-unsaturated carboxylic acid and furan ring, the carboxylate ion can be used as a nucleophile. Finally, synthesis of monomer **4** was achieved through a nucleophilic substitution reaction of 2-furanacrylic acid and dibromomethane with a yield of 84%.

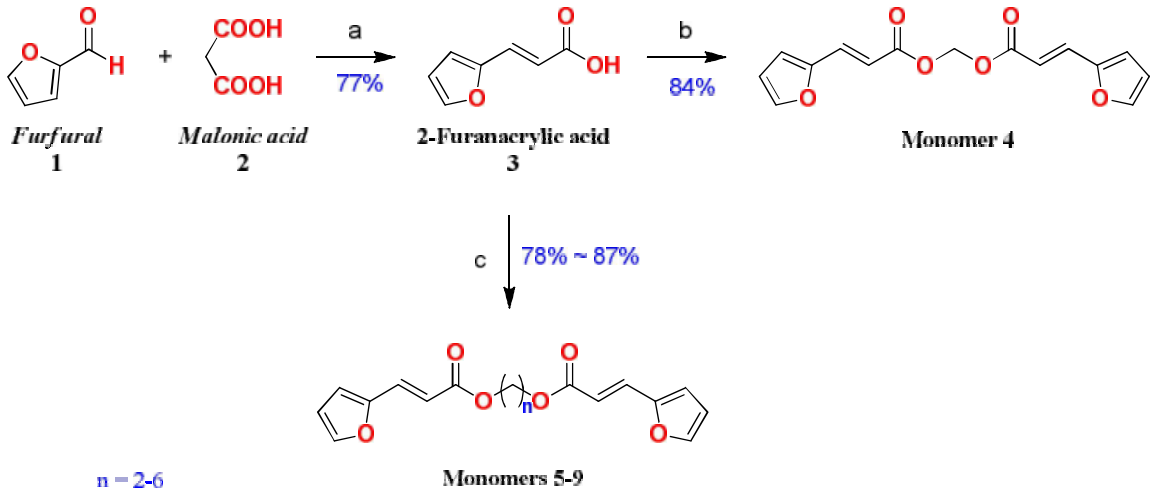

Scheme 1. The synthesis of monomers **4-9** from furfural. a) pyridine, 100 ºC, 14 h; HCl; b) dibromomethane, CsF, DMSO, 120 ºC, 3 h; c) $HO(CH_2)_nOH$, n =2-6, diols, DCC, DMAP, r.t., 8-16 h.

Synthesis of monomers **5**, **6**, **7**, **8** and **9** was started by activating 2-furanacrylic acid (**3**) and the diols used in this study were selected because they can be obtained from renewable resources. [57, 62, 64, 65, 71, 72] Some of the diols have been already used in different polyesters. For example, 1,2-ethanediol is used in polyethylene terephthalate (PET).[73-75] 1,3-propanediol can be produced from corn syrup and is the main component of polytrimethylene terephthalate (PTT), which can be used to make carpet fibers.[76] All of the nucleophilic substitution reactions can be completed in 8 to 16 h at room temperature with yields over 80%. Only the linker used in monomer **4** (dibromomethane) is not from bio-based chemicals, but the bio-ratio of the monomer by mass is still high.

1.4. Characterization

To investigate the orientation of monomers in the solid state, single crystals suitable for X-ray diffraction were obtained in different solvents. Crystalline states of monomers will help scientists find a way to design suitable monomers and predict their potential reactions. Selected crystalline data are listed in Table 1. The X-ray crystal structures of seven crystals showed the 2-furanacrylate group with a conjugated system preferred to align in the same plane to achieve maximum stability (Figure 2).

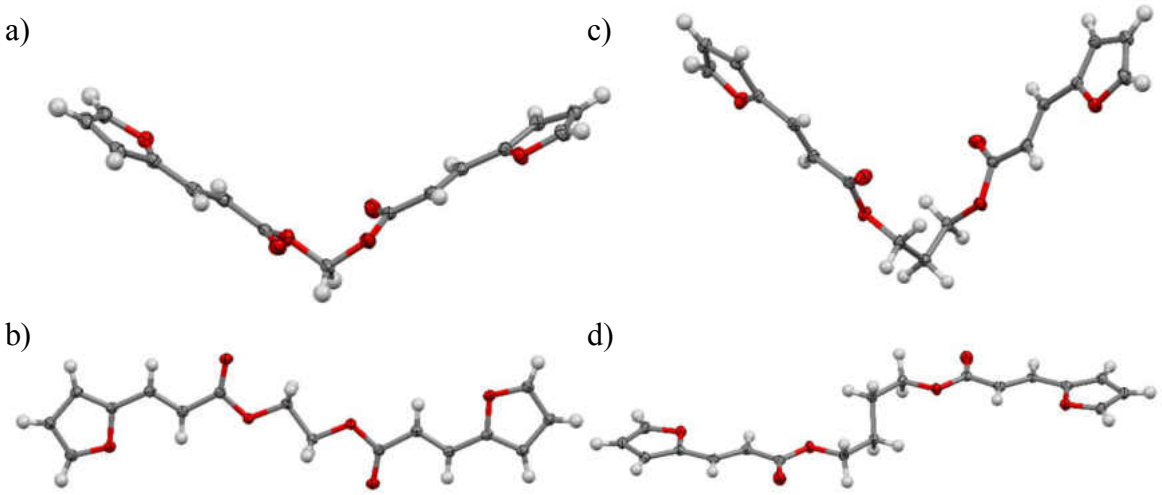

Figure 2. Oak Ridge Thermal-Ellipsoid Plot Program (ORTEP) drawing of monomer **4** (a), **5** (b), **6** (c), and **7** (d) with thermal ellipsoids at 50% probability.

Monomer **4** showed a V-shaped structure, because there is only one sp^3-hybridized carbon between the two 2-furanacrylate groups, preventing it from achieving a planar conformation. It forms monoclinic crystals in the $P2_1/n$ space group, with Z=15. Monomer **5** is planar with the two carbonyl groups pointing in opposite directions, giving the molecule an inversion center in between the two sp^3-hybridized carbons in the linker. It forms monoclinic crystals in the $P2_1/c$ space group, with Z=2. In monomer **6**, the central

linker is twisted such that the molecule has a V shape similar to monomer **4**. Also like monomer **4**, it forms monoclinic crystals, but they are in the C2/c space group with Z=8. Monomer **7** has an inversion center in the middle similar to monomer **5**. However, unlike monomer **5**, the middle two carbons in the linker are twisted, making the two 2-furanacrylate groups parallel to each other but offset from each other so the molecule is not planar. It also forms monoclinic crystals but in the space group $P2_1/n$ with Z=4.

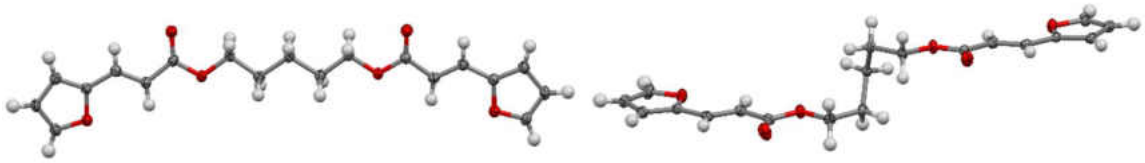

Figure 3. ORTEP drawing of monomer **8** with polymorphs **8a** (left) and **8b** (right).

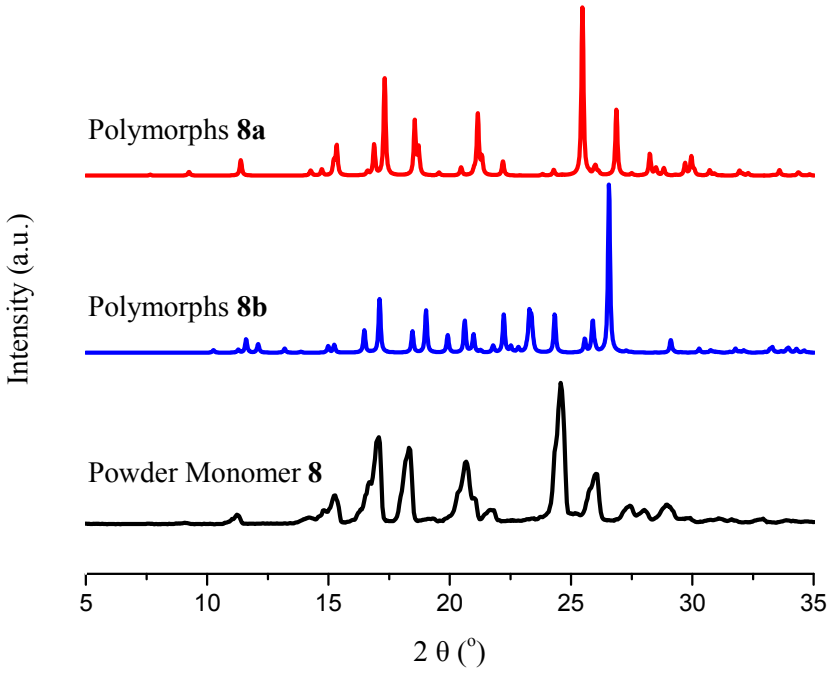

Figure 4. The comparison of powder X-ray diffraction results (black) of monomer **8** powder and simulation of polymorphs **8a** (red) and **8b** (blue).

Polymorphism was observed in monomer **8**. This is the ability of a compound to crystallize in two or more distinct crystal structures, called polymorphs. Two crystal structures form **8a** and **8b**, which were obtained in DMSO/H_2O and ethyl acetate, respectively. In **8a**, the 5-carbon linker arranges in a zig-zag pattern, making the molecule planar and giving it a mirror plane of symmetry through the central carbon atom. It forms orthorhombic crystals in the space group $Pna2_1$ with a Z value of 4. In **8b** on the other hand, the linker is twisted into more of a V shape. The 2-furanacrylate groups in **8b** are still parallel to one another but are offset, making the molecule non-planar. It forms triclinic crystals in the P-1 space group with a Z value of only 2. The X-ray diffraction results for monomer **8** are shown in Figure 3.

The monomer powders are microcrystalline. Powder X-ray diffraction (P-XRD) was used to study the structure of the monomer powder. The P-XRD data collected for monomer **8** indicated that the monomer powder has the same structure as **8a** (Figure 4). This phenomenon may indicate that polymorph **8a** is more stable that the other. Often polymorphous compounds form a kinetic polymorph, which crystallized more quickly but is not as stable, and a thermodynamic polymorph, which takes longer to form but is more stable.[77-81] The kinetic form may convert to the thermodynamic form over time, in which case it would be considered metastable. Conversely, the two forms may have a small enough difference in free energy, but both could be considered stable.[79-81] During crystallization, it was observed that polymorph **8a** did take considerably more time to crystallize when compared to **8b**. This shows that **8a** is most likely the thermodynamic form. It is important to note that since the crystal structure of the monomers determines if

and how polymerization occurs in the solid state, different polymorphs of the same monomer could potentially produce different polymers with distinct properties.

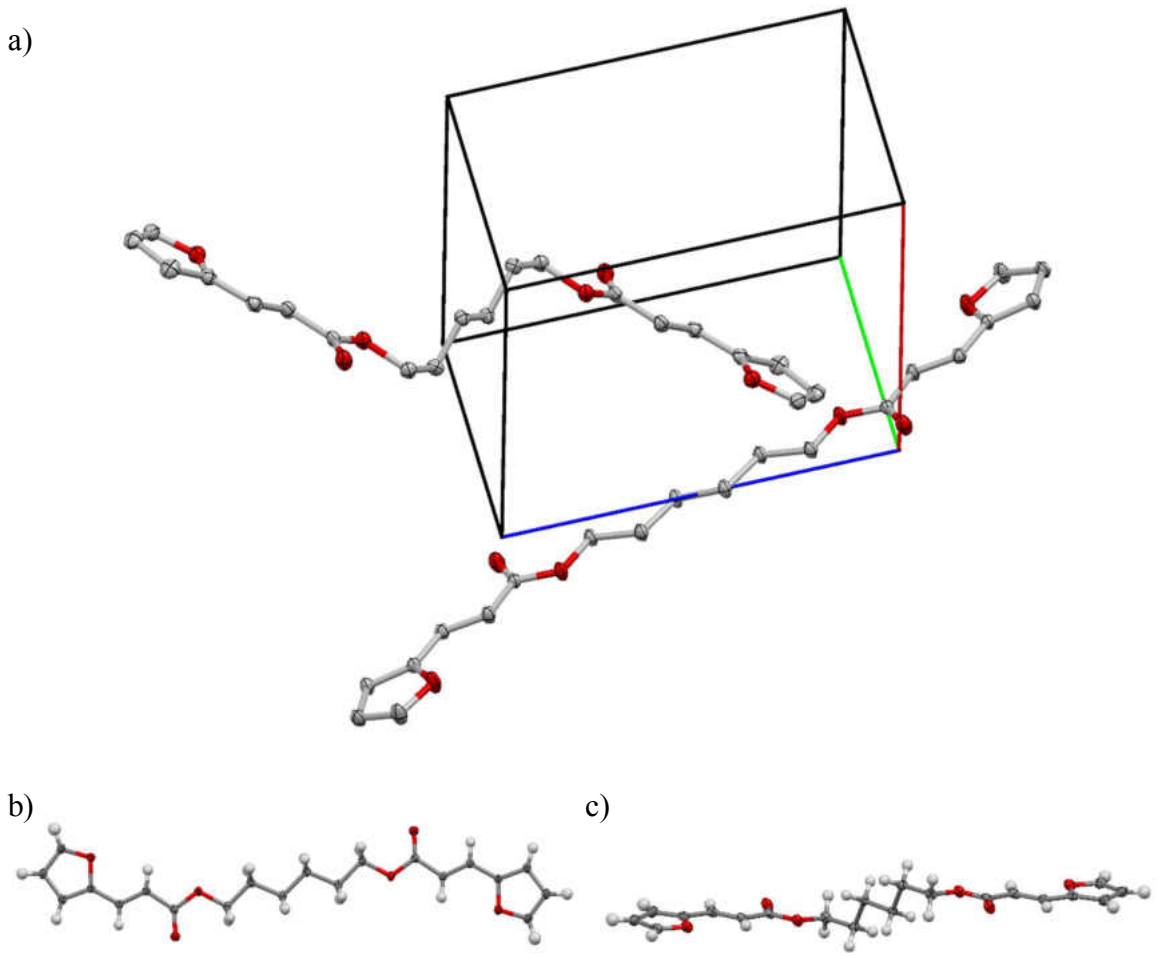

Figure 5. ORTEP drawing of monomer **9** with its unit cell (a). Isomer $\mathbf{9_\alpha}$ (b) and $\mathbf{9_\beta}$ (c).

Monomer **9** was shown to have two different conformational isomers in the same crystal: a planar one $\mathbf{9_\alpha}$ similar to monomers **5** and **8a** and a twisted one $\mathbf{9_\beta}$ similar to monomers **7** and **8b**, in which the 2-furanacrylate groups are parallel but offset. Interestingly, no polymorphism was observed (Figure 5). The two conformations exist within the same crystal structure, with alternating layers of the planar and twisted forms. This co-crystal is

triclinic and forms in the space group P-1, with a Z value of 2, similar to the crystals of monomer **8b**.

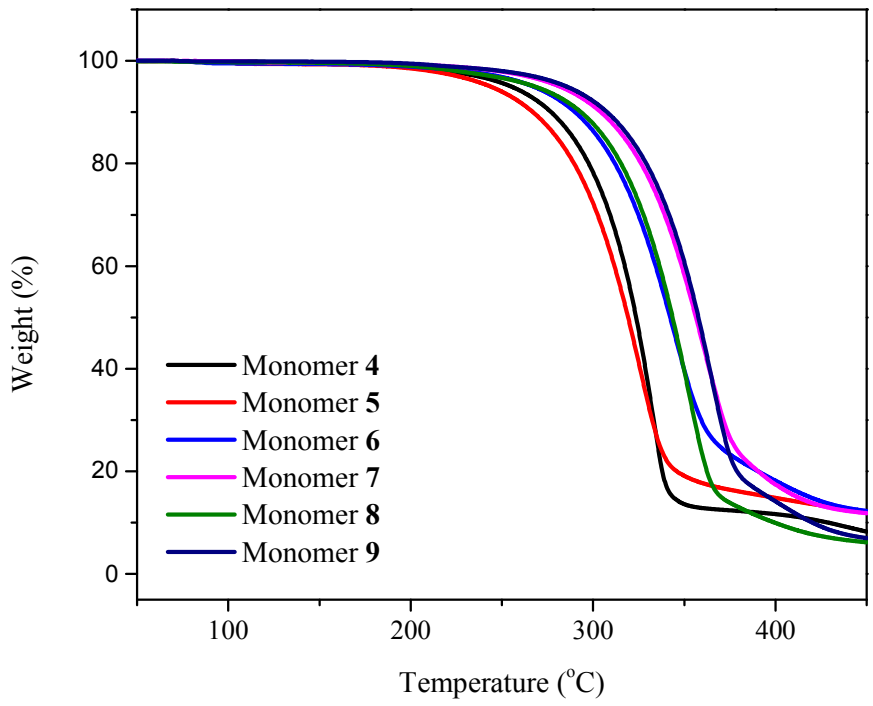

Figure 6. Thermostability study of monomers **4-9**.

Thermal gravimetric analysis (TGA) was performed to test the stability of the monomers at high temperatures (Figure 6). All of the monomers did not lose weight under 200 °C and lost most weight between 200 and 400 °C, but some decomposed at somewhat higher temperatures than others. It seems the monomers with an even number of carbons in the linker were more stable than the monomers with an odd number of carbons in the linker since monomers **7** and **9** decomposed at the highest temperatures. Monomers **6** and **8** decomposed at somewhat lower temperatures. However, the least stable monomers were **4**

and **5**. This is probably because they lack flexibility due to a low number of carbons in the linker.

These synthesized gemini monomers can be applied in the synthesis of polyladderane and linear polyesters, which will be discussed in the following chapters. For example, monomer **7** can be used to synthesize polyladderane. A ladderane has a unique chemical structure that includes two or more fused cyclobutane rings. Ladderanes are also found in nature in the ladderane lipid membranes of certain types of bacteria. Monomer **8** constructed from 2-furanacrylic acid and 1,5-pentanediol can be a precursor of sustainable polyester materials. The double bond conjugated with a carbonyl group in 2-furanacrylic acid can be a reacting center for polymerization in solid-state photoreaction. Two reacting centers are necessary because the [2 + 2] photoreaction will link the monomers together to form linear polyesters (Figure 7).

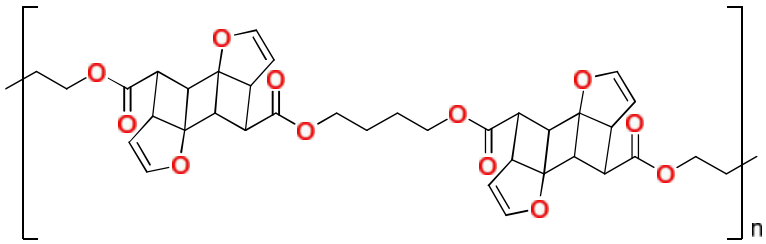

Polyladderane

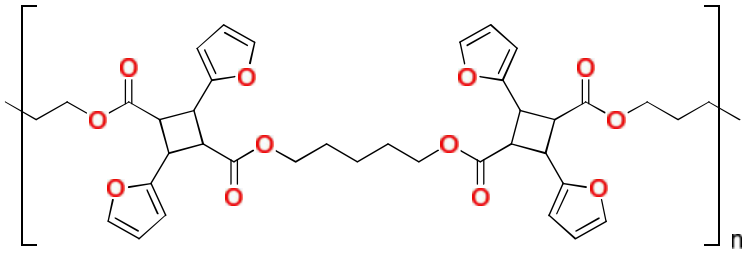

Linear Polyester

Figure 7. The polymers prepared from gemini monomers.

1.5. Conclusion

Six monomers were prepared from biomass derivate furfural. The monomers were characterized by XRD, P-XRD, and TGA. Seven crystal structures were collected and analyzed. Polymorphous crystalline states of monomer **8** were obtained. P-XRD data confirmed that the powders of monomer **8** have the same structure with **8a**. Conformational isomers were observed on monomer **9**. TGA showed high thermostability of the monomers. The study of the crystalline state of the monomers will benefit scientists who are working on crystal engineering, polyester materials, etc.

CHAPTER II

POLYLADDERANE SYNTHESIZED FROM 1,3-DIENE SYSTEM

2.1. Introduction

Ladderanes are unique ladder-like hydrocarbons containing two or more fused cyclobutane rings (Figure 8).[82] These ladder-like molecules and their derivatives have long been regarded as desirable synthetic targets due to their high ring strain and unique electronic properties.[83-85] These properties give them potential to be used as spacers, rigid rods, and optoelectronic devices.[86, 87] Ladderanes have been identified in nature as an essential component of biosystems called ladderane membrane lipids.[88-90] Although the biosynthesis mechanism of ladderane membrane lipids is still unknown,[91] the discovery of these ladder-like molecules has attracted attention from researchers in academia.[40, 92, 93]

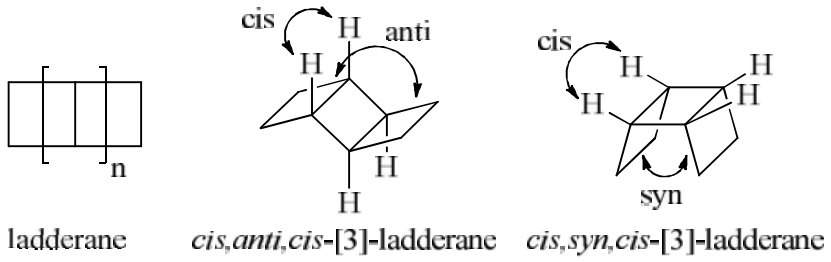

Figure 8. The backbone and stereochemistry of ladderane. left: the backbone of [n + 1]-ladderane; when two hydrogens between two rings are on the same side is cis-configuration. If the two outer rings are on different sides (middle), the ladderane has anti-configuration; same side (right) is syn-configuration.

Synthesis of ladderanes is challenging because of the high energy barrier and the ring strain.[94] The synthesis of ladderane-containing compounds has been achieved by several different synthetic approaches such as stepwise addition, [2 + 2] photocycloaddition, and oligomerization.[83-85,95-97] However, construction of polyladderane, a polymer containing the ladderane functional group, has not been realized even though such unique materials are of great interest for their fundamental significance and potential applications in a variety of technologies.[98-102]

The synthesis of polyladderane was achieved by [2 + 2] photocycloaddition reaction in the solid state with a conjugated diene. The main challenge of the solid-state reaction was to organize the double bonds in desired reactive orientations. The [2 + 2] photocycloaddition has specific reaction parameters: the two double bonds participating in the reaction must be separated by less than 4.2 Å and be aligned in parallel.[103] The strategy of our monomer design was to functionalize one end of the conjugated diene with an electron-withdrawing group such as an ester carbonyl group while the other end was substituted with an electron-donating group like a methyl group or an aromatic ring. Because of electrostatic interactions, conjugated dienes with different end groups prefer to pack into a crystal lattice in an electronically-complementary head-to-tail fashion (Figure 9a).[104-107] When two conjugated dienes are linked with an unreactive covalent spacer, the resulting gemini monomer will lead to the desired polyladderane (Figure 9b) after the [2 + 2] photopolymerization in the solid state.[52, 53, 108]

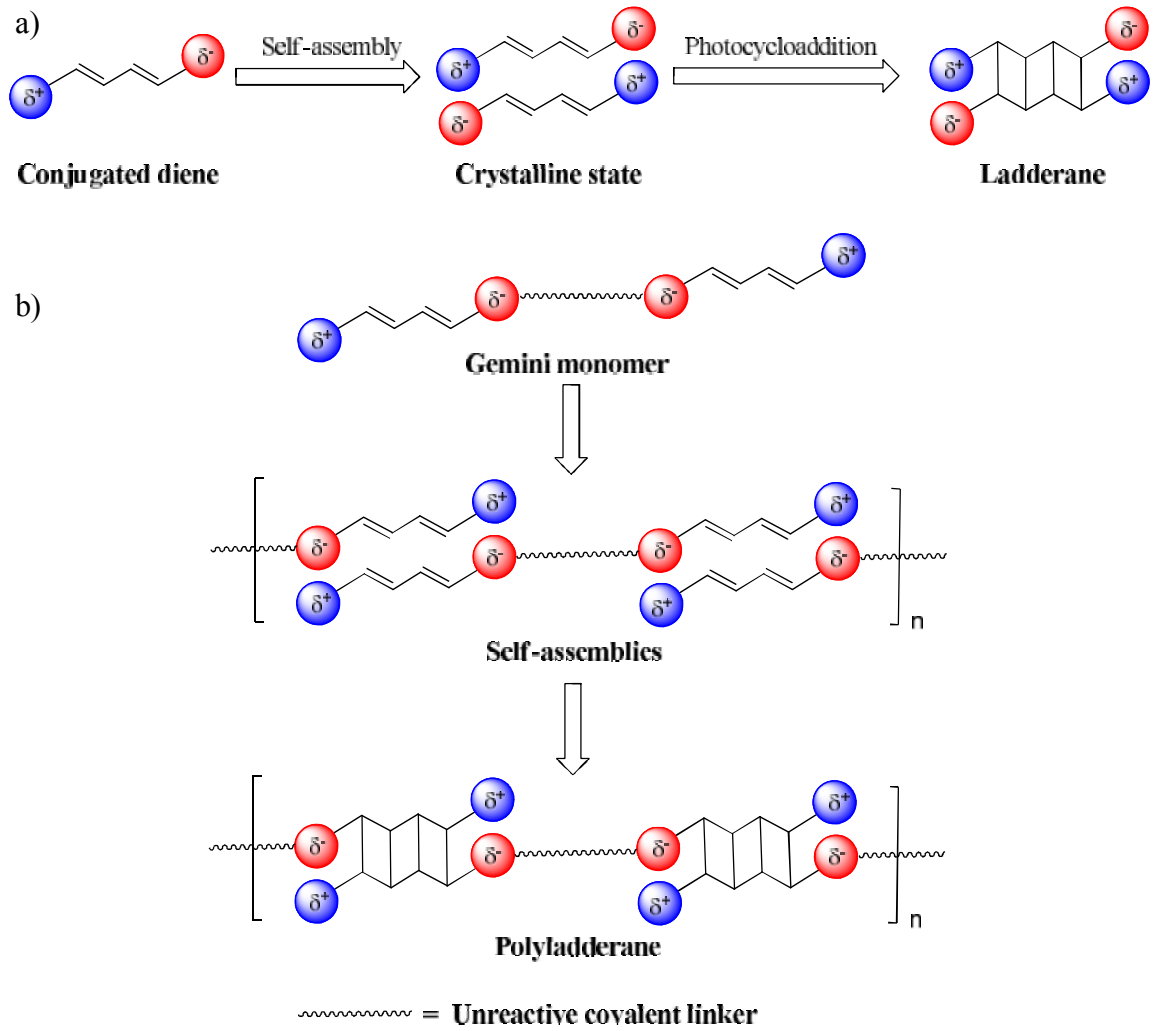

Figure 9. The strategy of polyladderane synthesis from designed gemini monomers.

2.2. Experimental Section

2.2.1. General Methods

All the reagents were purchased from Alfa Aesar, Sigma-Aldrich, Acros and used without further purification. The light source used for the photopolymerization was a Hanovia medium pressure mercury lamp (PC 451050, 450 W). The solution phase nuclear magnetic resonance (NMR) spectra were recorded using a Bruker AVANCE 500 MHz spectrometer (^{1}H: 500 MHz, ^{13}C: 125 MHz). All spectra were obtained in deuterium dimethyl sulfoxide

(DMSO-d_6). Single crystal X-ray data were recorded on Bruker Kappa Apex II Duo X-Ray Diffractometer with Mo *K*α (λ = 0.71073 Å) or Cu *K*α (λ = 1.54178 Å). Infrared (IR) spectroscopy was recorded on Thermo Scientific Nicolet iS5 FT-IR spectrometer. The mass spectrometric analyses were performed using a high-resolution time of flight G1969A with electrospray (atmospheric pressure chemical) ionization (Agilent, Santa Clara, CA, USA) and reported as m/z (relative intensity). Accurate masses are reported for the molecular ion $[M+Na]^+$, $[M+K]^+$, $[M+NH_4]^+$, or $[M]^+$. Melting points were measured on a MEL-TEMP device without correction. The mass spectrometric analyses were performed using a high-resolution time of flight G1969A with electrospray (atmospheric pressure chemical) ionization (Agilent, Santa Clara, CA, USA) and reported as m/z (relative intensity). X-ray powder diffraction (XRD) was performed on a X'PERT-PRO X-ray diffractometer (PANalytical, Netherlands) equipped with a 3 KW copper tube X-ray generator of λ = 0.1541 nm under 40 mA and 45 KV. Spectrum was collected at room temperature in a 2θ range of 3°~35° at a scanning rate of 3°/min. Thermogravimetric analysis (TGA) was performed with TA instrument SDT Q600 at a ramping rate 20 ºC/min under nitrogen protection. Mass spectrum was performed on the instrument of Waters SYNAPT G2Si. MALDI was performed on Waters SYNAPT G2-Si Q-TOF with MALDI source.

2.2.2. Synthesis of Monomer **12**

Sorbic acid (**10**) (1.6 g, 13 mmol), 1,4-butanediol (**11**) (0.6 g, 6 mmol), DCC (3.0 g, 14 mmol) and DMAP (2.0 g, 16 mmol) were dissolved in chloroform (20 mL). The mixture was stirred at room temperature for 16 h. The mixture was concentrated and purified by column chromatography using hexane and ethyl acetate (3 : 1) to give product monomer

12 (1.6 g, 86%) as a light yellow solid. M.p.: 69-70 °C, ^{1}H NMR (500 MHz, DMSO-d_6): δ 7.22 (m, 2H), 6.27 (m, 4H), 5.87 (d, J = 15.5 Hz, 2H), 4.10 (t, J = 5 Hz, 4H), 1.81 (d, J = 5.5 Hz, 6H), 1.67 (m, 4H); ^{13}C NMR (125 MHz, DMSO-d_6): δ 166.7 (C), 145.4 (CH), 139.3 (CH), 129.9 (CH), 118.9 (CH), 63.7 (2CH_2), 25.2 (2CH_2), 18.8 (CH_3); IR: 1700, 1642, 1616 cm^{-1}; UV/Vis: λ_{max} 259 nm; HRMS (m/z): $[M+Na]^+$ calcd. for $C_{16}H_{22}O_4Na$, 301.1415; found 301.1423.

2.2.3. Synthesis of Monomer **7**

The synthesis of monomer **7** has been discussed in Chapter I.

Intermediate **7b** (a dimer of **7**): ^{1}H NMR (500 MHz, DMSO-d_6): δ 7.53 (s, 2H), 7.00 (d, J = 15.5 Hz, 2H), 6.68 (s, 2H), 6.35 (s, 4H), 5.99 (d, J = 15.5 Hz, 2H), 5.0 (s, 2H), 4.17 (d, J = 10 Hz, 2H), 4.06 (s, 8H), 3.93 (t, J = 9 Hz, 2H), 3,76 (d, J = 8 Hz, 2H), 1.59 (s, 8H); ^{13}C NMR (125 MHz, DMSO-d_6): δ 171.1 (C), 165.3 (C), 151.6 (C), 148.2 (CH), 143.4 (CH), 143.1 (CH), 120.4 (CH), 110.9 (CH), 108.1 (CH), 102.3 (CH), 88.2 (C), 64.4 (2CH_2), 64.0 (2CH_2), 48.9 (2CH), 47.0 (2CH), 42.2 (2CH), 25.1 (2CH_2), 25.09 (2CH_2); HRMS (m/z): $[M+Na]^+$ calcd. for $C_{36}H_{36}O_{12}Na$, 683.2104; found 683.2123.

2.2.4. Crystallization

The crystals of **12** were obtained in ethyl acetate at room temperature. Monomer **12** (30 mg) was dissolved in solvent ethyl acetate (20 mL). The vial with monomer **12** solution was covered with a piece of aluminum foil which was punched with several holes. After four days' evaporation, crystals were obtained. The crystals of **7** were obtained in ethyl acetate and toluene (1 : 1). The vial was put in an ultrasonic cleaner (Bransonic® Models 1200) for a half hour. Then the mixture was filtered into a 20 mL vial with filter paper. The

vial with the clear solution was allowed to stay without a cover until the crystals were formed.

2.2.5. Photoreaction

Crystals were irradiated with ultraviolet light on a slide glass. 10 mg of monomer powder **12** or **7** was scattered on a slide glass and the sample was placed into a photoreactor. The process of photoreaction was monitored by FT-IR. The polymerization was accomplished in 36 hours.

The intermediate **7a** was obtained after 12 hours of the UV irradiation. The partial single-crystal-to-single-crystal (SCSC) transformation was achieved by using 10 mg of single crystals instead of the monomer powder **7** in the photopolymerization. X-ray diffraction was used to monitor the transformation.

Dimer $[M+K]^+$ calcd. $C_{36}H_{36}O_{12}K$, 699.1843; found 699.1871. Trimer $[M+K]^+$ calcd. $C_{54}H_{54}O_{18}K$, 1029.2947; found 1029.3008. Tetramer $[M+K]^+$ calcd. $C_{72}H_{72}O_{24}K$, 1359.4050; found 1359.4116.

2.3. Results and Discussions

The synthetic pathway of a designed polyladderane is shown in Scheme 2. Monomer **12** was synthesized by connecting two sorbic acids (**10**) with 1,4-butanediol (**11**) through an esterification reaction. To achieve polyladderane synthesis, the double bonds in the monomer molecules must be aligned in a head-to-tail reactive orientation in the solid state. To investigate the polymerization process, single crystals of monomer **12** suitable for X-

ray diffraction analysis were obtained in ethyl acetate. Single crystal structure analysis of monomer **12** confirmed that 1,3-dienes in monomers with the same color are packed in the desired head-to-tail fashion and are parallel with each other (Figure 10). The separation between two 1,3-dienes with the same color is about 3.80 Å, which is suitable for photoreaction (< 4.2 Å). As a result, two photocycloaddition reactions occur between 1,3-dienes forming three fused cyclobutane rings. The crystal packing of monomer **12** also shows that 1,3-dienes in monomers with different colors are not overlapped (Figure 10c), so they will not react with each other in the solid state.

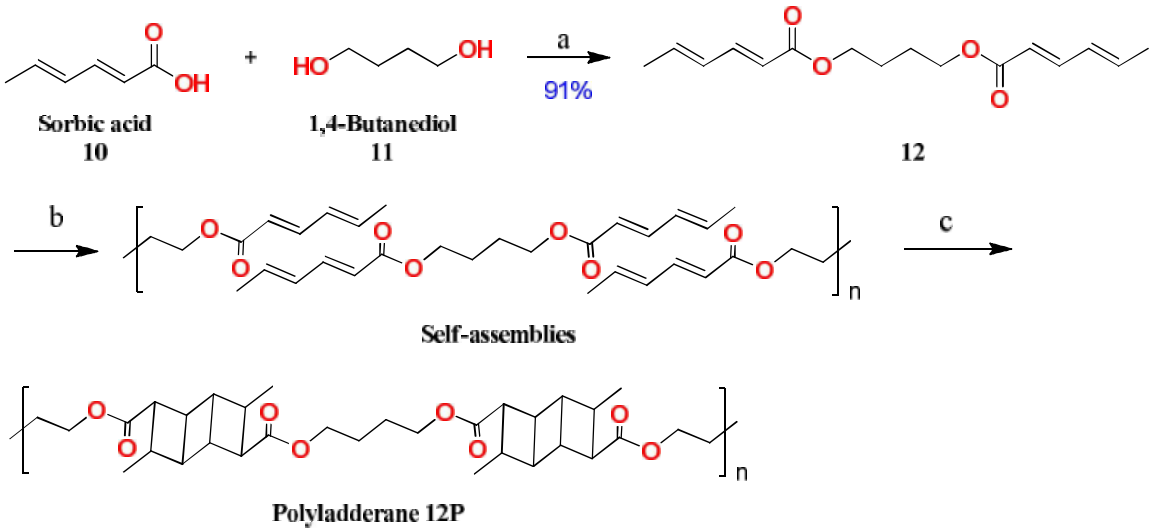

Scheme 2. Synthesis of polyladderane **12P**. a) DCC, DMAP, $CHCl_3$, r.t. 16 h. b) Self-assembly obtained in ethyl acetate. c) Topochemical photopolymerization with UV irradiation.

UV-Vis spectrum shows that monomer **12** has strong absorption in the range 229-303 nm. The photocycloaddition reaction was carried out with a UV-mercury lamp and monitored using FT-IR. The spectra of photoreaction shown in Figure 11 confirmed the completion of photoreaction. In FT-IR spectra, the characteristic absorption of C=O

stretching at 1704 cm^{-1} was shifted to 1723 cm^{-1}, which can be attributed to the deconjugation of the carbonyl group. Two C=C stretching bands (1640 and 1614 cm^{-1}) disappeared after photoreaction, which is consistent with completion of [2 + 2] photoreaction. The accomplishment of the photopolymerization was also confirmed by the disappearance of bands at 1003 cm^{-1} associated with the out-of-plane vibration of the C–H single bonds in the *trans*-CH=CH unit. The resulting polyladderane **12P** was insoluble in common organic solvents such as CH_3Cl, MeOH, DMSO, CH_3CN, acetone, and toluene.

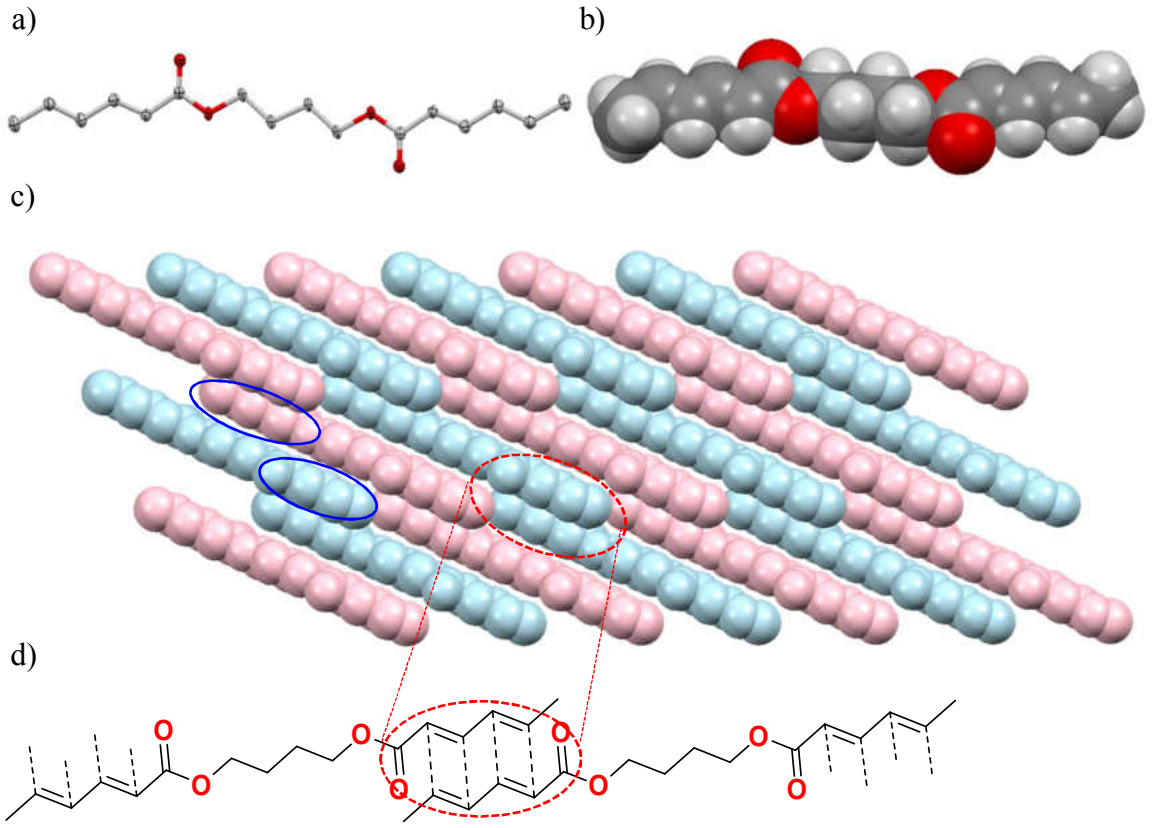

Figure 10. X-ray diffraction analysis of monomer **12**. a) Single crystal X-ray structure of monomer **12** ORTEP represents a 50% electron density of monomer crystal structure. b) The monomer crystal in space-fill style. c) Monomer stacking depicts that like-colored monomers are suitable for photocycloaddition reaction. Two solid blue circles show that diene segments of the different-colored monomers are not overlapped with each other. d) The black dashed lines indicate where new bonds form. (Hydrogen atoms are omitted for clarity in 10a and 10c. Colors are introduced arbitrarily for clarity in discussion and ease of visualization.)

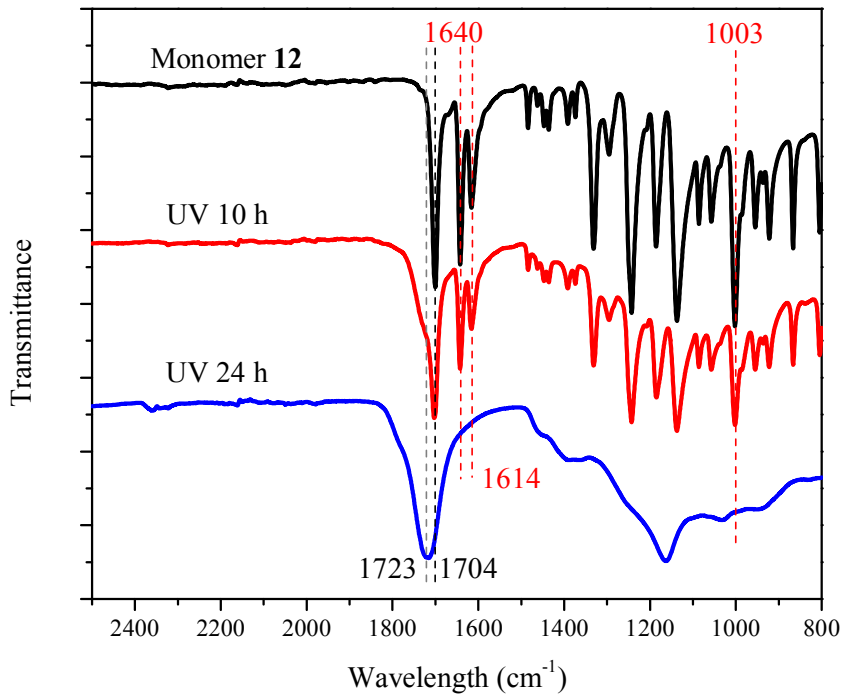

Figure 11. FT-IR spectra of monomer **12** and reaction mixture after 10 and 12 h of UV irradiation.

While working on the photopolymerization of monomer **12**, we noticed that it has a relatively low melting point (69-70 ºC) and high reactivity at room temperature making it difficult to achieve a single-crystal-to-single-crystal (SCSC) transformation, which represents a direct way to confirm the polyladderane structure. By judiciously choosing and testing different decorating functional groups or the covalent linker in this modular approach, the structure and property of the gemini monomer can be tuned. To continue studying polyladderane, a furan ring was introduced to stabilize the 1,3-diene and to increase the melting point of the monomer.

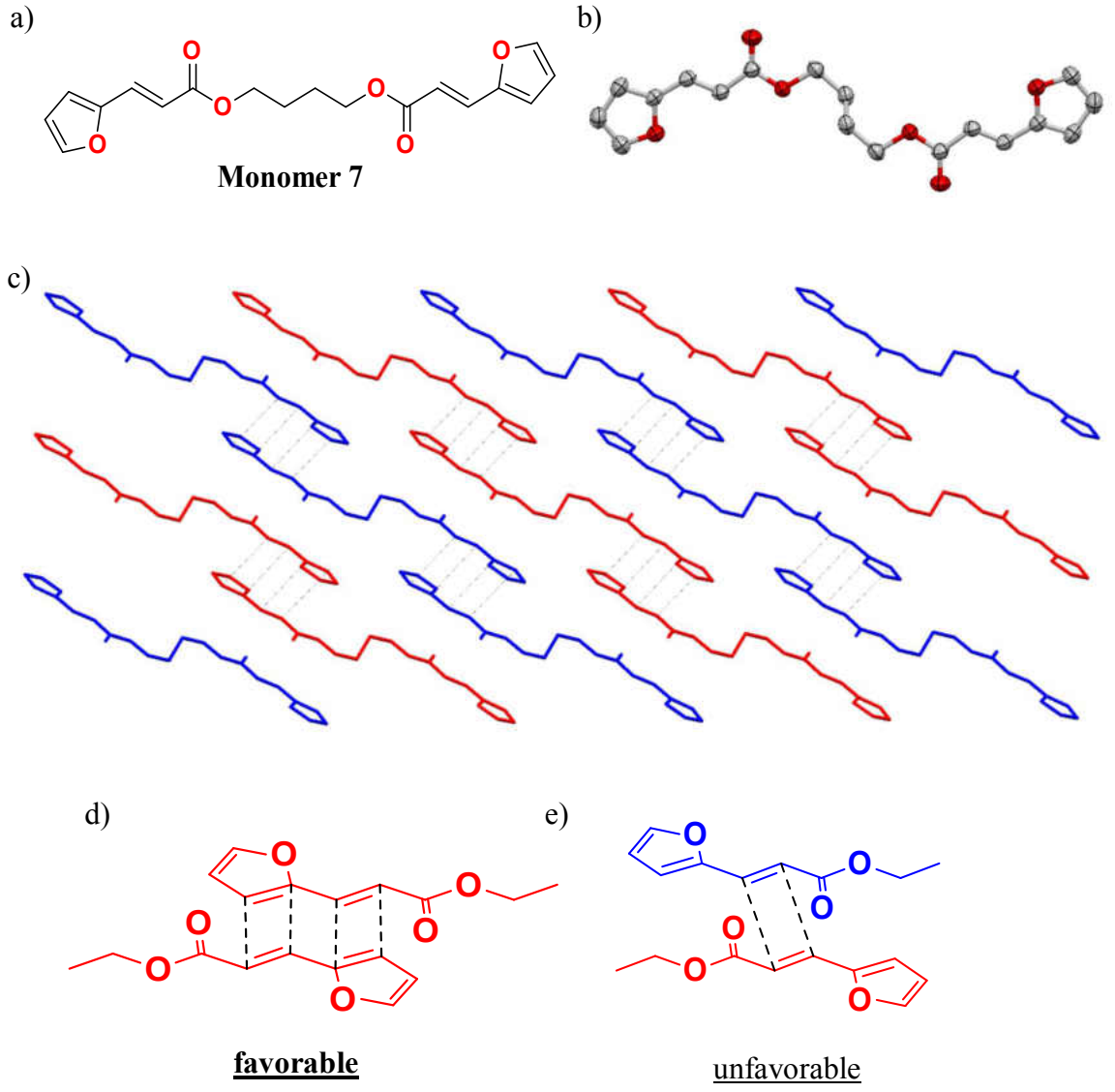

Figure 12. X-ray diffraction analysis of monomer **7**. a) Chemical structure of monomer **7**. b) Single crystal X-ray structure. c) Monomer stacking along the crystallographic *ac* plane. d) Chemical structures to show the spatial orientation of same colored monomers. e) Chemical structures show the spatial orientation of the different-colored monomers. (Hydrogens are omitted for simplification and colors are introduced arbitrarily for clarity in the discussion. Oak Ridge Thermal Ellipsoid Plot (ORTEP) perspective at 50% electron density of the monomer. Colors are introduced arbitrarily for clarity in discussion and ease of visualization.)

The synthesis of monomer **7** (mp: 114-115 ^{o}C) was similar to that of monomer **12**. The single crystal X-ray structure of monomer **7** shows the distance between 1,3- dienes in the closest monomers is 3.54 Å, exhibited in Figure 12d. The double bonds in the different-colored monomers are also parallel to each other, and the distance between them is 3.84 Å, which is also within the photoreactive range (< 4.2 Å). However, the distances of 1,3-dienes with same colors are 8.5 % closer than that of the double bonds in different colors.

Moreover, the π orbitals of adjacent C=C bonds with the same colors point almost directly toward each other, while the π orbitals of neighboring monomers with different colors are offset by more than 2 Å.[109] This orbital overlap is critical for the locally confined reaction in the solid state, which proceeds by the pathway with the smallest movement of atoms (Figure 12c-e). Therefore, in monomer **7** the photoreaction prefers to occur between 1,3-dienes in like-colored monomers. Photoreaction of monomer **7** will result in three fused cyclobutane rings to yield polyladderane **7P** in the crystalline state.

UV-Vis spectrum shows a broad absorption of **7** in solid state (241 to 373 nm) with a peak absorption around 300 nm. FT-IR spectra were used to monitor the photocycloaddition reaction of monomer **7**, showing that the reaction was completed after 36 hours under UV irradiation. While completion of photoreaction caused crystal **7** to become an amorphous solid and lose its crystalline state, partial polymerization resulted in the successful capture of a key polyladderane intermediate. Analysis of the partial single-crystal-to-single-crystal (SCSC) transformation indicated that about 10% of 1,3-dienes in partially polymerized **7a** were converted to *cis*,*anti*,*cis*-[3]-ladderanes (Figure 13). This partial single crystal X-ray structure of polyladderane provides a direct evidence for the aforementioned

analysis. Adjacent cyclobutane rings created in the photoreaction formed *cis*,*anti*,*cis*-[3]-ladderanes between monomers, connecting them to form polyladderanes.

a)

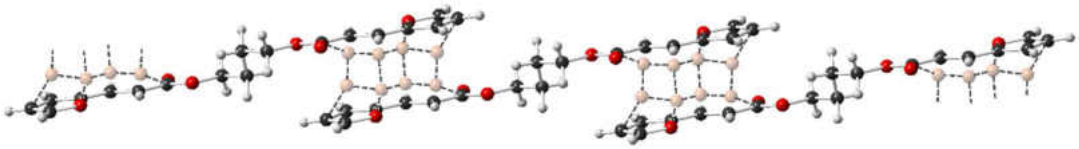

Intermediate **7a**

b) c)

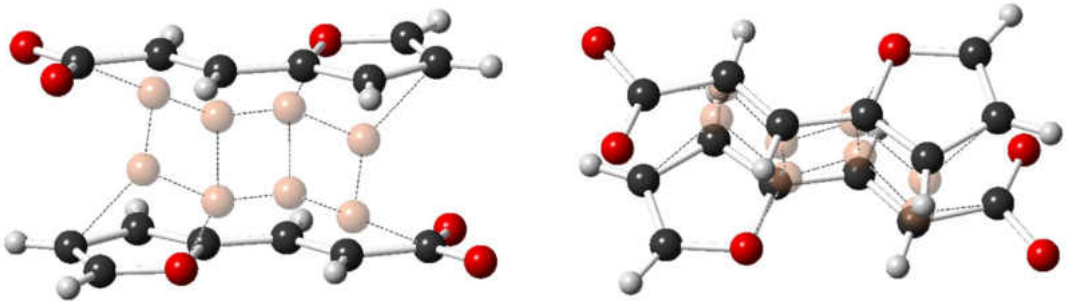

Figure 13. Single crystal X-ray structure of intermediate **7a**. a) Three monomers with corresponding polyladderanes. b) Front view of the *cis*, *anti*, *cis*-[3]-ladderanes. c) Top view of the three fused cyclobutane rings.

Another important intermediate obtained during the solid-state photoreaction provided additional evidence and insight into polyladderane formation. At the beginning of the photoreaction, a small amount of intermediate **7b** was successfully isolated with 1% yield after column chromatography (Figure 14a). Intermediate **7b** was characterized by HRMS, ^{1}H and ^{13}C NMR spectrum including COSY and DEPT. The structure of **7b** was confirmed to be a ladderane dimer of monomer **7**. Comparing to the ^{1}H NMR spectrum of **7b** (Figure 14b) with that of the monomer

7, three new peaks appeared in the spectrum of the dimer around 4 ppm (marked with blue stars) corresponding to the three protons on the newly formed ladderane. Figures 14c (DEPT-135) and 14d (DEPT-90) suggest that peaks with shifts 42.2, 47.0, and 48.9 ppm correspond to the three tertiary carbons of the *cis*,*anti*,*cis*-[3]-ladderane. The peak with chemical shift 88.2 ppm did not appear in DEPT-135 and DEPT-90 spectrum but showed in ^{13}C NMR spectrum (Figure 14e), indicating that it is a quaternary carbon atom, which corresponds to the carbon marked with a red star in the structure of ladderane (Figure 14a). The dimer intermediate **7b** was only observed at the beginning of the photoreaction. As the photoreaction proceeded, all monomers were consumed to produce polyladderane **7P**. Dimer, trimer, and tetramer were also observed in MALDI analysis at the first 12 h photoreaction. These results provided additional evidence for the polyladderane structures.

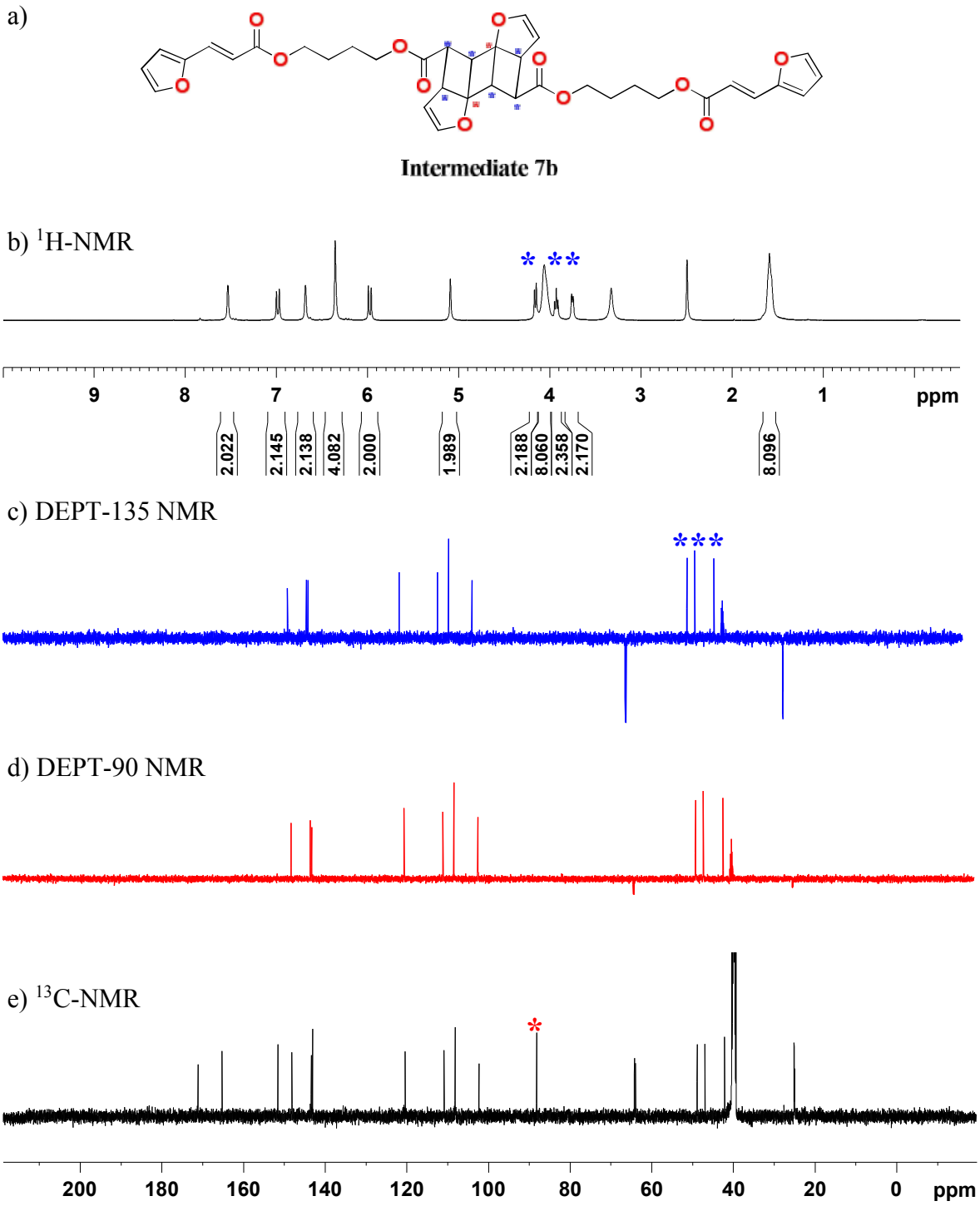

Figure 14. Ladderane dimer **7b**. a) The chemical structure of **7b**. b) ^{1}H-NMR spectrum of **7**. c) blue: DEPT-135 NMR spectrum of **7b**. d) red: DEPT-90 NMR spectrum of **7b**; e) black: ^{13}C-NMR spectrum of **7b**. Note: the NMR spectra were taken in DMSO-d_6 at room temperature.

It is worthwhile to mention that the overall synthesis of the polyladderanes is facile and mild. The starting materials are inexpensive and many of them, such as furfural and 1,4-butanediol, can be derived from renewable resources. In addition, the powder XRD patterns of the synthesized monomers **7** and **12**, without further processing, were nearly identical to those of the corresponding ground single crystals **7** and **12**, confirming that the powders are microcrystalline. The powder XRD results suggest that powders of monomers are also suitable for producing polyladderanes **7P** and **12P** on a larger scale. The recrystallization step can be skipped to synthesize both **7P** and **12P**.

2.4. Conclusion

A new class of polymer, polyladderane, was constructed stereoregularly from the designed gemini monomer through a photocycloaddition reaction under mild conditions in the solid state. The carbon−carbon single bonds formed stereospecifically during the [2 + 2] photopolymerization were directly revealed by the single crystal X-ray structure of a polyladderane intermediate. The isolation and characterization of a ladderane dimer in the beginning of the polymerization provided additional evidence and insight into polyladderane formation. The observation of the dimer, trimer, tetramer in MALDI analysis provided the third evidence of synthesized polyladderanes. The successful synthesis of polyladderane paves the way for the future study of its unique characteristics such as mechanical properties and opens up the possibility for applications in a variety of fields.

CHAPTER III

LINEAR POLYESTER SYNTHESIZED FROM FURFURAL-BASED MONOMER

3.1. Introduction

The most popular thermoplastic is polyester because of its impressive strength, thermostability, and transparency.[117-119] The polyester market underwent rapid expansion and there are broad development prospects. For example, polyethylene terephthalate (PET) is widely used for making beverage bottles and other plastic containers.[110-112 121, 127, 128] In fact, the popularity of PET was a long way. It took around 30 years for PET from discovery to bottle applications.[113] The other reasons for popularity of polyester attribute to its light-weight, low-cost and reusable ability.[114-119] With the limited fossil fuels and increasing carbon dioxide emissions, polyesters from sustainable resources are becoming fantastic synthetic targets.[9-13, 33, 52, 54, 118-126] As one of the promising renewable building blocks, furfural has recently attracted more and more attention from academic and industrial researchers for synthesizing new materials. [3, 4, 6, 15, 20, 22, 23, 127-129] In fact, an increasing number of companies has dedicated to developing sustainable thermoplastics.[112, 116, 119, 130-132]

Solvent-free and solid-state polymer synthesis have been widely accepted by scientists under green chemistry conditions.[133-137] The advantages of solvent-free reactions are

obvious, such as easy operating, low costs, low energy consumption, and reducing pollution, which are important in applications of industry.[134-139] Moreover, since incrystalline state the molecules are regularly pre-organized, the reactions occurred in solid-state are more efficient and selective than solution reaction.[39, 47, 54, 137, 140-142] Due to the pre-organized molecules, the structures of synthesized materials are predictable. Hence, solvent-free reactions provide a promising way to design and synthesize new materials with complicated structures, which may not be achieved by solution reactions. In solid-state reactions, topochemistry plays a crucial role because topochemical synthesis can efficiently avoid crosslinking and side reactions. [42, 47, 52, 54, 142-144]

For green chemistry, the using of solar energy in chemistry has a quiet great development.[36, 145-149] Sunlight, as a natural light resource, is much safer than an ultraviolet lamp, which is normally used in photoreactions. Furthermore, sunlight is inexpensive, clean, and essentially inexhaustible, which makes the solvent-free polymer synthesis process more environmentally friendly. [36, 145, 146, 149] According to the rules of green chemistry, a linear polyester based on furfural and it derivate were synthesized through solvent-free polymer synthesis. Based on the mass calculation, the bio-ratios of the synthesized polyester achieved to 100%. In our study, it has been proven that sunlight is as efficient as an ultraviolet lamp.

3.2. Experimental Section

3.2.1. General Methods

All the reagents were purchased from Alfa Aesar, Sigma-Aldrich and used without further purification. The light sources used for the photopolymerization were sunlight and a Hanovia medium pressure mercury lamp (PC 451050, 450 W). The optical filter used for the photoreaction with mercury lamp was ZRR0340 Red Rejection UV Filter from Asahi Spectra USA Inc. The solution phase nuclear magnetic resonance (NMR) spectra were recorded with Bruker AVANCE 500 MHz NMR Spectrometer (^{1}H: 500 MHz, ^{13}C: 125 MHz). All spectra were obtained in deuterium dimethyl sulfoxide (DMSO-d_6). Single crystal X-ray data were recorded on Bruker Kappa Apex II Duo X-Ray Diffractometer with Mo $K\alpha$ (λ = 0.71073 Å) or Cu $K\alpha$ (λ = 1.54178 Å). Melting points were measured on a MEL-TEMP device without correction. Infrared (IR) spectroscopy was recorded on Thermo Scientific Nicolet iS5 FT-IR spectrometer. The mass spectrometric analyses were performed using a high-resolution time of flight G1969A mass spectrometer with electrospray (atmospheric pressure chemical) ionization (Agilent, Santa Clara, CA, USA) and reported as m/z (relative intensity). X-ray powder diffraction (XRD) was performed on a X'PERT-PRO X-ray diffractometer (PANalytical, Netherlands) equipped with a 3 KW copper tube X-ray generator of λ = 0.1541 nm under 40 mA and 45 KV. Spectra were collected at room temperature in a 2θ range of 3°~35° at a scanning rate of 3°/min. Scanning electron microscope (SEM) and transmission electron microscopy (TEM) were recorded with Hitachi SU8010 UHR Cold-Emission FE-SEM. Copper Grids are FCF200-Cu-50 (Formvar Carbon Film on 200 Square Mesh Copper Grids) and CF213-25 (C-Flat 1.2 Micron Hole 2 μm Space 200 Mesh). Silicon wafer chips were purchased from West

Chester (Silicon Wafer Chip 5×7 mm, PK/186). Thermogravimetric analysis (TGA) was performed with TA instrument SDT Q600 at a ramping rate 20 ºC/min under nitrogen protection.

3.2.2. Synthesis of 2-Furanacrylic Acid **3**

The synthesis of 2-furanacrylic acid has been discussed in Chapter I.

3.2.3. Synthesis of Monomer **8**

The synthesis of monomer **8** has been discussed in Chapter I.

3.2.4. Crystallization

The crystals of **8** were obtained in DMSO/H_2O (3 : 1) at room temperature. Monomer **8** (20 mg) was added to solvent DMSO/H_2O (20 mL). The vial of the suspended mixture was put in an ultrasonic cleaner (Bransonic® Models 1200) for a half hour. The mixture was filtered into a 20 mL vial with filter paper. The vial with the clear solution was allowed to stay without a cover until the crystals were formed.

3.2.5. Photoreaction

Crystals were irradiated in sunlight on a slide glass. 10 mg of monomer **8** was scattered on a slide glass and the sample was placed outdoors for photoreaction. The process of photoreaction was monitored by FT-IR. The photoreaction of monomer **8** was carried out in 3 days with 8 h of solar irradiation per day.

During the UV photoreaction, 10 mg of monomer **8** crystal powder was scattered on a glass plate and covered by a ZRR0340 Red Rejection UV Filter. The combined plates with the monomer **8** were put in a photoreactor equipped with Hanovia medium pressure

mercury lamp (PC 451050, 450 W). Due to its low melting point of monomer **8** (66-67 °C), the photoreaction was further cooled with a fan besides the immersion cooling well and the polymerization was carried out near room temperature. The polymerization was accomplished in 24 h.

Monomer **8** powder (2.0 g) was scattered on a 2" × 2" glass plate and covered by ZRR0340 Red Rejection UV Filter. The combined plates with monomer **8** were put in photoreactor and the powder was scattered every 2 h until the reaction completed in 24 h.

For the partial single-crystal-to-single-crystal (SCSC) transformation, 4 mg of single crystals were used instead of the monomer powder **8** in the photopolymerization. The intermediate crystal **8c** was obtained after 2 days of the UV irradiation.

3.3. Results and Discussions

Monomer **8** was synthesized from furfural (Scheme 3). The building block of the monomer is 2-furanacrylic acid, which can be prepared by Knoevenagel condensation between furfural and malonic acid, and followed by decarboxylation. The newly-formed exocyclic carbon-carbon double bond (C=C) extended the branch of furfural and will be used for the solid-state [2 + 2] photoreaction. A photostable 1,5-pentanediol (**13**) linker was then introduced to connect two 2-furanacrylic acid molecules together to form the new monomer **8**. An important factor in the selection of 1,5-pentanediol as the linker was that both of them can be produced from furfural as well.[61, 65, 129]

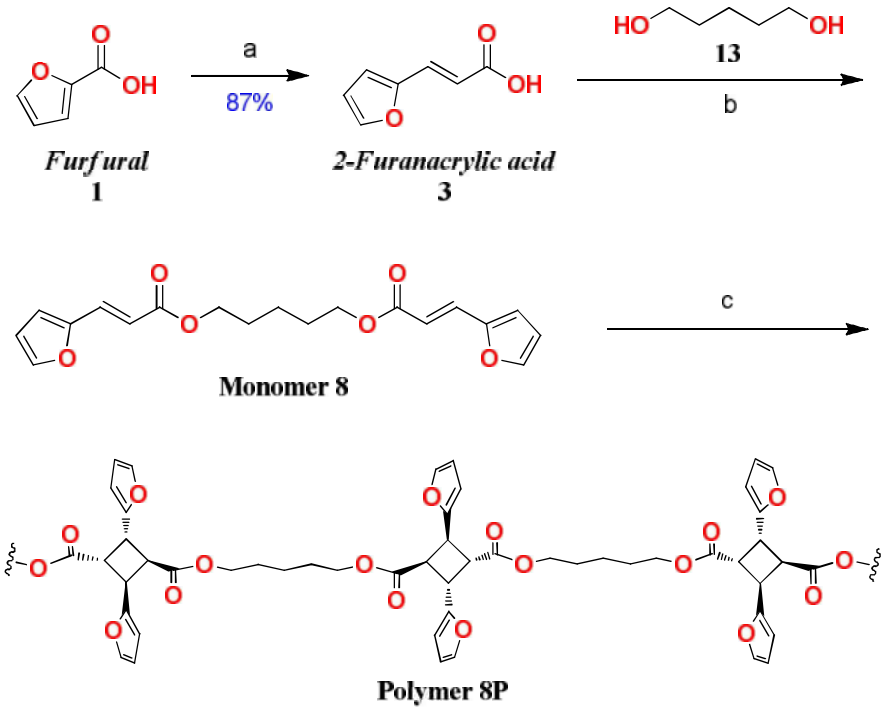

Scheme 3. The synthesis of monomer **8**. a) Malonic acid, pyridine, 100 ºC, 14 h; then HCl. b) DCC, DMAP, ACN, r.t., 12 h. c) Topochemcial photopolymerization with 24 h sunlight.

The powder of monomer **8** polymerized under sunlight within 24 hours in the solid state. To investigate the solvent-free polymerization, crystals of monomer **8** suitable for single-crystal X-ray diffraction (XRD) were obtained from DMSO/H_2O (3 : 1) at room temperature. Powder X-ray diffraction (P-XRD) was used for structural characterization of powder monomer **8**, which showed that the packing of monomer powder was the same as that of the single crystal structure. This indicated that the crystal structure of monomer **8** was suitable to analyze and interpret the solid state polymerization of both the crystals and powder. The crystal structure of monomer **8** reveals that the distance between the closest C=C bonds shown with same colors in Figure 15 (colors are introduced arbitrarily for clarity in discussion and ease of visualization) is around 3.68 Å. The distance between the

closest C=C bonds with the different colors is around 4.14 Å. Because the adjacent C=C bonds with same colors are 12.5% closer than different colored double bonds in the crystal (3.68 *vs.* 4.14 Å, Figure 15c), the [2 + 2] photoreaction between the C=C bonds of monomer **8** with the same colors is preferred.[109, 150]

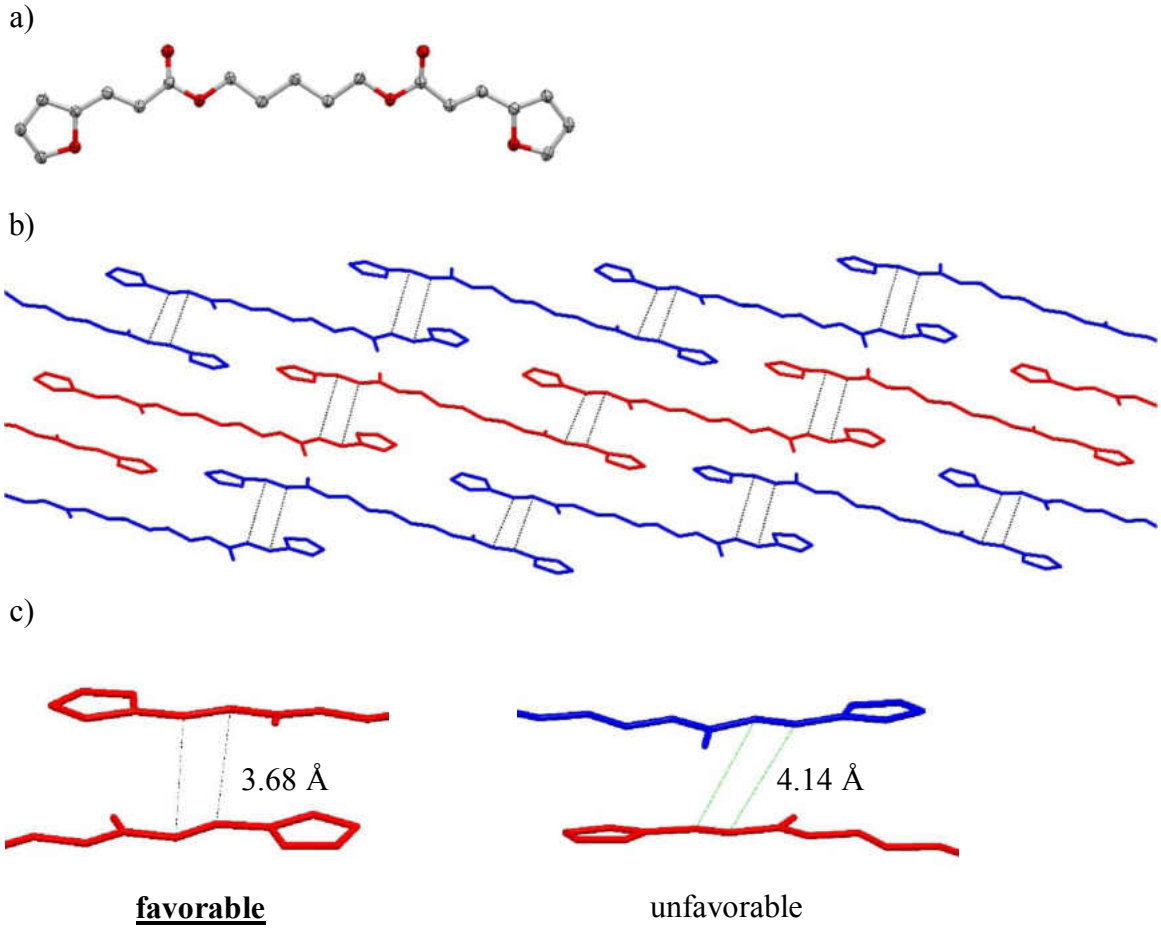

Figure 15. Three views of the crystal structure of monomer **8** (hydrogens are omitted for simplification and colors are introduced arbitrarily for clarity in the discussion.). a) ORTEP perspective at 50% electron density of the monomer **8** crystal structure. b) A side view of the crystal packing shown in capped sticks model. The closest C=C bonds are connected with dotted lines. c) The distances between C=C bonds in adjacent monomers. The dotted lines showing where the new C−C bonds could form.

Moreover, the π orbitals of adjacent C=C bonds with the same colors are directly pointing toward each other while the π orbitals of neighboring monomers with different colors are offset by more than 2 Å. This orbital overlap is critical for the locally confined reaction in the solid state, which proceeds with the minimum movement of atoms (Figure 15b-c). Therefore, the preorganization of the reactive centers in the self-assembly prefers that monomer **8** reacts with its two nearest same-colored neighbors to form the linear polyester as shown in Scheme 3.[42, 151]

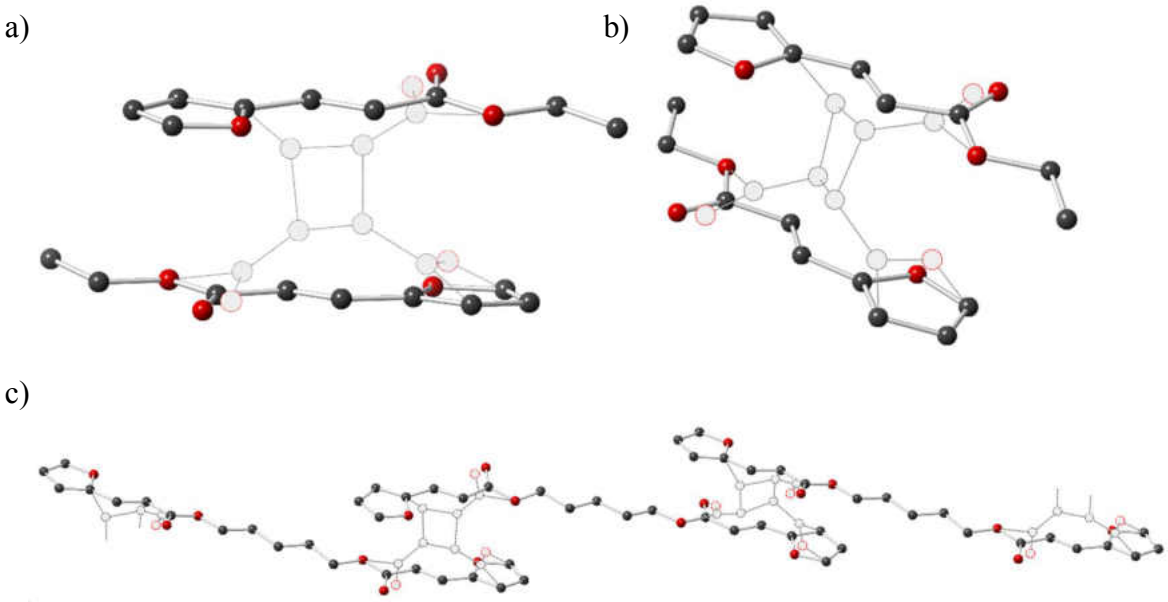

Figure 16. The X-ray single crystal structure of intermediate **8c** (The 15% of polymer is shown in gray and only part of the monomer/polymer is shown for simplicity.). a) Front view of the cyclobutane ring in the crystal. b) A different view of the cyclobutane showing the stereoregularity of the polymerization. c) Three monomers with the corresponding linear polymeric product.

The X-ray crystal structure with partial polymeric products was consistent with the above analysis of spatial approximation of the neighboring C=C bonds. Although crystal **8** lost its crystallinity gradually under UV irradiation and became an amorphous solid, a single-

crystal-to-single-crystal (SCSC) transformation was still observed at the beginning of the polymerization process. Figure 16 shows the partially polymerized crystal structure with 15% of the C=C double bonds converted into cyclobutane rings. With the formation of the cyclobutane ring, the two carbonyl groups moved closer to adapt to the change of the structure in the solid state correspondingly. Meanwhile, the distance between the closest different-colored C=C bonds increased for about 0.03 Å. The partial SCSC transformation was readily repeatable. In the seven similar SCSC photopolymerization experiments, cyclobutane rings were only observed between the same-colored monomers and no cyclization was detected between the different-colored monomers. Such excellent selectivity can be ascribed to the formation of the cyclobutane ring between the two closest monomer arms, which causes a see-saw action whereby other monomer arms are made to react with monomers of the same color.

It is also noteworthy that SCSC experiment shows that monomer **8** underwent [2 + 2] photopolymerization in a known stereospecific manner.[52, 144] Only one of the five possible stereoisomers of the [2 + 2] head-to-tail cyclobutane dimer was observed in all of the seven SCSC experiments. This stereospecificity is because topochemical reaction normally proceeds with minimum movement of atoms. Stereoregularity is an essential property of polymers with stereocenters that directly affects the performance of the polymeric materials. Stereoregular polymers normally have many mechanical properties that are better than those of corresponding nonstereoregular polymers.[152]

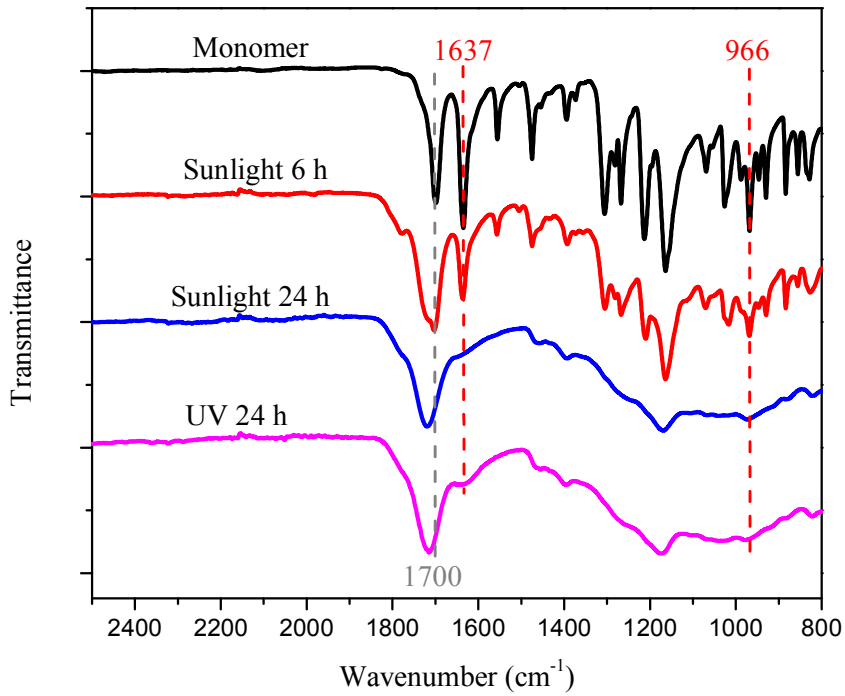

Figure 17. The photopolymerization of monomer **8**: FT-IR spectra show that the photoreaction was completed in 24 h under sunlight and UV irradiation.

The photopolymerization process was monitored by using FT-IR spectroscopy (Figure 17). The changes in FT-IR spectra shows the complete consumption of exocyclic C=C bonds, which is consistent with the formation of polyester **8P**. The IR spectra of monomer **8** exhibited a strong band at 1700 cm^{-1} attributed to the stretching mode of the carbonyl groups. A new band appeared after irradiation, which indicated that the chemical environment of carbonyl groups was changing due to the de-conjugation (Scheme 3). The carbonyl band shifted from 1700 to 1723 cm^{-1} after 24 h irradiation, which signaled the completion of the photoreaction. The accomplishment of the photopolymerization was also confirmed by the disappearance of bands at 1637 cm^{-1} and 966 cm^{-1} associated with the

stretching of the exocyclic C=C double bond and the out-of-plane twisting vibration of the C-H single bonds in the *trans*-CH=CH unit, respectively. If a noteworthy amount of cross-linking had occurred (the [2 + 2] side photoreaction between monomers with different colors), a peak for the unreacted exocyclic C=C bond would have remained in the IR spectra after the completion of the photoreaction.[52]

The UV-Vis spectrum of monomer **8** showed that a broad absorption range from 250 to 370 nm in the solid state. The results of FT-IR spectroscopy indicate that the photopolymerization processes by sunlight and ultraviolet lamps were nearly identical (Figure 17). The photoreaction was so effective that even the small fraction of UV irradiation present in sunlight was sufficient to complete the reaction.

Polyester **8P** was found to be insoluble in common organic solvents (e.g., acetone, acetonitrile, ethyl acetate, toluene, DMF and DMSO) and acidic conditions (e.g., conc. HCl or 1M TFA), but decomposed in conc. aq. KOH solution. TGA of polyester **8P** showed nearly no weight loss below 150 ^{o}C. When the polymeric product was sonicated in water, nanofiber was observed under transmission electron microscopy (TEM, Figure 18).

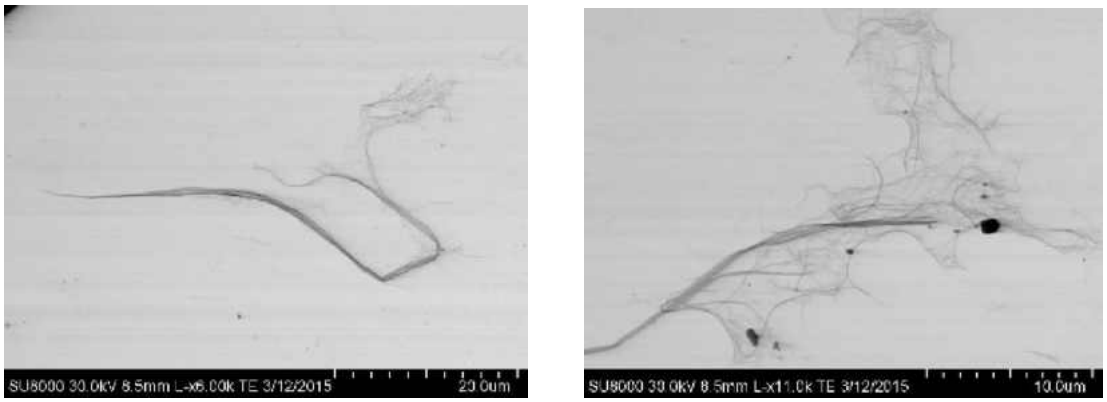

Figure 18. TEM images of the linear polyester **8P** after exfoliation.

Similar to the design of PET, the novel polyester **8P** contains alternating rigid (the cyclobutane with two aromatic substituents) and flexible (the linear aliphatic linker) moieties in the polyester chain. Considering that the species $HO(CH_2)_nOH$ (n = 2-4) can also be produced from biomass[129] and are commercially available, there is an opportunity to further tune the properties of the 100% bio-based polyesters according to future academic study or industrial production requirements. The scope of this topochemical photoreaction and the properties of the novel bio-based linear polyesters are currently under investigation.

3.4. Conclusion

A novel linear polyester was successfully synthesized from a furfural-based monomer through solvent-free photoreaction using sunlight or a UV lamp. The locally confined topochemicial polymerization process avoided cross-linking. The single crystal X-ray structures of the key photoreactive assembly and partially polymerized intermediate proved that the monomers underwent stereoregular [2 + 2] photopolymerization in the solid state. The newly formed four-membered cyclobutane rings connected monomers in one direction that resulted in the linear polyester. FT-IR spectra confirmed the completion of the polymerization and showed sunlight was an efficient light source for the photoreaction. The polyester was formed from 100% biomass-derived chemicals via a green chemistry approach and showed promising chemical and thermal stability. The balance between the rigid and flexible moieties in the polyester chain may be fine-tuned using other commercially available bio-based diols. This research opens a new means for the construction of novel biobased polyesters from furfural and its derivatives.

CHAPTER IV

SYNTHESIS OF TWO-DIMENSIONAL POLYMERS BY TOPOCHEMICAL PHOTOPOLYMERIZATION

4.1. Introduction

The synthesis of new materials is an essential element in the advancement of modern science and technology. The emerging two-dimensional (2D) polymers are valuable synthetic targets for their potential applications ranging from membranes to optics.[153-161] 2D polymers are regarded as potential synthetic analogs of graphene. Carbon fiber represents one of the most influential and practical applications of graphene sheets. Because of the exceptional tensile strength, high stability, and light weight of graphene sheets, carbon fiber has been used in aerospace, automobile, sporting goods, and civil engineering applications.[162,163] However, the precise introduction of organic functional groups at the atomic level to tune the properties of graphene is difficult due to the harsh conditions in preparing graphene.[164] Distinct from graphene, a 2D polymer prepared by organic synthesis offers more flexibility in structural tailoring and opportunity for atomic level structure-property investigations.

Although there are several reports on preparing 2D polymers and discussing the possibilities of using them as porous materials and optics,[155-161] their potentials to serve as Strong and Lightweight Materials (SLIM) have not been fully realized. In our efforts to synthesize SLIM, we have recently achieved polymeric ladders from two-armed symmetric

monomers via topochemical polymerization.[54] Expanding this approach to the next level, we report herein the synthesis and characterization of a stereoregular 2D polymer from four-armed symmetric monomers. To construct ladder and 2D polymers, monomers with multiple reactive centers are needed. In classic solution phase polymerization, the potential for cross-linking between the monomers poses a challenge. We have been exploring one aspect of this challenge by pre-organizing the monomers with multiple reactive centers using weak intermolecular forces under mild conditions before the photopolymerization.[54,143, 144]

2D polymers are theorized to be stronger than traditional polymers because each monomer is connected with its neighbors by multiple covalent bonds in an organized way. Moreover, solid-state polymerization offers a unique opportunity to synthesize macromolecules with regio- and stereo-specificity because topochemical reaction normally proceeds with minimum movement of atoms.[165-169] Stereoregularity is an important property of polymers with chiral centers that directly determines the performance of the polymeric materials. Stereoregular polymers often have an array of mechanical properties that are superior to those of corresponding non-stereoregular polymers.[152] However, it is challenging to unambiguously characterize the structure of 2D polymer, especially its stereochemistry. The novel stereoregular 2D polyester in this article was achieved by the photo-curing of a crystalline intermediate and fully characterized by FT-IR spectroscopy, solid state NMR, and the product of polymer hydrolysis.

4.2. Experimental Section

4.2.1. General Methods

All the reagents were purchased from Alfa Aesar, Sigma-Aldrich and used without further purification. Thin layer chromatography (TLC) was performed on silica gel W/UV 200 μm pre-coated plates. The light sources used for the photopolymerization were sunlight, a Hanovia medium pressure mercury lamp (PC 451050, 450 W), or sixteen RPR-3500A lamps in a Rayonet Photochemical Reactor. The solution phase nuclear magnetic resonance (NMR) spectra were recorded with Bruker AVANCE 500 MHz NMR Spectrometer (^{1}H: 500 MHz, ^{13}C: 125 MHz). All spectra were obtained in deuterium dimethyl sulfoxide (DMSO-d_6) or deuterium oxide (D_2O). For DMSO-d_6 or D_2O solution, the chemical shifts were reported as parts per million (ppm) with tetramethylsilane as a standard. Coupling constants were reported in Hertz (Hz). Data for ^{1}H NMR spectra were reported as follows: chemical shift (ppm: referenced to parts per million), brs = broad singlet, s = singlet, d = doublet, t = triplet, q = quartet, dd = doublet of doublets, dt = doublet of triplets, ddd = doublet of doublet of doublets, p = pentet, h = heptet, m = multiplet, coupling constant (Hz), and integration. Single crystal X-ray data were recorded on Bruker Kappa Apex II Duo X-Ray Diffractometer with Mo *K*α (λ = 0.71073 Å) or Cu *K*α (λ = 1.54178 Å). Melting points were measured on a MEL-TEMP device without correction. Infrared (IR) spectroscopy was recorded on Thermo Scientific Nicolet iS5 FT-IR spectrometer. The mass spectrometric analyses were performed using a high-resolution time of flight G1969A with electrospray (atmospheric pressure chemical) ionization (Agilent, Santa Clara, CA, USA) and reported as m/z (relative intensity). Accurate masses are reported for the molecular ion $[M+Na]^+$, $[M+H]^+$, $[M+NH_4]^+$, or $[M]^+$. X-ray Powder Diffraction (XRD) was performed on a X'PERT-PRO X-ray diffractometer (PANalytical, Netherlands) equipped with a 3 KW copper tube X-ray generator of λ = 0.1541 nm under

40 mA and 45 KV. Spectra were collected at room temperature in a 2θ range of 3°~35° at a scanning rate of 3°/min. Differential scanning calorimetry (DSC) was recorded with Perkin Elmer Jade DSC with a ramping rate of 10 ^{o}C/min under nitrogen protection. Heat flow was recorded from both the first heating and cooling curve. Thermogravimetric analysis (TGA) was recorded with TA instrument SDT Q600 at a ramping rate 20 ^{o}C/min under nitrogen protection. Mass spectra were performed on the instrument of Waters SYNAPT G2Si. Scanning electron microscope (SEM) and transmission electron microscopy (TEM) were recorded with Hitachi SU8010 UHR Cold-Emission FE-SEM. Copper Grids are FCF200-Cu-50 (Formvar Carbon Film on 200 Square Mesh Copper Grids) and CF213-25 (C-Flat 1.2 Micron Hole 2 μm Space 200 Mesh). Silicon wafer chips were purchased from West Chester (Silicon Wafer Chip 5×7 mm, PK/186).

4.2.2. Synthesis of Monomer **16**

Cinnamic acid (**14**) (988 mg, 6.6 mmol), 1,2,4,5-tetrakis(bromomethyl)benzene (**15**) (500 mg, 1.1 mmol), and K_2CO_3 (921 mg, 6.6 mmol) or Na_2CO_3 (700 mg, 6.6 mmol) were added to dimethyl sulfoxide (50 mL). The mixture was stirred at room temperature for 16 hours. TLC showed the reaction was completed. Then the mixture was slowly poured into ice water (300 mL). The precipitate was filtered and washed with ethanol (50 mL × 2) to give product (2*E*,2'*E*,2"*E*,2'''*E*)-benzene-1,2,4,5-tetrayltetrakis(methylene)tetrakis (3-phenylacrylate) (**16**) (670 mg, 84%) as a white solid. M.p.: 188-189 °C; TLC (hexanes : ethyl acetate, 3:1 v/v): R_f = 0.54; ^{1}H NMR (500 MHz, DMSO-d_6): δ 7.62-7.68 (m, 14H), 7.31-7.40 (m, 12H), 6.64 (d, J = 20 Hz, 4H), 5.38 (s, 8H); ^{13}C NMR (125 MHz, DMSO-d_6): δ 166.2 (4C), 145.4 (4CH), 135.5 (4C), 134.2 (4CH), 131.7 (4C), 130.9 (4CH), 129.2

(4CH), 128.7 (2CH), 117.9 (4CH), 63.5 (4CH_2); IR: 1707, 1635, 1575, 1495, 979 cm^{-1}; UV/Vis: λ_{max} 275 nm; HRMS (m/z): $[M+Na]^+$ calcd. for $C_{46}H_{38}O_8Na$, 741.24643; found 741.23698.

4.2.3. Synthesis of Monomer **20**

Malonic acid (**2**) (10.0 g, 96.1 mmol) was added slowly to solvent pyridine (40 mL). The mixture was stirred at 45 ºC until a colorless solution was obtained. 12.7 g (96.1 mmol) of *trans*-cinnamaldehyde was added to the solution at 60 ºC and stirred for 10 min. Another 12.7 g (96.1 mmol) of *trans*-cinnamaldehyde (**18**) was added slowly to the solution and the solution was allowed to be heated at 80 ºC for 14 hours. The reaction mixture was poured into ice and HCl solution. The precipitate was filtered to give the crude product. Then the crude product was dissolved in EtOAc (500 mL) and washed with brine (300 mL). The organic layer was dried to give desired product (2*E*,4*E*)-5-phenylpenta-2,4-dienoic acid (**19**) (15.1 g, 91%) as a white solid. ^{1}H NMR (DMSO-d_6, 500 MHz): δ 6.01 (d, J = 15 Hz, 1H), 7.02 (m, 2H), 7.30 (m, 4 H), 7.54 (d, J = 10 Hz, 2 H), 12.26 (s, 1H). ^{13}C NMR (DMSO-d_6, 125 MHz): δ 167.9 (C), 144.6 (CH), 140.1 (CH), 136.3 (C), 129.3 (CH), 129.2 (CH), 127.5 (CH), 126.9 (CH), 122.6 (CH).

The (2*E*,4*E*)-5-phenylpenta-2,4-dienoic acid (compound **19**, 3.8 g, 21.8 mmol), 1,2,4,5-tetrakis(bromo-methyl)benzene (2.0 g, 4.4 mmol) and CsF (4.0 g, 26.7 mmol) were added to DMSO (100 mL). The mixture was heated to 165 ºC with stirring for 5 hours. A clear and light yellow solution was obtained. TLC showed the starting material 1,2,4,5-tetrakis(bromo-methyl)benzene had disappeared. Then the mixture was poured into ice-water (300 mL) and filtered to give the crude product as a yellow solid. The crude product was washed with EtOAc (100 mL) to give the desired product

(2*E*,2'*E*,2"*E*,2'"*E*,4*E*,4'*E*,4"*E*,4'"*E*)-benzene-1,2,4,5-tetrayltetrakis (methylene)tetrakis(5-phenylpenta-2,4-dienoate) (**20**) (3.3 g, 90%) as a white solid. M.p.: 204-205 °C; ^{1}H NMR (500 MHz, DMSO-d_6): δ 7.61 (s, 2H), 7.45-7.46 (m, 12H), 7.31-7.32 (m, 12H), 7.09 (s, 8H), 6.14 (d, J = 15 Hz, 4H), 5.31 (s, 8H); ^{13}C NMR (125 MHz, DMSO-d_6): δ 166.1 (4C), 145.7 (4CH), 141.3 (4CH), 136.1 (4C), 135.5 (4C), 129.5 (2CH), 129.2 (4CH), 129.2 (4CH), 127.6 (4CH), 126.6 (4CH), 120.8 (4CH), 63.3 (4CH_2); IR: 1704, 1628, 1594, 1448 cm^{-1}; UV/Vis: λ_{max} 307 nm; HRMS (m/z): $[M+Na]^+$ calcd. for $C_{54}H_{46}O_8Na$, 845.30904; found 845.30905.

4.2.4. Crystallization

The crystals of **16** were obtained in ethyl acetate. The monomer **16** (20 mg) was added to solvent ethyl acetate (200 mL). The vial of the suspended mixture was put in an ultrasonic cleaner (Bransonic® Models 1200) for 1 hour at 57 ºC. The mixture was filtered into a 250 mL Erlenmeyer flask with filter paper. The flask was put on the heating plate without cover at 55 ºC until the solution evaporated to 20 ml. The rest of the solution was transferred into a 20 mL vial. The vial was kept at 55 ºC until the crystals formed.

A photo-stable crystal form of the monomer **16** was also discovered during the solvent screening. This photo-stable form was found in DMF by using pure compound **16** after column chromatography while the photo-reactive form was obtained in ethyl acetate with crude monomer direct from synthesis without further purification. The crystal **20** was obtained from DMF at 100 ºC. No polymorphism has been observed for monomer **20** so far.

4.2.5. Photopolymerization

Method A, sunlight irradiation: Monomer **16** were irradiated in sunlight on a transparent glass slide. 10 mg of ground crystals were evenly scattered on a glass slide and the sample was placed outdoors for photoreaction. The process of photoreaction was monitored by FT-IR. The photoreaction of monomer **16** was found to be completed after 24 hours, which was carried out in 2 days with 12 hours solar radiation per day. The product **16P** of photoreaction was obtained and it was found to be insoluble in normal organic solvents.

Method B, UV irradiation: A transparent glass slide which held 10 mg of monomer **16** was placed in a photochemical reactor. The photochemical reactor was equipped with a Hanovia medium pressure mercury lamp (PC 451050, 450 W) or sixteen RPR-3500A lamps. The polymerization reaction was monitored by FT-IR and completed in 24 hours.

4.2.6. Solid-State NMR

The solid state ^{13}C NMR spectra were recorded on a 500MHz Bruker Avance III spectrometer. ^{13}C cross polarization (CP) magic angle spinning (MAS) spectra were recorded at a sample rotation rate of 12.5 kHz using total spinning sideband suppression sequence (TOSS).[170] Monomer **16** required a recycle delay of 30s. 243 transients were accumulated with a total experiment time of approximately 2 hours and 2 minutes. Polymer **16P** required a recycle delay of 3s. 2187 transients were accumulated with a total experiment time of approximately 3 hours and 16 minutes. Monomer **20** shows high crystallinity yet relatively short relaxation rates on ^{1}H. The monomer **20** and polymer **20P** do not have significantly different ^{1}H relaxation behavior.

4.2.7. Hydrolysis

The polymer **16P** (100 mg) was added to a solution of KOH (50%, 100 mL). The mixture was heated to 100 ºC for 16 hours. After cooling to room temperature, the mixture was diluted with water (100 mL) and adjusted pH to 2 with concentrated HCl. The aqueous solution was extracted with ethyl acetate (100 mL × 3). The combined organic layers were dried over sodium sulfate and concentrated. The residue was purified by column chromatography eluted with ethyl acetate and hexane (20 : 1) to give pure α-truxillic acid (60 mg, yield: 74%) as a white solid. 10 mg of the isolated α-truxillic acid was recrystallized in ethanol. The single crystal X-ray structure is disordered and consistent with the reported crystal data of α-truxillic acid (**17**).[171] M.p.: 276-277 ºC (lit.[172, 173] 274-278 ºC); ^{1}H NMR (500 MHz, DMSO-d_6): δ 12.13 (s, 2H), 7.32-7.37 (m, 8H), 7.24-7.25 (m, 2H), 4.28 (dd, J = 10 Hz, 10 Hz, 2H), 3.81 (dd, J = 10 Hz, 10 Hz, 2H); ^{13}C NMR (125MHz, DMSO-d_6): δ 173.01, 139.49, 128.20, 127.68, 126.71, 46.18, 41.06. NMR data are consistent with the reported values.[174, 175]

A 2-aminoethanaminium salt of the above isolated α-truxillic acid was obtained, in which the α-truxillic acid anions showed no disorder. In this experiment, 10 mg of α-truxillic acid was dissolved in 3 mL of methanol. To the solution was added 0.2 mL of ethylenediamine. The mixture was kept at room temperature until the crystals (**17a**) were formed. M.p.: 230-231 ºC. ^{1}H NMR (500 MHz, D_2O): δ 7.35 (m, 8H), 7.23-7.26 (m, 2H), 4.18 (dd, J = 7.5 Hz, 7.5 Hz, 2H), 3.70 (dd, J = 7.5 Hz, 7.5 Hz, 2H), 2.91 (s, 8H); ^{13}C NMR (125MHz, D_2O): δ 181.06, 141.88, 128.77, 127.90, 126.81, 49.86, 42.93, 39.96.

4.2.8. Exfoliation

After the photoreaction of crystals **16** (1 mg), the polymer **16P** was added into a mixture of DMF (dimethylformamide) and water (5:95, 10 mL). The suspension was heated to 100 ^{o}C for 4 days without stirring. The exfoliation process was monitored by SEM and TEM. One drop of the suspension was placed on copper grids and observed by electronic microscopy after evaporation of the solvent.

4.3. Results and Discussions

In the study, monomer **16** was synthesized in 84% yield by linking four cinnamic acid molecules together with 1,2,4,5-tetrakis(bromomethyl)benzene (**15**) via nucleophilic substitution as shown in Scheme 4. The monomer powder **16** polymerized under sunlight within 24 hours in quantitative yield. To understand the solid-state polymerization, we prepared single crystals of the four-armed symmetric monomer **16** suitable for X-ray diffraction analysis from ethyl acetate.[176] Without further processing, the powder XRD pattern of the synthesized monomer **16** was nearly identical to that of the ground single crystals confirming that the powder is microcrystalline. The powder XRD results showed that the crystal structure of the monomer **16** was suitable to analyze and interpret the solid state polymerization of both the crystals and powder. The monomers stacked along the crystallographic *a* axis with a repeating distance of 5.8 Å, which was too far for the C=C bonds to react with each other along this stacking direction in the solid-state (Figure 19b). Meanwhile, the X-ray structure also revealed the intramolecular [2 + 2] cycloaddition to be unfavorable because the two pairs of C=C bonds are not paralleled and are separated from each other more than 4.2 Å (Figure 19a), which is

the minimum viable distance for the [2 + 2] photoreaction in the solid state.[42, 177-180] Nevertheless, the crystal structure completed a two-dimensional assembly based on π-π interactions of the conjugated arms between the nearest monomers in the crystallographic *bc* plane.[181-186] The four reactive C=C bonds in each monomer were all parallel to the double bonds in the closest four adjacent monomers, respectively. The distances between the reactive sp^2 hybridized carbons in the neighboring monomers were approximately 3.9 Å (Figure 19c). In the presence of light, the [2 + 2] cycloaddition locked the two-dimensional assembly into a covalently bonded two-dimensional polymer.[187-189]

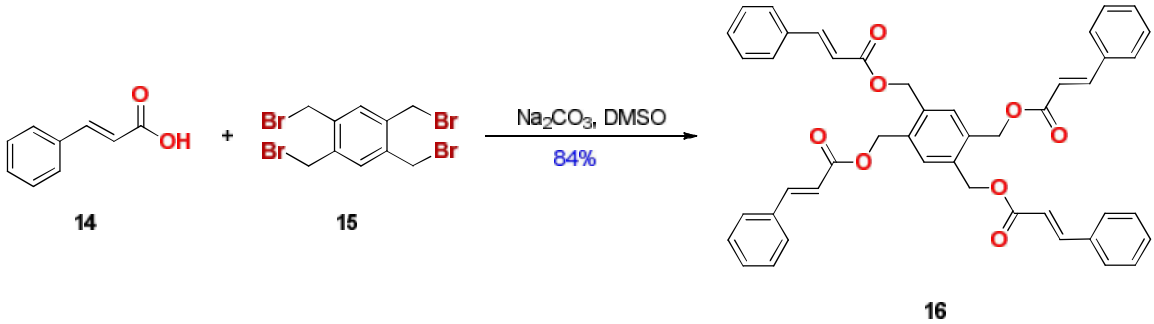

Scheme 4. The synthesis of monomer **16** from cinnamic acid (**14**) and 1,2,4,5-tetrakis(bromomethyl)benzene (**15**).

The sunlight polymerization process was monitored with respect to time using FT-IR spectroscopy. The IR spectra in Figure 20a show that the characteristic absorption peak of C=O stretching at 1708 cm^{-1} shifted to 1726 cm^{-1} in 24 hours due to the de-conjugation of the carbonyl group. The disappearance of C=C stretching (1637 cm^{-1}) and the out-of-plane twisting vibration of the carbon-hydrogen single bonds in the *trans*-CH=CH (980 cm^{-1}) after the reaction were consistent with completion of the [2 + 2] photopolymerization.

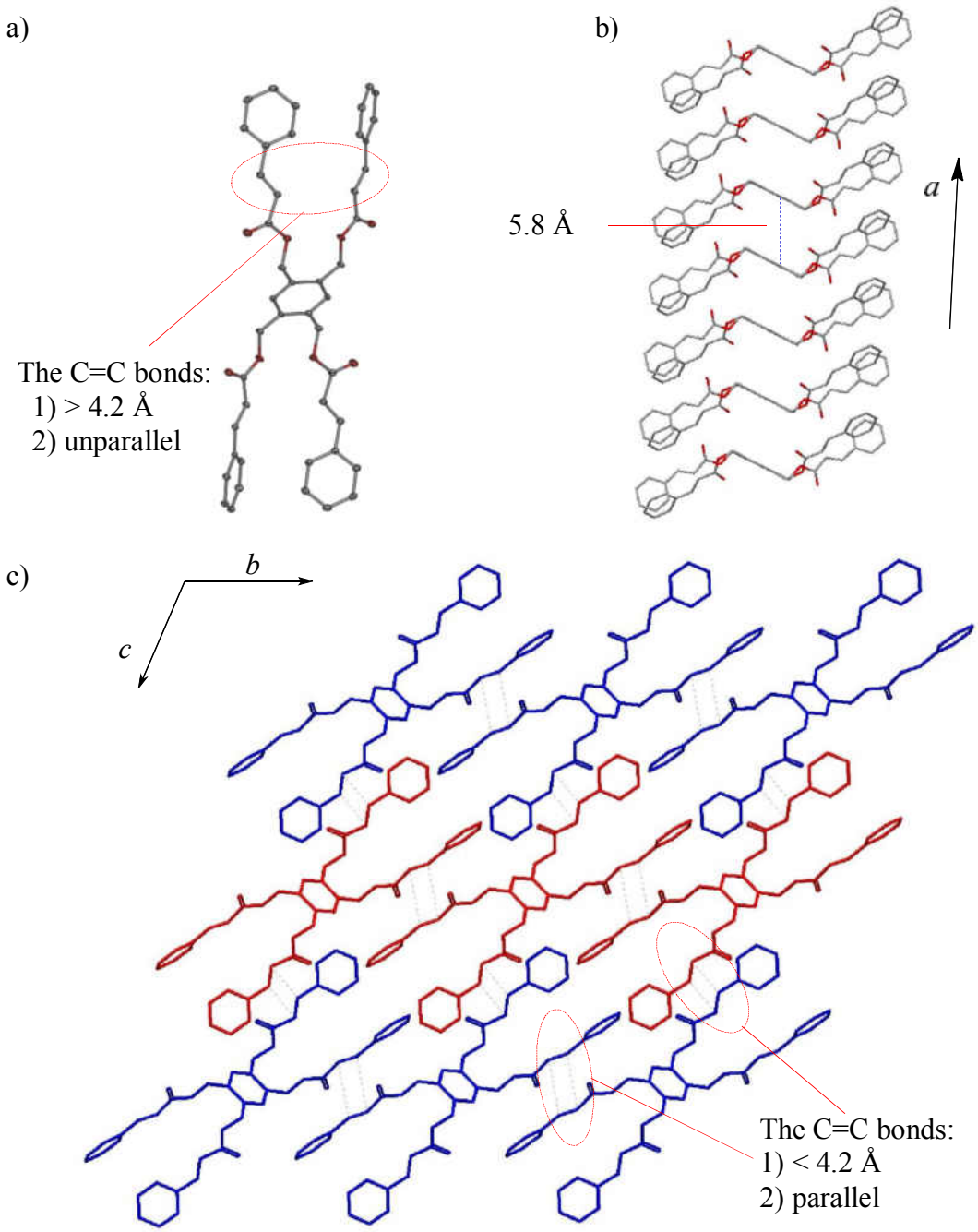

Figure 19. X-ray single crystal structure of monomer **16** (hydrogen atoms are omitted for clarity): a) Oak Ridge Thermal Ellipsoid Plot (ORTEP) representation at 50% electron density of the monomer crystal structure showing the intramolecular [2 + 2] cycloaddition is unfavorable; b) monomers stacking along the crystallographic *a* axis showing the C=C bonds are too far from each other to react in this direction; c) 2D assembly of the monomers in the crystallographic *bc* plane showing the intermolecular [2 + 2] polymerization is favorable (the dotted lines showing where the new C-C bonds form). Reprinted with permission from (Wang, Z.; et al., *Macromolecules* **2015**, *48* (9), 2894-2900.). Copyright (2015) American Chemical Society.

The polymer was also successfully obtained through UV irradiation. The UV-Vis spectra show that monomer **16** absorbed irradiation at values of 240-310 nm in an acetonitrile solution and at values of 240-325 nm in the solid state. When an optical filter was used to remove the irradiation below 380 nm of a mercury lamp, no reaction was observed for monomer **16** in 24 hours. Thus, the photopolymerization in the solid state is highly efficient because the low concentration of UV irradiation present in sunlight was enough to complete the reaction. The IR spectra of polymers obtained from the two different light sources were nearly identical (Figure 20).

Although 2D polymers are interesting synthetic targets and have great potential for applications,[153-161] the discovery and development of the 2D polymer have lagged behind other classic polymers, such as linear and cross-linked polymers. One persistent challenge is the characterization of 2D polymers due to poor solubility. In this study, a comparison of the solid-state ^{13}C-NMR spectra of the monomer **16** and polymer **16P** confirmed the formation of the 2D polymer in the crystalline solid by showing the disappearance of two olefin peaks at 118 and 146 ppm concurrent with the appearance of peaks from cyclobutane around 44 ppm (the three key peaks are marked with red stars in Figure 20b). The spectrum of polymer **16P** looks rather amorphous compared to the sharper resonances of the monomer.

a)

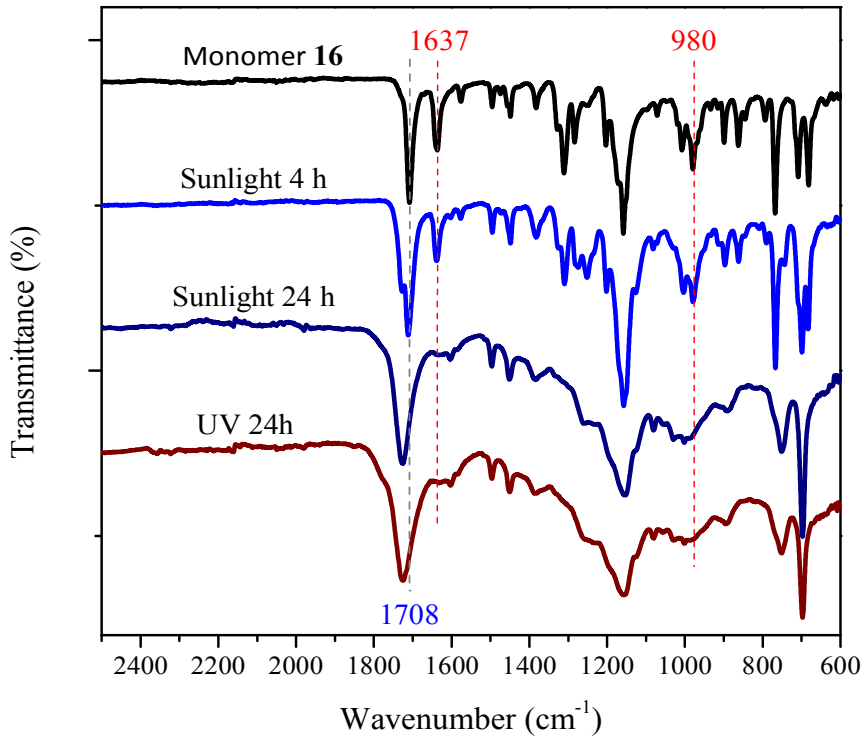

b)

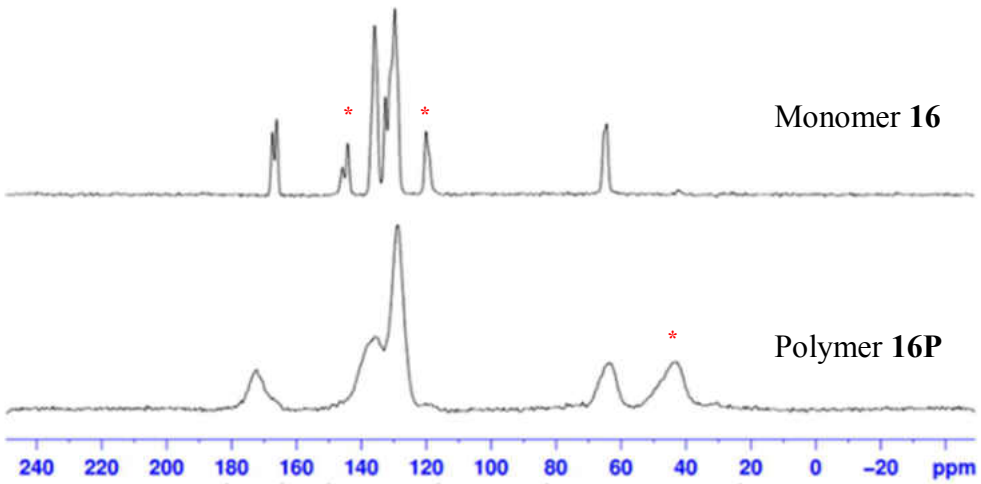

Figure 20. a) FT-IR spectra showing the [2 + 2] photopolymerization completed by using sunlight or UV irradiation. b) Solid-state ^{13}C-NMR spectra of the monomer **16** and polymer **16P**. Reprinted with permission from Wang, Z.; et al., *Macromolecules* **2015**, *48* (9), 2894-2900. Copyright (2015) American Chemical Society.

a)

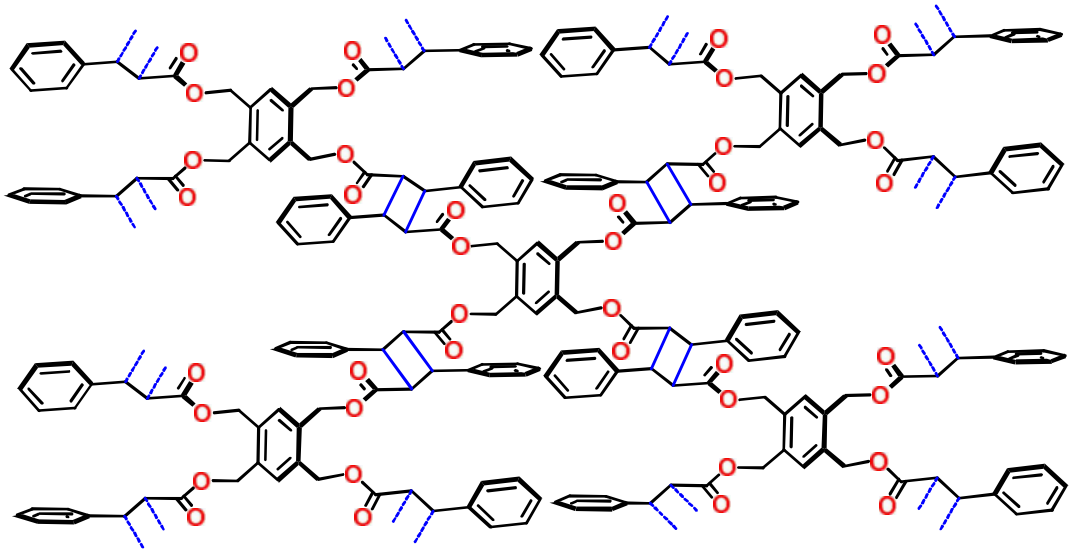

16P

b)

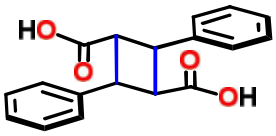

17

c)

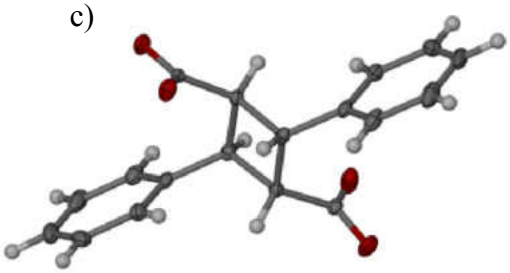

Figure 21. The newly formed C-C single bonds are shown by the α-truxillic acid from hydrolysis of the 2D polyester: a) the chemical structure of 2D polyester **16P** (newly formed bonds are in blue and only five repeating units are shown for simplicity); b) the chemical structure of α-truxillic acid **17**; c) ORTEP representation of the isolated α-truxillic acid salt crystal structure. (Ellipsoids displayed at 50% probability and aminium cations are omitted for clarity.)

Given the ester structure of the 2D polymer, hydrolysis offers another facile way to confirm the macromolecular structure (Figure 21a). The conversion of the hydrolysis reaction was nearly 100%. No undimerized cinnamic acid was observed in the hydrolysis process, which confirmed the completion of polymerization. The

α-truxillic acid (head-to-tail dimer of cinnamic acid shown in Figure 21b, c was isolated as a polymer hydrolysis product in 72% yield after column chromatography that directly revealed the newly formed C-C bonds (shown in blue).[171, 190, 191] The results of hydrolysis unequivocally confirmed the polymerization and displayed excellent stereoregularity of the [2 + 2] photopolymerization because only one of the five possible stereoisomers of truxillic acid was observed (Figure 21). Meanwhile, the absence of β-truxinic acid (head-to-head dimer[192]) illustrated that intramolecular [2 + 2] cycloaddition did not occur.The eight carbon-carbon single bonds that each monomer formed with its four adjacent neighbors all resulted in chiral centers. All the chiral centers were generated stereospecifically since the monomer of this topochemical polymerization can only react with the neighboring monomer in a pre-organized way (Figure 20 and 21).[165-169]

Different chemical and physical properties of the 2D stereoregular polymer were studied. Polymer **16P** was insoluble in common organic solvents such as MeOH, CH_3CN, Toluene, $CHCl_3$ and DMSO. It tolerated bases (e.g., Et_3N and NaOH) and acids (e.g., 1 M HCl and TFA) at room temperature. However, it was degradable in aqueous potassium hydroxide at 100 ^{o}C and was oxidized by concentrated sulfuric acid.

a)

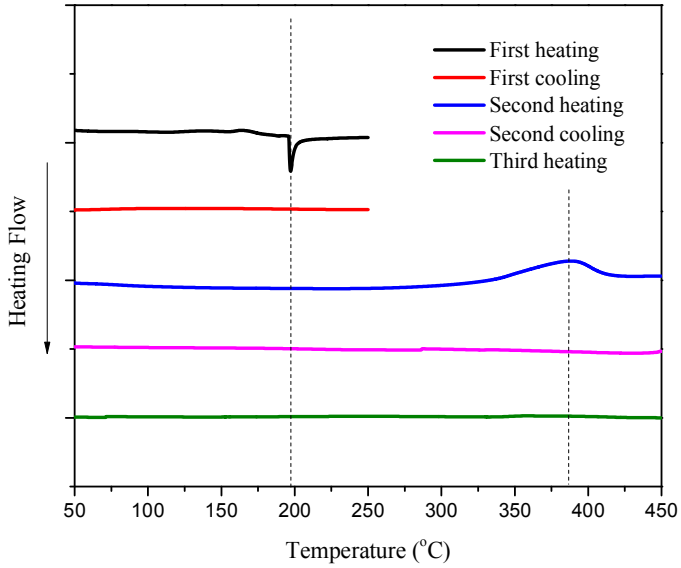

b)

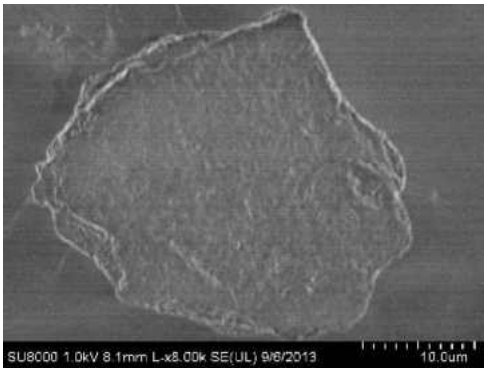

c)

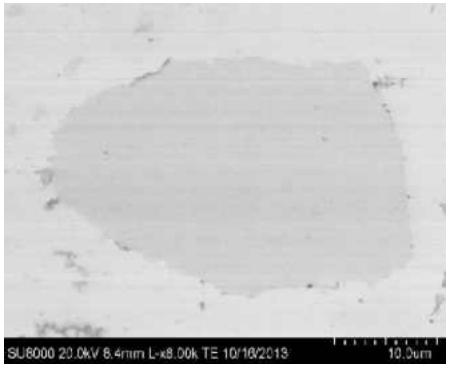

d)

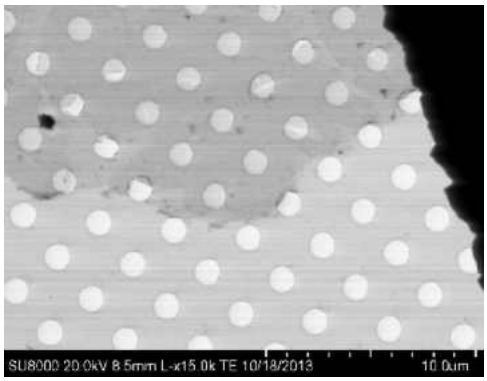

e)

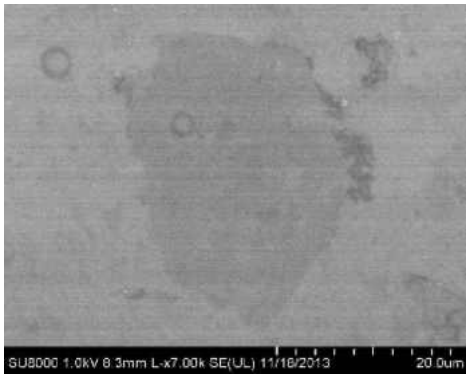

Figure 22. a) DSC of polymer **16P** was operated under nitrogen (20 mL/min) with rate 10 ºC/min; b) SEM image of a multi-layered material of **16P**; c) SEM image of an ultra-thin polymeric sheet of **16P** obtained by exfoliation; d) TEM images of an ultra-thin polymeric sheet with cracks and holes after exfoliation; e) TEM images of an ultra-thin polymeric sheet obtained by exfoliation.

The thermogravimetric analysis of the 2D polymer showed a slight weight loss around 200 ºC. The differential scanning calorimetry curve (DSC, Figure 22a) of polymer **16P** showed an endothermic peak near 200 ºC, but the 2D polymer did not melt even when heated at 350 ºC. This endothermic peak disappeared during the sequential heating cycles, which might indicate an annealing process. The heat released tension built within the 2D polymer structure during the photopolymerization reaction due to the restricted movement of atoms in the solid state.

Since there are only weak interactions between the polymeric layers,[181-186,193, 194] the 2D polymers were exfoliated into extremely thin sheets by heating in a DMF/H_2O (5 : 95) solution at 100 ºC. The scanning electron microscope (SEM) and transmission electron microscopy (TEM) images of a multilayered crystal before exfoliation and ultrathin sheets after exfoliation are shown in Figure 22b-e. A deepened exploration of this novel polymer may expose innovative properties and subsequent possibilities.[153, 154, 195]

We also investigated a similar monomer capable of 2D polymerization. Indeed, generality is a challenge in solid-state synthesis because topochemicial reactions are often sensitive to small structural changes,[196, 197] so judicious design and tests are necessary. With this in mind, the monomer **20** with two conjugated C=C bonds on each of the four arms was synthesized from a cinnamic aldehyde, malonic acid and the same tetrabromo-linker in three steps with 81% overall yield (Scheme 5).

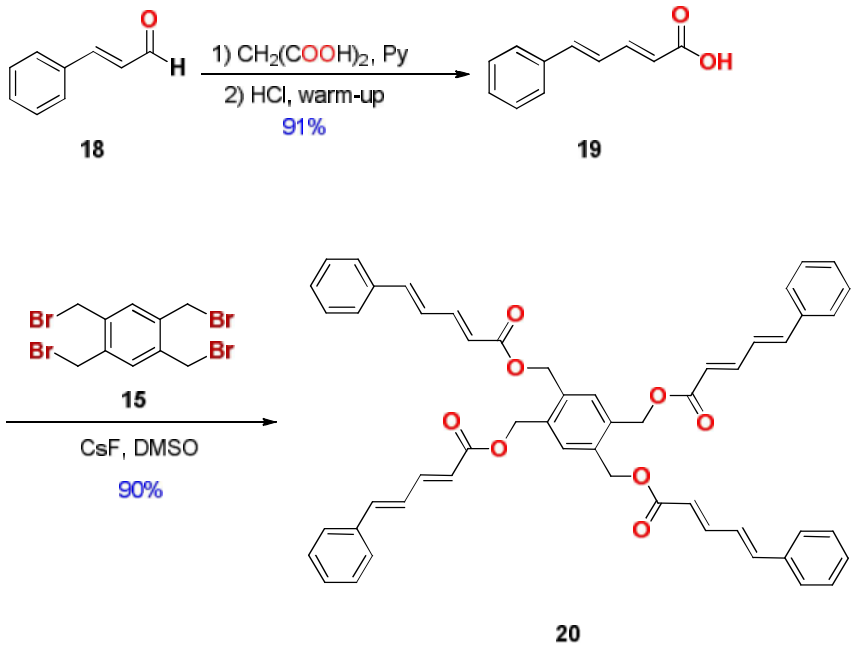

Scheme 5. The synthesis of monomer **20** from a cinnamic aldehyde, malonic acid and 1,2,4,5-tetrakis(bromomethyl)benzene.

The crystal structure of monomer **20** adopted a conformation and packing very similar to those of monomer **16** (Figure 23). The monomer **20** also stack along the crystallographic *a* axis with a repeating distance of 5.8 Å, which is too far for the conjugated C=C bonds to react with each other by 1,4-polymerization in the solid state.[12,198] However, the crystals of compound **20** were photoreactive as well and polymerized readily in 24 hours upon exposure to UV or sunlight. Interestingly, both the IR and solid state ^{13}C NMR spectra showed that there was still a small portion of the olefins that remained untouched after the polymerization stopped although all of the C=C double bonds were pre-organized in such way that each bond could be photodimerized (Figure 23c).

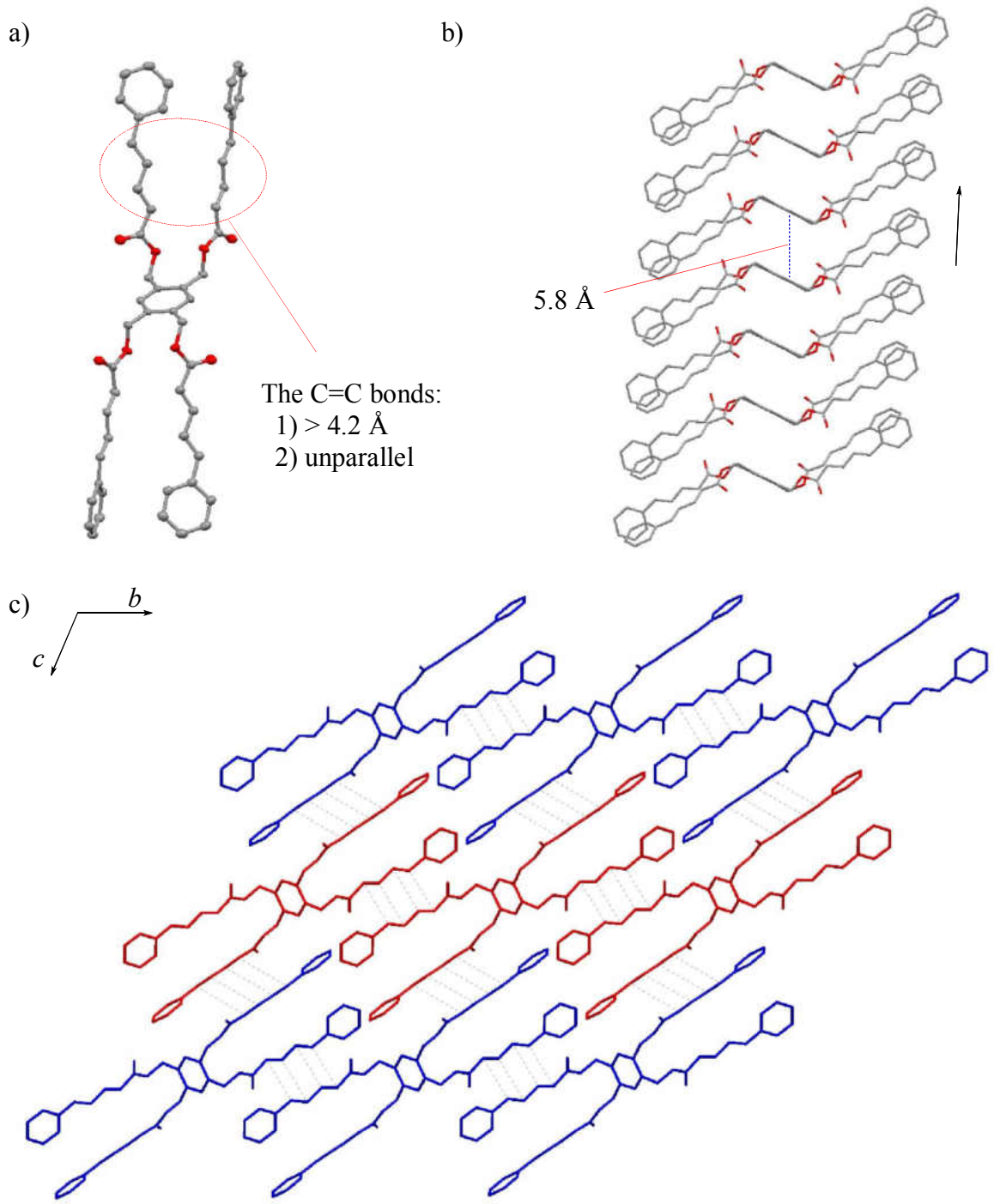

Figure 23. X-ray single crystal structure of the monomer **20** (hydrogen atoms are omitted for clarity): a) Oak Ridge Thermal Ellipsoid Plot (ORTEP) representation at 50% electron density of the monomer crystal structure showing the intramolecular [2 + 2] cycloaddition is unfavorable; b) monomers stacking along the crystallographic *a* axis showing the C=C bonds are too far from each other to react in this direction; c) 2D assembly of the monomers in the crystallographic *bc* plane showing the intermolecular [2 + 2] polymerization is favorable (the dotted lines showing where the new C-C bonds could form).

A close examination of the crystal packing showed that there was a competing [2 + 2] dimerization for the reaction between the blue and red monomers since they were slightly offset (Figure 24, colors introduced arbitrarily for clarity in the discussion). Although the olefins were aligned for the formation of the three-ladderane linkage,[82, 88, 199-201] the two C=C bonds closer to the ester groups could also react with each other. Since the separation between the double bonds was about 0.3 Å shorter in the latter option, it was easier to react. Therefore, two C=C bonds close to the phenyl rings were left untouched. The olefins with the same colors were aligned well to form the ladderane linkage exclusively and there was no competing [2 + 2] dimerization reaction between the blue monomers or the red ones.

Thus, only two of the eight C=C double bonds in each monomer were left after the photopolymerization. This analysis of spatial approximation is consistent with the FT-IR and solid state NMR spectra of the polymeric product. The solid state NMR spectra of monomer **20** and polymer **20P** showed a remarkable amorphous broadening of all aliphatic resonances and some broadening of the CH and C=O resonances where the aromatic core shows few spectral differences after the photopolymerization. Nevertheless, a 2D polymeric matrix was formed after the photodimerization of each reactive arm on monomer **20**.

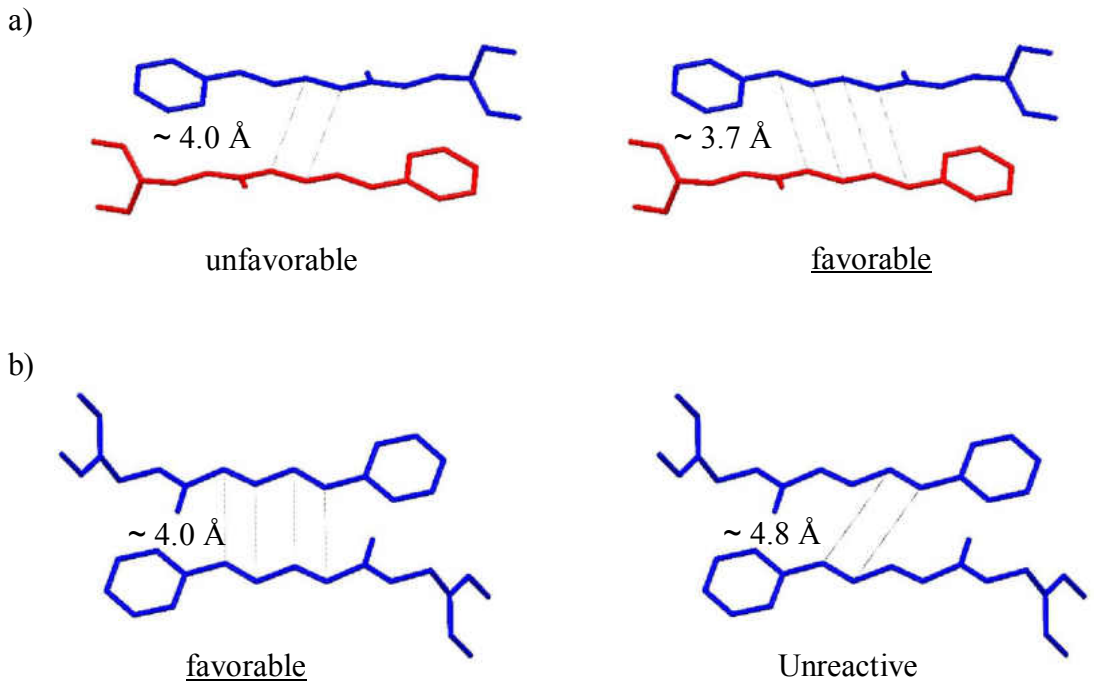

Figure 24. a) The two competing [2 + 2] dimerization reactions in the solid-state between the blue and red monomers (the dotted lines showing where the new C-C bonds could form). b) The olefins with the same colors were aligned well to form the ladderane linkage exclusively. Reprinted with permission from Wang, Z.; et al., *Macromolecules* **2015**, *48* (9), 2894-2900. Copyright (2015) American Chemical Society.

4.4. Conclusion

Stereoregular 2D polyester **16P**, which could not be easily obtained by alternative synthetic routes, was prepared by topochemical polymerization. The locally confined polymerization avoids cross-linking by pre-organizing the multiple reactive centers in the solid state.[54,143, 144,187-189] The stereoregular 2D polymer structure was unambiguously confirmed by revealing the newly formed carbon-carbon single bonds through the single crystal structure of its hydrolysis product. We have also extended the synthetic approach to another monomer with two

conjugated carbon-carbon double bonds on each of the four arms. The starting materials, reagents, and necessary preparations implemented in the experiments were inexpensive and common, showing the possibility of scaling up the facile and efficient 2D polymer synthesis. The novel stereoregular 2D polyesters have potential in a variety of applications. One can envision that the application of such strong and lightweight organic materials may usher in the next generation of fuel-efficient transportation on all scales, from aircraft to automobile.

CHAPTER V

CYCLOBUTANEDIACID-BASED MONOMERS FOR THE SYNTHESIS OF POLYCYCLOBUTANE MATERIALS

5.1. Introduction

In spite of inherent ring strain, cyclobutane units are present in a wide range of natural products.[91, 202-207] Cyclobutane derivatives can be generated in metabolisms and play a significant role in biology system.[205, 206, 208] It has also been found that cyclobutane derivatives can be precursors in drug discovery programs.[209-215] Cyclobutane ring has two conformations, planar and puckered, which bring the semi-flexible and semi-rigid properties.[216, 217] This semi-rigid structure of cyclobutane ring can be potentially functionalized, which is a feature of drug-target interaction.[218-220] In fact, this feature is also important for martial design. The derivatives of cyclobutanes have been employed as highly useful starting materials in total synthesis.[221-227]

On the other hand, diacids have been studied for a long time in material science and are widely used in modern materials.[120, 228-232] Nylon 66 is an example of a highly successful material based on the aliphatic diacid, adipic acid.[132, 233, 234] In addition to aliphatic diacids, aromatic diacids have also found applications in materials. For instance, terephthalic acid, or benzene-1,4-dicarboxylic acid, is a chemical synthesized from compounds in crude oil.[235-237] It is a key building block in polyethylene terephthalate (PET), which is widely used to make plastic beverage bottles (Figure 25).[112, 116] Growth in manufacture polyester

fiber has greatly increased the global demand for terephthalic acid, with production reaching over 47 million tons in 2012.[238-240] Meantime, scientists are trying to find a biomass-based diacid that could be used as an alternative to terephthalic acid.[241-243] The furan-based building block 2,5-furandicarboxylic acid (FDCA) is one of the prime candidates and has been named one of the top-12 value-added chemicals for "green" chemistry.[14, 15] The FDCA based polymer polyethylene 2,5-furandicarboxylate (PEF) is being considered as an alternative thermoplastic to PET.[241, 243-245]

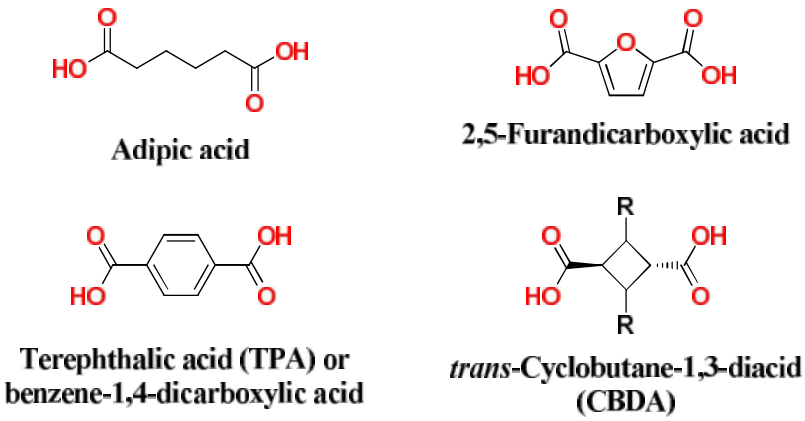

Figure 25. Building blocks for materials synthesis.

Furthermore, diacids also have played an important role in the synthesis of metal-organic frameworks (MOFs).[246-250] Omar M. Yaghi and his coworkers reported MOF-5 in 2003, in which TPA is the main backbone of the structure.[251-253] Other diacids, including oxalic, malonic, succinic, glutaric, phthalic acids have been used in MOFs as well.[247, 248, 252, 254]

Cyclobutane-1,3-diacid (**CBDA**) previously has not been widely regarded as a building block for materials synthesis, because of the concern of its stability caused by ring strain of the four-membered ring.[216, 255, 256] Compared to five- and six-membered rings, four-membered rings are indeed more unstable.[216, 255, 256] However, this relatively low stability

has been found to still be more than enough for using **CBDA** as a building block in materials. For this reason, **CBDA** has numerous possible applications in the synthesis of polymers, MOFs, and more. Herein one of the applications of this new building block is demonstrated. In our study, four polyesters were synthesized from **CBDA** and tests showed the polymers to have high thermostability.

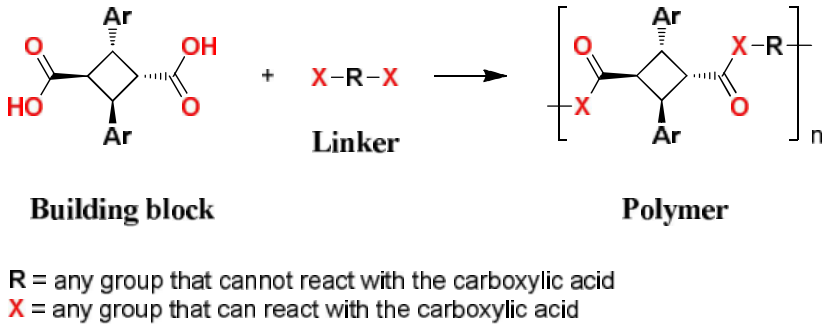

Figure 26. The strategy of using **CBDA** as a building block. Any bifunctional groups that can react with carboxylic acid can be used as a linker.

To apply *trans*-cyclobutane-1,3-dicarboxylic acid in the synthesis of polymers, a linker with bifunctional groups, capable of reacting with a carboxylic acid is necessary (Figure 26). Examples of such linkers are diols, which can be used to synthesize polyesters, and diamines, which can be used to prepare polyamides. **CBDA** with aromatic rings (furan ring, benzene ring, etc) is a good building block for polyesters. In our previous work, we have introduced furan ring as an aromatic ring to synthesize linear polyester. In this study, either *trans*-2,4-diphenyl-1,3-cyclobutanedicarboxylic acid or α-truxillic acid (**CBDA-1**) will be introduced as a building block for synthesizing polyesters via a traditional method.

5.2. Experimental Section

5.2.1. General Methods

All chemicals and reagents were purchased from MC&B Manufacturing Chemists, Alfa Aesar, Sigma-Aldrich, Matrix and Acros. The light source used for the photodimerization was sunlight or a Hanovia medium pressure mercury lamp (PC 451050, 450 W). The solution phase nuclear magnetic resonance (NMR) spectra were recorded with Bruker AVANCE 500 MHz NMR Spectrometer (^{1}H: 500 MHz, ^{13}C: 125 MHz). All spectra were obtained in deuterium dimethyl sulfoxide (DMSO-d_6), deuterium water (D_2O) or deuterium chloroform ($CDCl_3$). Infrared (IR) spectroscopy was recorded on a Thermo Scientific Nicolet iS5 FT-IR spectrometer. The mass spectrometric analyses were performed using a high-resolution time of flight G1969A with electrospray (atmospheric pressure chemical) ionization (Agilent, Santa Clara, CA, USA) and reported as m/z (relative intensity). Accurate masses are reported for the molecular ion $[M+Na]^+$, $[M+K]^+$ or $[M]^+$. Single crystal X-ray data were recorded on Bruker Kappa Apex II Duo X-Ray Diffractometer with Mo *K*α (λ = 0.71073 Å) or Cu *K*α (λ = 1.54178 Å). Melting points were measured on a MEL-TEMP device without correction. Powder X-ray Diffraction (P-XRD) was performed on an X'PERT-PRO X-ray diffractometer (PANalytical, Netherlands) equipped with a 3 KW copper tube X-ray generator of λ = 0.1541 nm under 40 mA and 45 KV. Spectra were collected at room temperature in a 2θ range of 3°~35° at a scanning rate of 3°/min. Differential scanning calorimetry (DSC) was recorded with Perkin Elmer Jade DSC with a ramping rate of 10 ºC/min under nitrogen protection. Heat flow was recorded from both the first heating and cooling curve. Thermogravimetric analysis (TGA) was performed with TA instrument SDT Q600 at a ramping rate 20 ºC/min under nitrogen

protection. MALDI was performed on the instrument of Waters SYNAPT G2Si with MALDI source.

5.2.2. Synthesis of *trans*-2,4-Diphenyl-1,3-cyclobutanedicarboxylic Acid (**CBDA-1**) (**17**) Using Solid-state Photodimerization

CBDA-1 (**17**). Commercially available *trans*-cinnamic acid (2.0 g) was scattered on a 10" × 10" glass plate. The plate was put outside in sunlight or in a photoreactor with a mercury lamp. The process of photodimerization was monitored by FT-IR which showed the completion in sunlight was 8 h and in UV was 6 h. 1.96 g of **CBDA-1** (**17**) was obtained. M.p.: 276.2-277.5 ^{o}C. ^{1}H-NMR (500 MHz, DMSO-d6): δ 12.11 (s, 2H), 7.32-7.37 (m, 8H), 7.23-7.26 (m, 2H), 4.29 (dd, J = 7.5 Hz, 10.5 Hz, 2H), 3.81 (dd, J = 7.5 Hz, 10.5 Hz, 2H); ^{13}C-NMR (125MHz, DMSO-d6): δ 173.2 (2C), 139.8 (2C), 128.5 (2CH), 127.9 (2CH), 127.0 (2CH), 46.5 (2CH), 41.4 (2CH). HRMS (m/z): $[M]^{+}$ calcd. for $C_{18}H_{16}O_4$, 296.1048; found 296.1009.

5.2.3. Crystallization

trans-Cinnamic acid (**14**): 60 mg of *trans*-cinnamic acid was added to a mixture of ethyl acetate and acetonitrile (1:1, 20 mL). The mixture was allowed to stand in the fume hood until single crystals were formed.

CBDA-1 (**17**): 10 mg of CBDA-1 was dissolved in 20 mL of ethanol. The mixture was sonicated for 30 min. The obtained clear solution was allowed to stand at room temperature without cover for three days or until the crystals were formed.

α-Truxillate-dibutylaminium (**17b**): 20 mg of CBDA-1 was dissolved in DMF (5 mL) in a 20 mL vial. To this solution was added a mixture of ethanol (5 mL), water (5 mL) and *n*-

butylamine (0.5 mL). The mixture was heated to 70 ºC with stirring for 10 mins. Crystals were obtained in around three days. ^{1}H-NMR (500 MHz, $CDCl_3$): δ 7.36-7.39 (m, 8H), 7.27-7.29 (m, 2H), 4.20 (dd, J = 7.5 Hz, 10.5 Hz, 2H), 3.72 (dd, J = 7.5 Hz, 10.5 Hz, 2H), 2.92 (t, J = 7.5 Hz, 4H), 1.55–1.61 (m, 4H), 1.32-1.38 (m, 4H), 0.89 (t, J = 7.5 Hz, 6H); ^{13}C-NMR (125MHz, DMSO-d6): δ 181.0 (2C), 141.9 (2C), 128.7 (2CH). 127.9 (2CH), 126.8 (2CH), 49.9 (2CH), 42.9 (2CH), 39.5 ($2CH_2$), 29.0 ($2CH_2$), 19.3 ($2CH_2$), 13.0 ($2CH_2$).

5.2.4. Synthesis

General method:

CBDA-1 (**17**) (1.0 g, 3 mmol), ethylene glycol (0.2 g, 3 mmol), N,N'-dicyclohexylcarbodiimide (DCC, 0.7 g, 3.6 mmol) and 4-dimethylaminopyridine (DMAP, 0.5 g, 4 mmol) were added to solvent acetonitrile (ACN, 20 mL). The mixture was stirred at room temperature for 20 h and then poured into 20 mL of chloroform. The mixture was filtered *via* column chromatography to give product poly(ethylene-α-truxillate) (PEAT, 1.0 g, 87%) as a white solid.

Poly(ethylene-α-truxillate) (PEAT) (**21P**):

MS $[M+Na]^+$: 989.3472, 1051.3832, 1311.4465, 1373.5010, 1633.5853, 1695.6365; ^{1}H-NMR (500 MHz, $CDCl_3$): δ 7.16-7.31 (m, 10H), 4.37-4.41 (m, 2H), 3.88-3.92 (m, 2H), 3.45-3.56 (m, 2H), 3.33-3.34 (m, 2H); ^{13}C-NMR (125MHz, $CDCl_3$): δ 171.4, 138.9, 130.4, 128.4, 127.4, 127.3, 66.3, 62.2, 61.7, 60.9, 46.5, 41.3, 29.7.

Poly(1,4-butylene-α-truxillate) (PBAT) (**22P**):

MS $[M+Na]^+$: 1073.4794, 1423.6332, 1513.6512, 1773.7697, 1863.8007, 2123.8440, 2213.9534; ^{1}H-NMR (500 MHz, $CDCl_3$): δ 7.20-7.33 (m, 10H), 4.41 (dd, J = 7.5 Hz, 10.5 Hz, 2H), 3.89 (dd, J = 7.5 Hz, 10.5 Hz, 2H), 3.46-3.57 (m, 4H), 0.89-0.92 (m, 4H); ^{13}C-NMR (125MHz, $CDCl_3$): δ 171.8, 138.8, 128.4, 127.5, 127.1, 63.8, 46.8, 41.4, 24.5.

Poly(1,5-pentylene-α-truxillate) (PPAT5) (**23P**):

MS $[M+Na]^+$: 1115.4766, 1219.5552, 1479.7136, 1588.7213, 1843.8148, 1947.8933, 2207.9763; ^{1}H-NMR (500 MHz, $CDCl_3$): δ 7.20-7.31 (m, 10H), 4.43 (dd, J = 7.5 Hz, 10.5 Hz, 2H), 3.93 (dd, J = 7.5 Hz, 10.5 Hz, 2H), 3.56-3.66 (m, 4H), 1.04-1.10 (m, 4H), 0.76-0.77 (m, 2H); ^{13}C-NMR (125MHz, $CDCl_3$): δ 171.9, 138.8, 128.3, 127.5, 127.1, 64.2, 46.7, 41.4, 27.7, 21.8.

Poly(1,6-hexylene-α-truxillate) (PHAT) (**24P**):

MS $[M+Na]^+$: 1157.5259, 1275.6173, 1535.7283, 1653.8168, 1913.9023, 2031.9886, 2292.0740; ^{1}H-NMR (500 MHz, $CDCl_3$): δ 7.20-7.30 (m, 10H), 4.45 (dd, J = 7.5 Hz, 10.5 Hz, 2H), 3.95 (dd, J = 7.5 Hz, 10.5 Hz, 2H), 3.68-3.72 (m, 2H), 3.59-3.62 (m, 2H), 1.13 (s, 4H), 0.88 (s, 4H); ^{13}C-NMR (125MHz, $CDCl_3$): δ 171.9, 138.8, 128.3, 127.5, 127.1, 64.4, 46.8, 41.4, 28.0, 25.2.

5.3. Results and Discussions

In this study, an example of CBDA, *trans*-2,4-diphenyl-1,3-cyclobutanedicarboxylic acid (**CBDA-1**) (**17**), will be demonstrated. Although **CBDA-1** has been observed for decades,[52, 108, 257] using **CBDA-1** as a building block has not been studied because of the relatively unstable cyclobutane ring. Whereas thermogravimetric analysis (TGA) showed **CBDA-1** can be stable at temperature 275 ^{o}C and lost 5% weight at 307 ^{o}C (Figure 27a).

The weight loss in TGA before 330 ºC may due to evaporation because **CBDA-1** will melt at around 276 ºC. **CBDA-1** lost all weight at 378 ºC. Between 307 and 378 ºC, it lost 95% weight which suggested that **CBDA-1** totally decomposed among these temperatures. DSC showed **CBDA-1** was melt before 300 ºC and started decomposing at 330 ºC in the first heating process (Figure 27b). After decomposition, DSC showed nothing changed in the first cooling and second heating processes. The DSC analysis is consistent with TGA results. TGA and DSC results indicated that **CBDA-1** is stable enough to be used in materials. Therefore, **CBDA-1** could be a broad building block for materials.

CBDA-1 can be synthesized from *trans*-cinnamic acid directly in sunlight through a photodimerization reaction.[52, 108, 257] In fact, cinnamic acid has two forms, cis and trans isomers, but the trans form is dominant, existing nature in a number of plants.[258-260] Using **CBDA-1** as a building block is not only beneficial because it can be produced from bio-based chemicals, but also because it has a rigid structure, clarity, and high thermostability. These features of **CBDA-1** can enhance the physical properties of synthesized polyesters such as transparency and glass transition temperature (T_g).[53, 75, 112, 116] Based on these advantages of **CBDA-1**, several semi-rigid, semi-flexible polyesters have been developed from **CBDA-1** by linking it with flexible-chain diols in this study. The strategy used in synthesizing the building block **CBDA-1** from *trans*-cinnamic acid in this work was solvent-free [2 + 2] photodimerization reaction by irradiation in sunlight or ultraviolet. Solid state synthesis has many advantages including no waste, low energy consumption, avoiding undesired reactions and high yield. These features are quite important in manufacture applications.

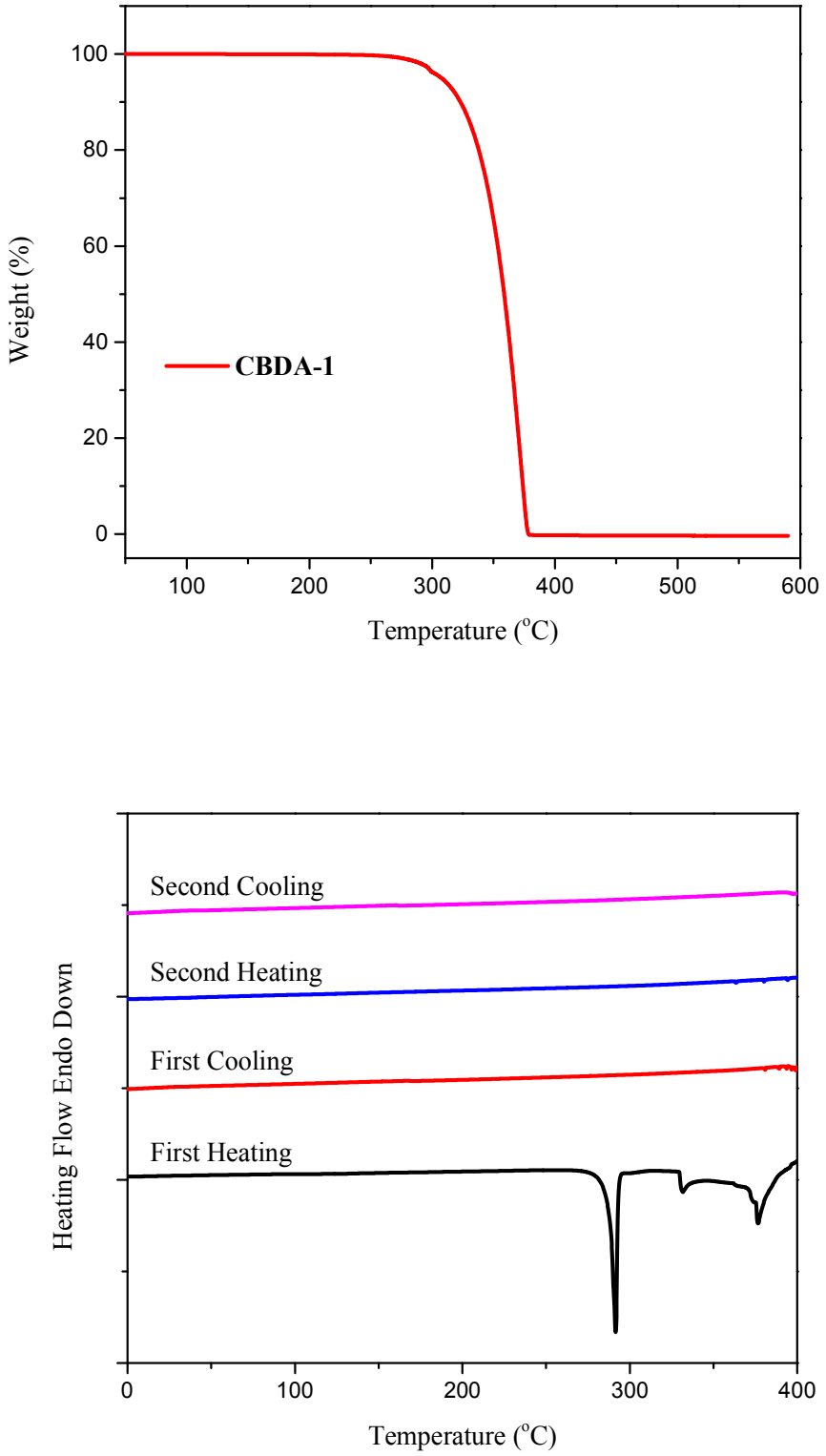

Figure 27. TGA (a) and DSC (b) analysis of building block **CBDA-1**.

The synthesis of poly-α-truxillate started from the photodimerization reaction of *trans*-cinnamic acid (Scheme 6). As a building block, **CBDA-1** was connected with different linear diols such as ethylene glycol, 1,3-propanediol, 1,4-butanediol, 1,5-petanediol, and 1,6-hexanediol through a condensation reaction. The above diols can be obtained from biomass as well, which makes it possible to achieve a 100% bio-ratio in the polyesters.[14]

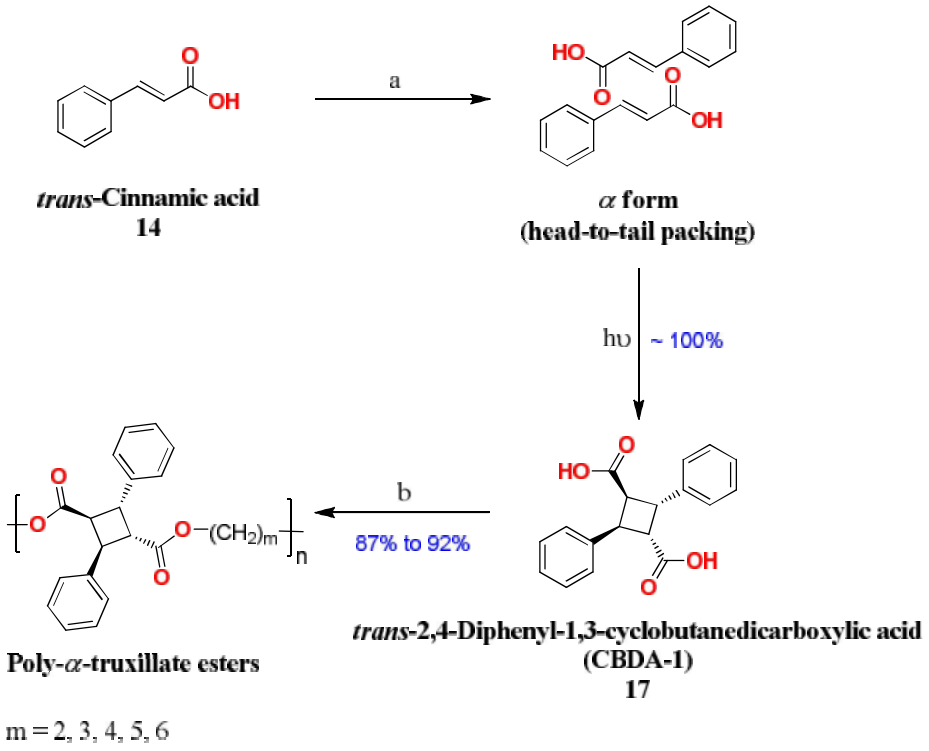

Scheme 6. The synthesis of **CBDA-1** and poly-α-truxillate. a) The commercially available *trans*-cinnamic acid is in α-form (head-to-tail packing). Further crystallization processes are not necessary. b) DCC, DMAP, ACN, r.t., 18 h.

To investigate the packing of commercial *trans*-cinnamic acid, single crystals of purchased *trans*-cinnamic acid were obtained in a mixed solvent of ethyl acetate and acetonitrile (1 : 1). X-ray diffraction analysis indicated that the packing of commercial *trans*-cinnamic acid is α-form (head-to-tail) (Figure 28a). The head-to-tail packing also can

be obtained in a variety of solvents such as acetonitrile, acetone, toluene, etc. This result is consistent with the reported phenomenon that head-to-tail packing is the dominant packing method for *trans*-cinnamic acid. Powder X-ray diffraction of the commercial *trans*-cinnamic acid gave almost the same results as the single crystal simulation, proving the commercial *trans*-cinnamic acid has the same structure as the single crystal structure. (Figure 28c). Consequently, the commercial *trans*-cinnamic acid powder can be used to produce the building block **CBDA-1** directly without further recrystallization.

After confirming the packing of commercial *trans*-cinnamic acid, the powder of *trans*-cinnamic acid was put outside in sunlight for 12 h to produce the building block **CBDA-1**. The photodimerization process was monitored by FT-IR and NMR. Both of them showed the completion of the photodimerization with a yield of 98%. The 2% loss may have been due to sublimation of *trans*-cinnamic acid. To characterize the structure of the obtained **CBDA-1**, a single crystal was obtained in ethanol. However, the X-ray diffraction result showed a highly disordered structure which has been reported.[52, 257] To get a legible single crystal structure of **CBDA-1**, a salt of **CBDA-1**, α-truxillate-dibutylaminium was prepared in solvents of ethanol/water/dimethylformamide (1 : 1 : 1), and butylamine. A salt will not destroy nor change the structure of **CBDA-1**, but can be used to avoid the disorder of **CBDA-1** molecules. Figure 28 shows three views of synthesized **CBDA-1**. The single crystal X-ray structure clearly showed the newly formed cyclobutane ring and the configuration. Two carboxylic groups are on opposite side of the cyclobutane ring which makes it suitable for chain construction.

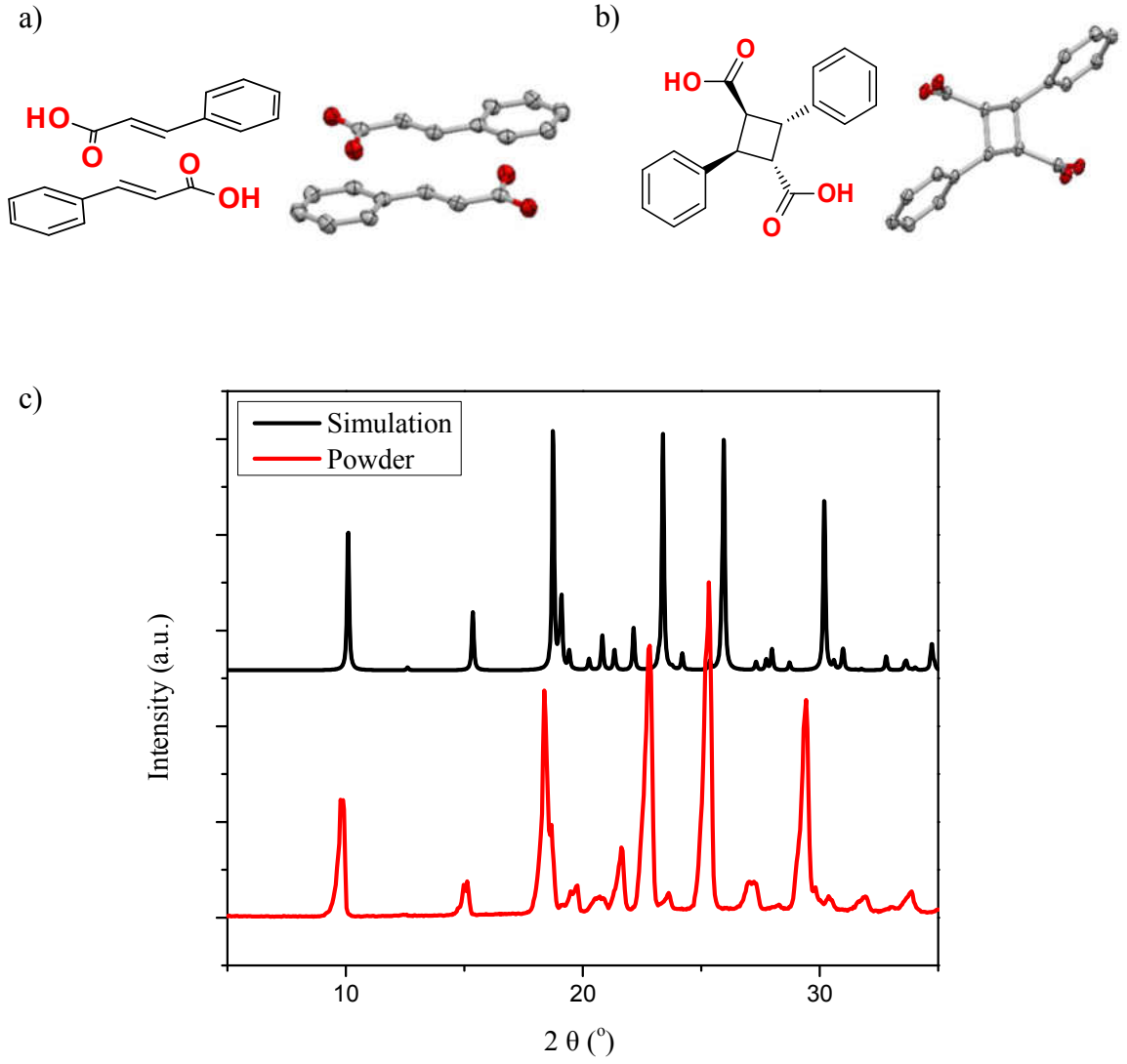

Figure 28. The study of commercial *trans*-cinnamic acid and its α-form dimer. a) Single crystal X-ray structure of *trans*-cinnamic acid with α-form packing (head-to-tail), which is suitable for the photodimerization reaction. b) Single crystal X-ray structure of α-truxillate which revealed the newly formed cyclobutane ring. c) Powder XRD comparison of single crystal simulation (black line) and powder *trans*-cinnamic acid (red line). Note: Oak Ridge Thermal Ellipsoid Plot (ORTEP) represents at 50% electron density of monomer crystal structure (hydrogen atoms are omitted for clarity)

The obtained **CBDA-1** was connected with each other by linear diols through a condensation reaction. Five poly-α-truxillate were produced, poly(ethylene-α-truxillate) (PEAT), poly(propylene- α-truxillate) (PPAT3), poly(1,4-butylene- α-truxillate) (PBAT), poly(1,5-pentylene- α-truxillate) (PPAT5), poly(1,6-hexylene- α-truxillate) (PHAT), among which PPAT3 is a liquid. All poly-α-truxillates were expected to be fully amorphous. However, powder X-ray diffraction patterns of these four poly-α-truxillates (PPAT3 not included) showed that the polymers are semi-crystalline. PPAT 3 is a liquid at room temperature.

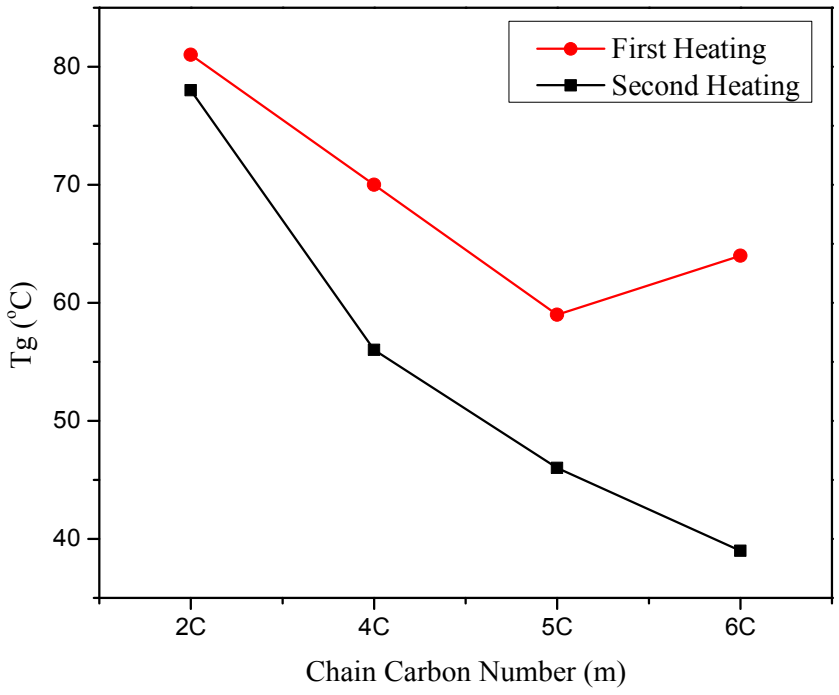

Figure 29. The plot of first and second heating T_g of poly-α-truxillate against carbon chain length of linear diols.

Differential scanning calorimetry (DSC) revealed the glass transition temperature (T_g) of four polyesters. Figure 29 shows a decreasing trend of T_gs when the carbon chain length was increased. T_g of PEAT is 81 °C whereas T_g of PPAT is 64 °C. The trend shown in the T_gs may be attributed to the increasing flexibility of longer carbon chains, with increasing chain length. It is easier for the polyester to rotate or twist. After the first heating and cooling process, in the second heating process, the DSC curve showed an obvious decreasing trend of T_gs. Compared with the first heating T_g, the second heating T_gs showed lower temperatures. This phenomenon may be due to the annealing effect of the first heating process. After heating polyesters to 250 °C, they will be scattered and mixed equally, which may lead the decreasing T_gs.

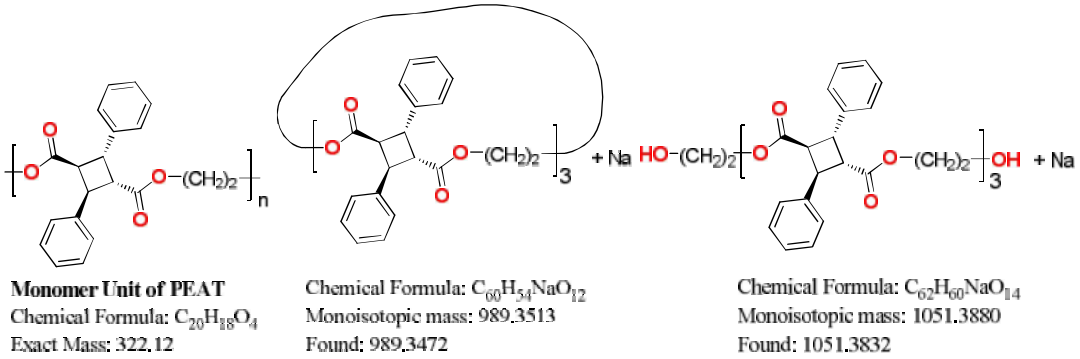

Figure 30. a) The repeating unit of PEAT. b) and c) Cycled PEAT and chain PEAT.

Two series of peaks in mass spectra of PEAT were observed (Figure 30). They have a repeating unit with *m/z* = 322.12 that corresponds with the unit mass of PEAT ($C_{20}H_{18}O_4$ *m/z* = 322.12). One repeating peak of PEAT is '*m/z* = 322.12×n + 22.99 (Na)' which indicates that some cycled polyesters exist in the product. For example, a trimer was observed with '*m/z* = 322.12×3 + 22.99 = 989.35'. Another repeating peak of PEAT is 'm/z

= 322.12×n + 62.04 (end-group) + 22.99 (Na)'. This result suggests there are chain polyesters with end-group HO-$(CH_2)_2$- and –OH that exist in the product. For example, 'm/z = 322.12×3 + 62.04 + 22.99 = 1051.39'. The MS analysis of PEAT revealed both chain and cycled fragments are present in PEAT. This phenomenon of two different repeating peaks in MS spectra was also observed in PBAT, PPAT5, and PHAT.

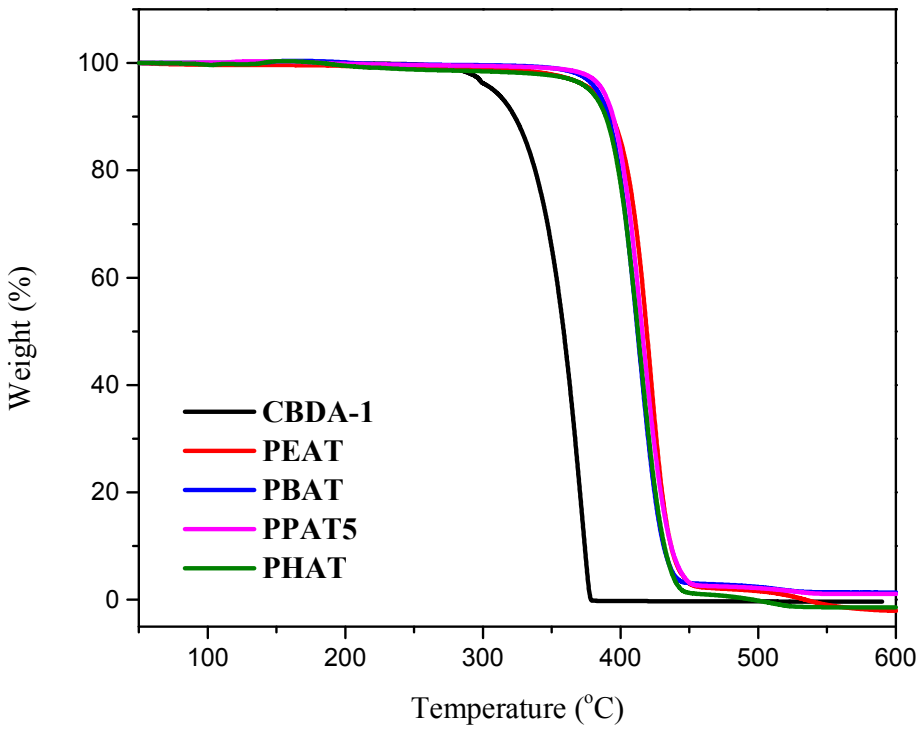

Figure 31. Thermostability test of poly-α-truxillate esters. TGA results were recorded from 30 °C to 600 °C with a heating rate of 20 °C min^{-1} under an N_2 atmosphere.

Thermogravimetric analysis (TGA) shows that the synthesized poly-α-truxillate esters have higher stability than the building blocks. Although DSC showed the T_g decreased as the carbon chain length increased, there is no dramatic stability difference between these

polyesters (Figure 31). The decomposition of poly-α-truxillate polyesters occurred around 395 ^{o}C. As the temperature kept going up, the polyesters fully decomposed at around 450 ^{o}C. Compared with PET, the poly-α-truxillate esters have similar thermostability but have a 100% bio-ratio.

5.4. Conclusion

A new building block **CBDA** is introduced in this study. A series of semi-flexible polyesters have been successfully synthesized from the building block **CBDA-1**. Commercial *trans*-cinnamic acid has been confirmed to have a head-to-tail packing pattern which is suitable for easy producing **CBDA-1**. The X-ray diffraction result is consistent with previous reports that the head-to-tail packing of *trans*-cinnamic acid is the dominant packing way. Solvent-free [2 + 2] photodimerization provided a convenient method for synthesis **CBDA-1** from *trans*-cinnamic acid. Several polyesters have been presented in this work, which shows **CBDA-1** is a promising building block for polyesters. DSC data showed the glass transition temperature decreased as the carbon chain length increasing. TGA revealed the thermal properties of the newly synthesized polyesters and showed similar thermostability to PET. These studies proved that **CBDA-1** can be a promising replacement of terephthalic acid. As a building block, **CBDA** provides a new opportunity to synthesize polymers such as polyesters and polyamides.

CHAPTER VI

SUMMARY AND OUTLOOK

Polycyclobutanes (**PCBs**) are the polymers with cyclobutane rings as their building blocks or backbone.[42, 44, 47, 108, 140, 261-268] In spite of inherent ring strain, cyclobutane units are present in a wide range of natural products.[91, 202-207] The cyclobutane derivatives can be generated in metabolisms and play a significant role in the biological system.[205, 206, 208-215] Cyclobutane ring has two conformations, planar and puckered, which bring the semi-flexible and semi-rigid properties.[216, 217] The semi-rigid structure of cyclobutane ring can provide PCBs semi-flexible characteristics which may change their chemical or physical properties. Cyclobutane rings can be easily formed via [2 + 2] cycloaddition.[91, 203, 218, 224, 225, 269, 270] The most popular approach to preparing cyclobutane derivatives is a photochemical process.[92, 270] When reactions occur in the solid-state, they avoid organic solvents and harsh conditions which create a more environmentally-friendly setting for synthesizing particular compounds.[40, 92, 96, 165, 271, 272]

This dissertation described the work on PCBs in a classical way. To construct PCBs, diolefins are necessary. Therefore, gemini monomers with diolefins were introduced to construct PCBs. When the double bonds on gemini monomers are in a suitable orientation, they will undergo the [2 + 2] photocycloaddition reaction with irradiation in the crystalline state. Two PCBs, linear polyester, and polyladderane, were synthesized from gemini

monomers and the structures were confirmed by SCSC results (Figure 32a and b). PCBs also can be applied to 2D polymers. Two 2D polymers were synthesized from cinnamic acid based monomers via [2 + 2] photoreaction (Figure 32c).

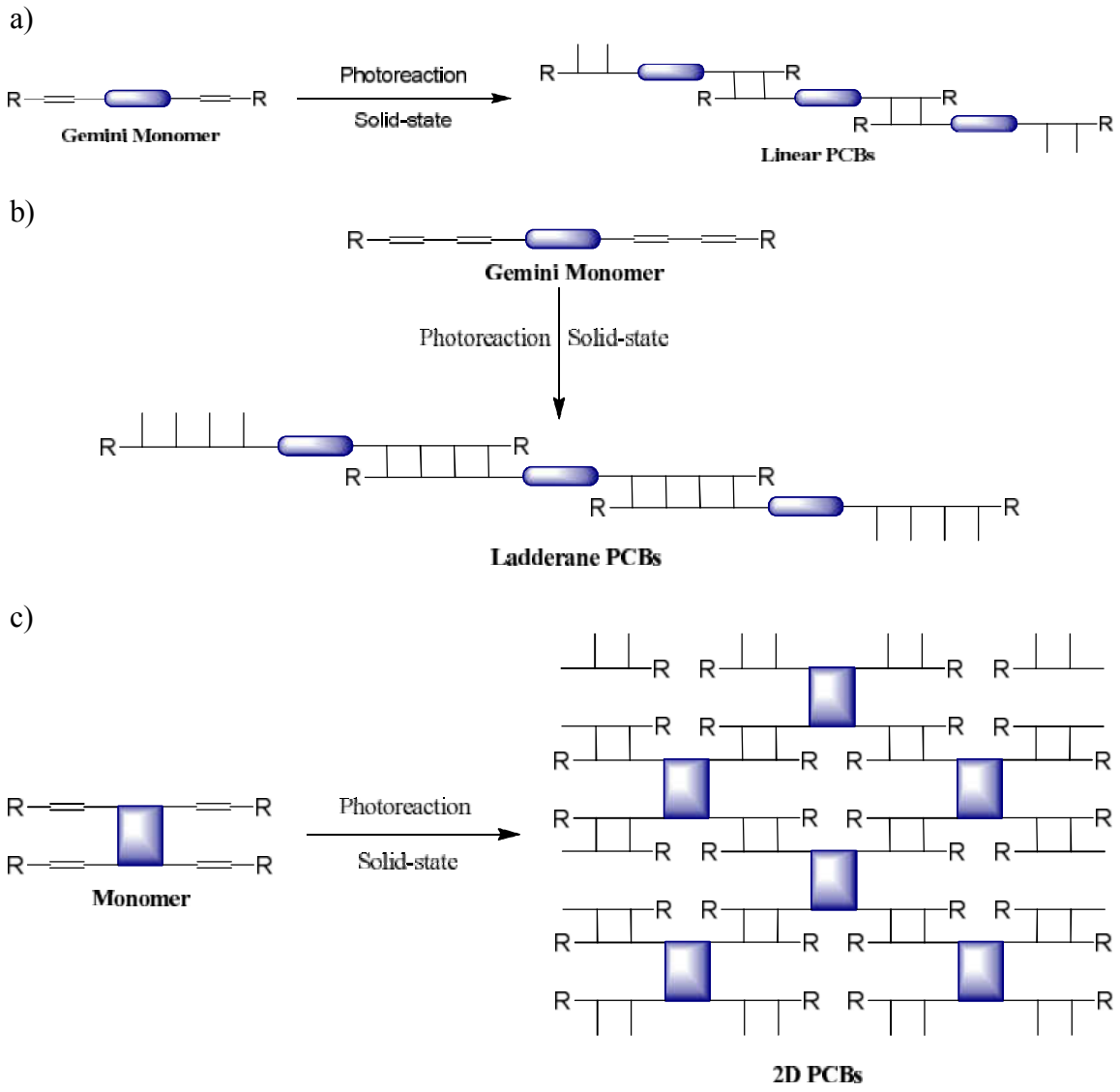

Figure 32. Summary of different PCBs synthesized by solid-state photopolymerization.

Since many scientists in academia and industry are not familiar with solid-state photoreactions, several PCBs were synthesized by the classical solution polymerization process. CBDA, which is a cyclobutane diacid, has been regarded as a building block for the synthesis of PCBs. An example of CBDA was introduced to illustrate how PCBs can be prepared in a solution reaction (Figure 33). Firstly, CBDA-1 was synthesized in solid-state via photodimerization reaction. The thermal and chemical stability of CBDA-1 indicated that it was a good building block to synthesize PCBs in solutions. Four PCBs examples PEAT, PBAT, PPAT5, and PHAT were successfully prepared from CBDA-1 via solution polymerization.

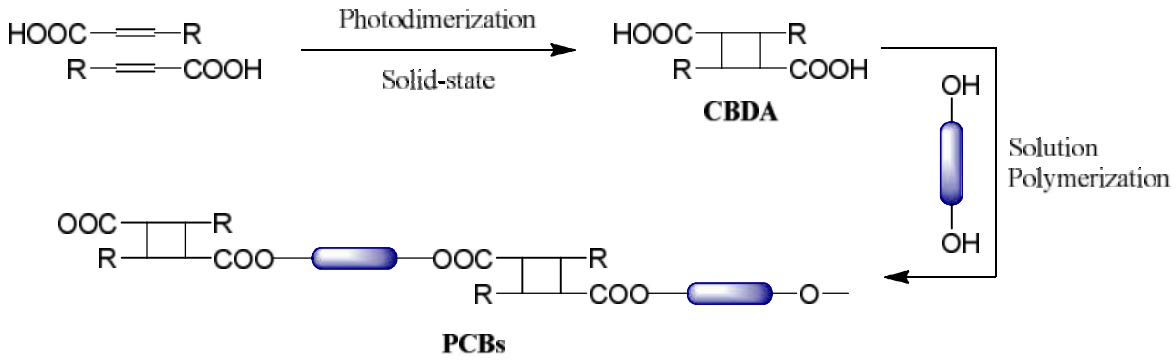

Figure 33. PCBs synthesized *via* classical solution polymerization.

This dissertation demonstrated two different approaches to synthesize PCBs. Both solid-state reaction and the conventional organic synthesis are reliable methods in PCBs synthesis. PCBs with semi-flexible structures showed high thermostability and chemical stability. The examples exhibited in this dissertation paved the way to PCBs.

APPENDIX

APPENDIX A

Selected NMR Spectra

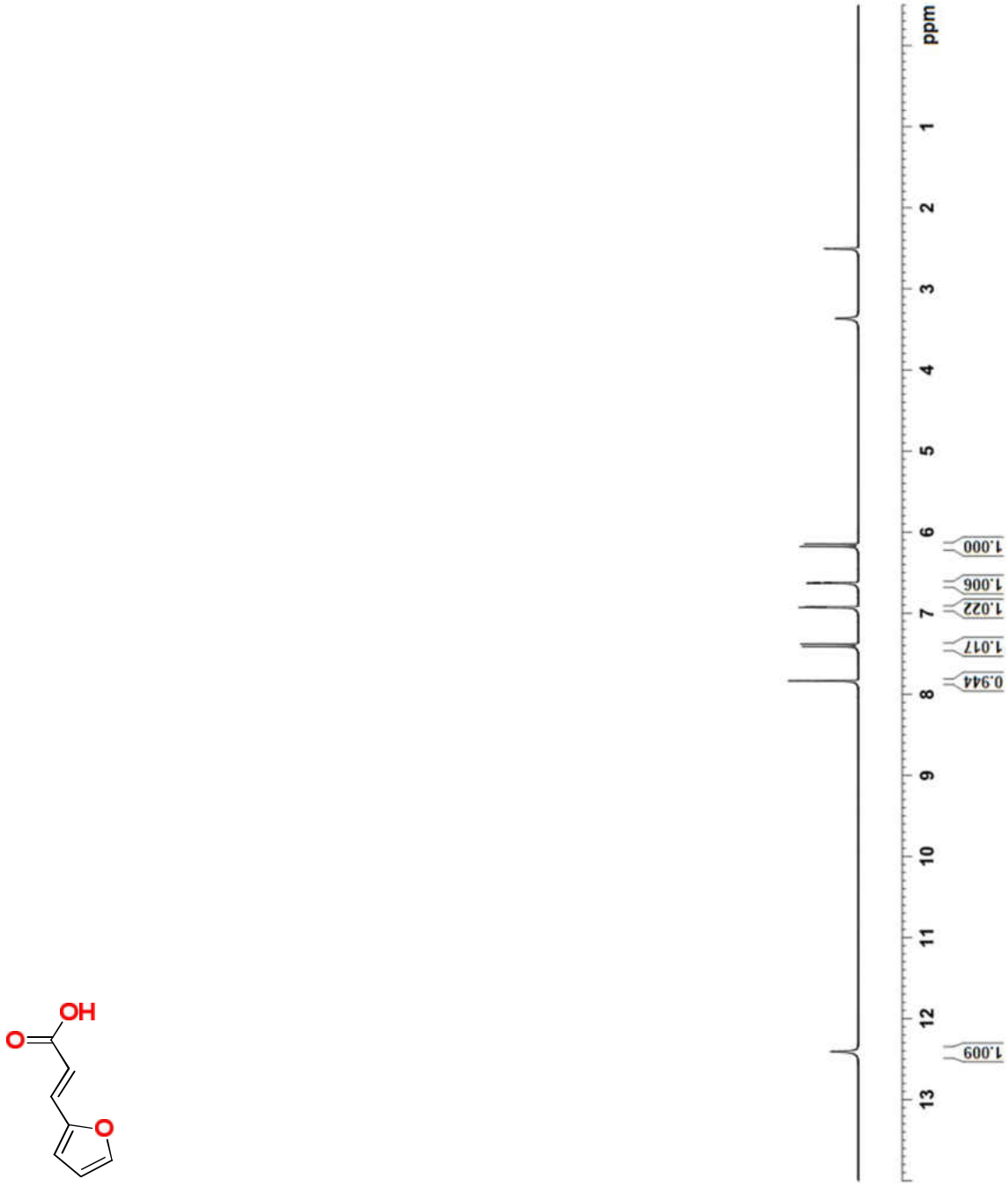

Figure 34. ^{1}H-NMR spectrum of **3** in DMSO-d_6 at room temperature.

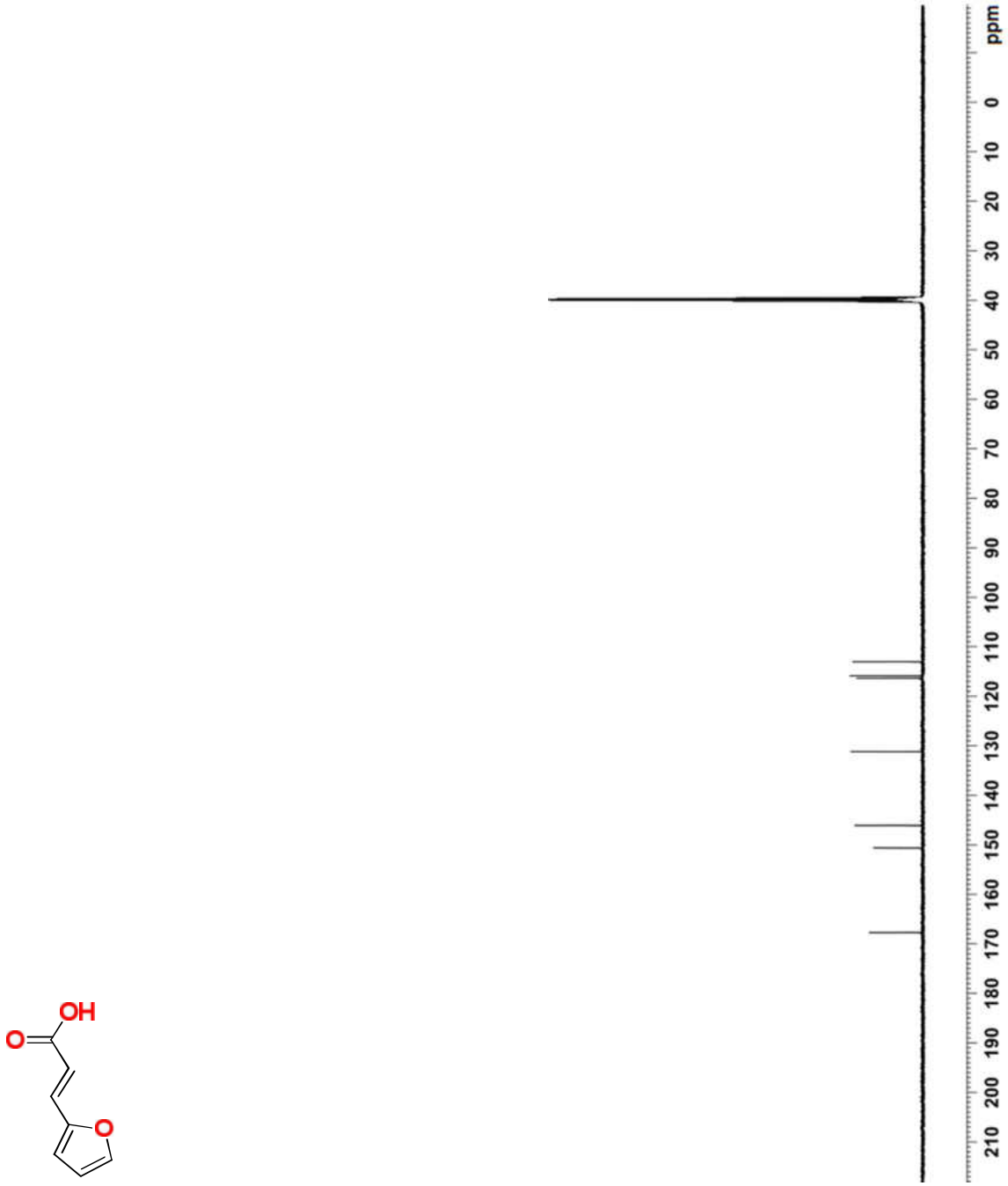

Figure 35. ^{13}C-NMR spectrum of **3** in DMSO-d_6 at room temperature.

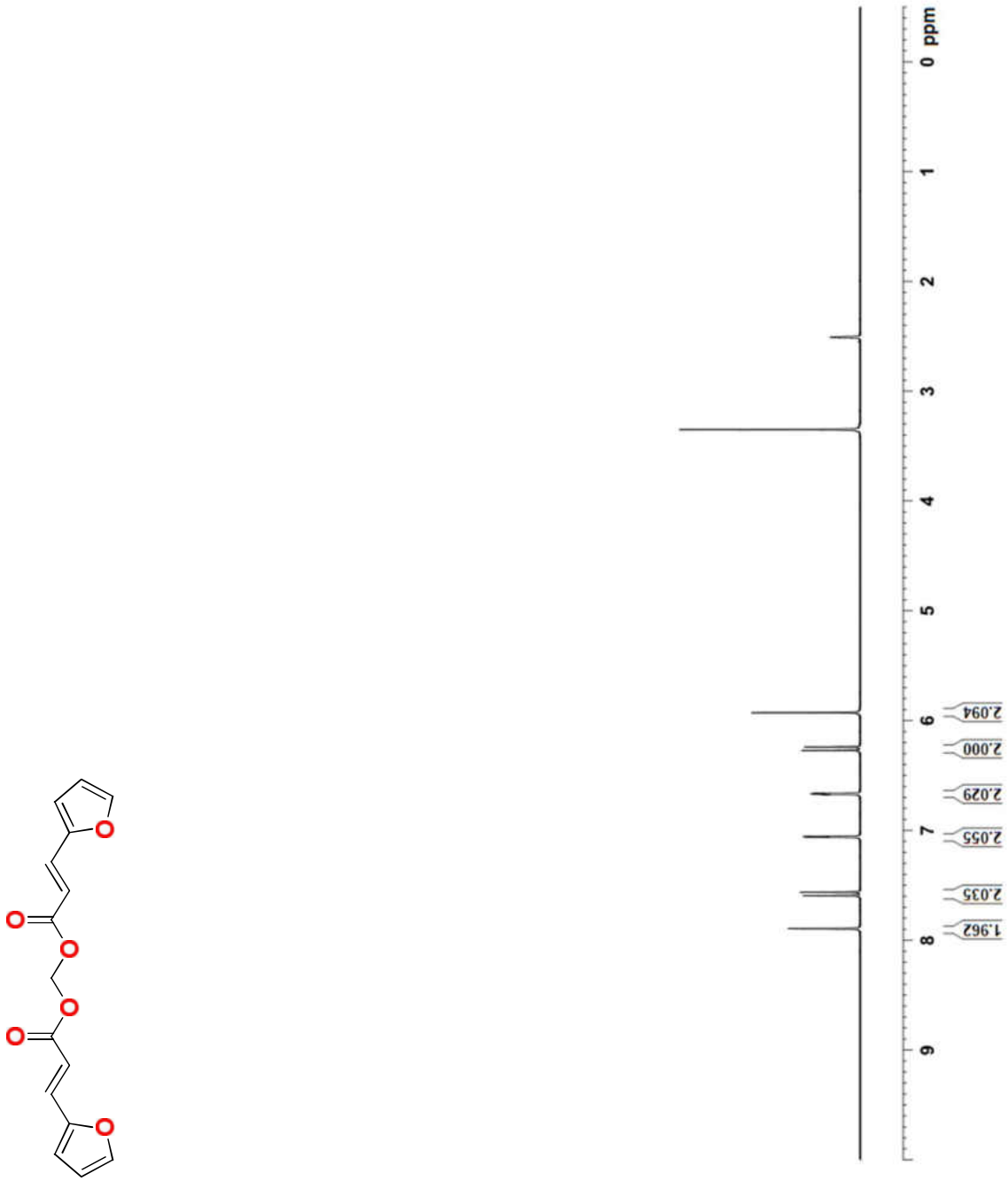

Figure 36. ^{1}H-NMR spectrum of monomer **4** in DMSO-d_6 at room temperature.

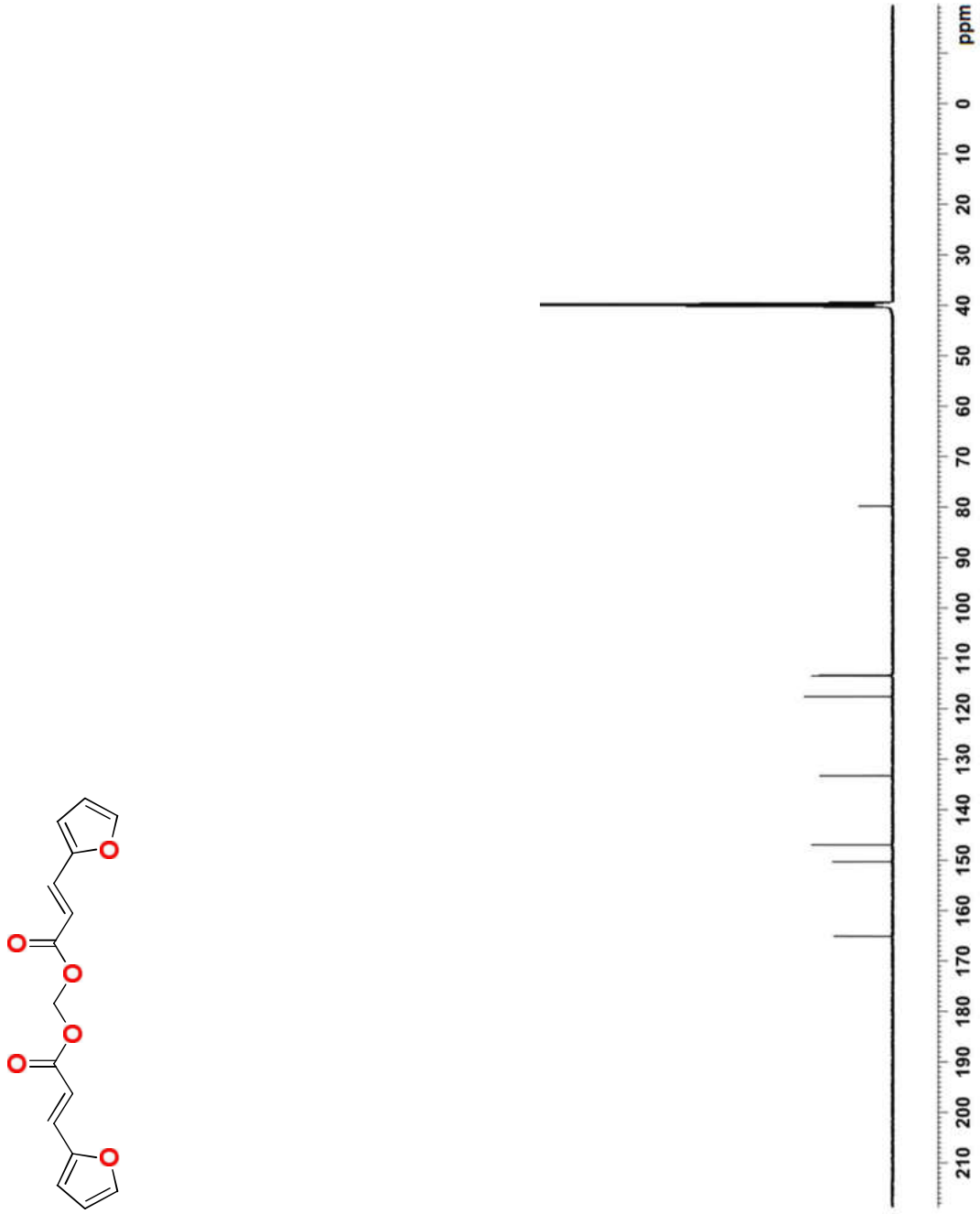

Figure 37. ^{13}C-NMR spectrum of monomer **4** in DMSO-d_6 at room temperature.

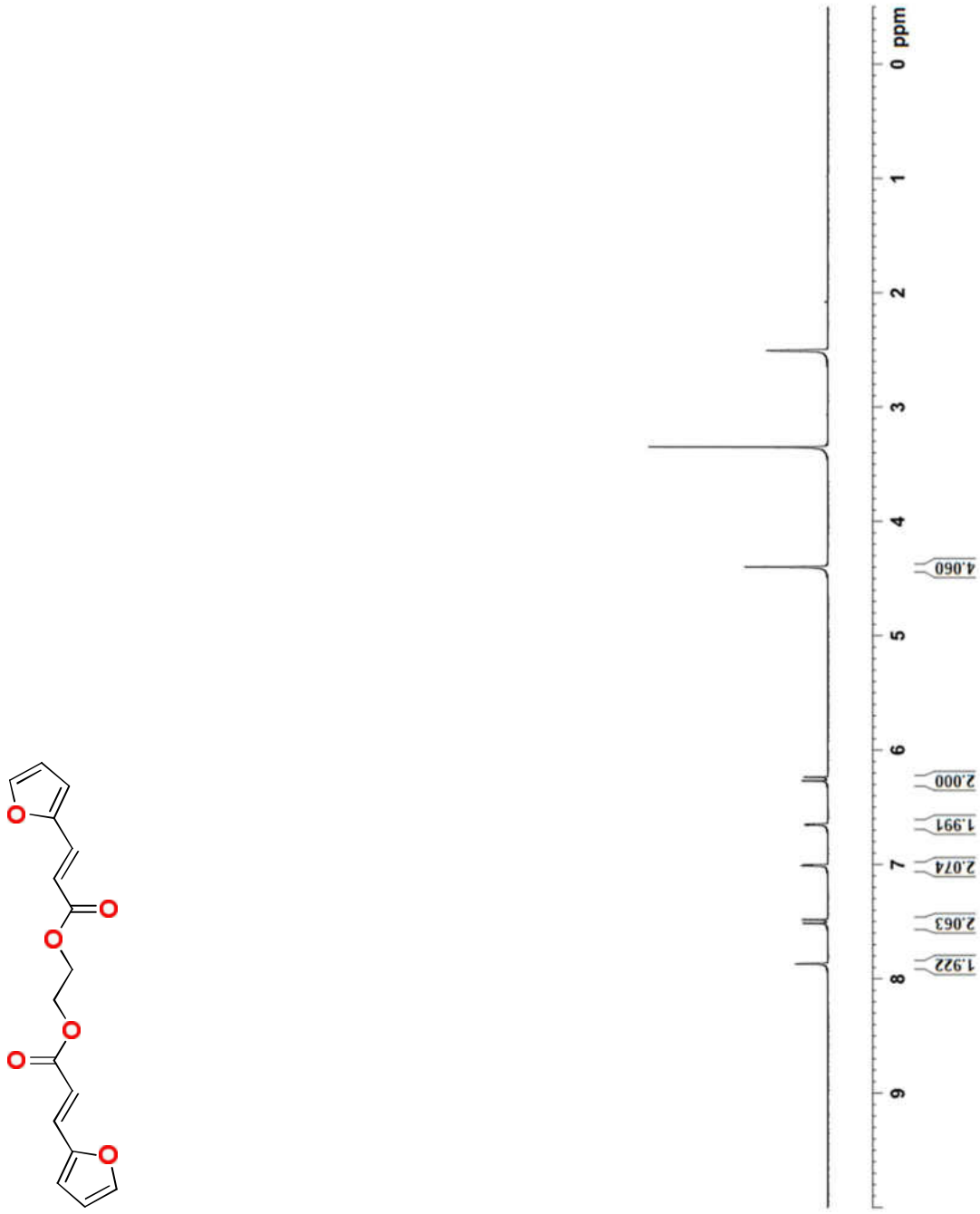

Figure 38. ^{1}H-NMR spectrum of monomer **5** in DMSO-d_6 at room temperature.

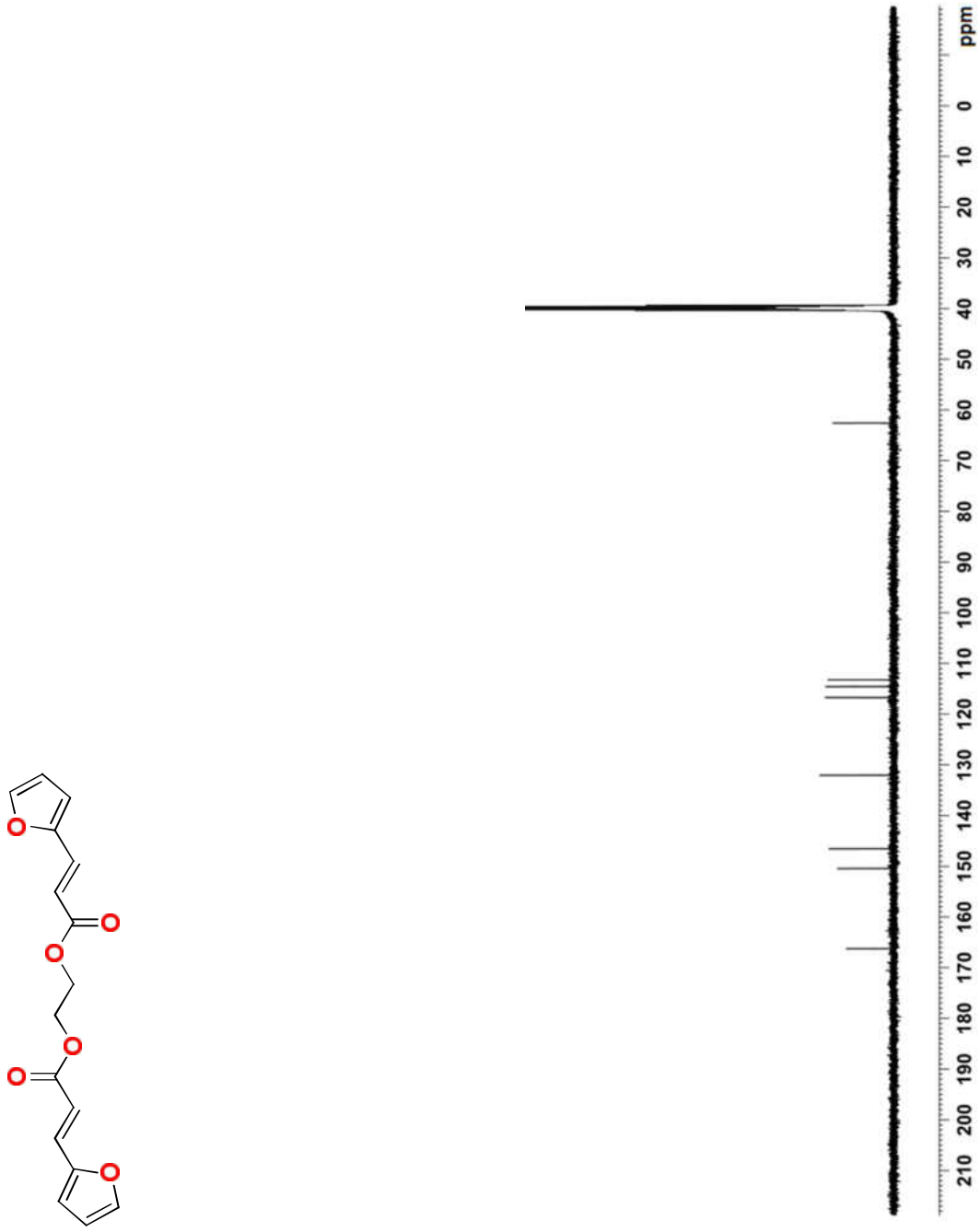

Figure 39. ^{13}C-NMR spectrum of monomer **5** in DMSO-d_6 at room temperature.

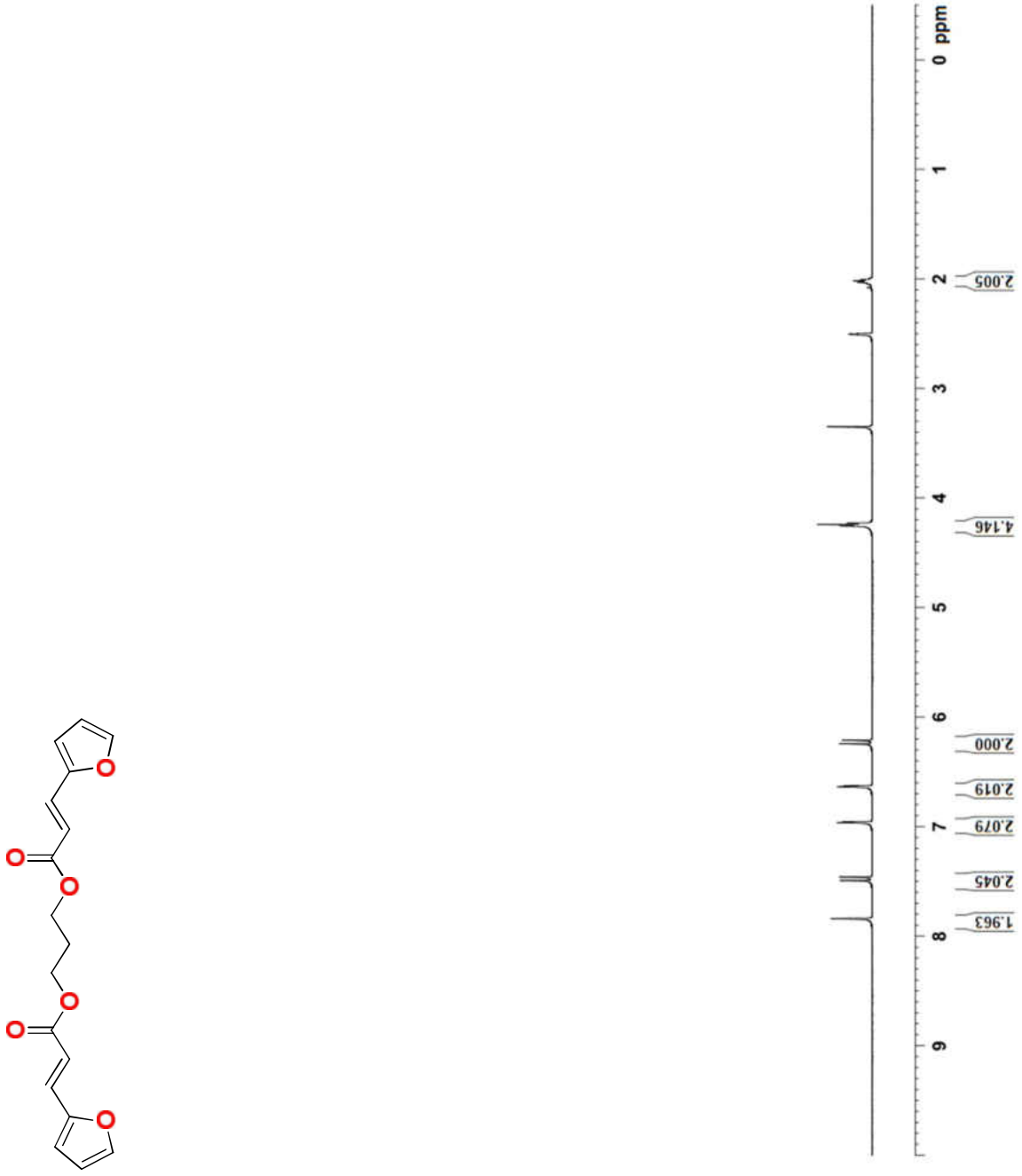

Figure 40. ^{1}H-NMR spectrum of monomer **6** in DMSO-d_6 at room temperature.

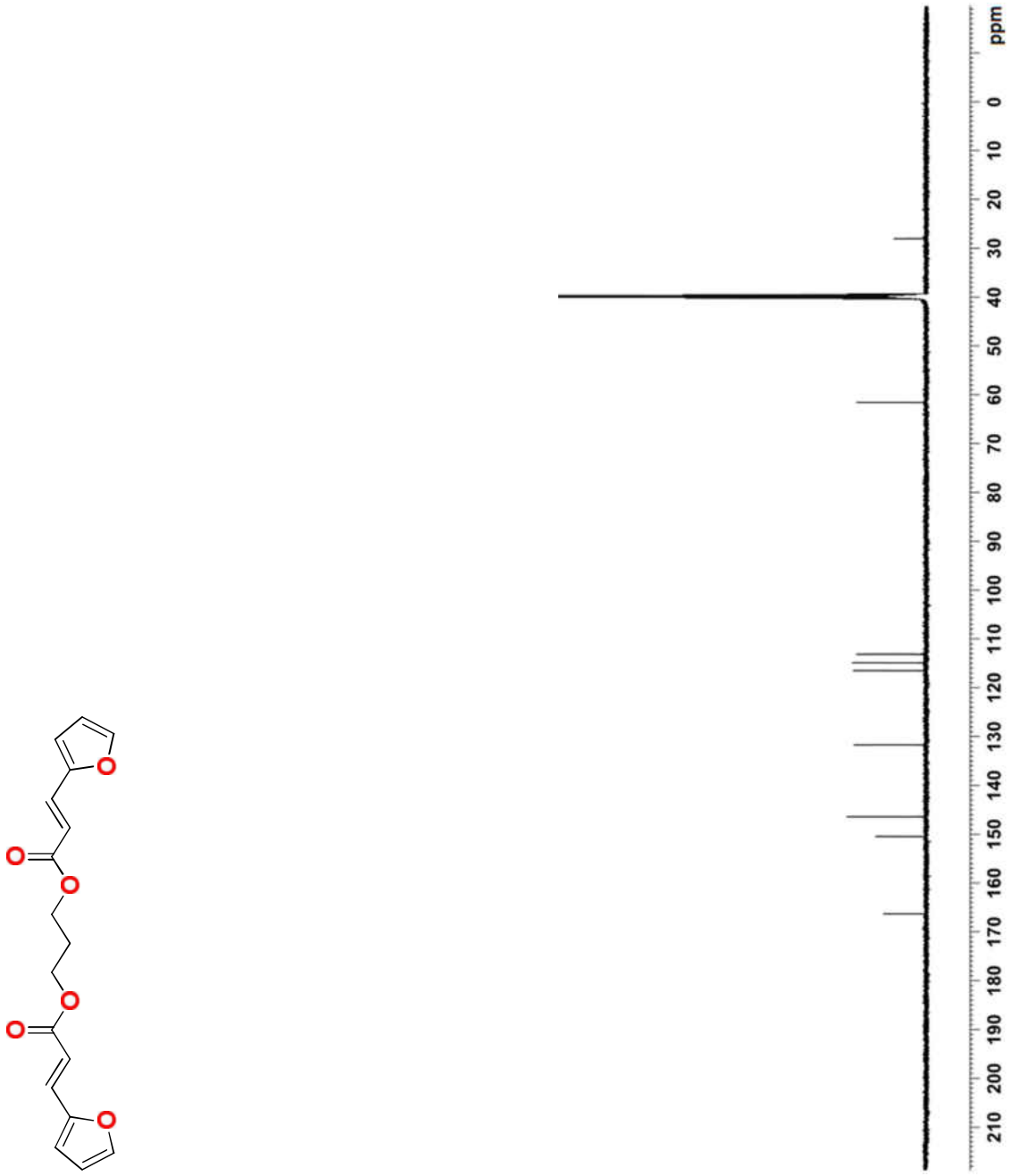

Figure 41. ^{13}C-NMR spectrum of monomer **6** in DMSO-d_6 at room temperature.

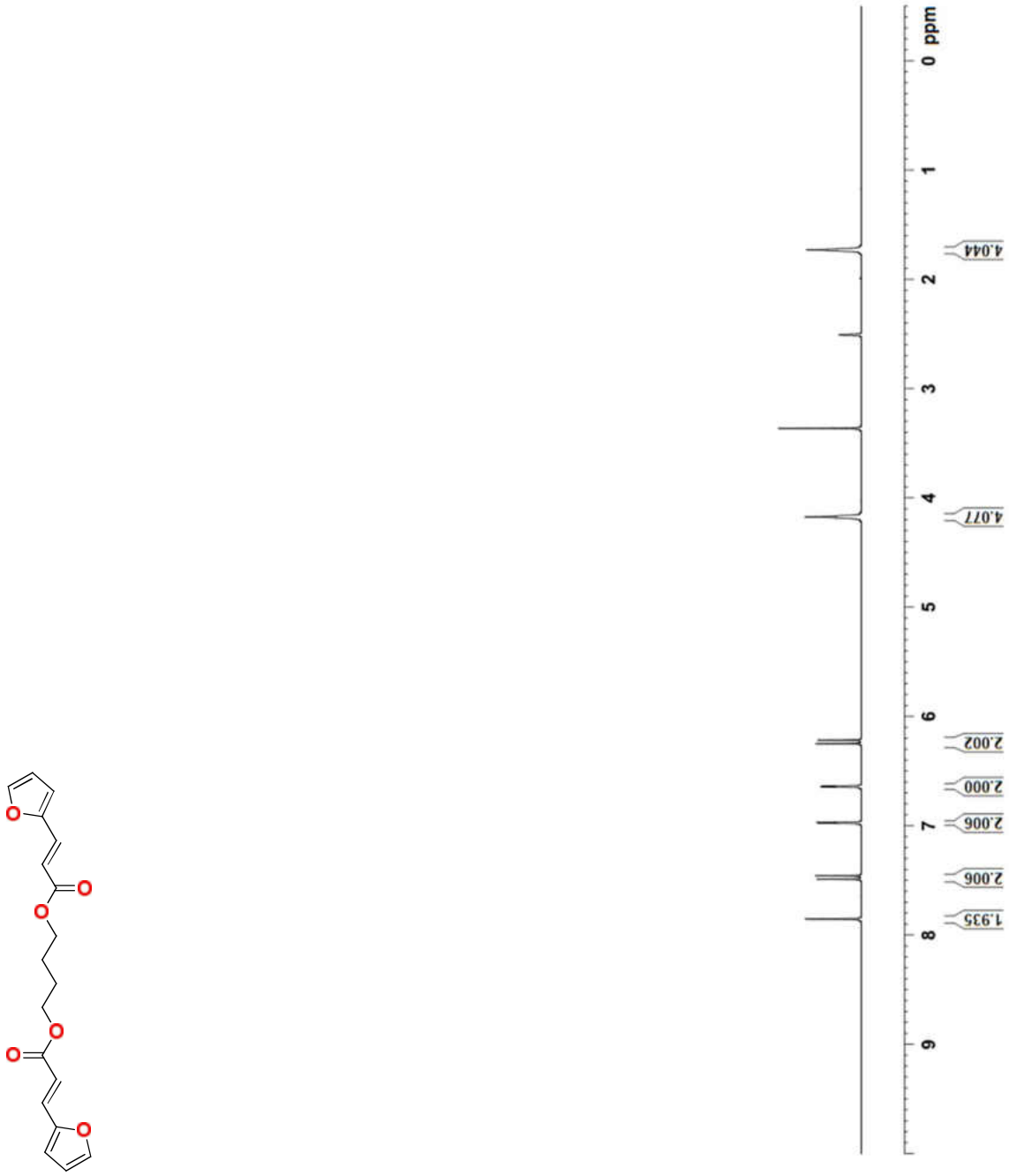

Figure 42. ^{1}H-NMR spectrum of monomer **7** in DMSO-d_6 at room temperature.

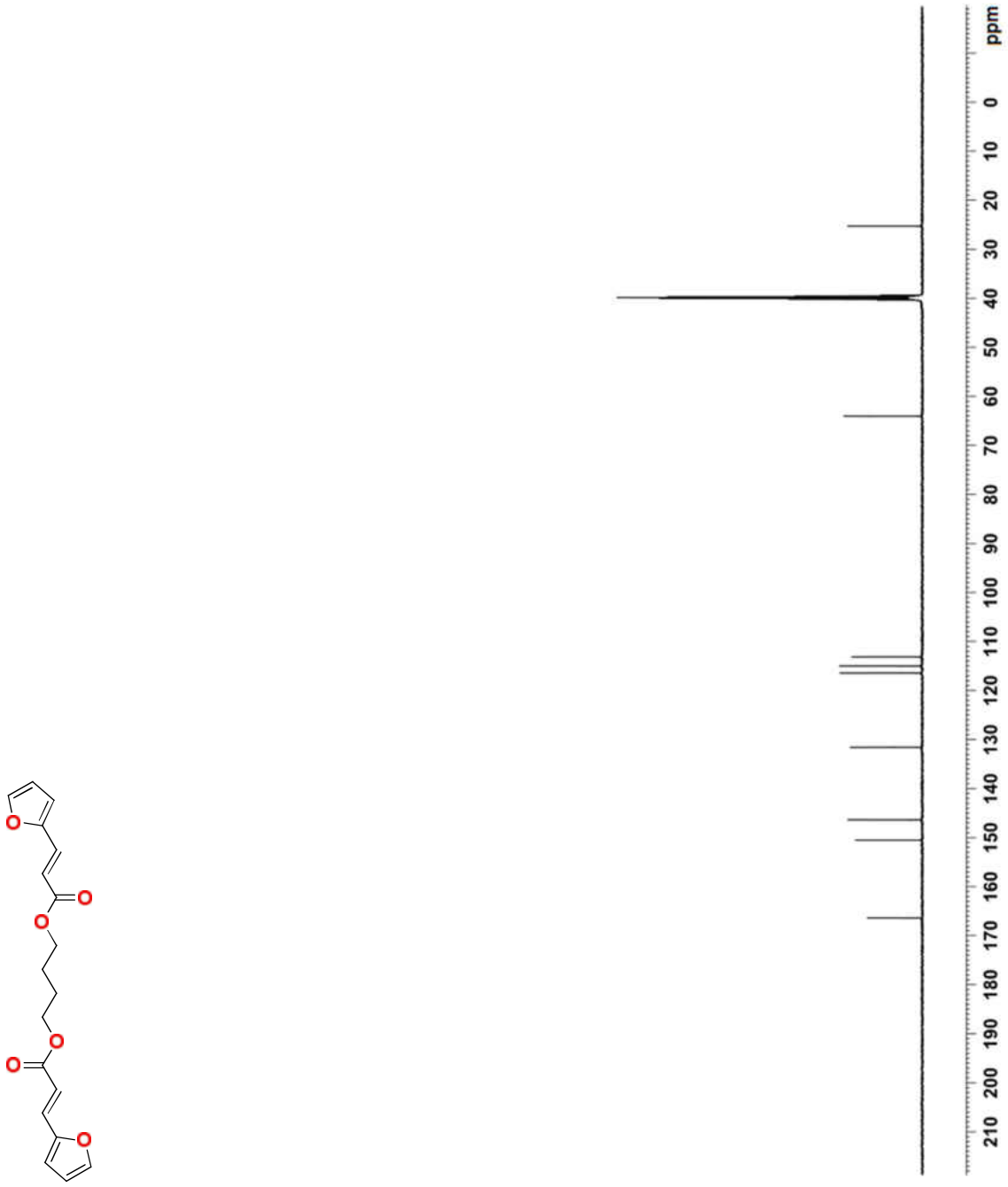

Figure 43. ^{13}C-NMR spectrum of monomer **7** in DMSO-d_6 at room temperature.

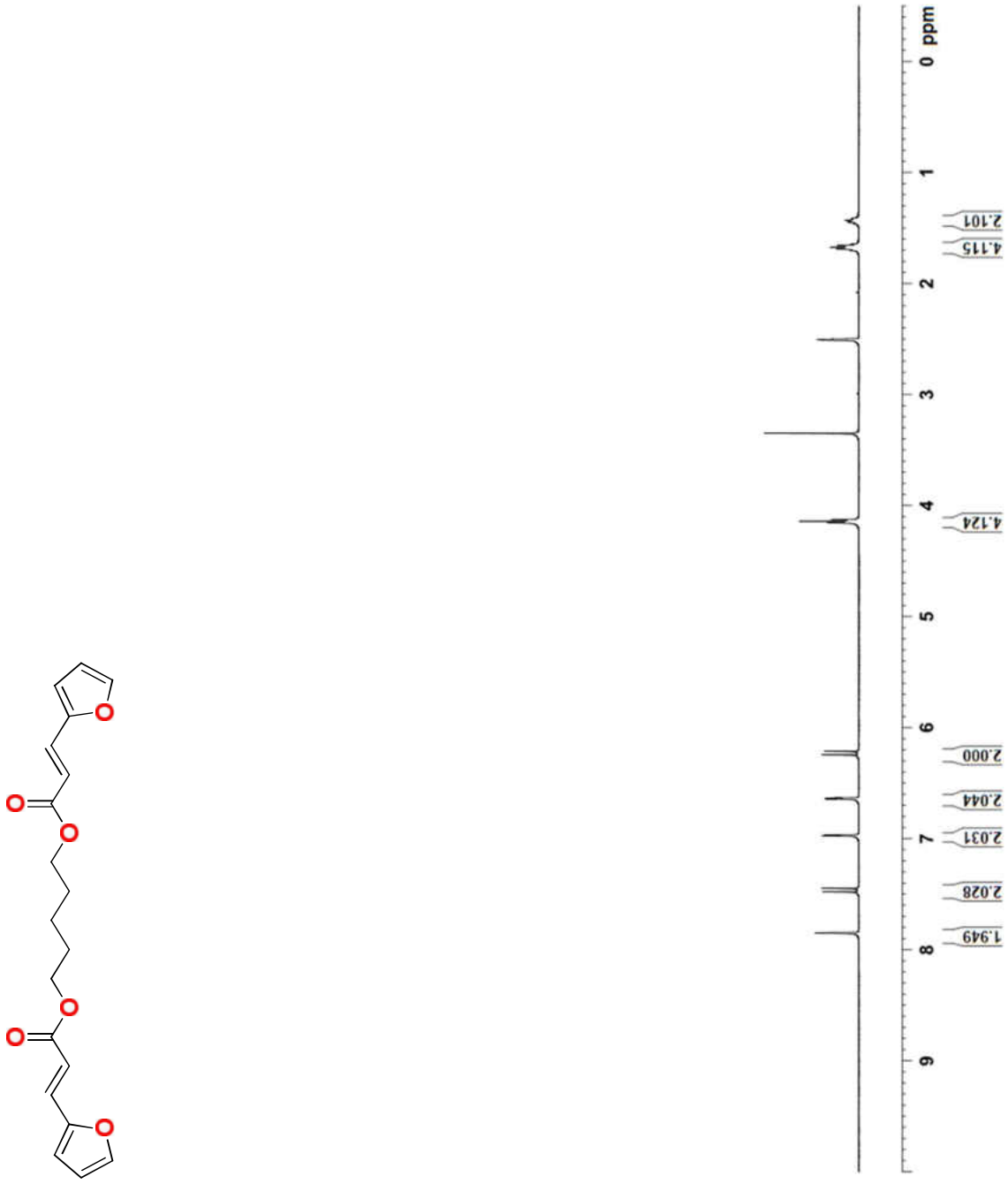

Figure 44. ^{1}H-NMR spectrum of monomer **8** in DMSO-d_6 at room temperature.

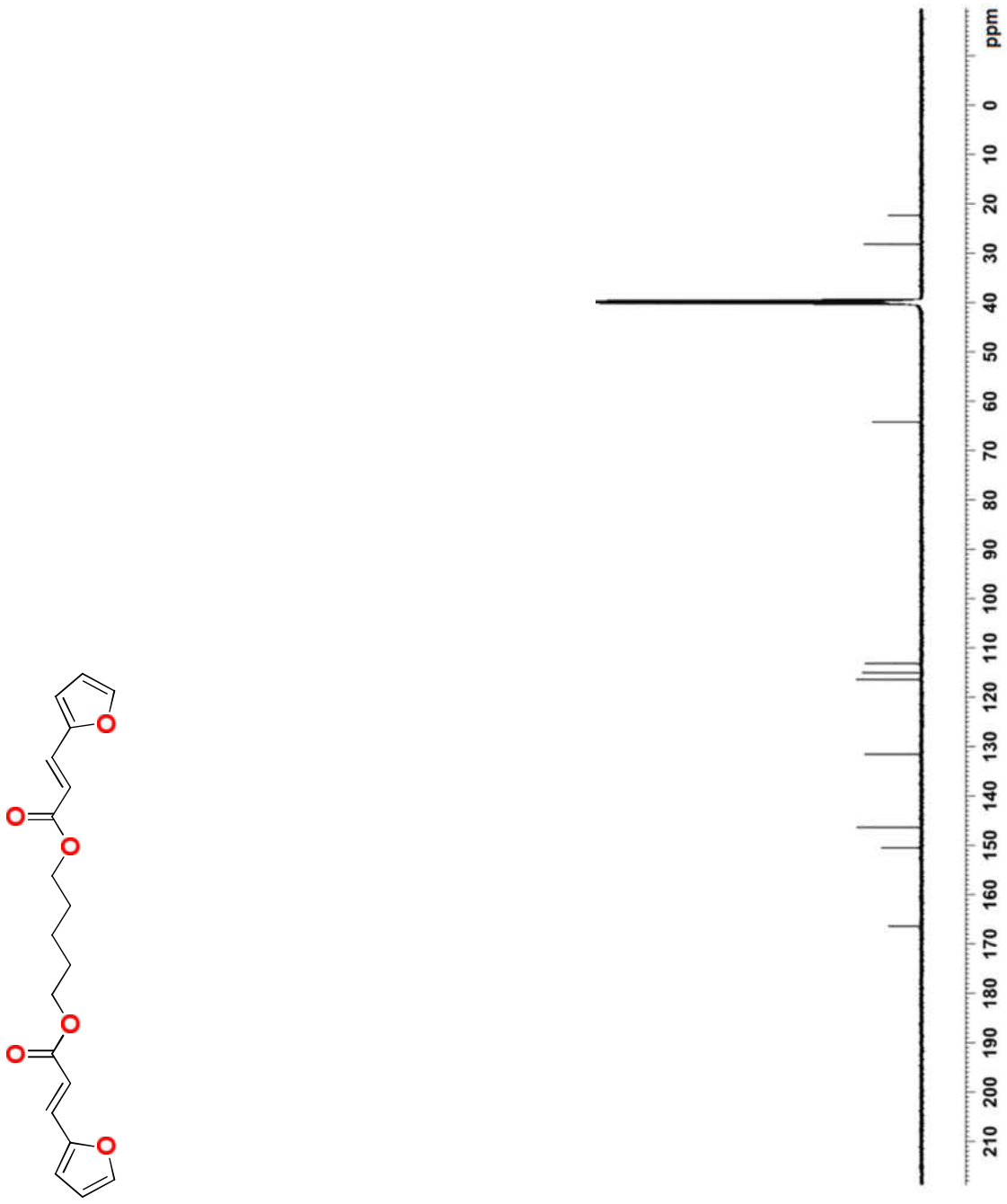

Figure 45. ^{13}C-NMR spectrum of monomer **8** in DMSO-d_6 at room temperature.

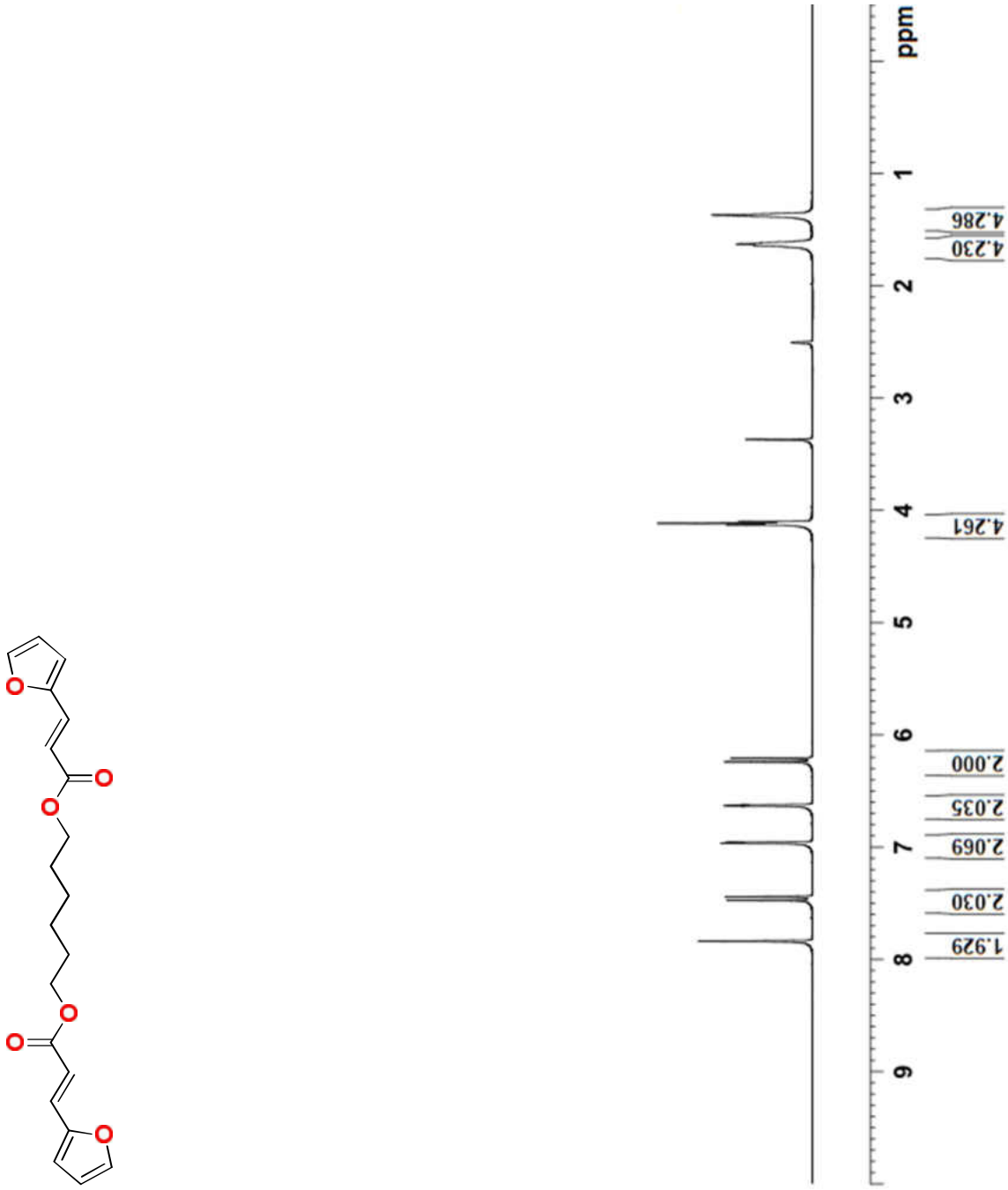

Figure 46. ^{1}H-NMR spectrum of monomer **9** in DMSO-d_6 at room temperature.

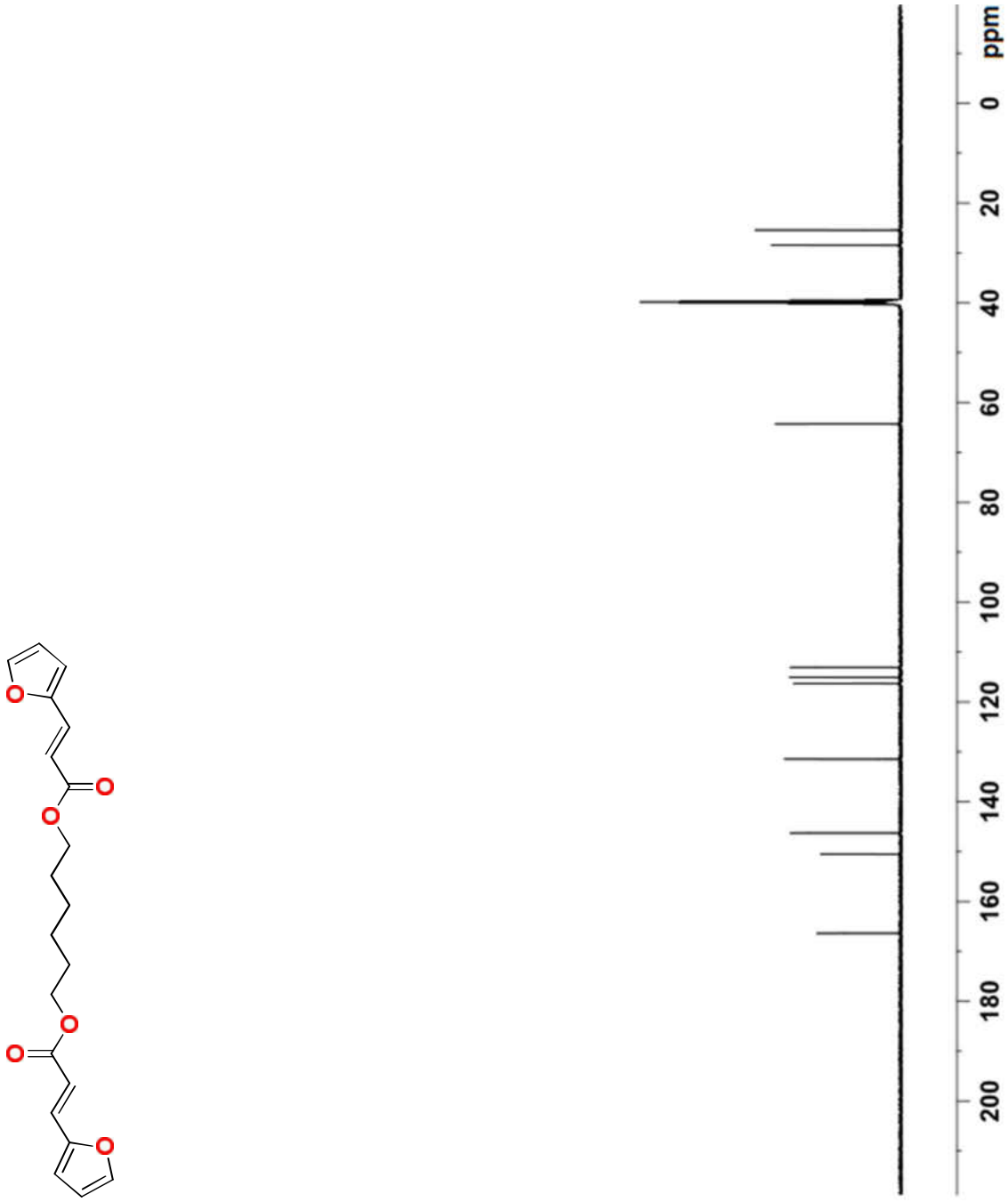

Figure 47. ^{13}C-NMR spectrum of monomer **9** in DMSO-d_6 at room temperature.

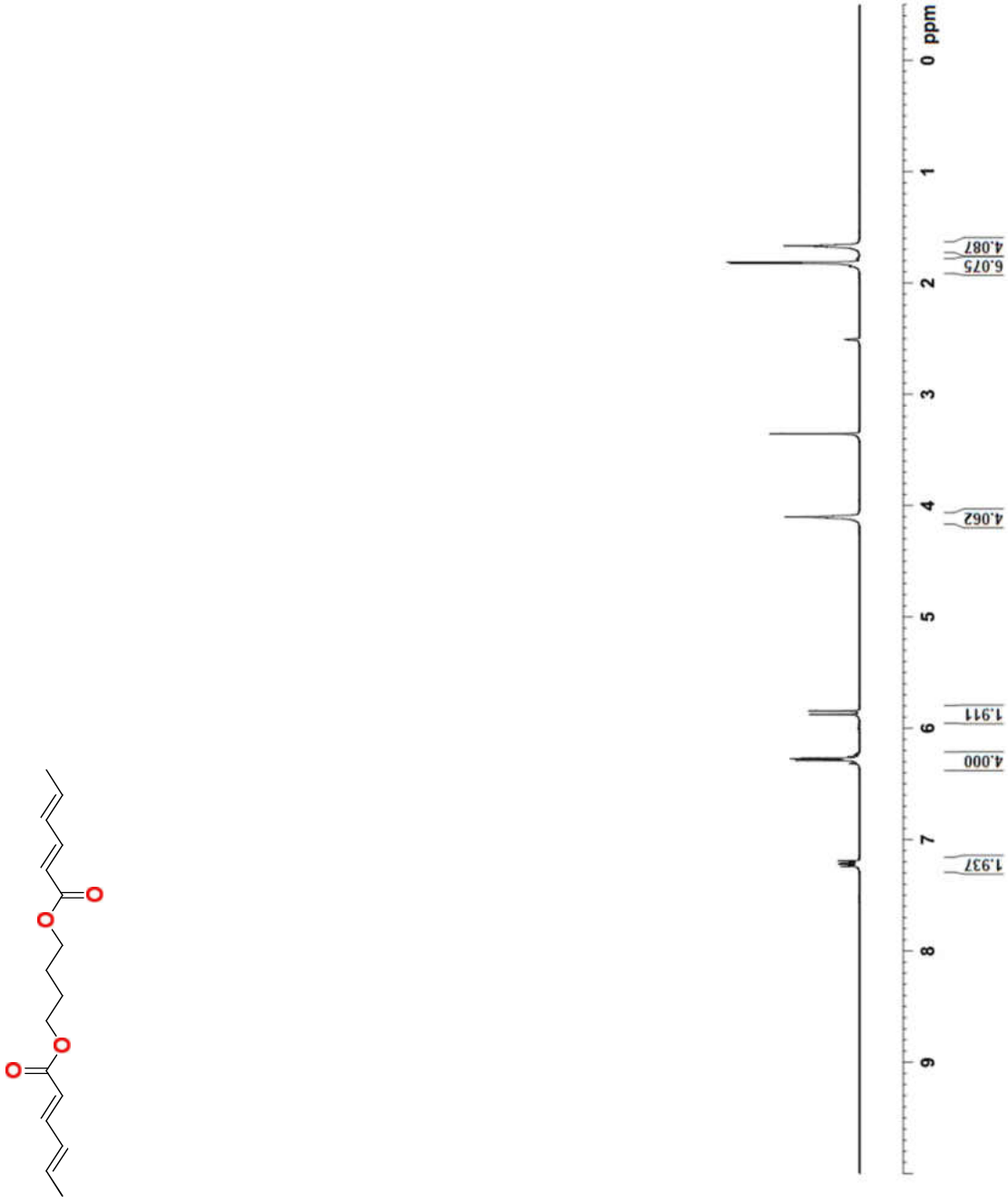

Figure 48. ^{1}H-NMR spectrum of monomer **12** in DMSO-d_6 at room temperature.

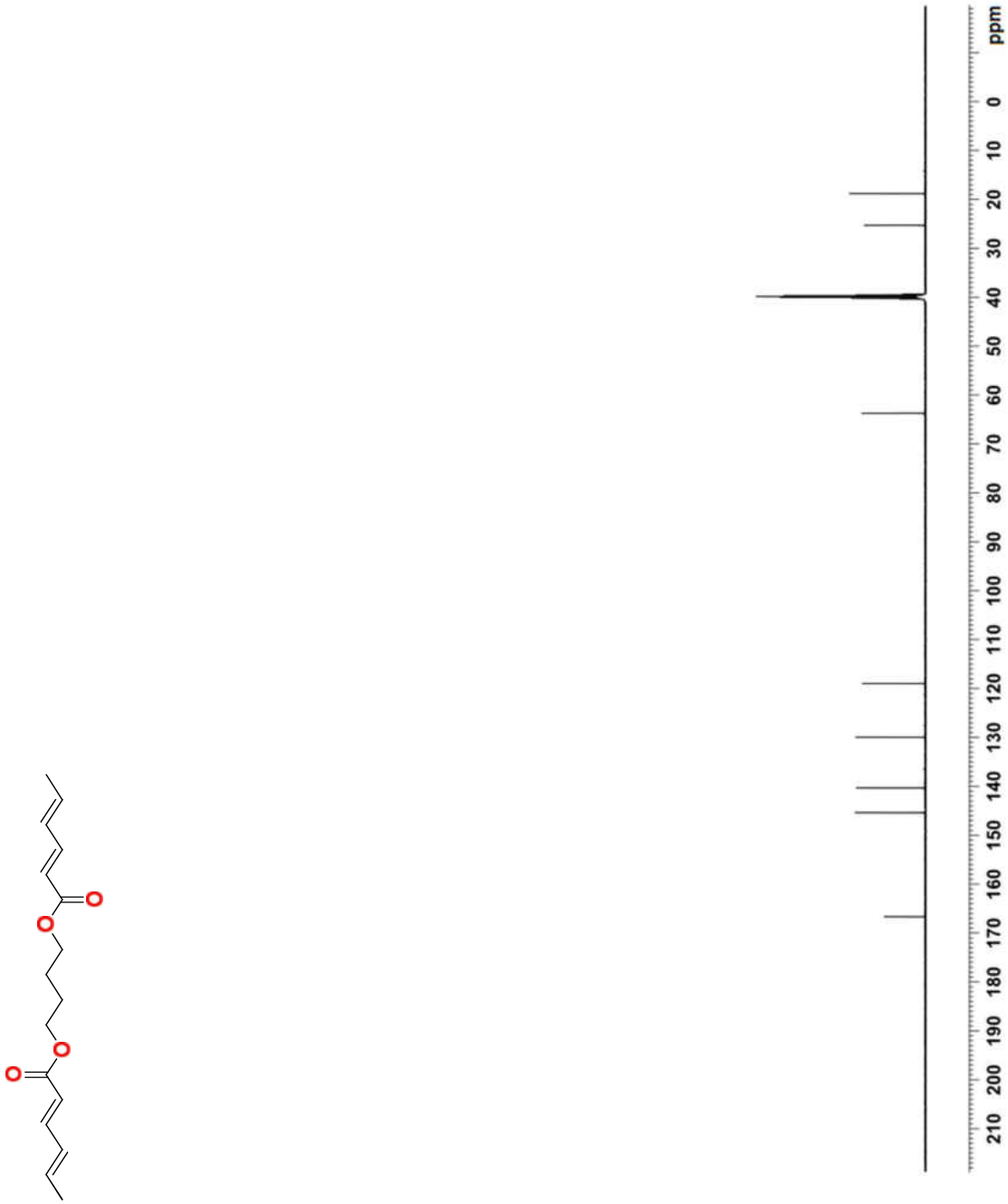

Figure 49. ^{13}C-NMR spectrum of monomer **12** in DMSO-d_6 at room temperature.

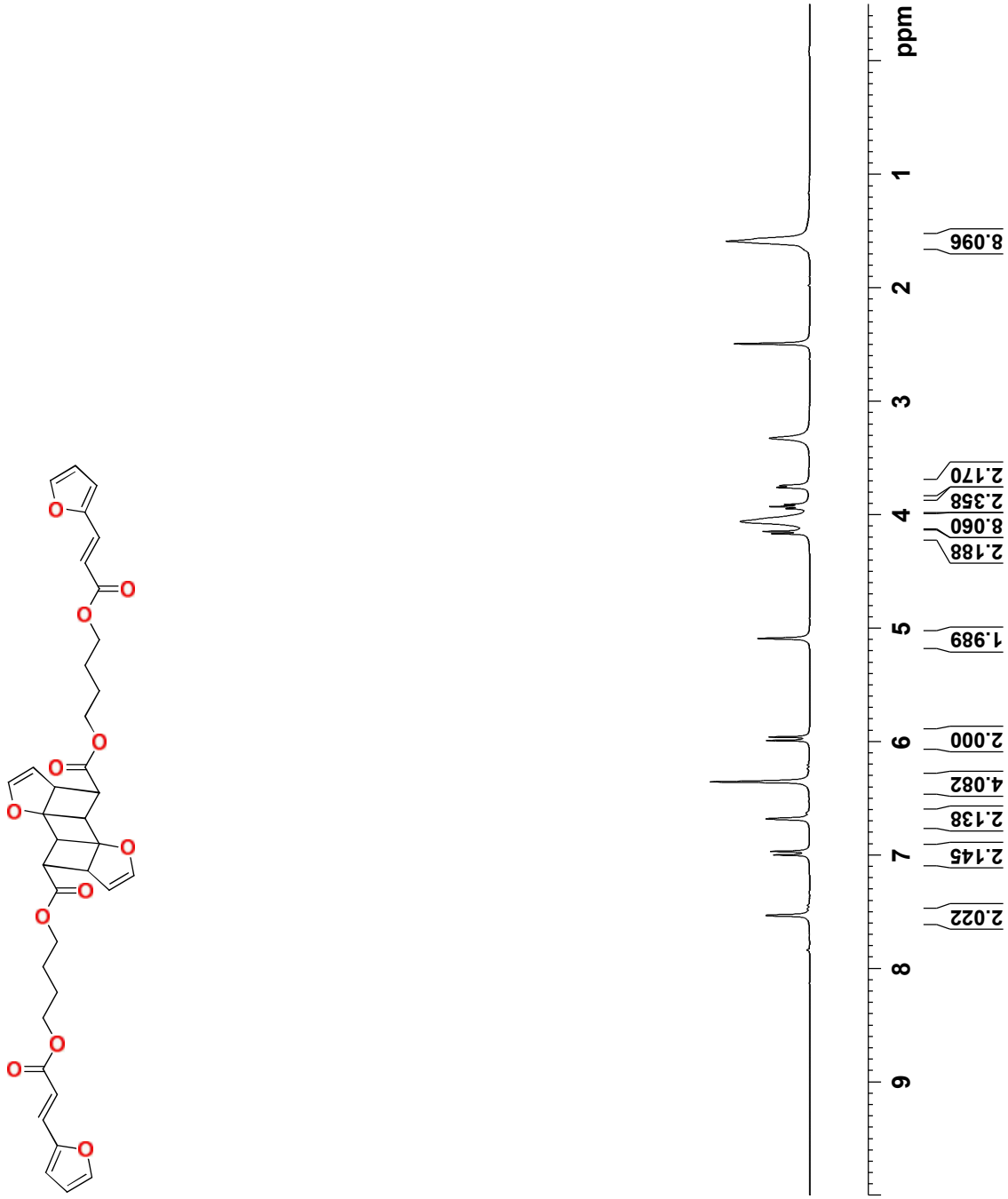

Figure 50. ^{1}H-NMR spectrum of **7b** in DMSO-d_6 at room temperature.

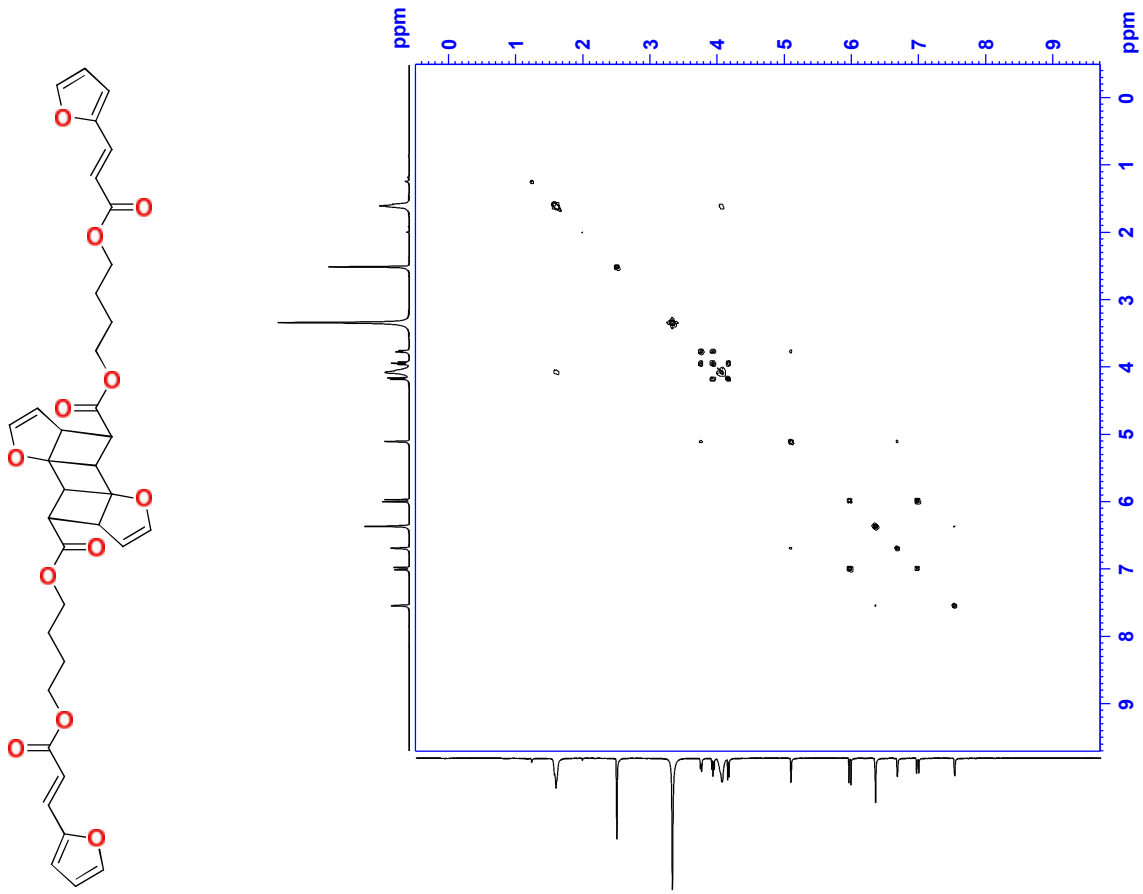

Figure 51. COSY NMR spectrum of **7b** in DMSO-d_6 at room temperature.

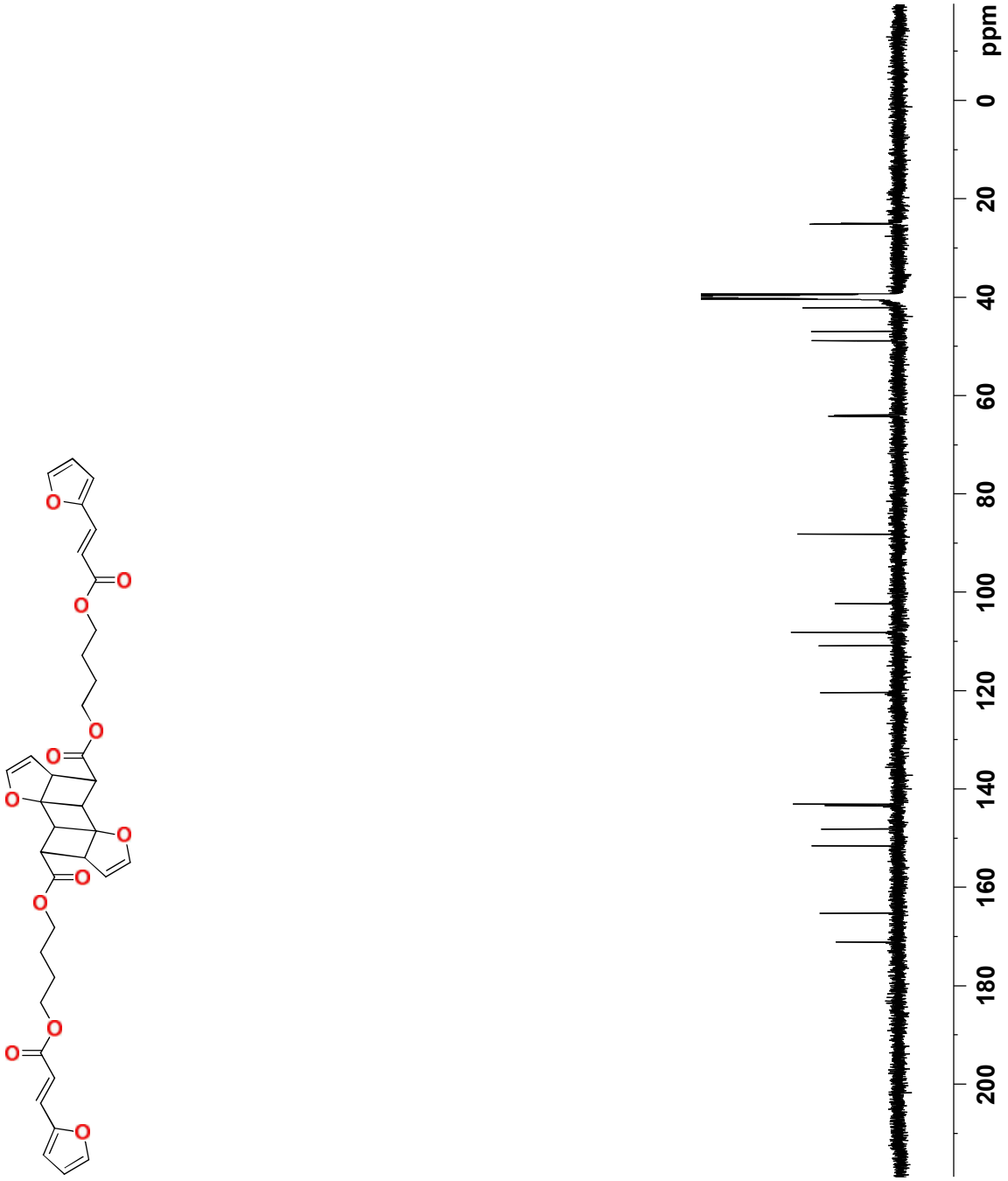

Figure 52. ^{13}C-NMR spectrum of **7b** in DMSO-d_6 at room temperature.

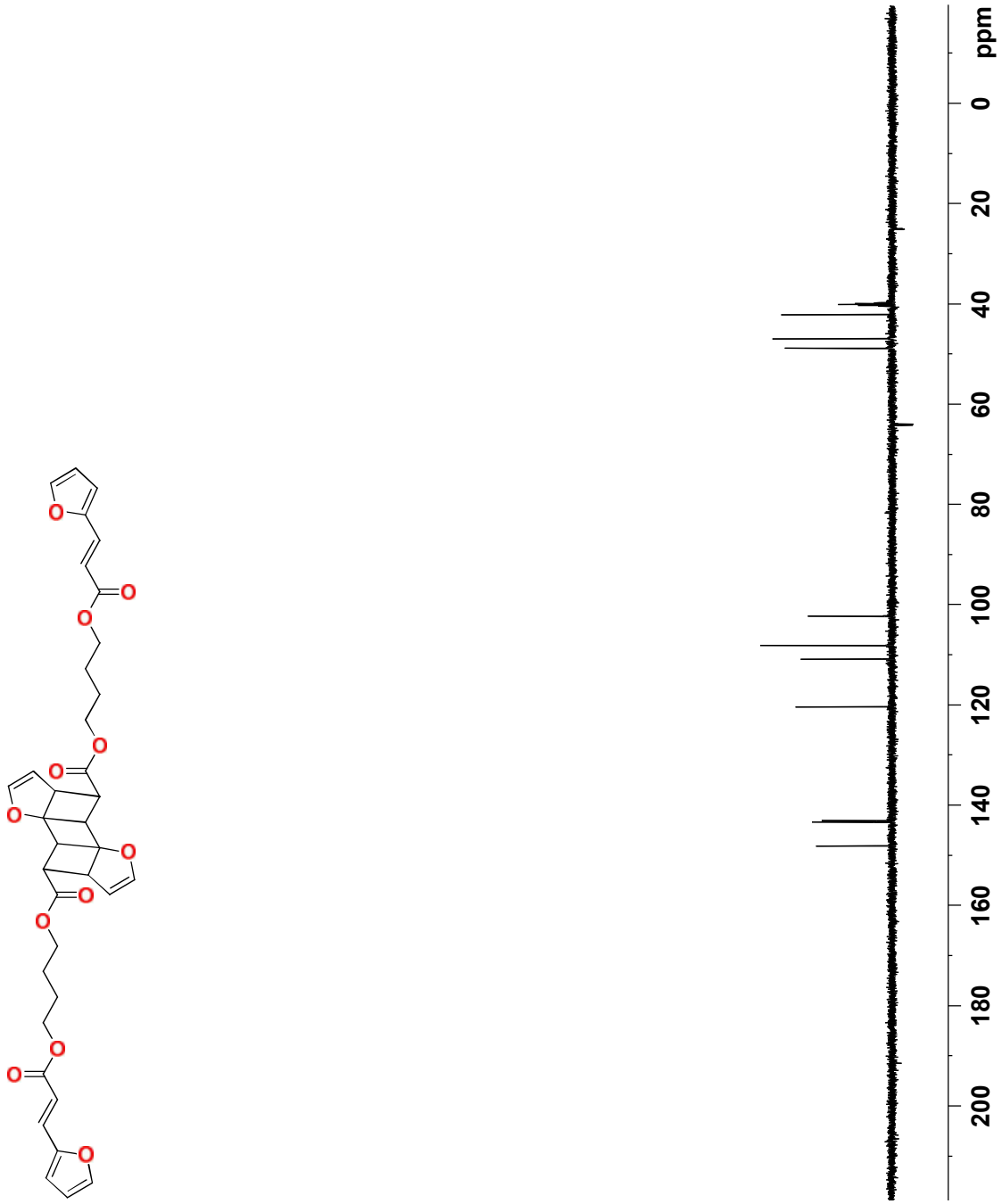

Figure 53. DEPT 90 NMR spectrum of **7b** in DMSO-d_6 at room temperature.

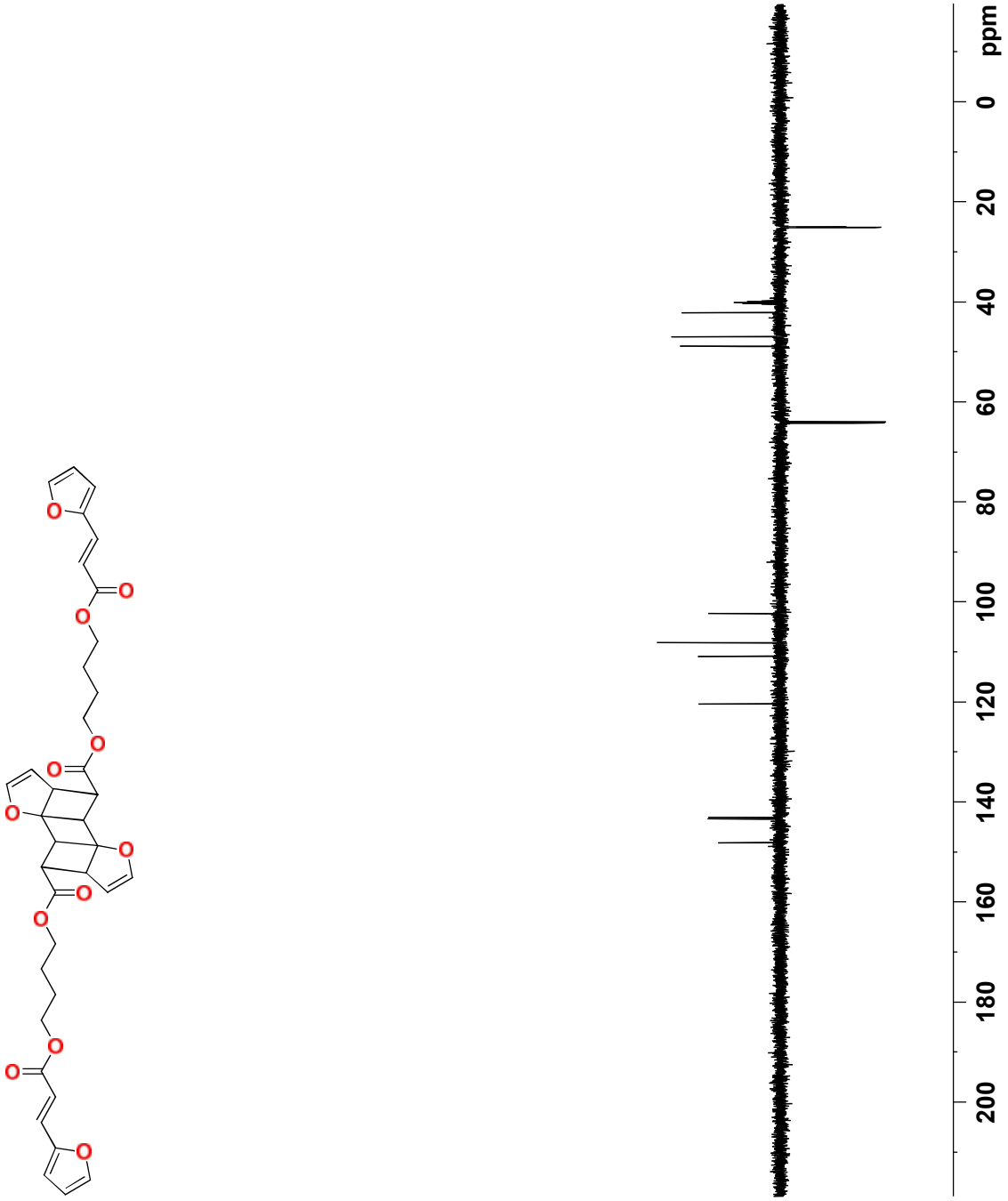

Figure 54. DEPT 135 NMR spectrum of **7b** in DMSO-d_6 at room temperature.

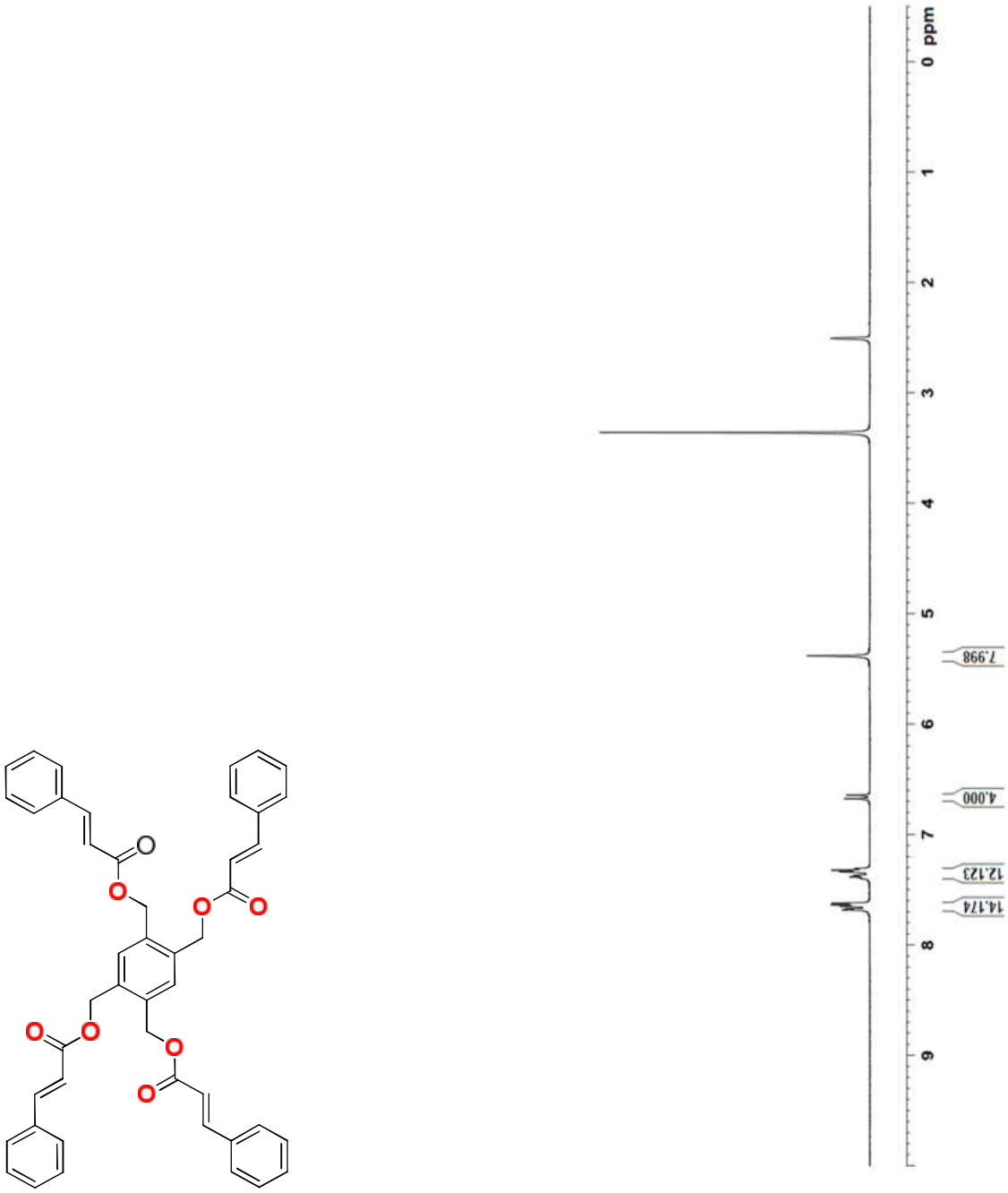

Figure 55. ^{1}H-NMR spectrum of monomer **16** in DMSO-d_6 at room temperature.

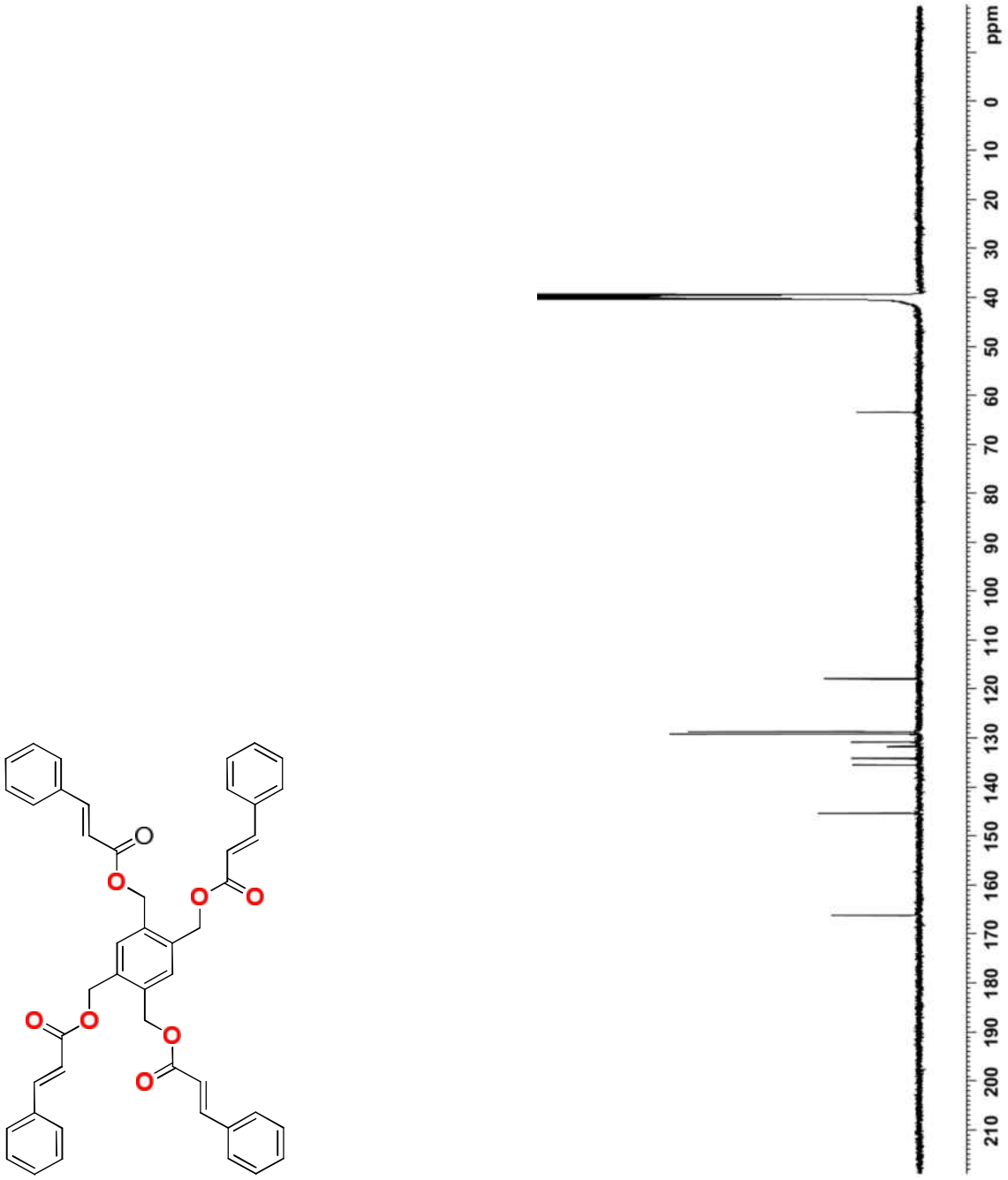

Figure 56. ^{13}C-NMR spectrum of monomer **16** in DMSO-d_6 at room temperature.

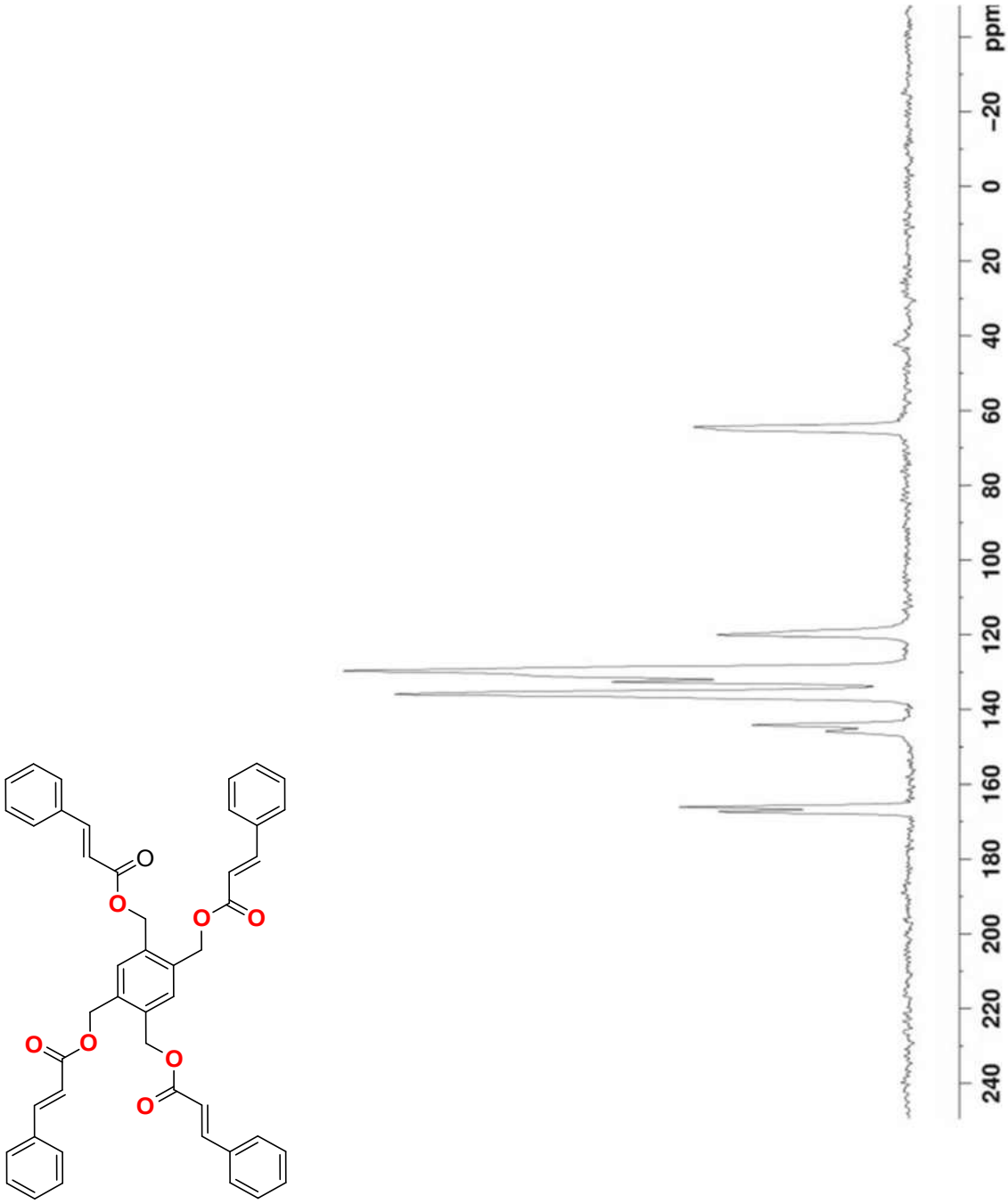

Figure 57. Solid-state NMR spectrum of monomer **16**.

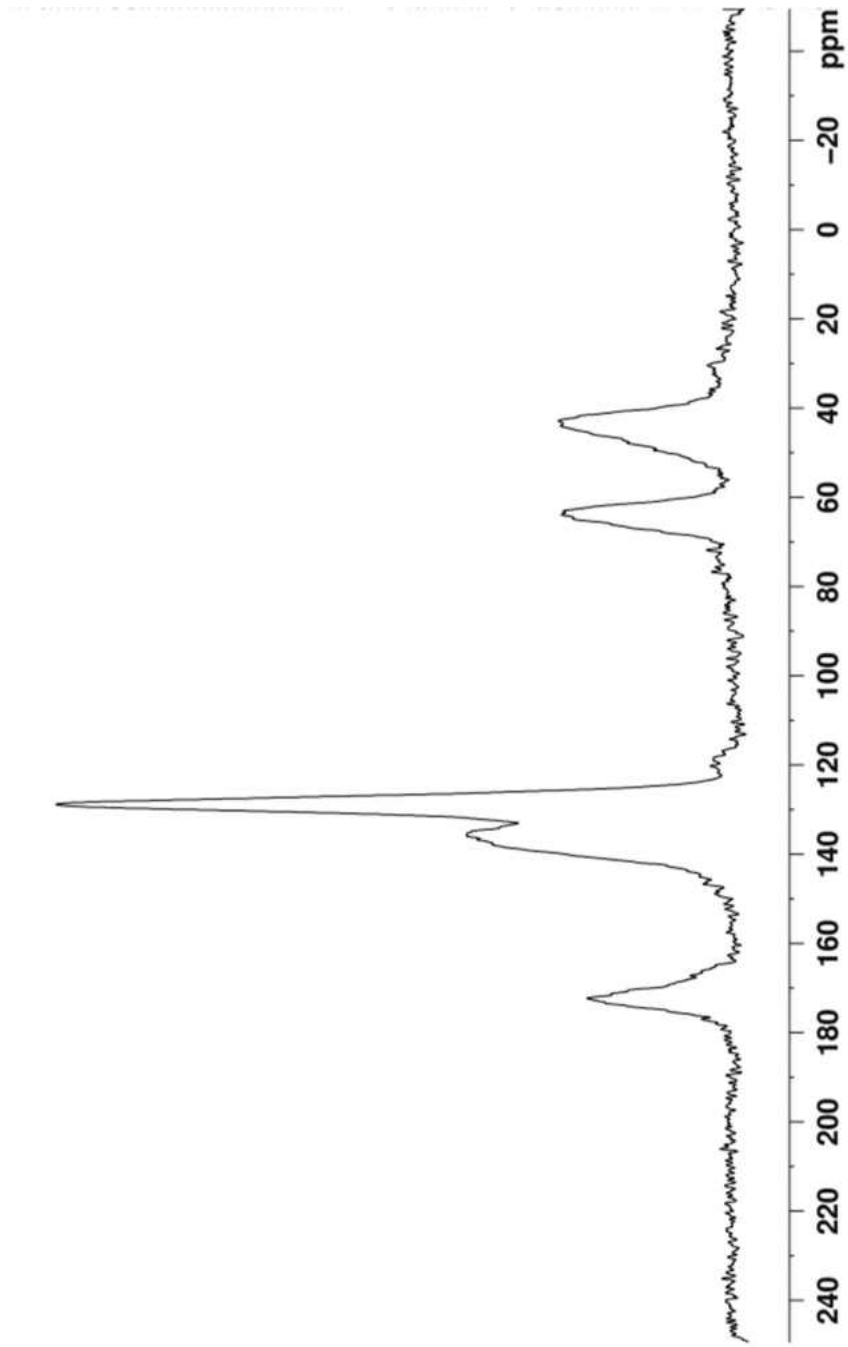

Figure 58. Solid-state NMR spectrum of **16P**.

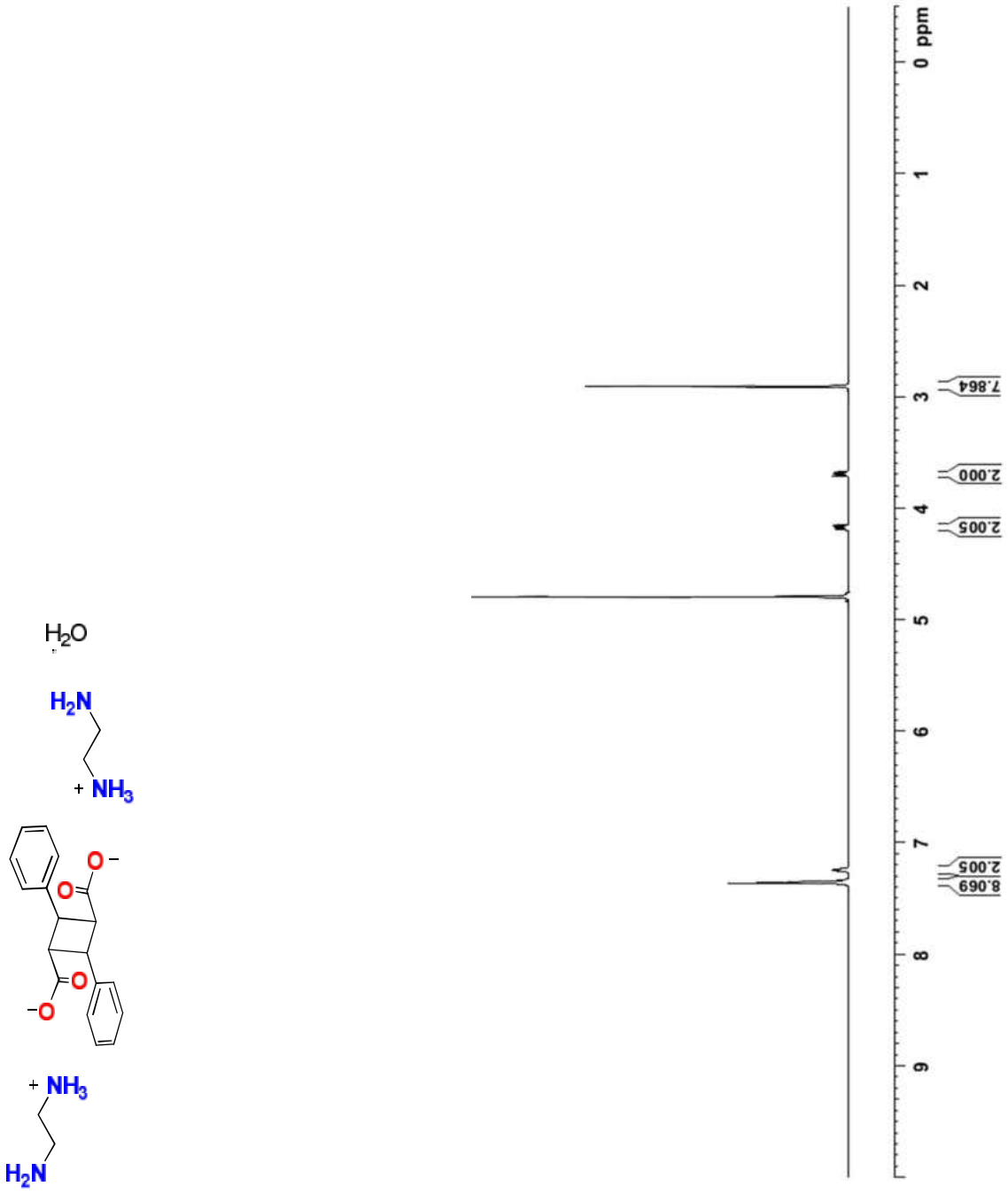

Figure 59. ^{1}H-NMR spectrum of **17a** in D_2O at room temperature.

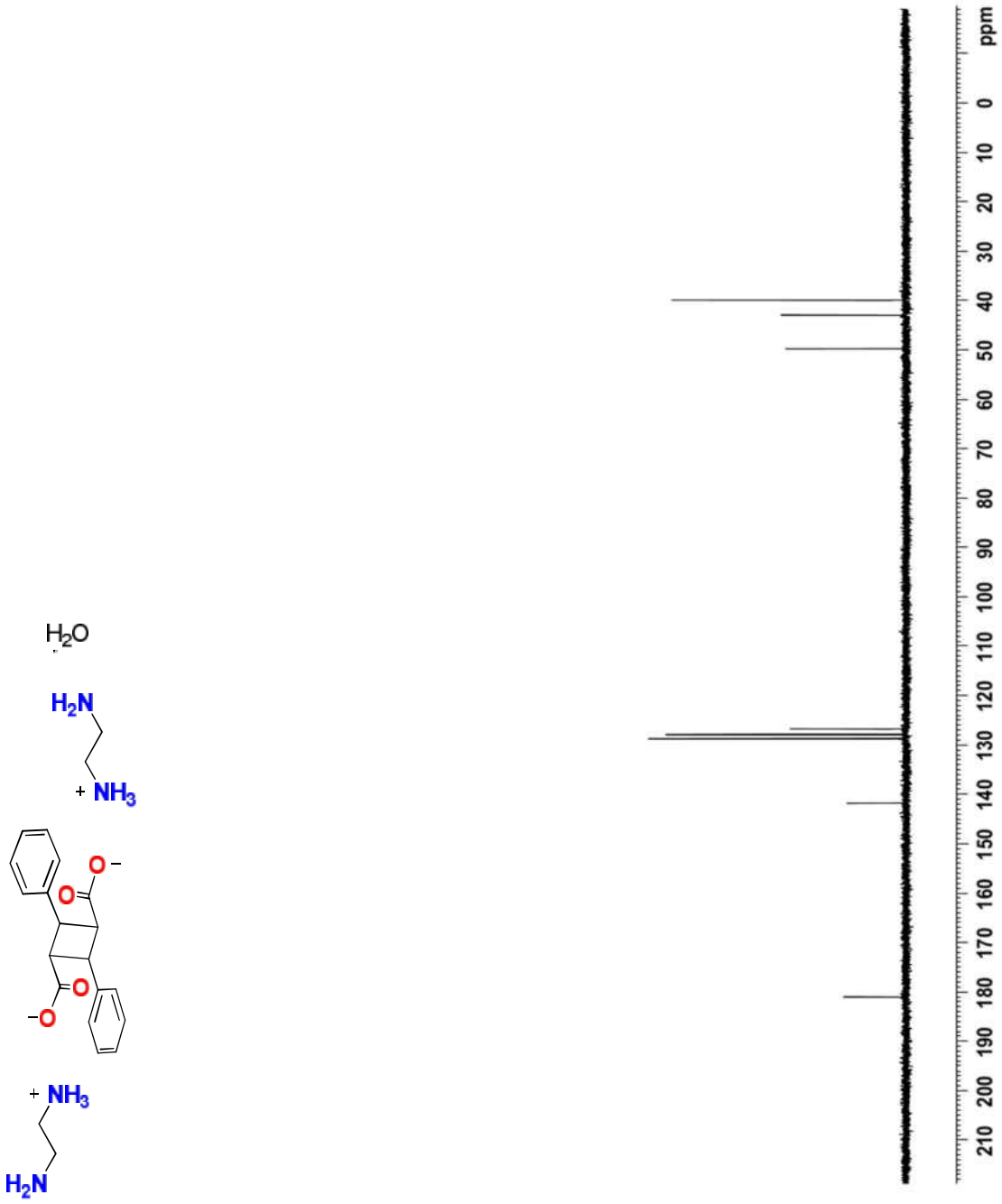

Figure 60. ^{13}C-NMR spectrum of **17a** in D_2O at room temperature.

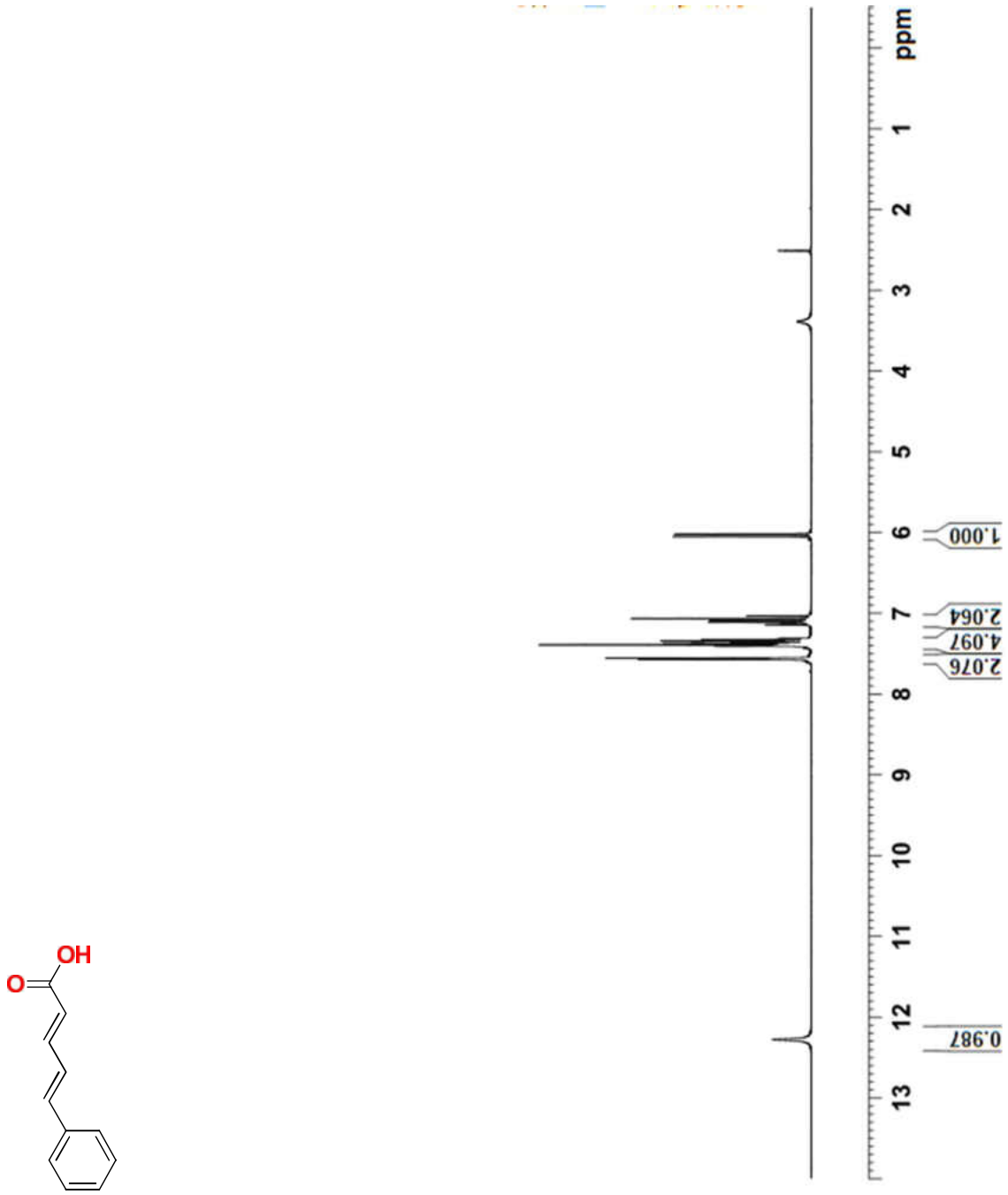

Figure 61. ^{1}H-NMR spectrum of **19** in DMSO-d_6 at room temperature.

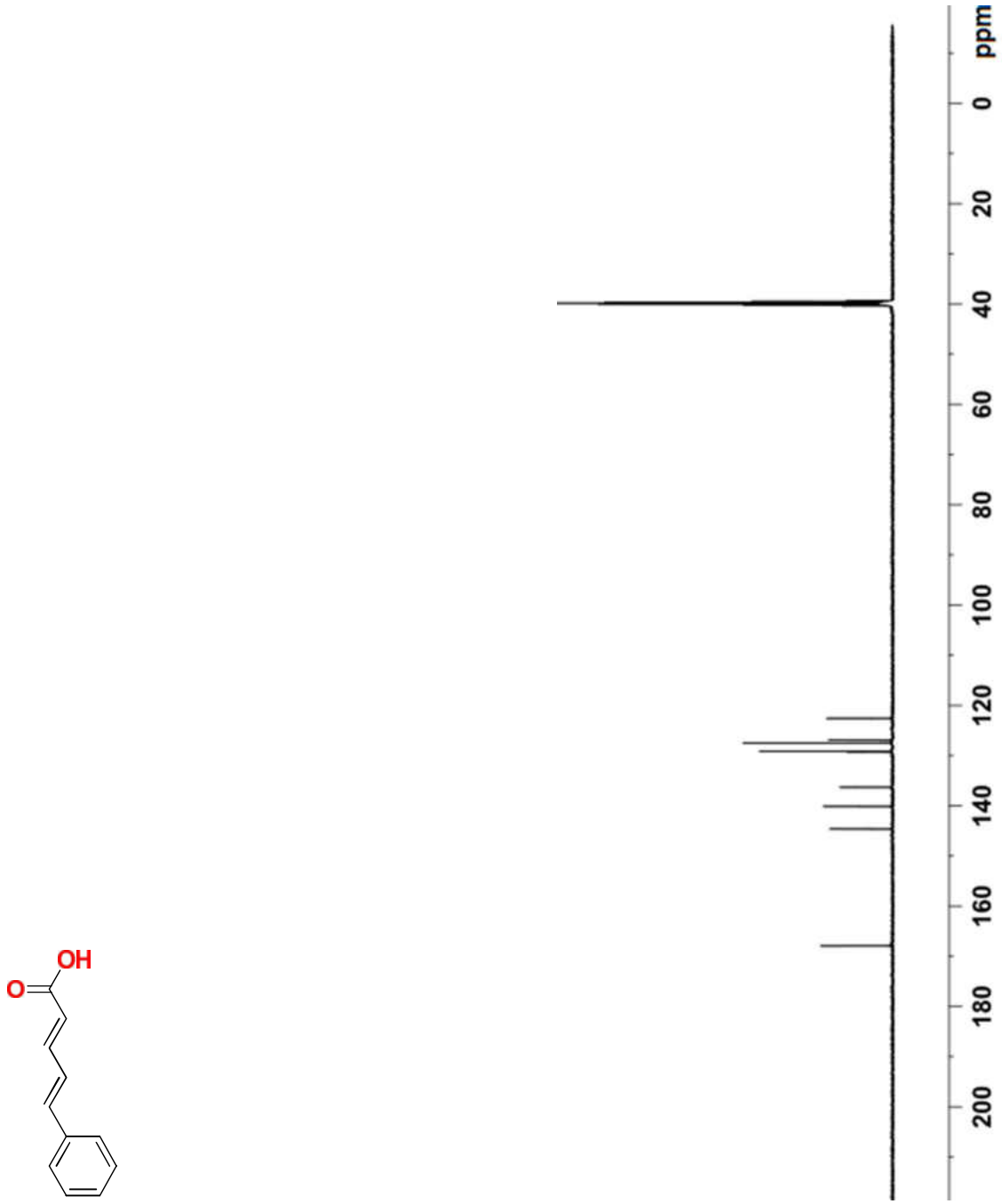

Figure 62. ^{13}C-NMR spectrum of **19** in DMSO-d_6 at room temperature.

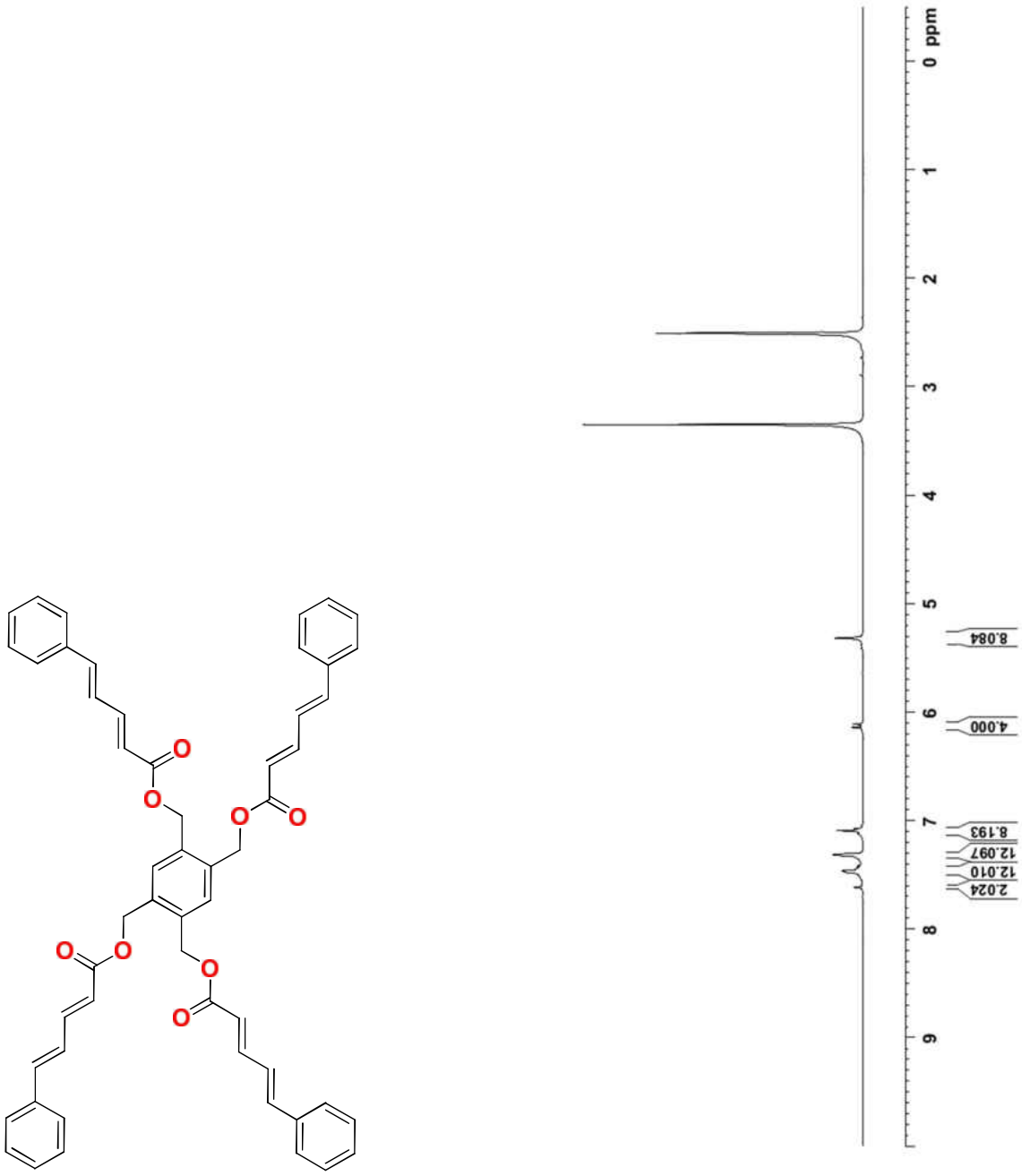

Figure 63. ^{1}H-NMR spectrum of monomer **20** in DMSO-d_6 at room temperature.

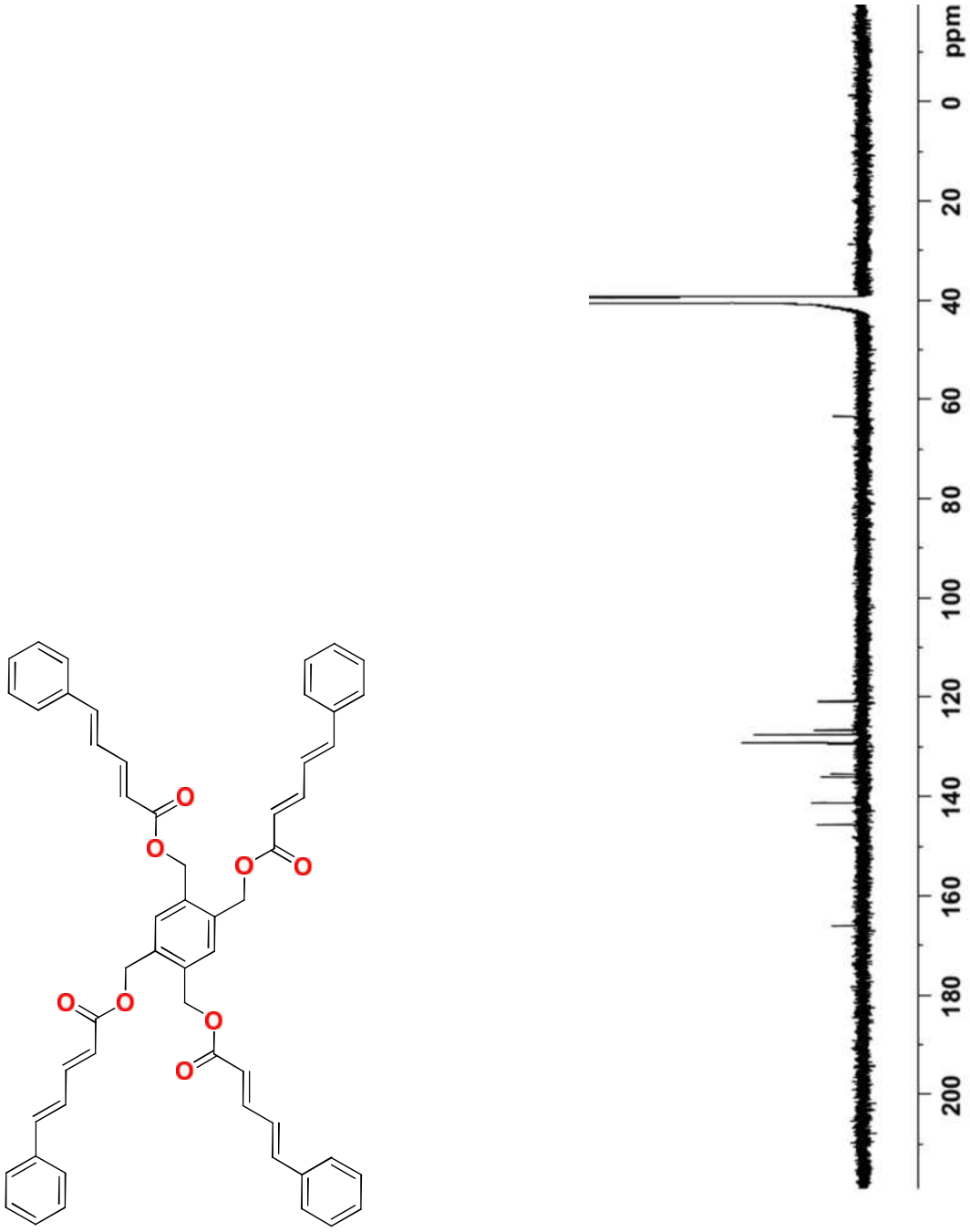

Figure 64. ^{13}C-NMR spectrum of monomer **20** in DMSO-d_6 at room temperature.

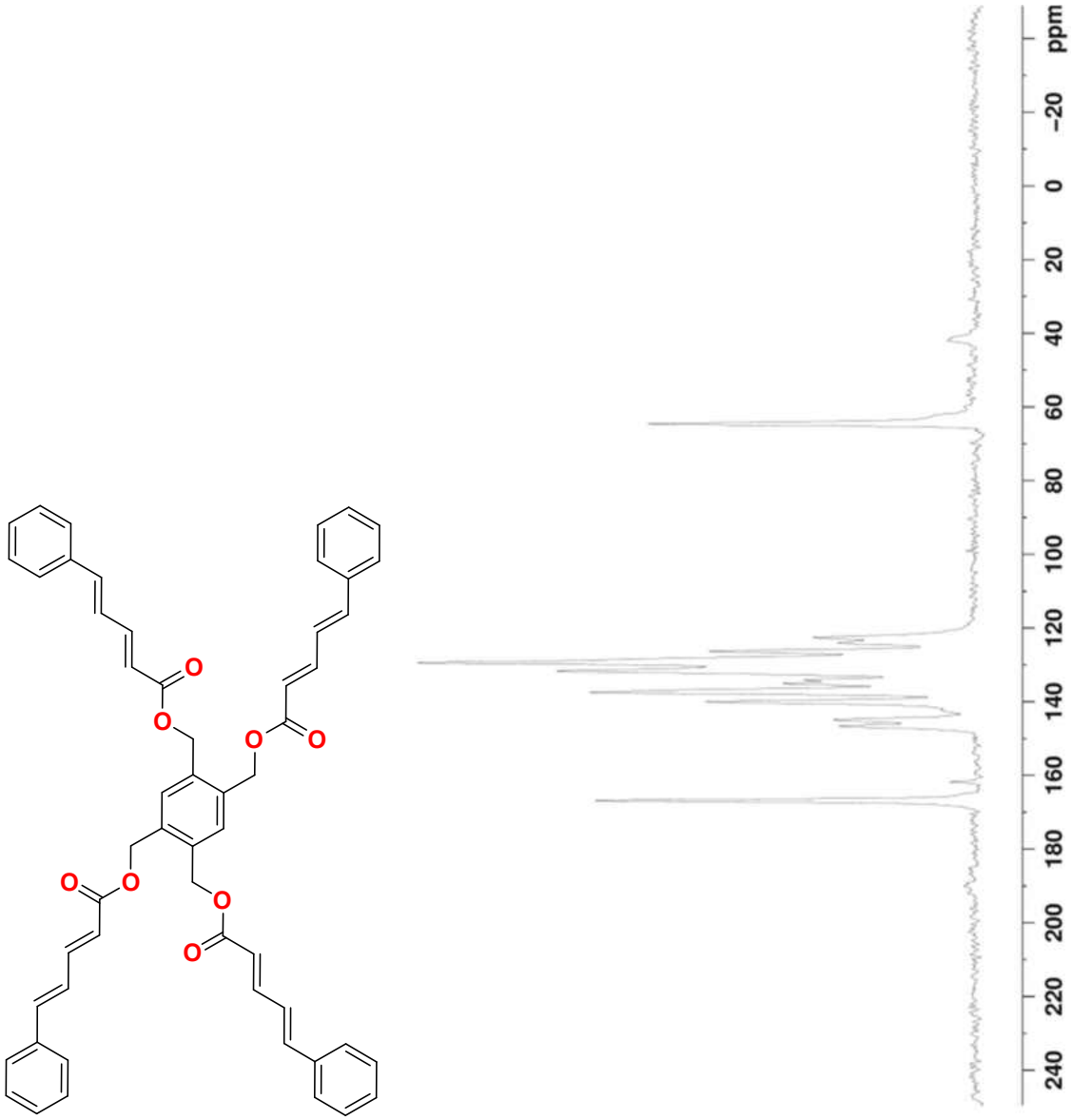

Figure 65. Solid-state NMR spectrum of monomer **20**.

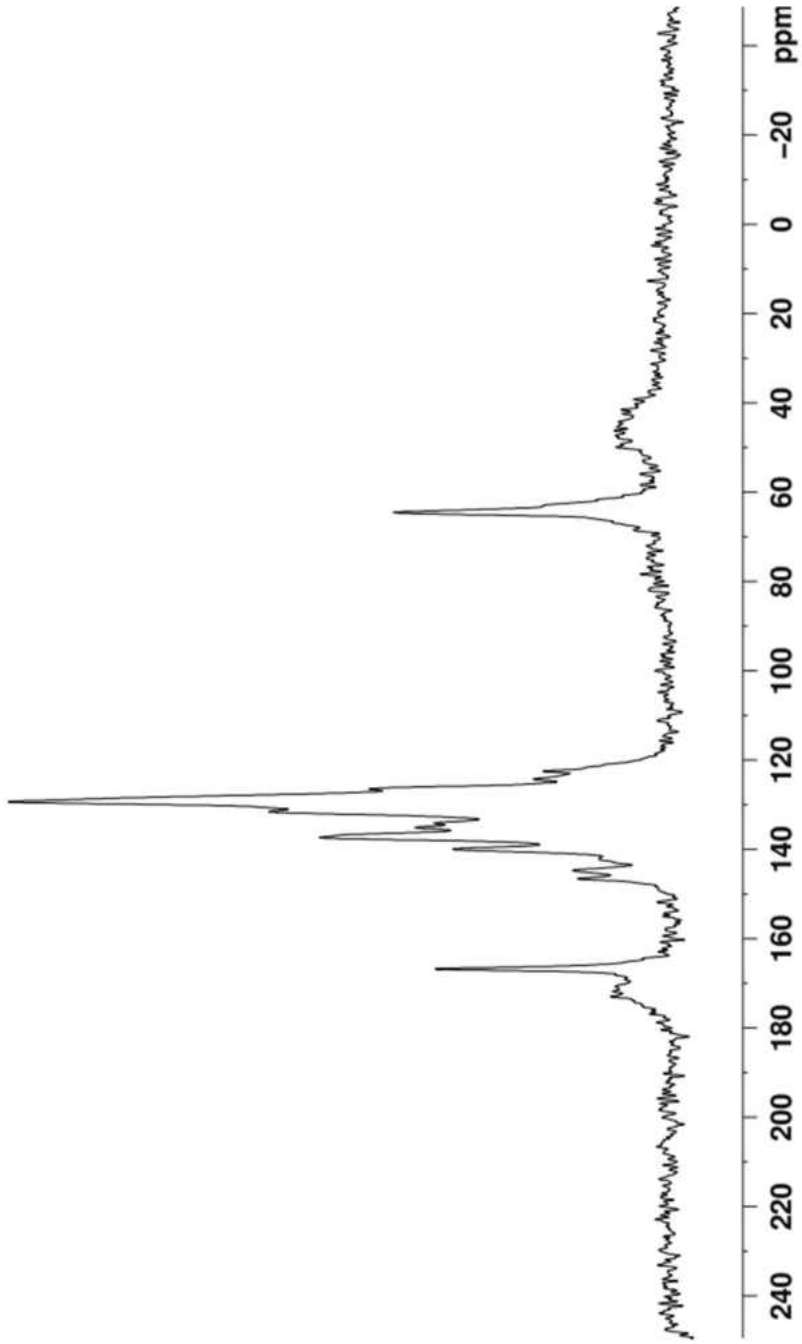

Figure 66. Solid-state NMR spectrum of **20P**.

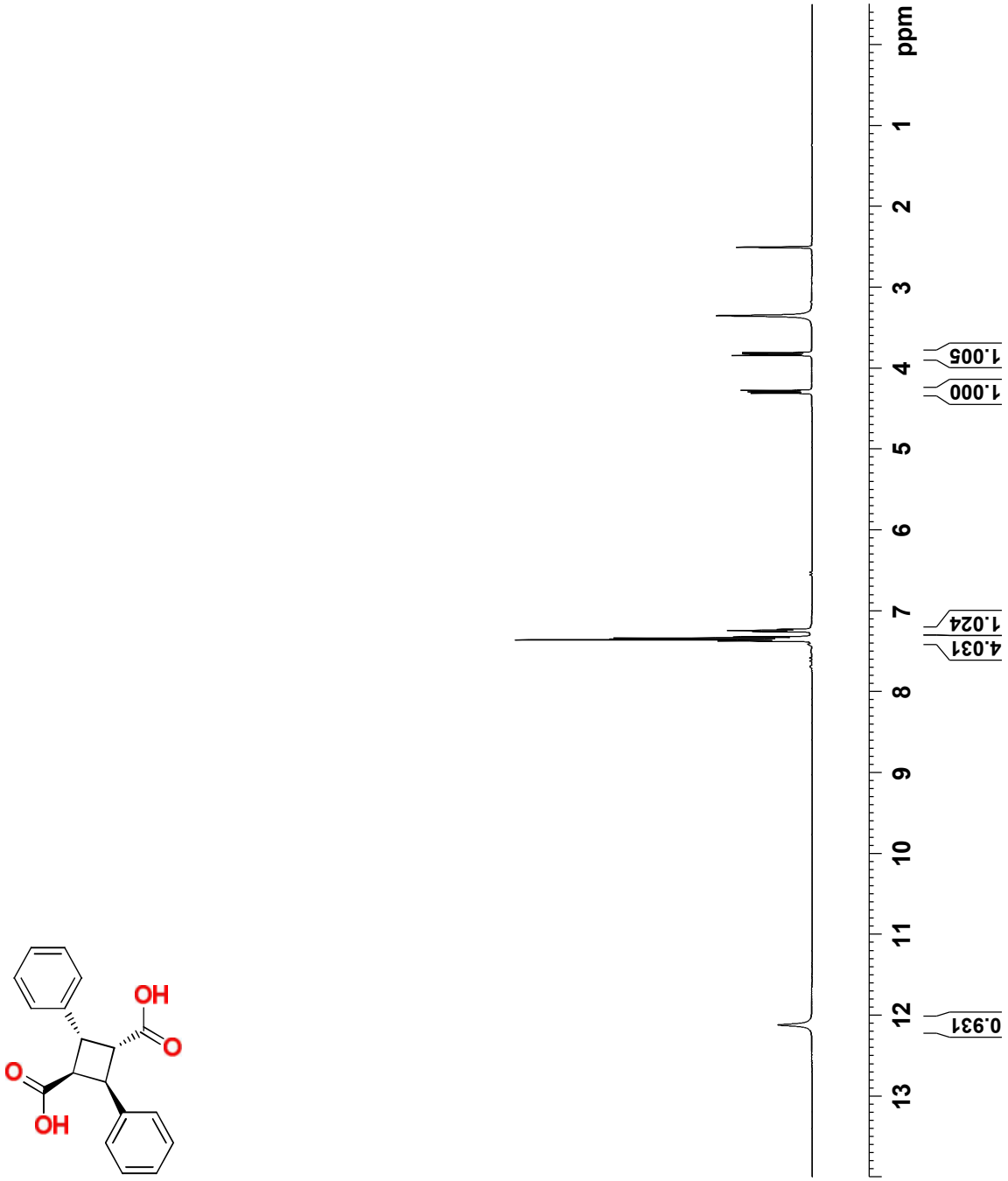

Figure 67. ^{1}H-NMR spectrum of **17** in DMSO-d_6 at room temperature.

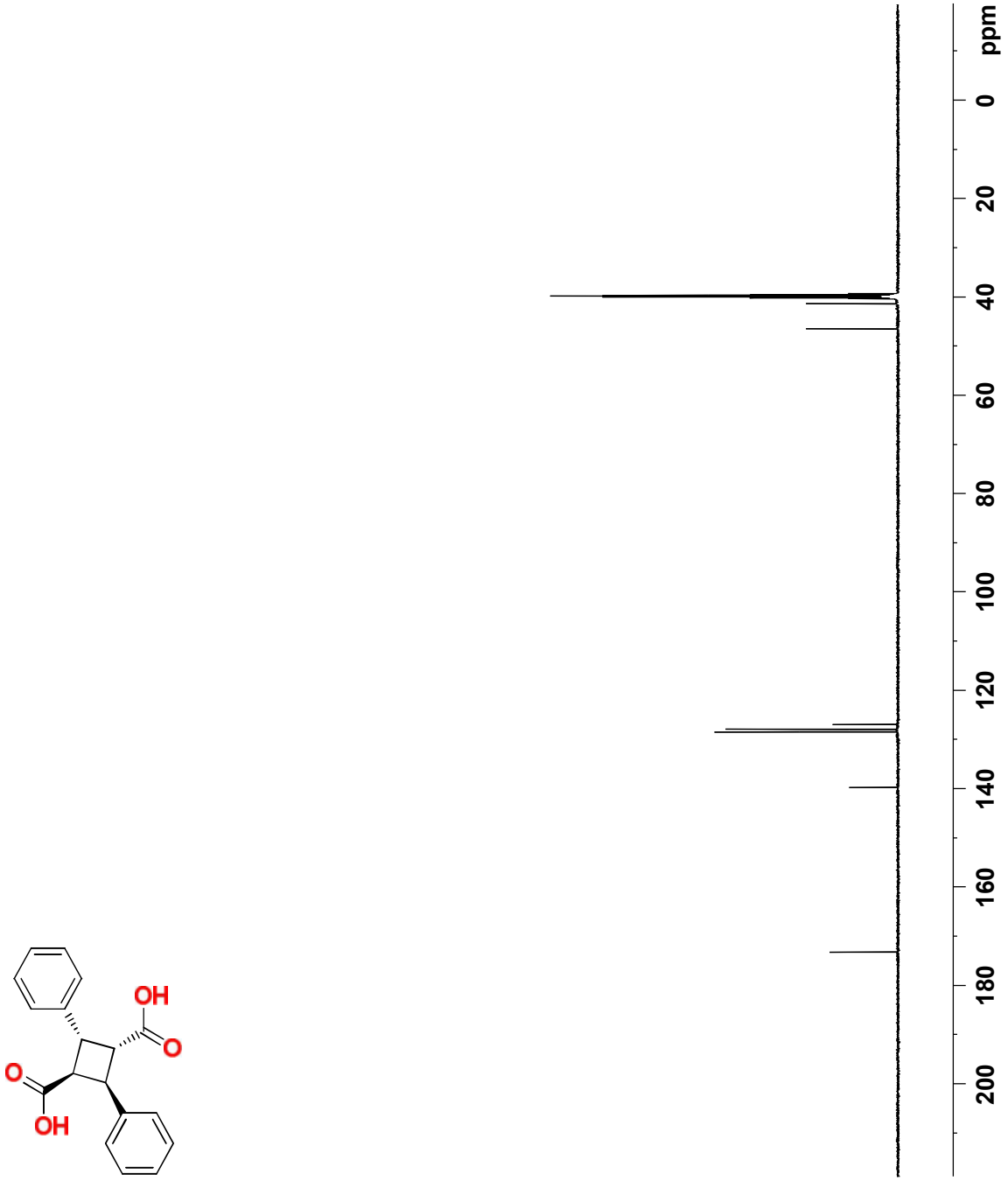

Figure 68. ^{13}C-NMR spectrum of **17** in DMSO-d_6 at room temperature.

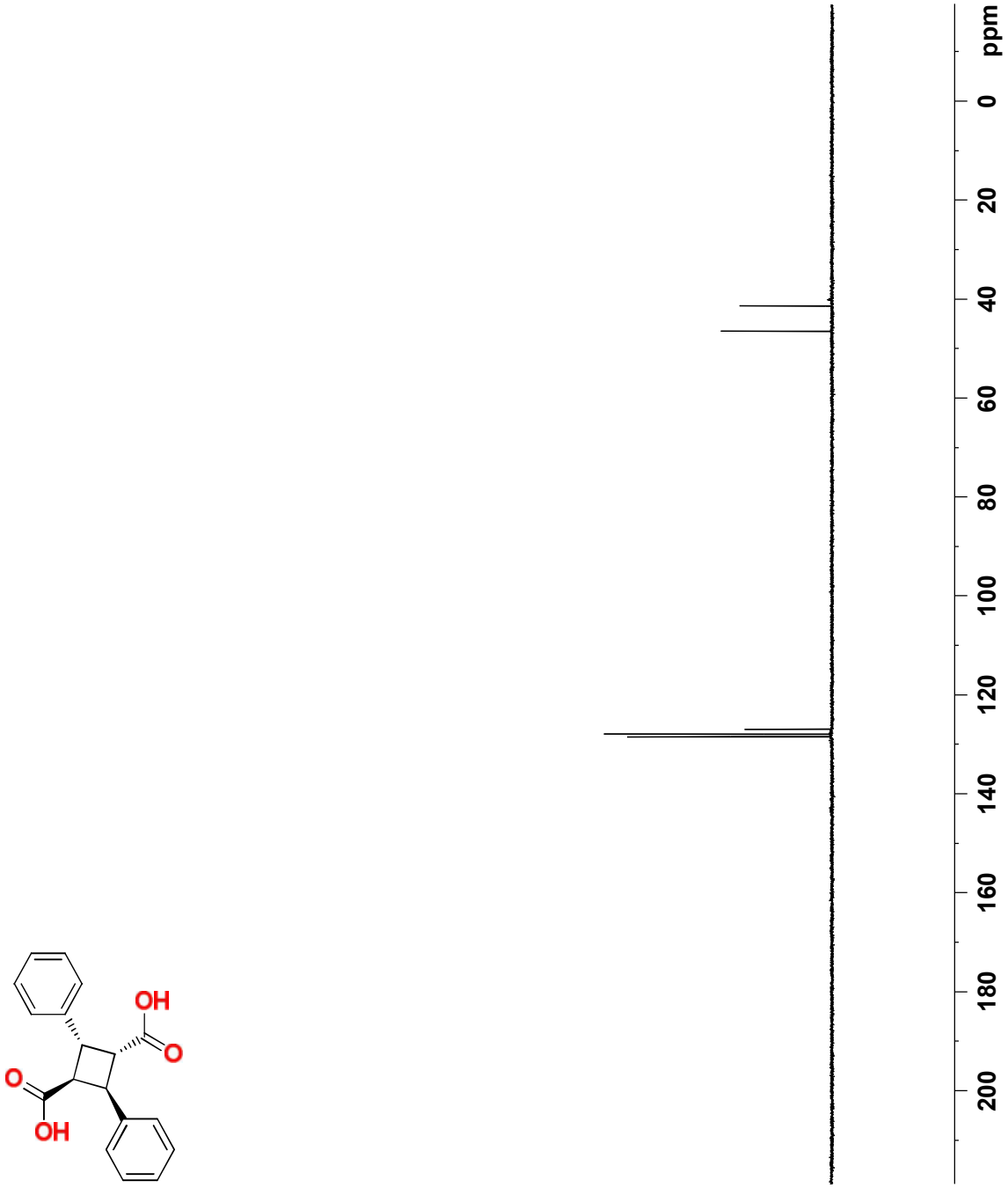

Figure 69. DEPT 135 NMR spectrum of **17** in DMSO-d_6 at room temperature.

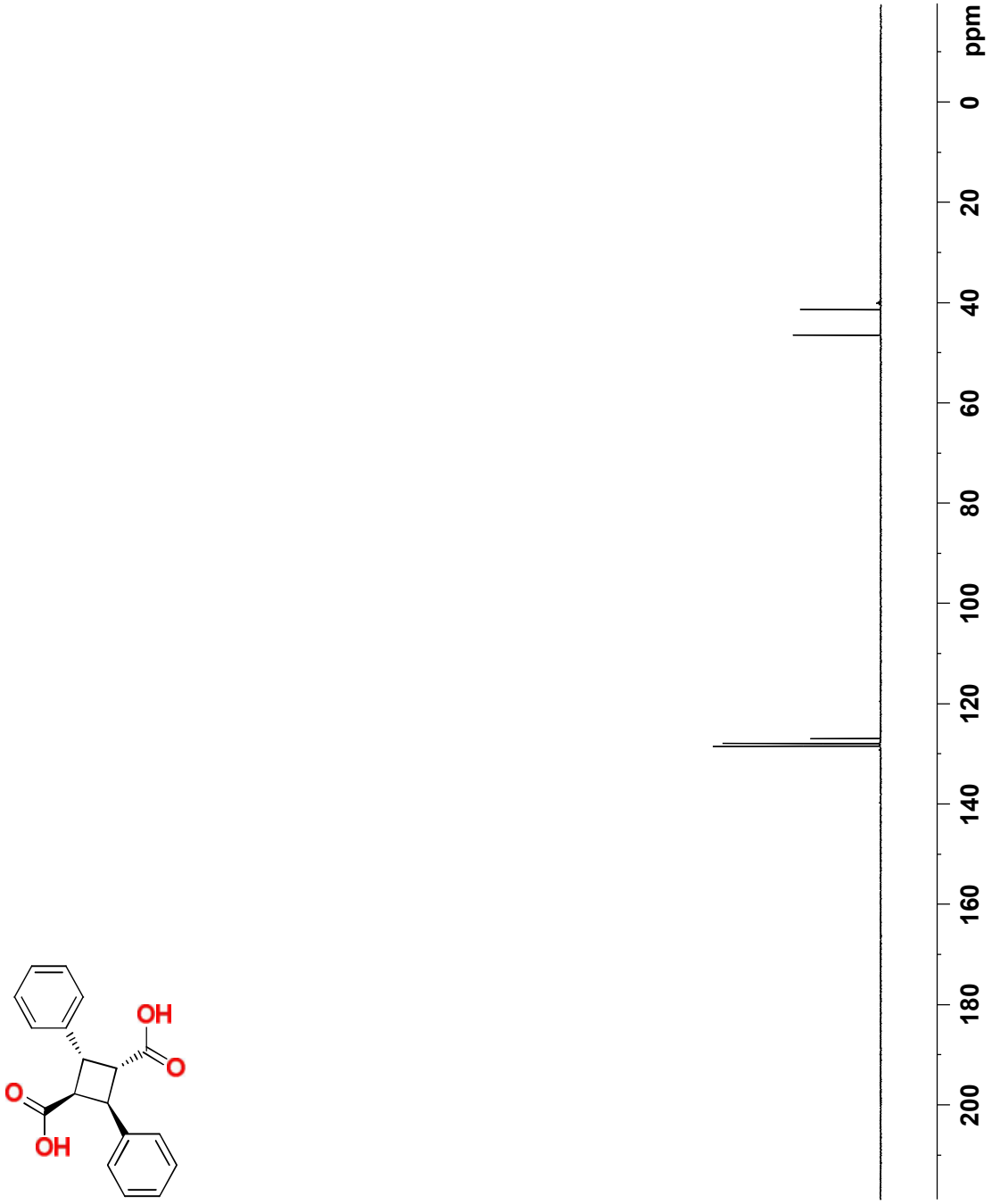

Figure 70. DEPT 90 NMR spectrum of **17** in DMSO-d_6 at room temperature.

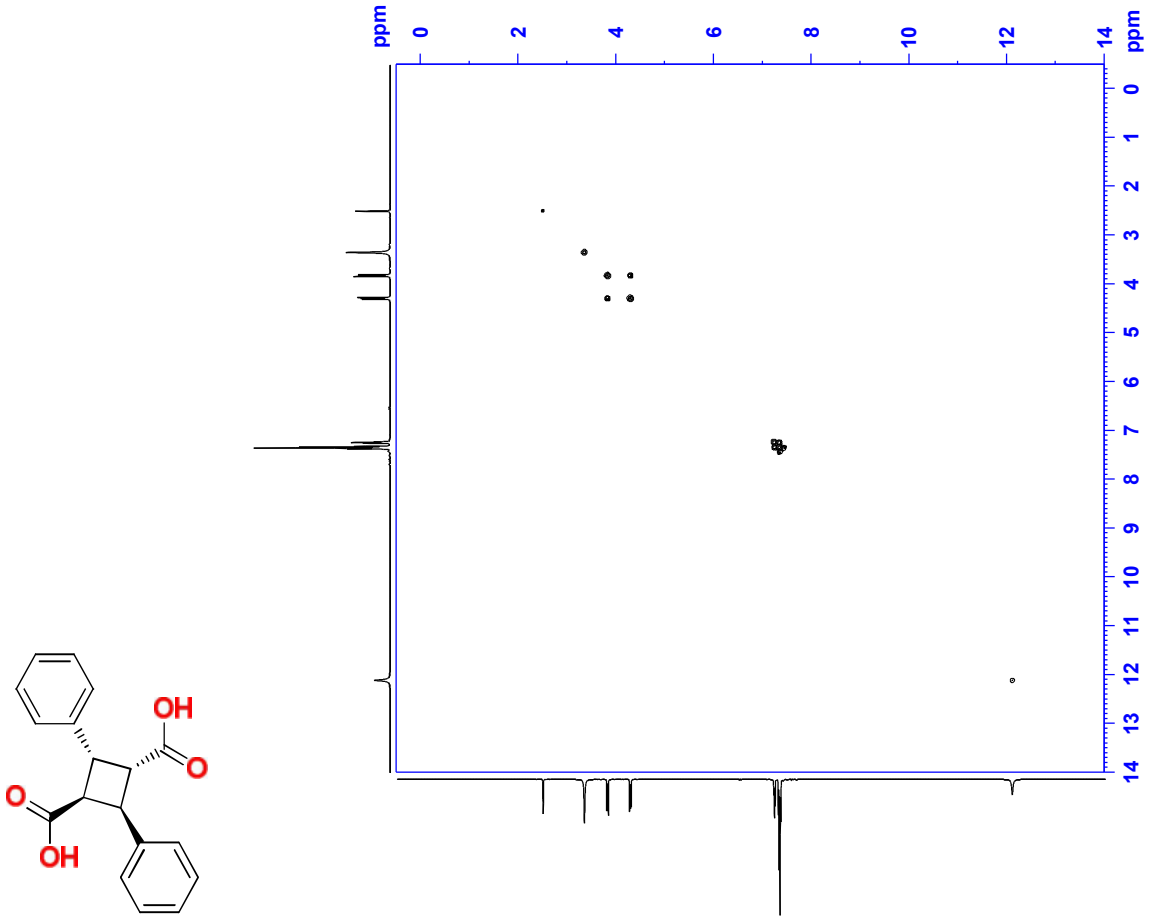

Figure 71. COSY NMR spectrum of **17** in DMSO-d_6 at room temperature.

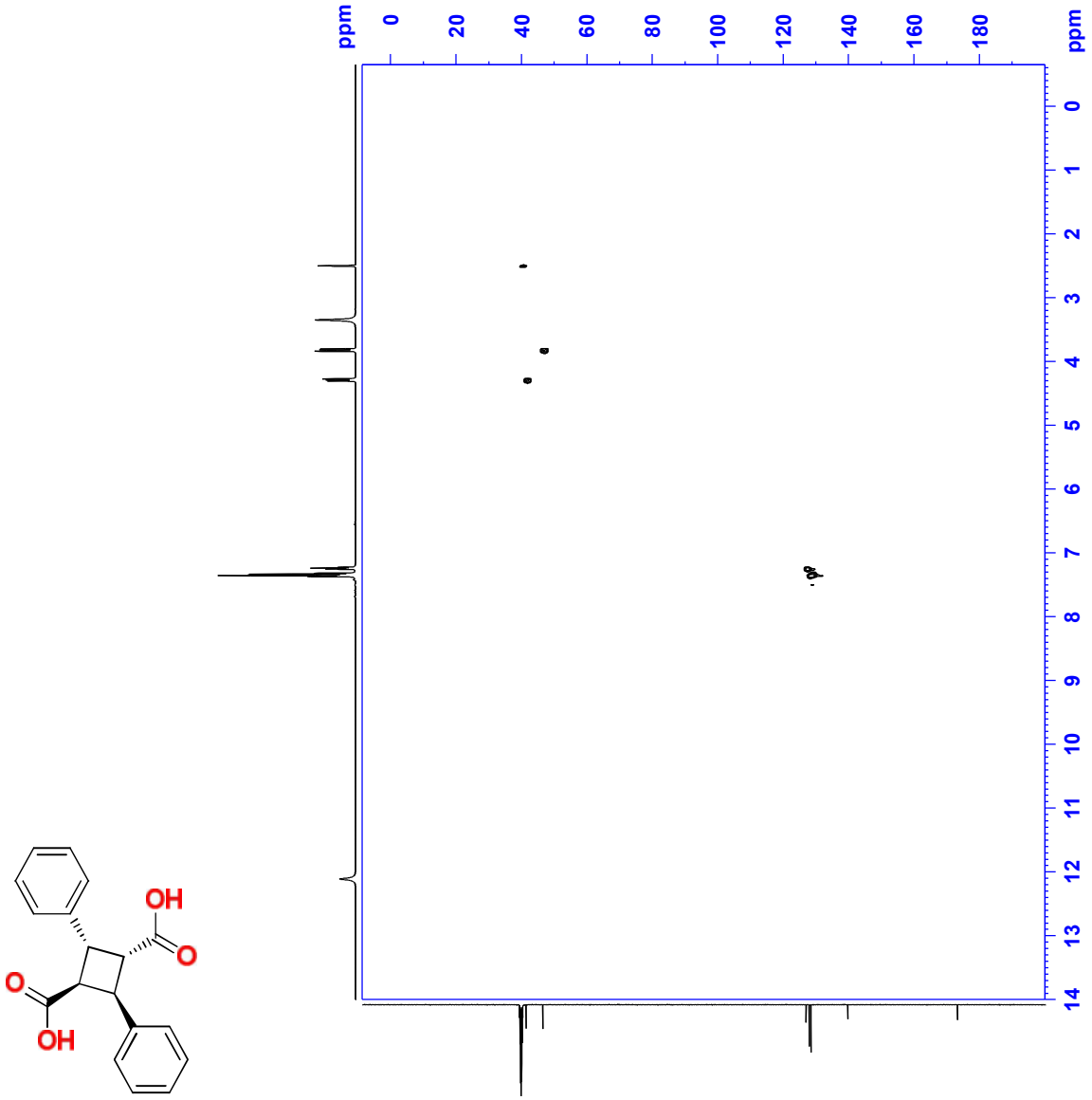

Figure 72. HSQC NMR spectrum of **17** in DMSO-d_6 at room temperature.

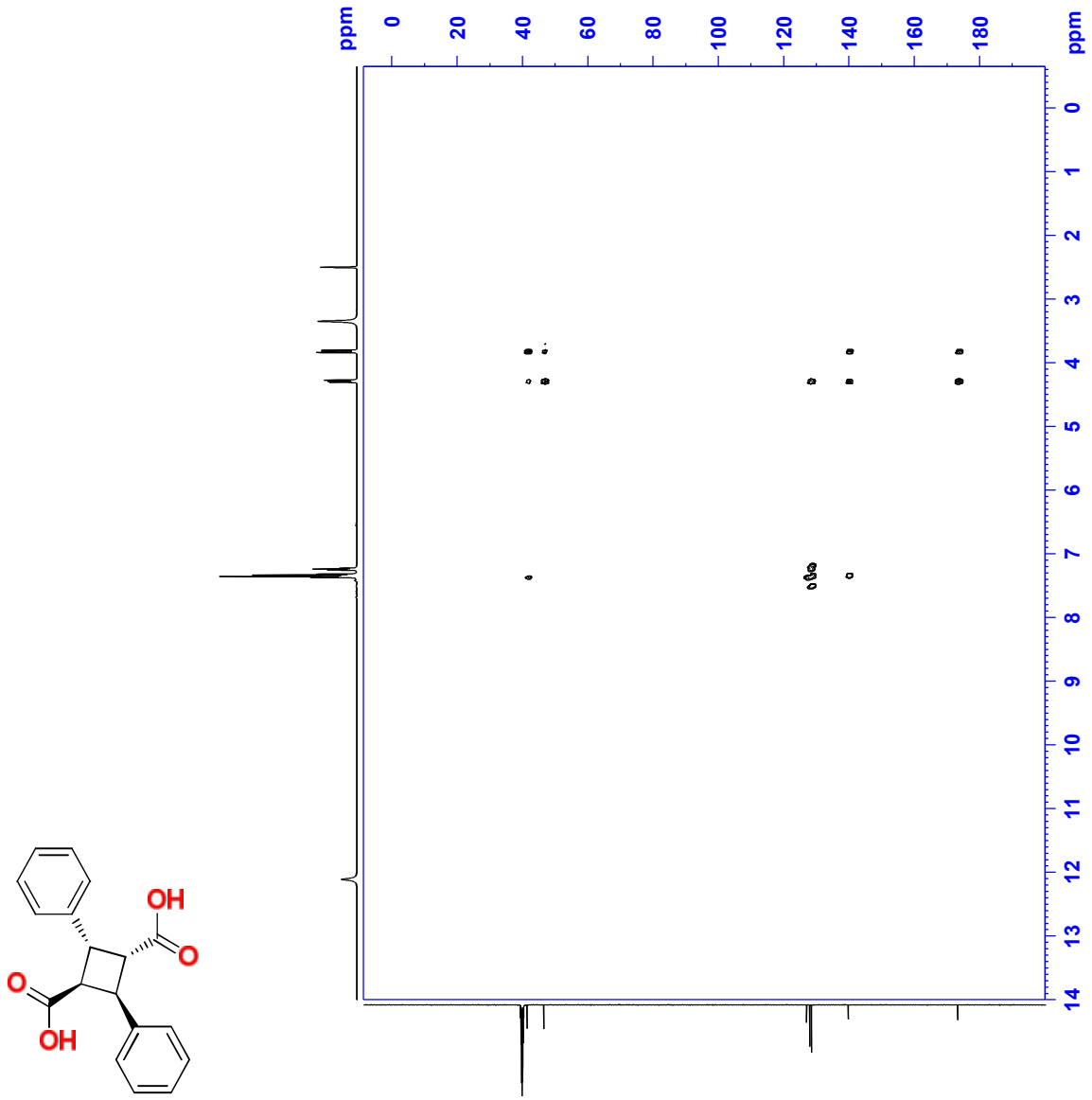

Figure 73. HMBC NMR spectrum of **17** in DMSO-d_6 at room temperature.

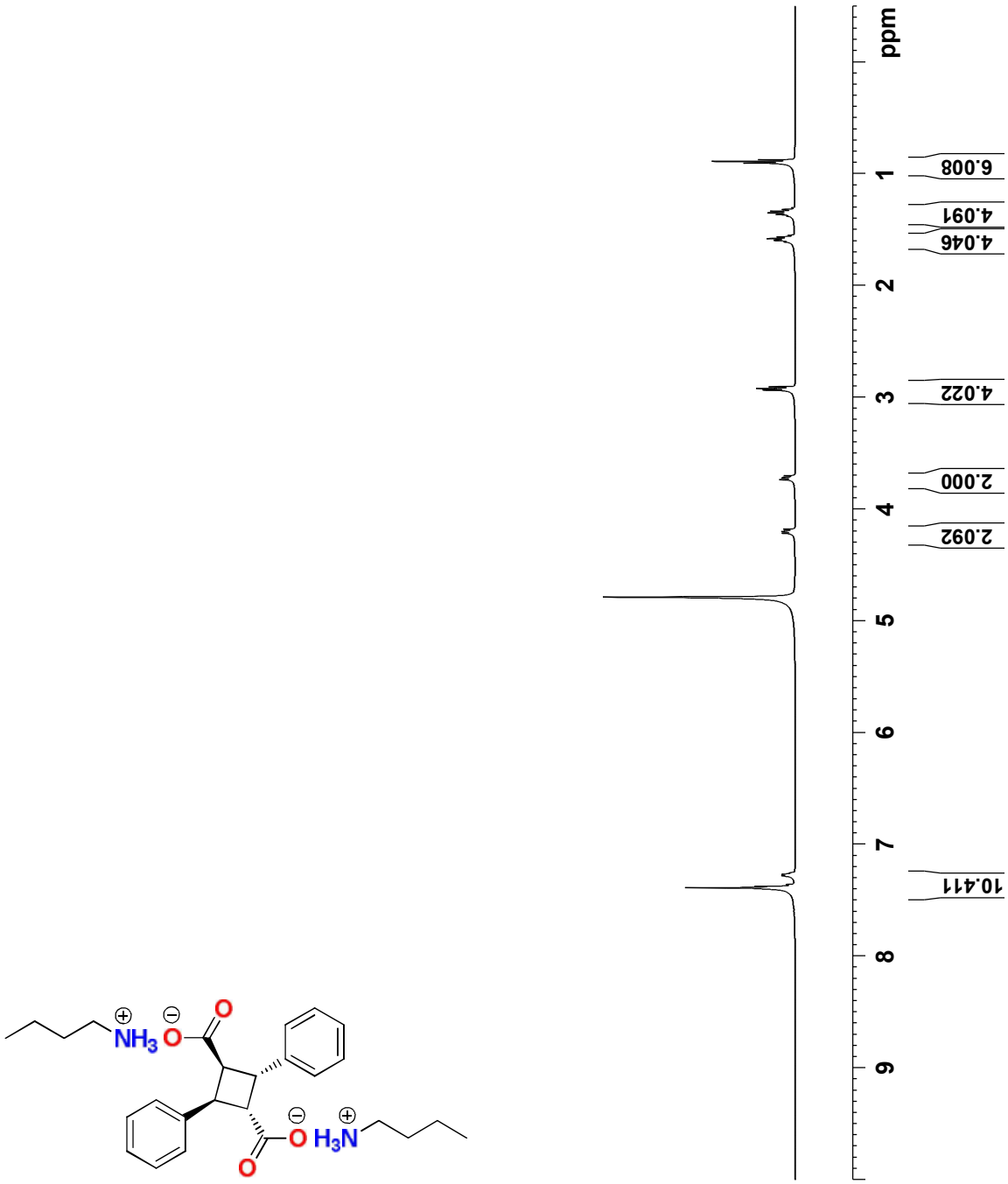

Figure 74. ^{1}H-NMR spectrum of **17b** in D_2O at room temperature.

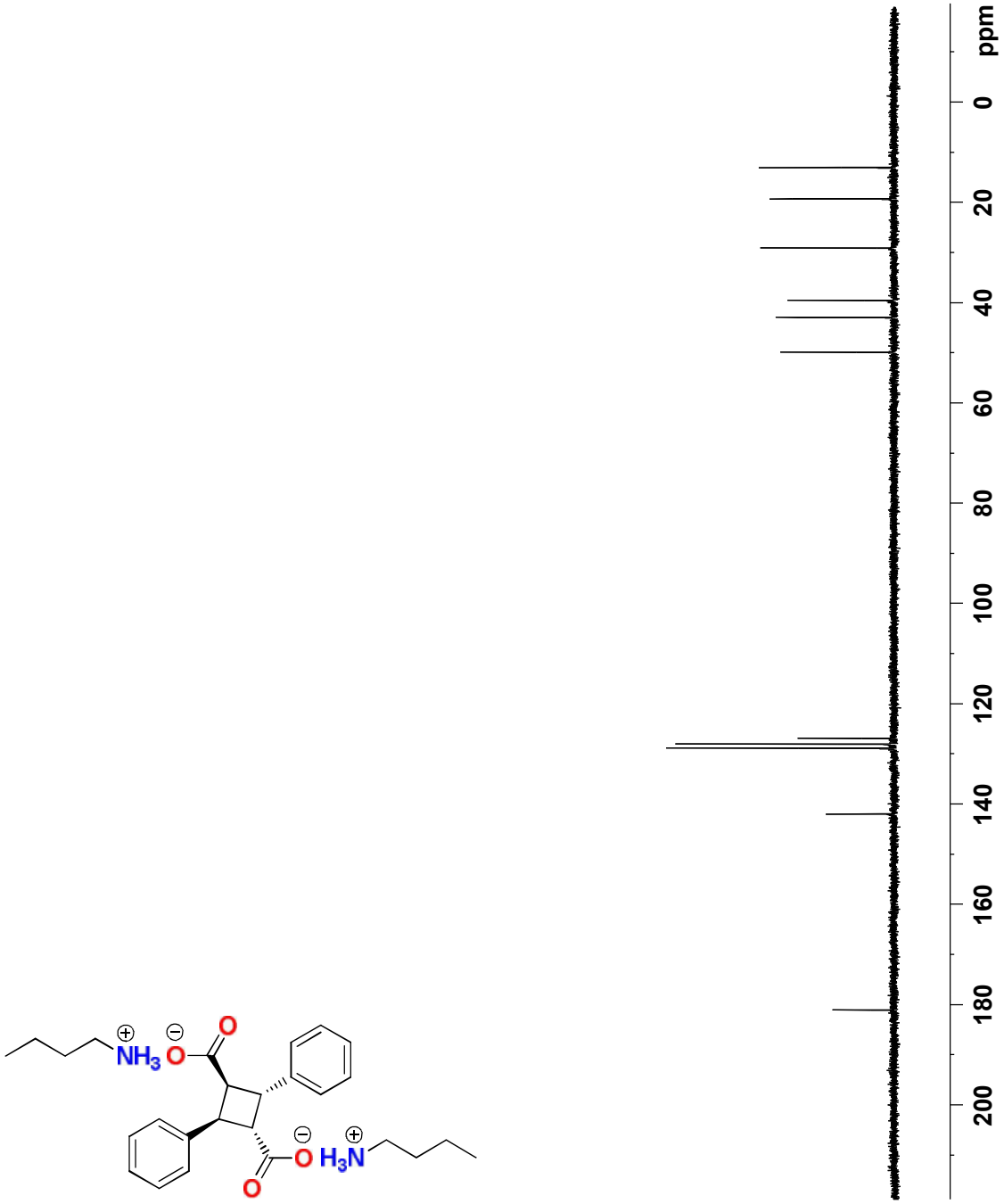

Figure 75. ^{13}C-NMR spectrum of **17b** in D_2O at room temperature.

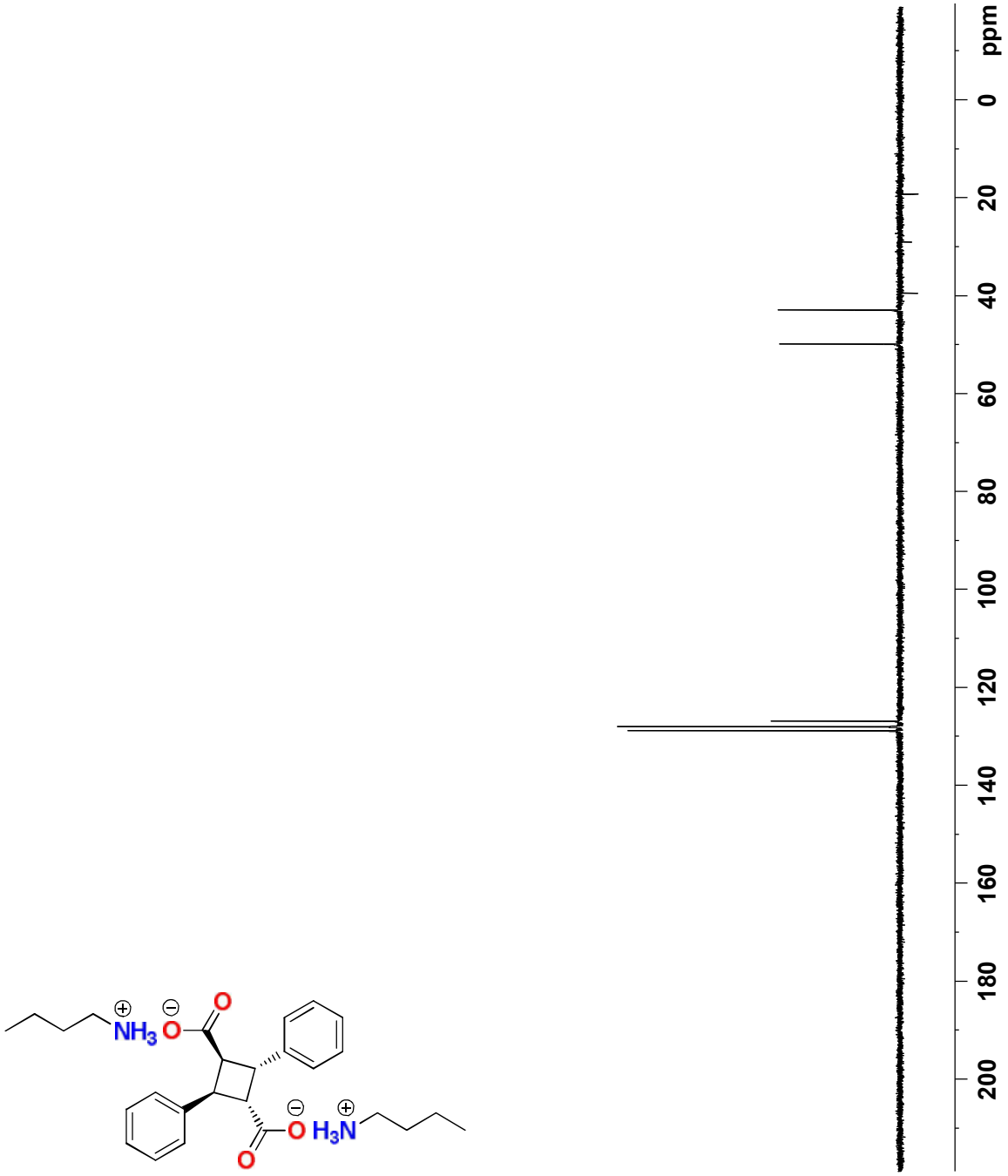

Figure 76. DEPT 90 NMR spectrum of **17b** in D_2O at room temperature.

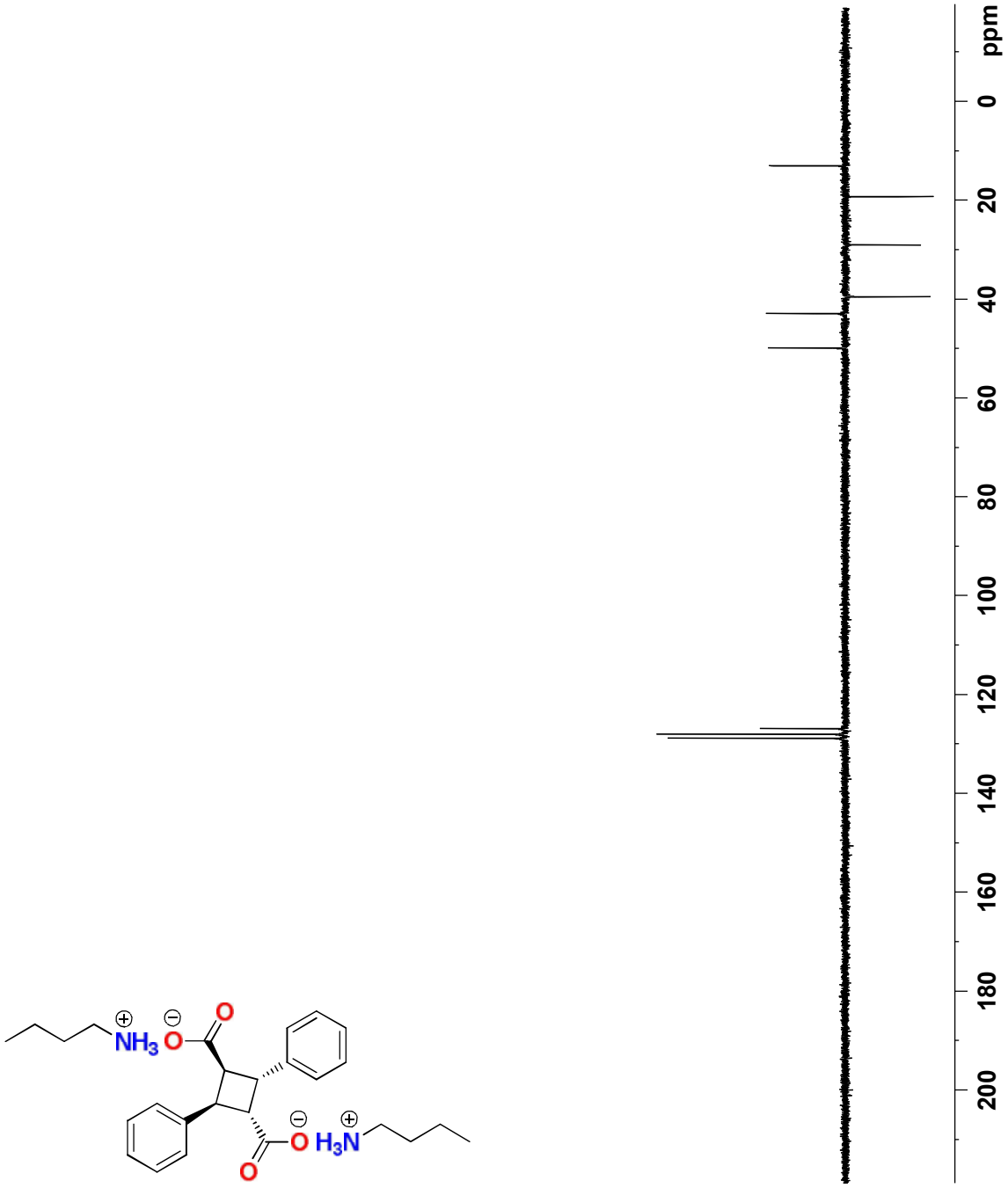

Figure 77. DEPT 135 NMR spectrum of **17b** in D_2O at room temperature.

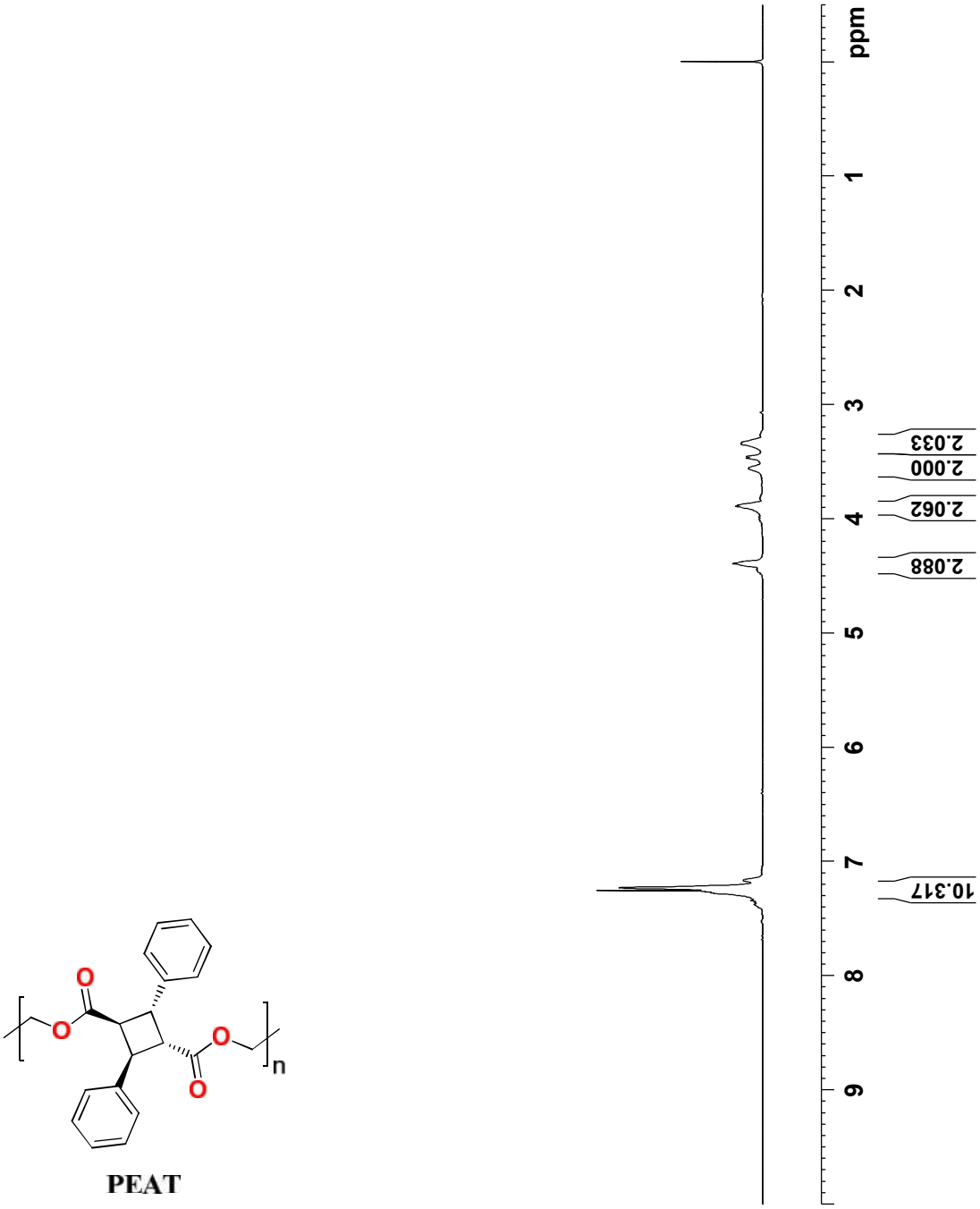

Figure 78. ^{1}H-NMR spectrum of **21P** in $CDCl_3$ at room temperature.

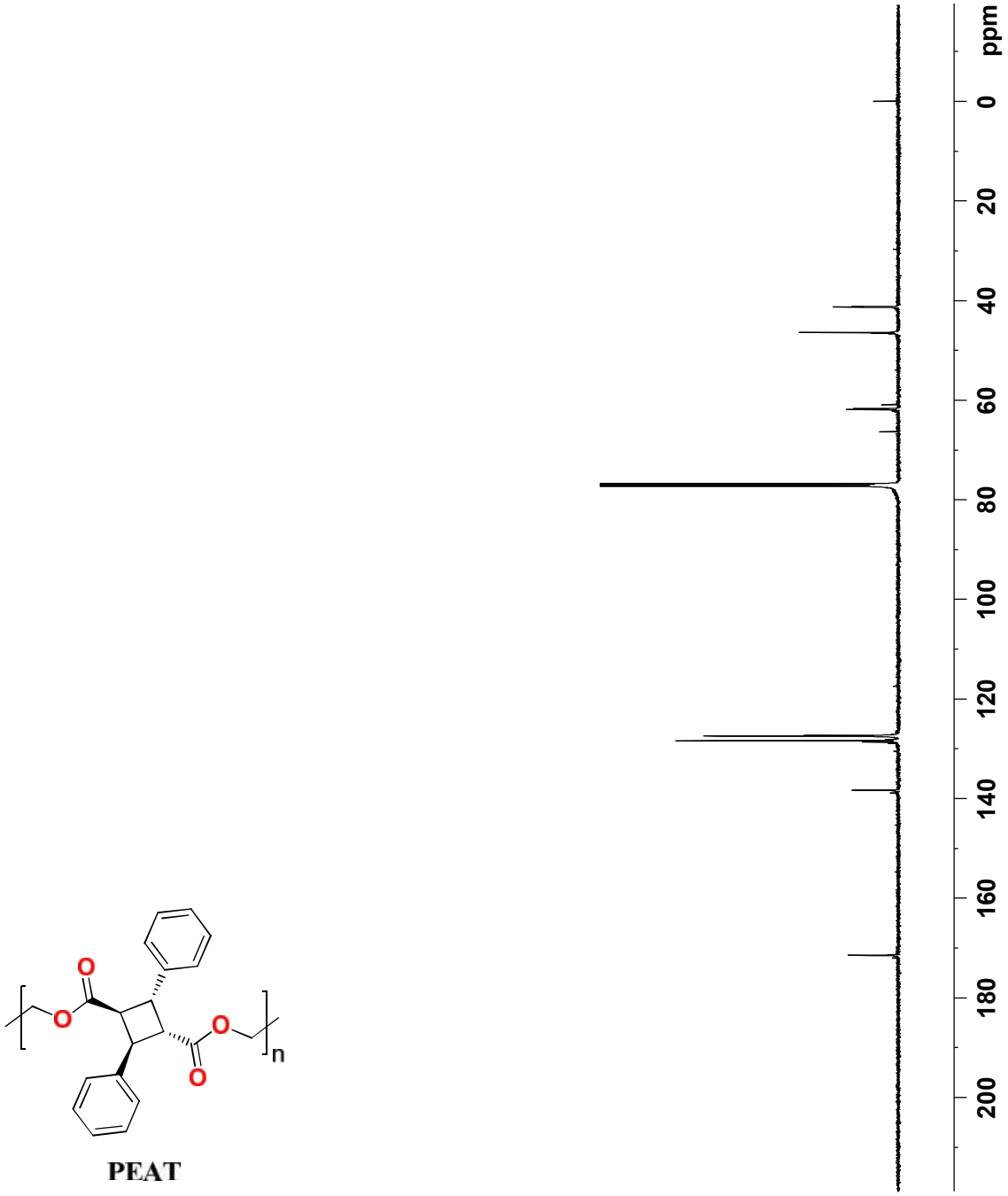

Figure 79. ^{13}C-NMR spectrum of **21P** in $CDCl_3$ at room temperature.

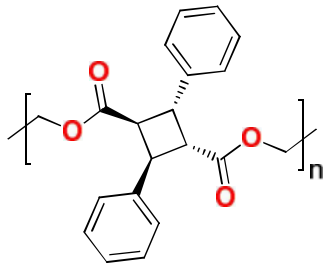

PEAT

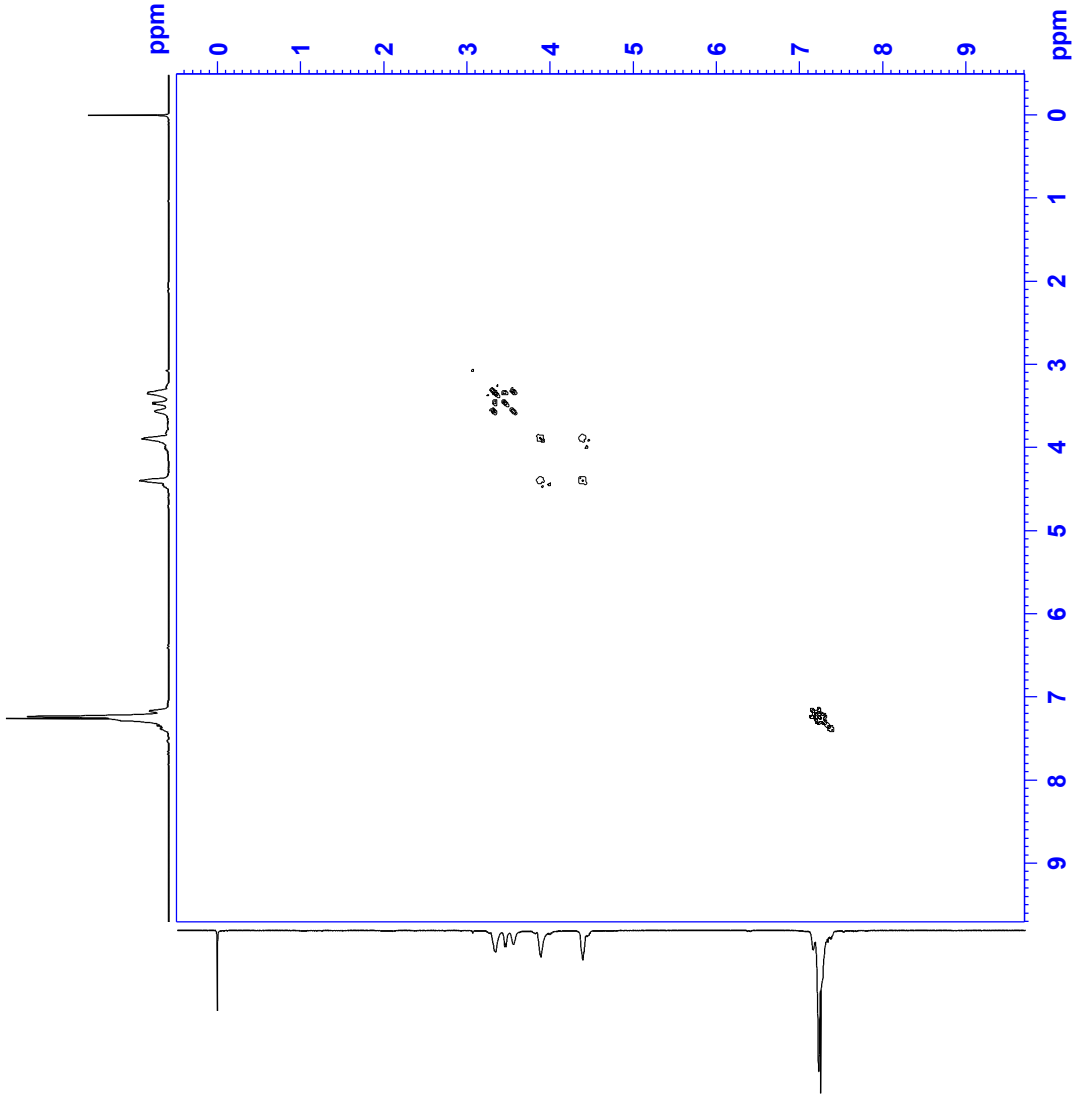

Figure 80. COSY NMR spectrum of **21P** in $CDCl_3$ at room temperature.

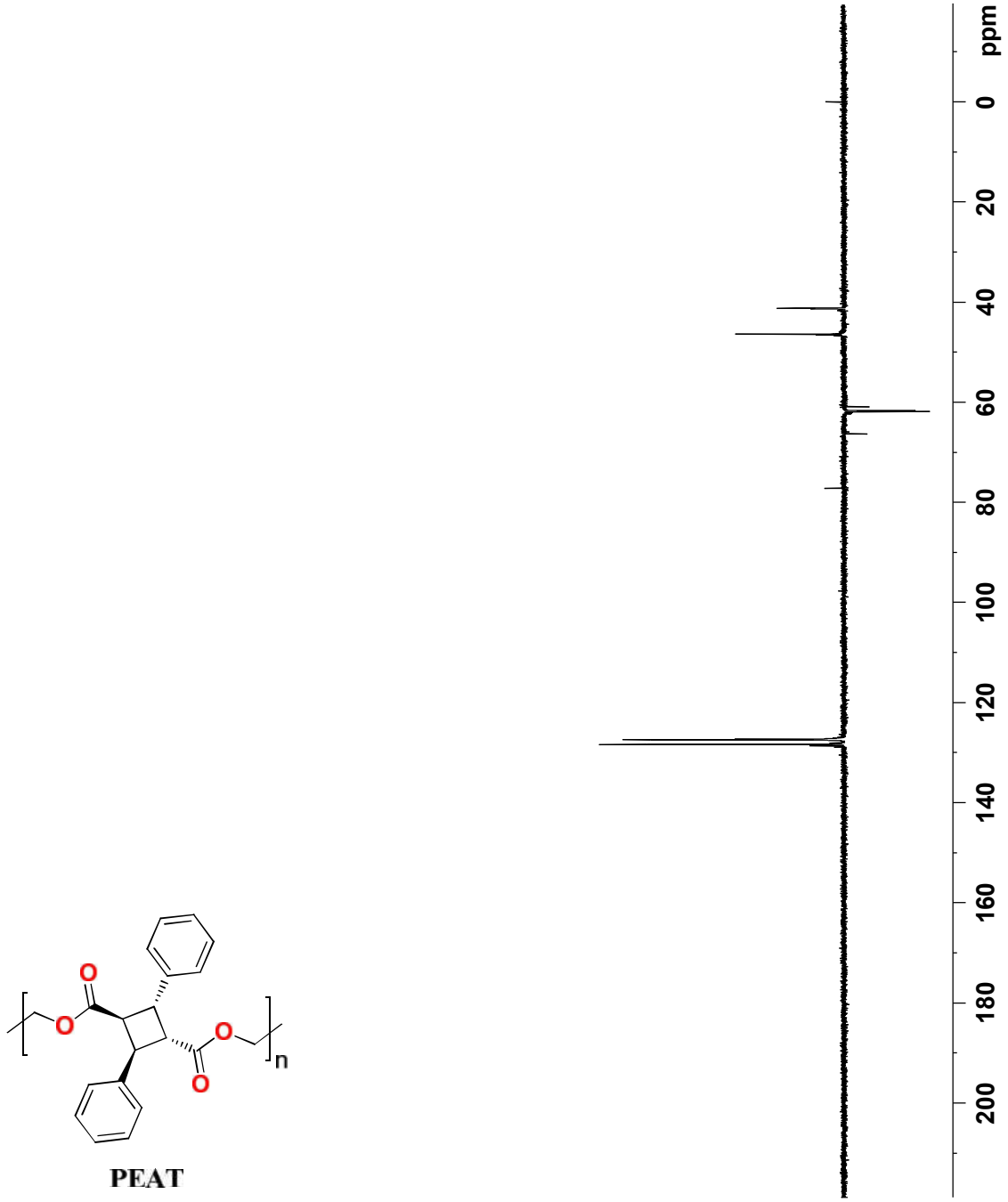

Figure 81. DEPT 135 NMRspectrum of **21P** in $CDCl_3$ at room temperature.

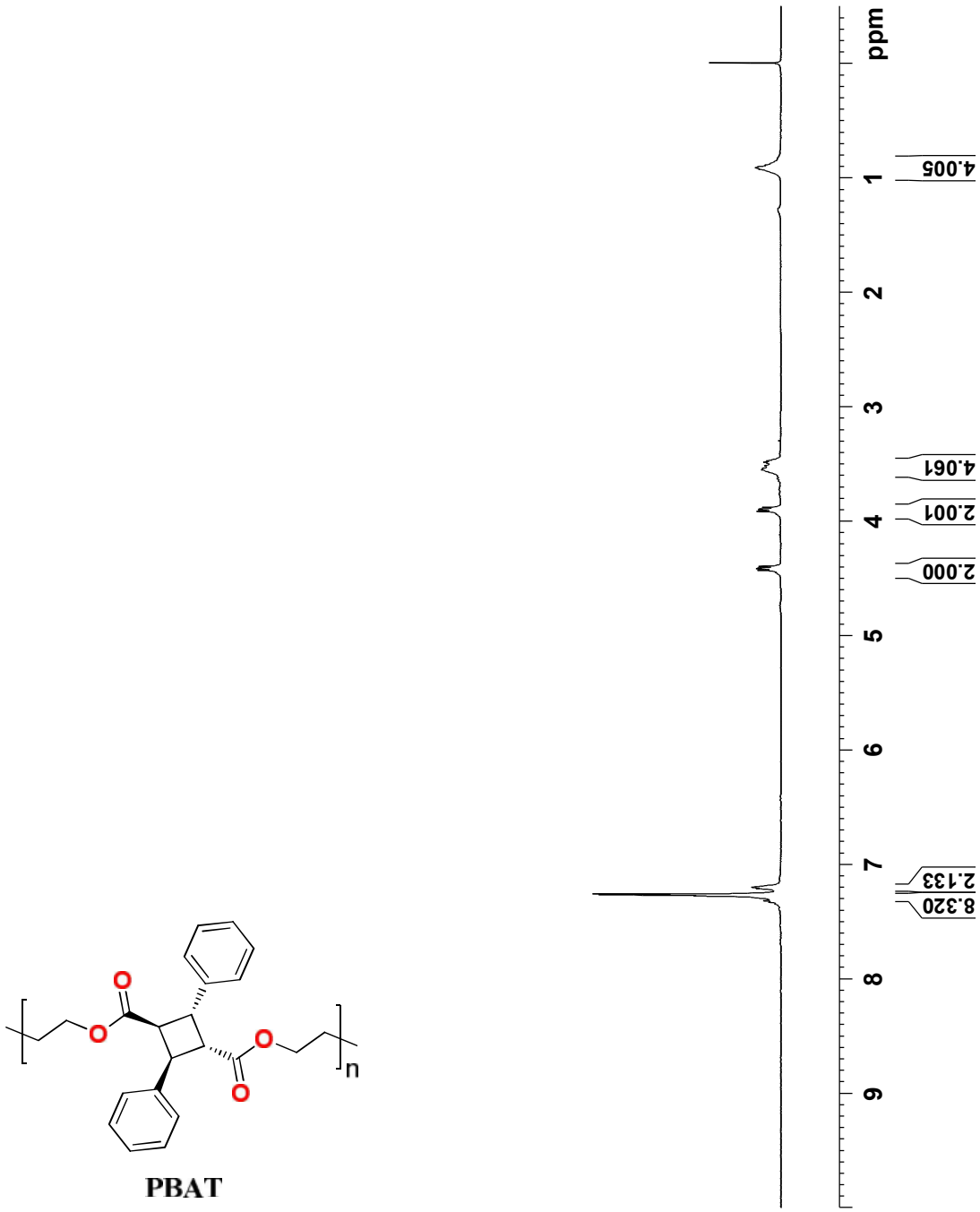

Figure 82. ^{1}H-NMR spectrum of **22P** in $CDCl_3$ at room temperature.

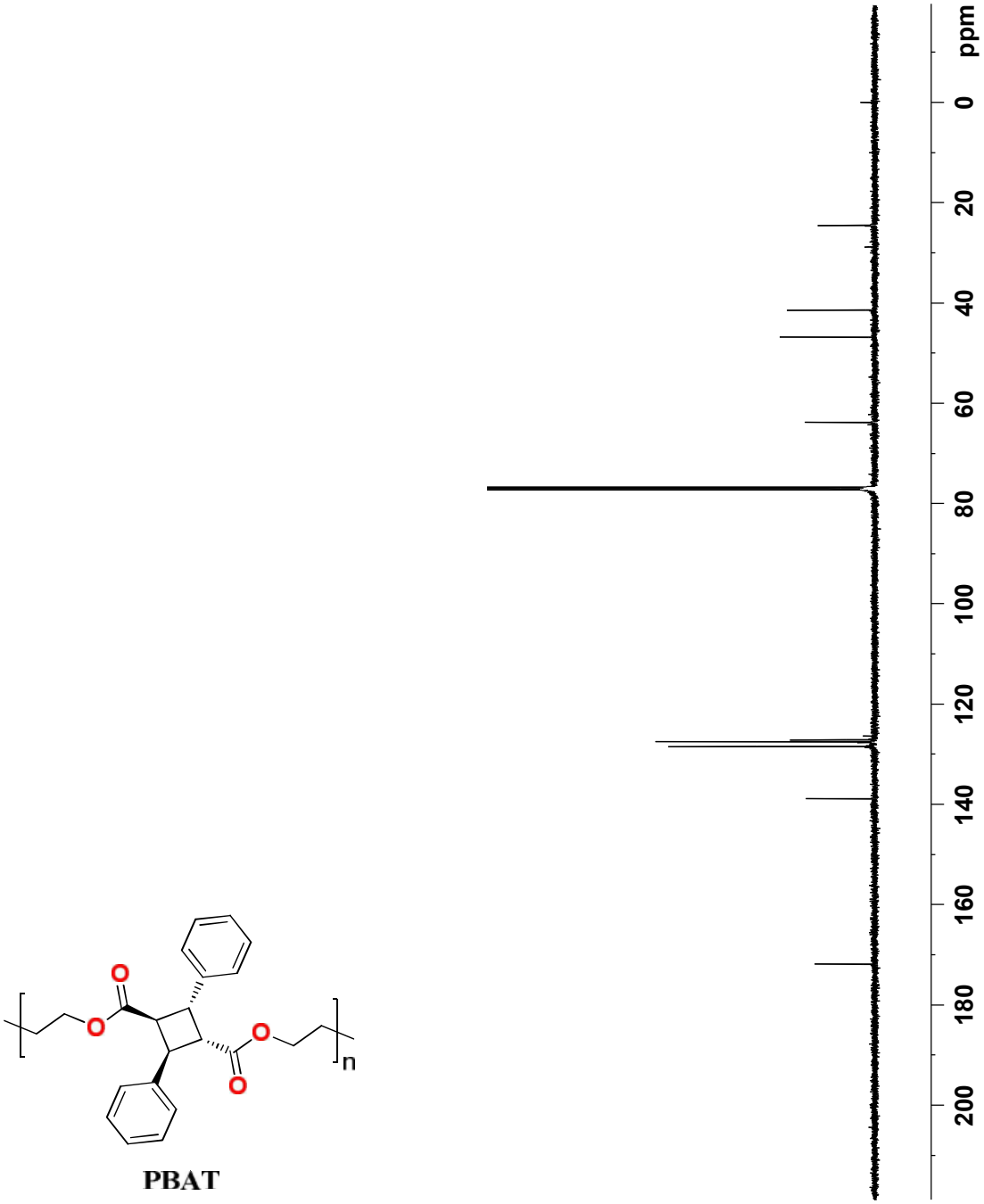

Figure 83. ^{13}C-NMR spectrum of **22P** in $CDCl_3$ at room temperature.

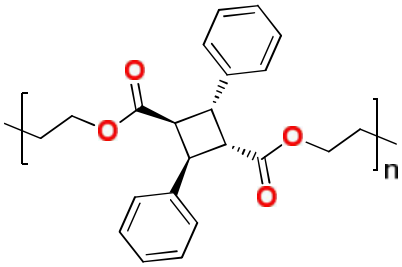

PBAT

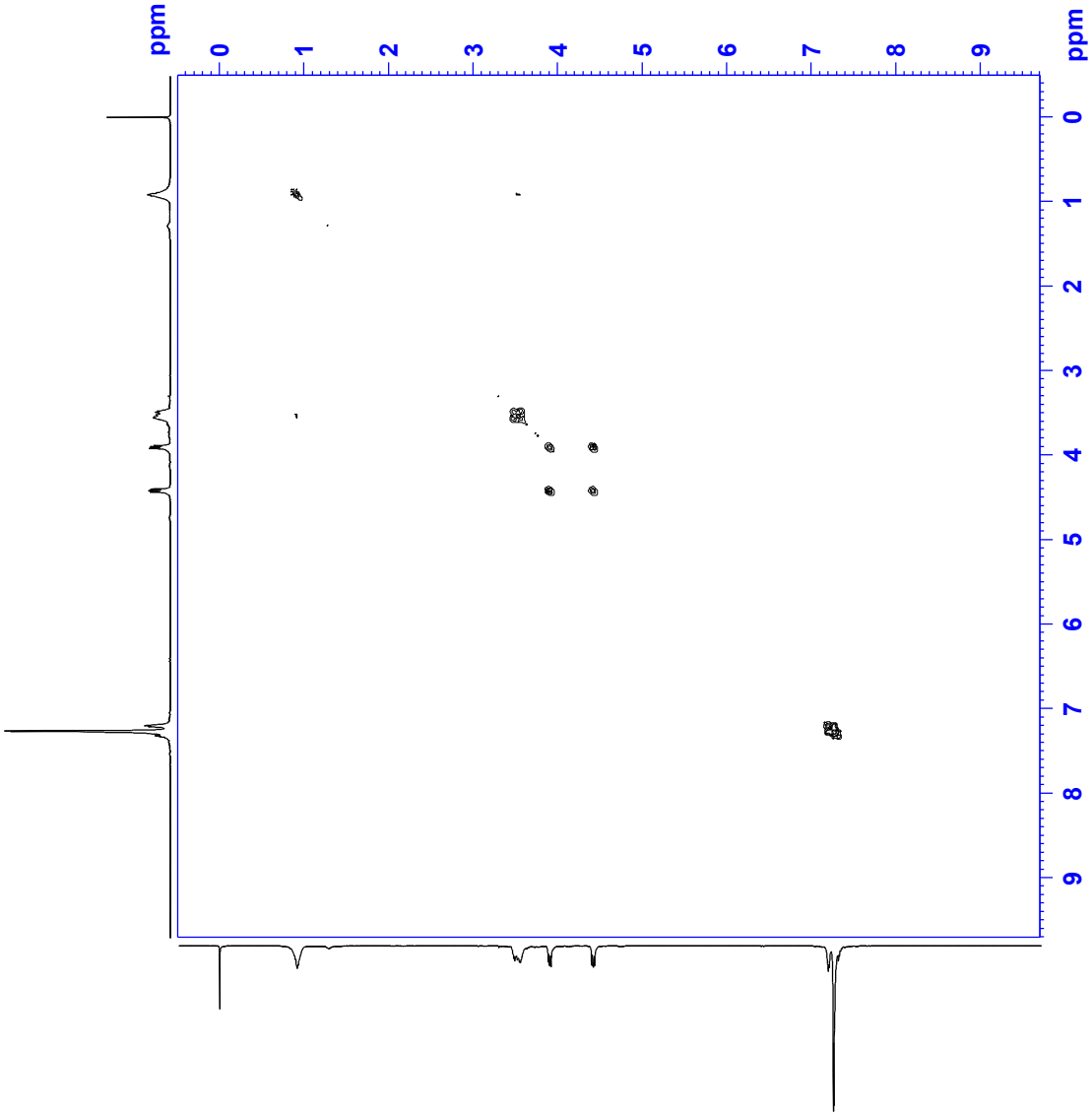

Figure 84. COSY NMR spectrum of **22P** in $CDCl_3$ at room temperature.

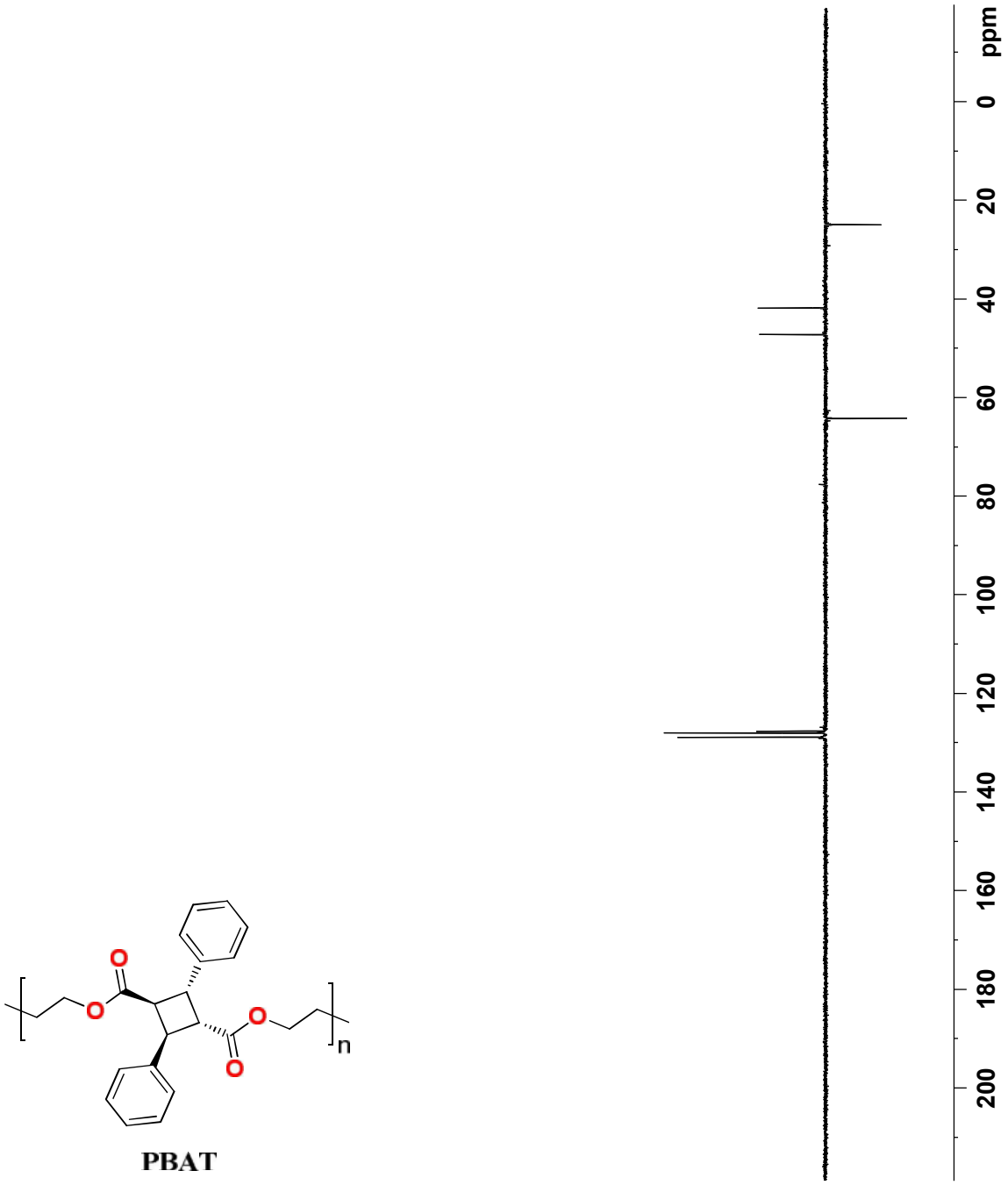

Figure 85. DEPT 135 NMR spectrum of **22P** in $CDCl_3$ at room temperature.

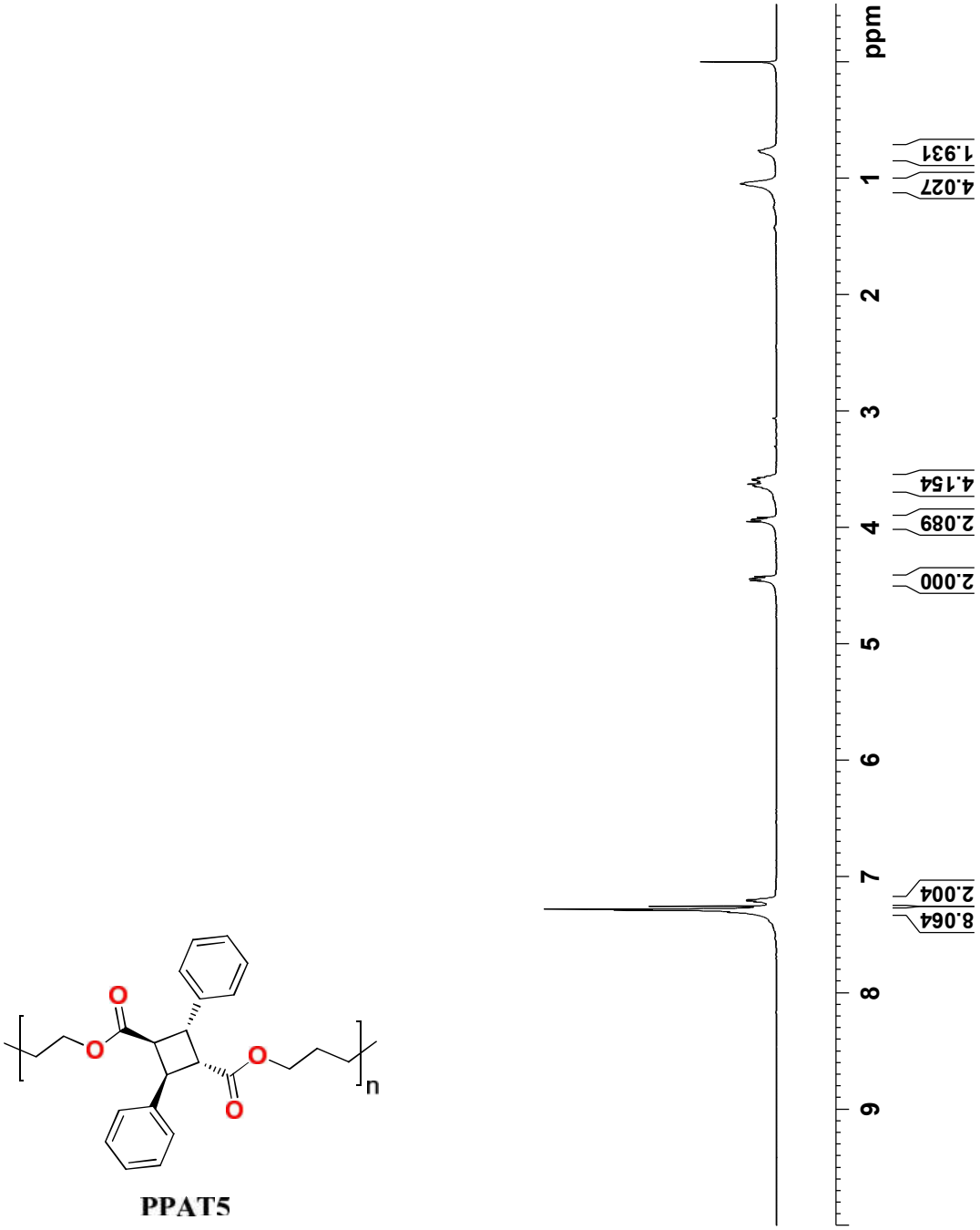

Figure 86. ^{1}H-NMR spectrum of **23P** in $CDCl_3$ at room temperature.

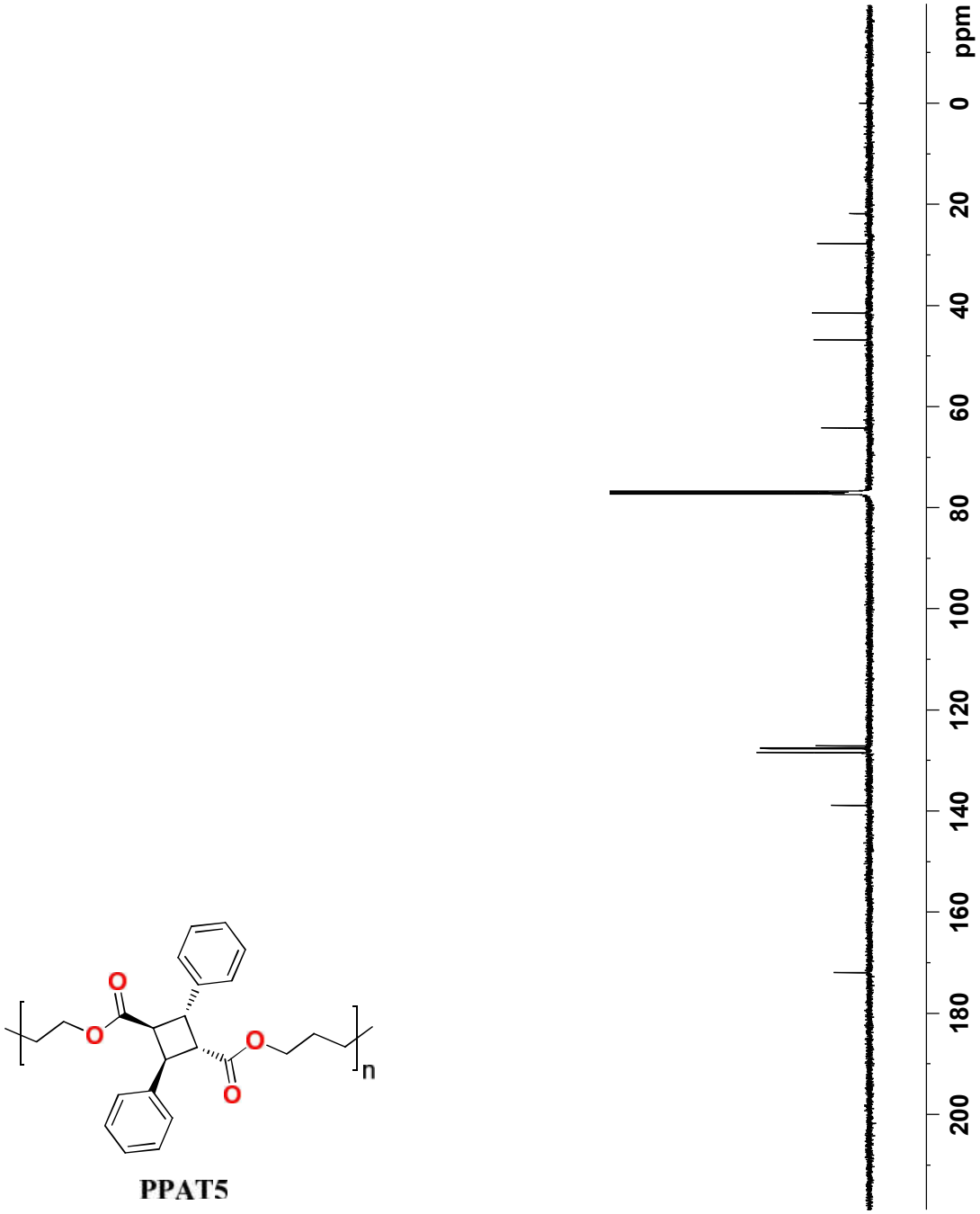

Figure 87. ^{13}C-NMR spectrum of **23P** in $CDCl_3$ at room temperature.

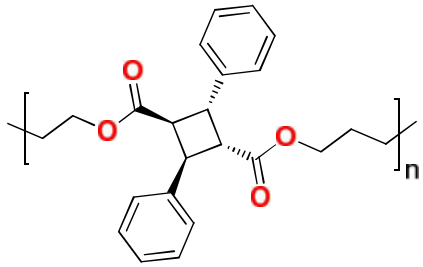

PPAT5

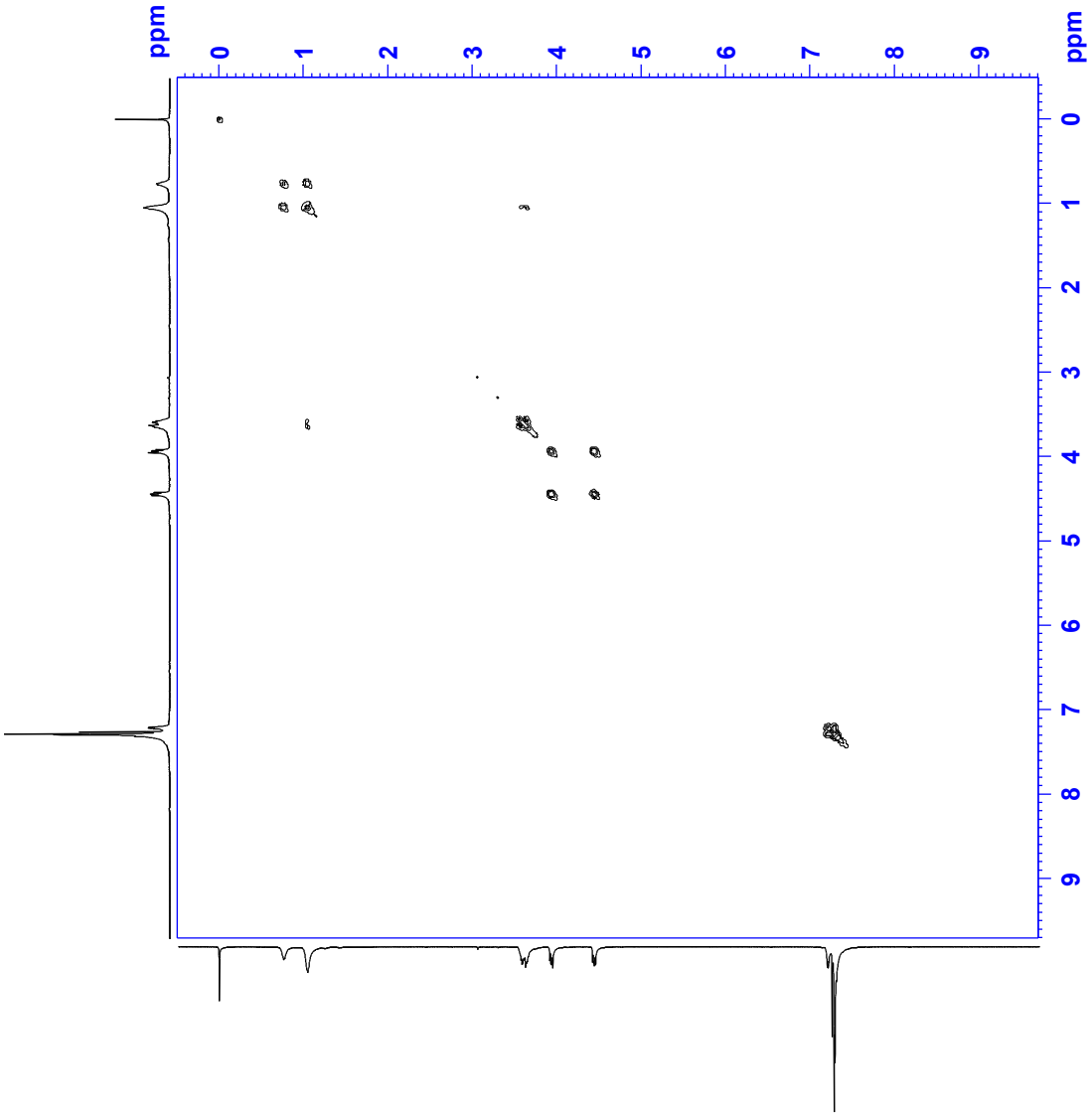

Figure 88. COSY NMR spectrum of **23P** in $CDCl_3$ at room temperature.

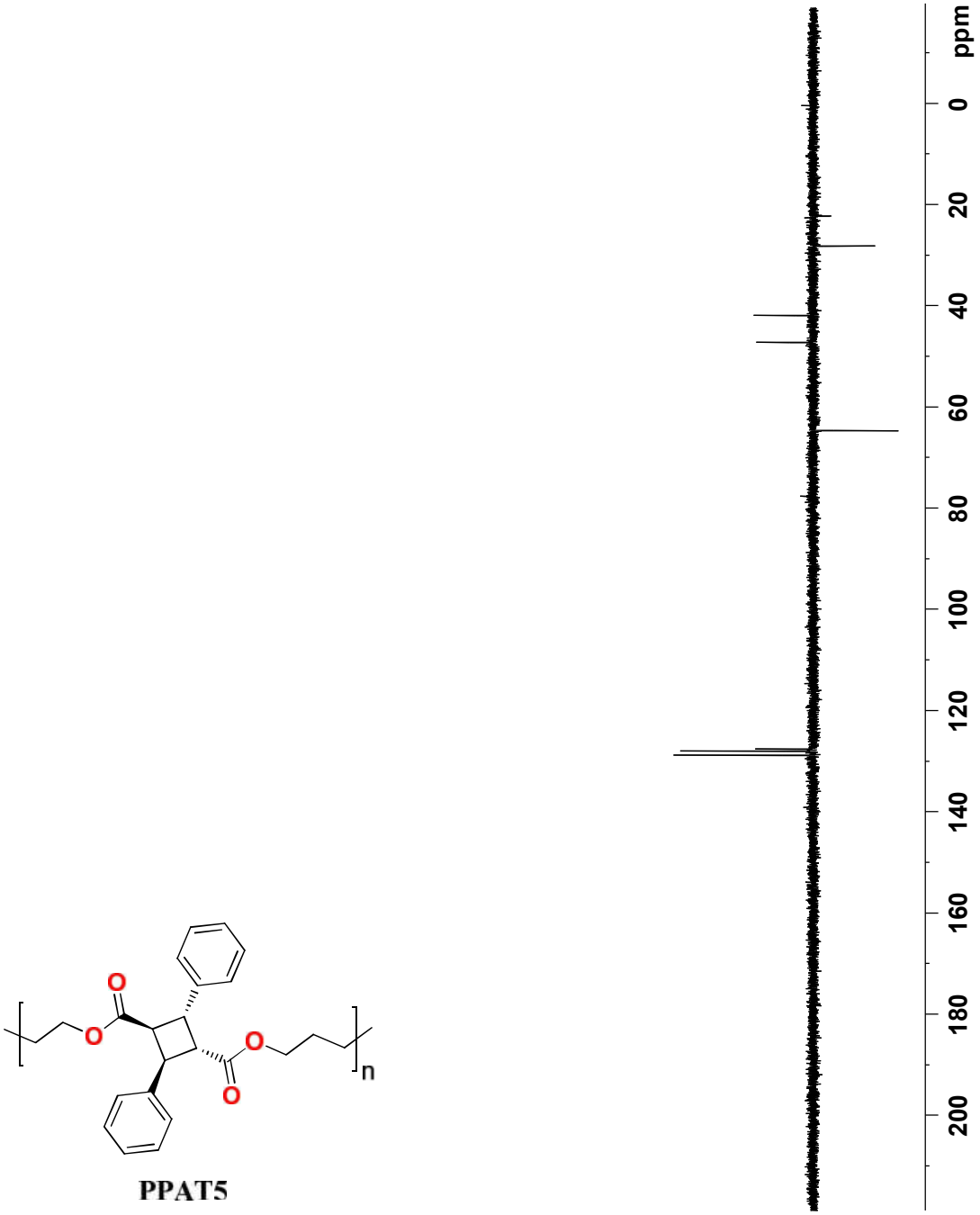

Figure 89. DEPT 135 NMR spectrum of **23P** in $CDCl_3$ at room temperature.

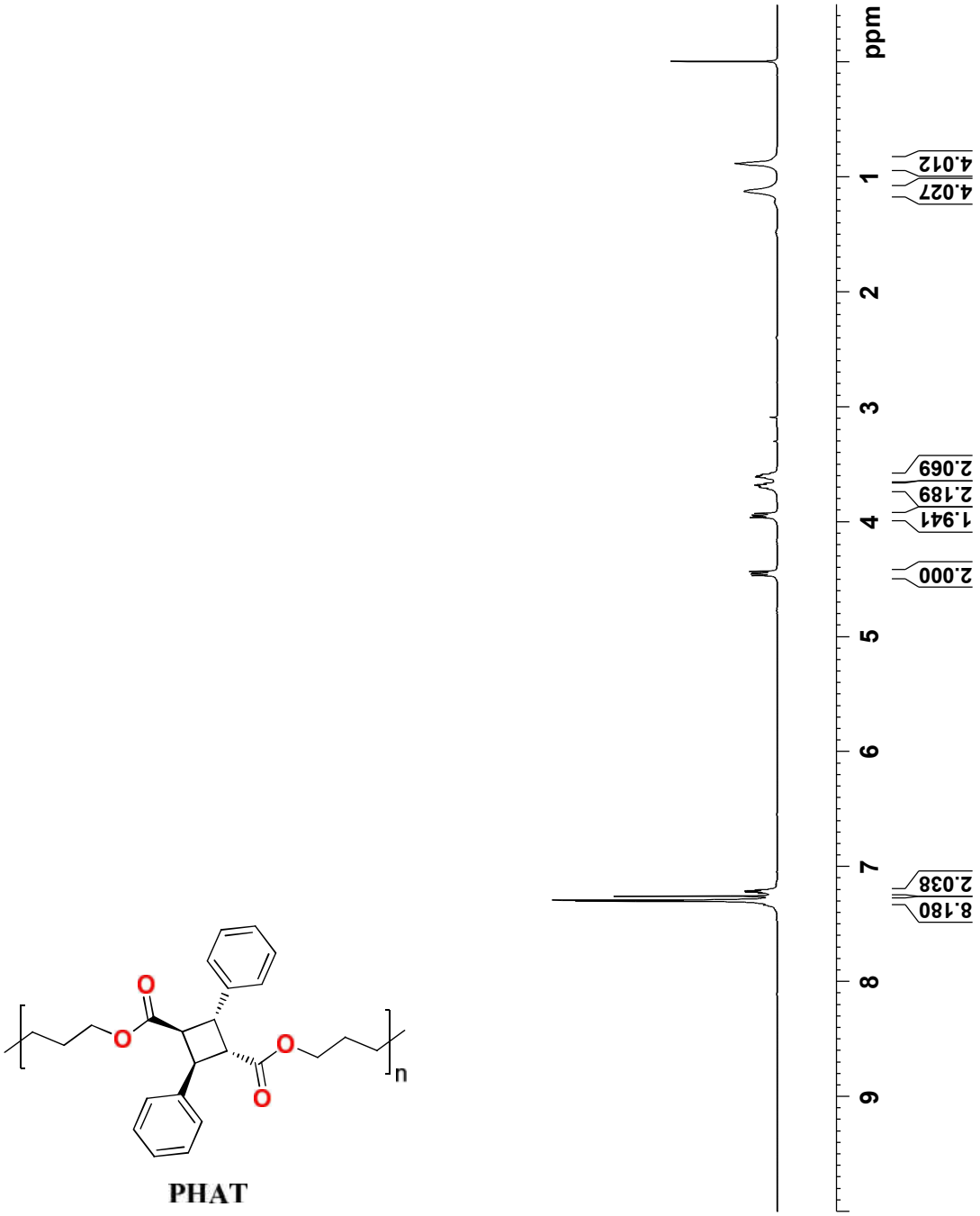

Figure 90. ^{1}H-NMR spectrum of **24P** in $CDCl_3$ at room temperature.

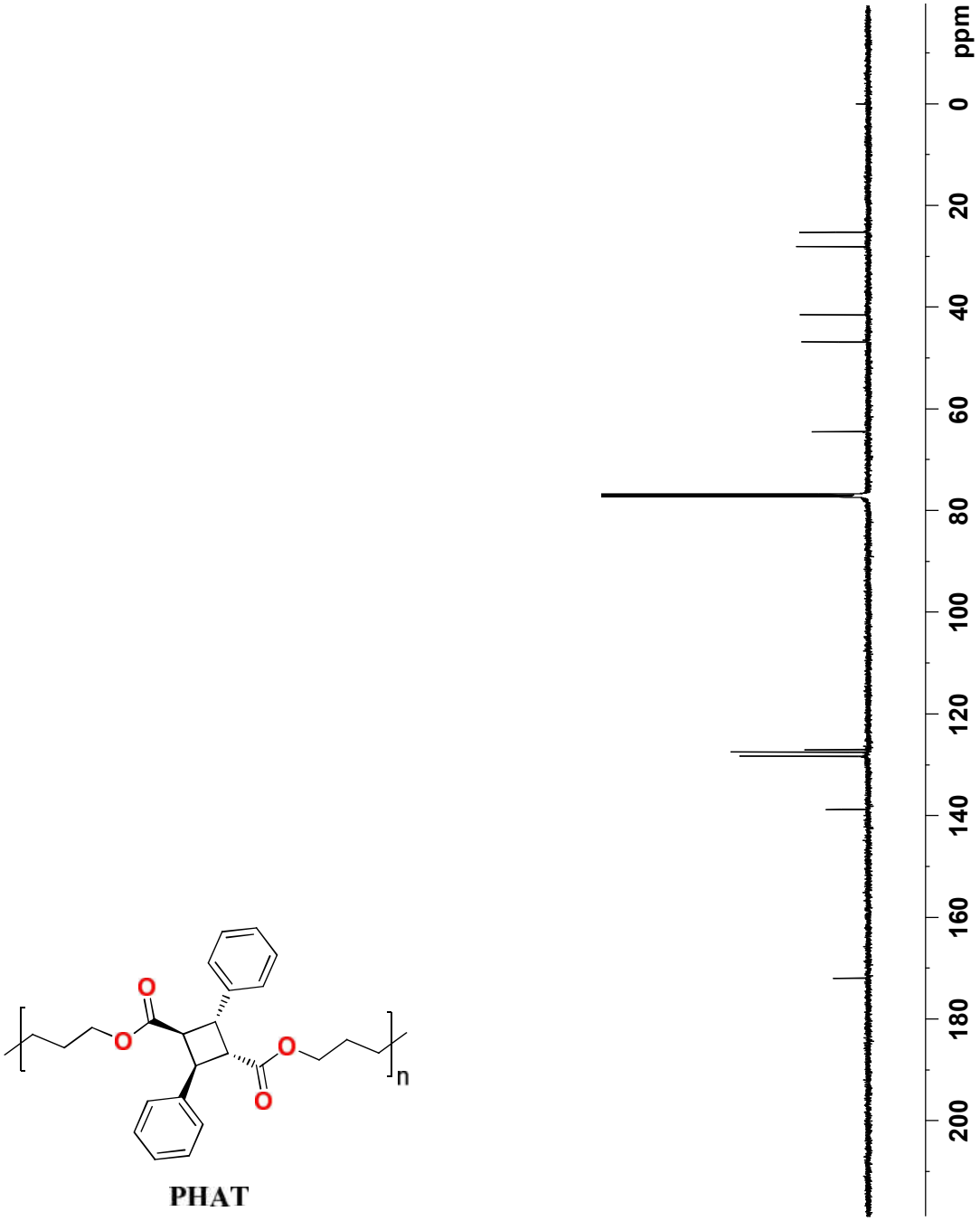

Figure 91. ^{13}C-NMR spectrum of **24P** in $CDCl_3$ at room temperature.

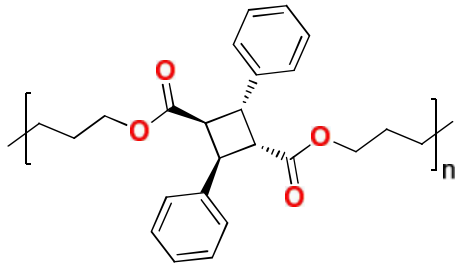

PHAT

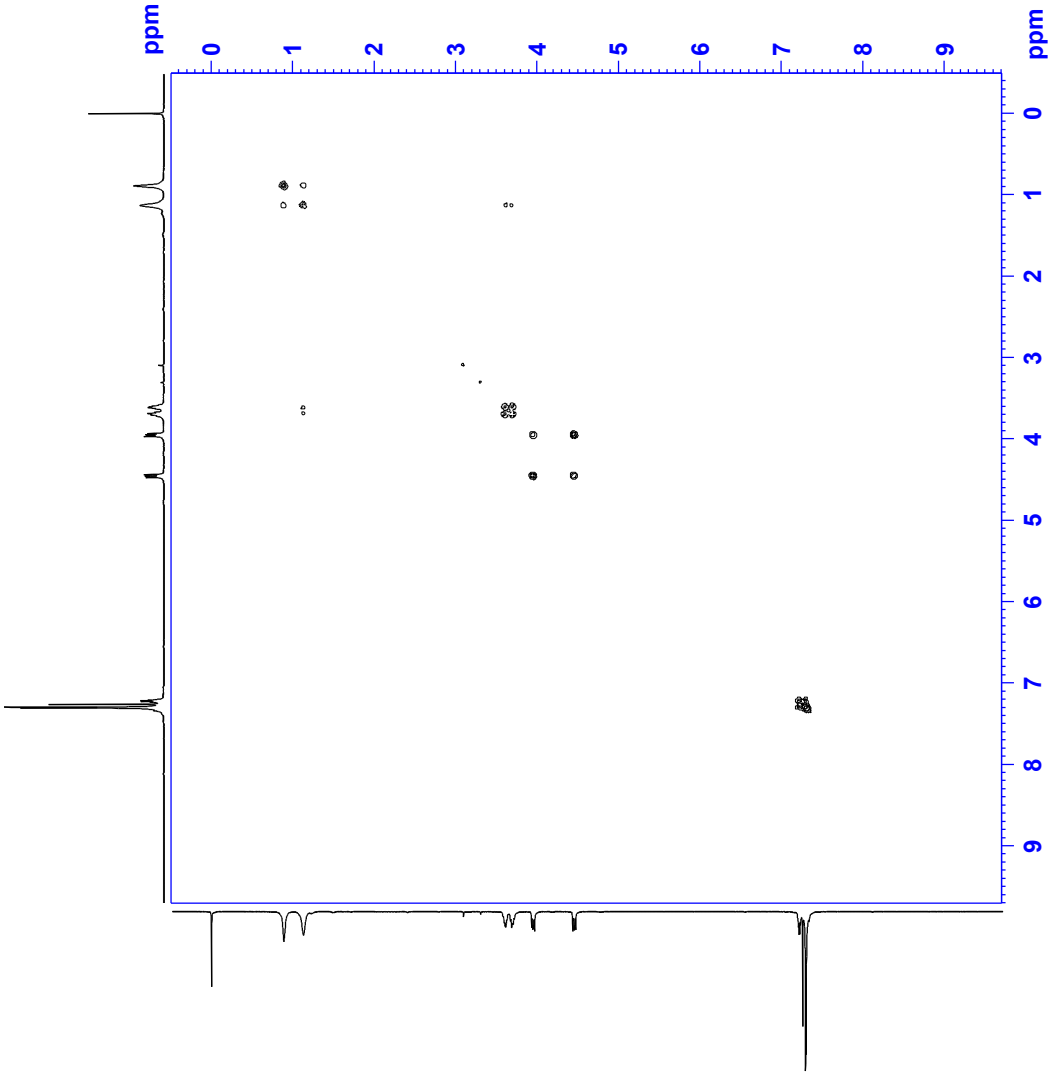

Figure 92. COSY NMR spectrum of **24P** in $CDCl_3$ at room temperature.

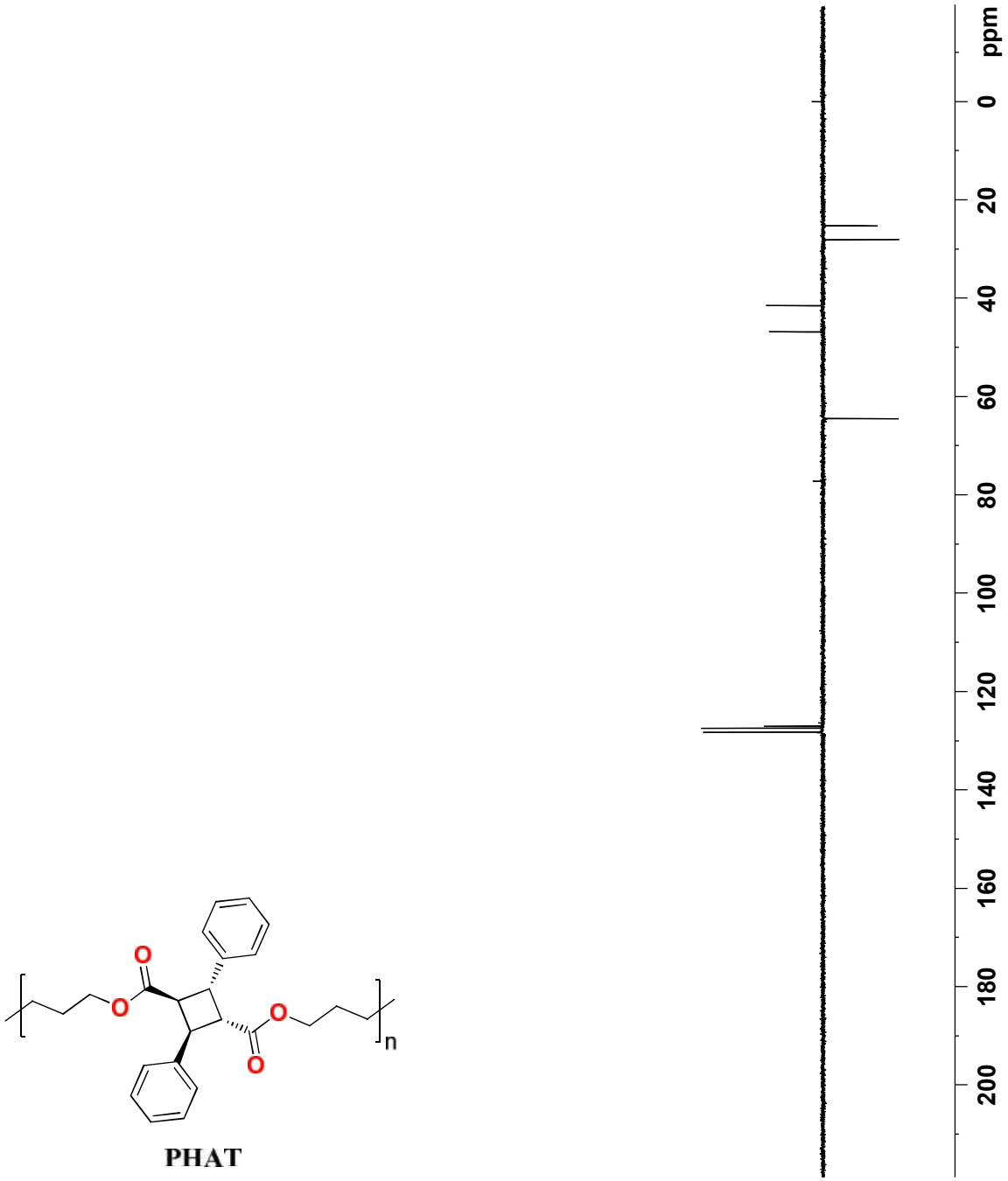

Figure 93. DEPT 135 NMR spectrum of **24P** in $CDCl_3$ at room temperature.

APPENDIX B

Selected IR Spectra

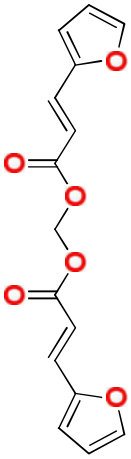

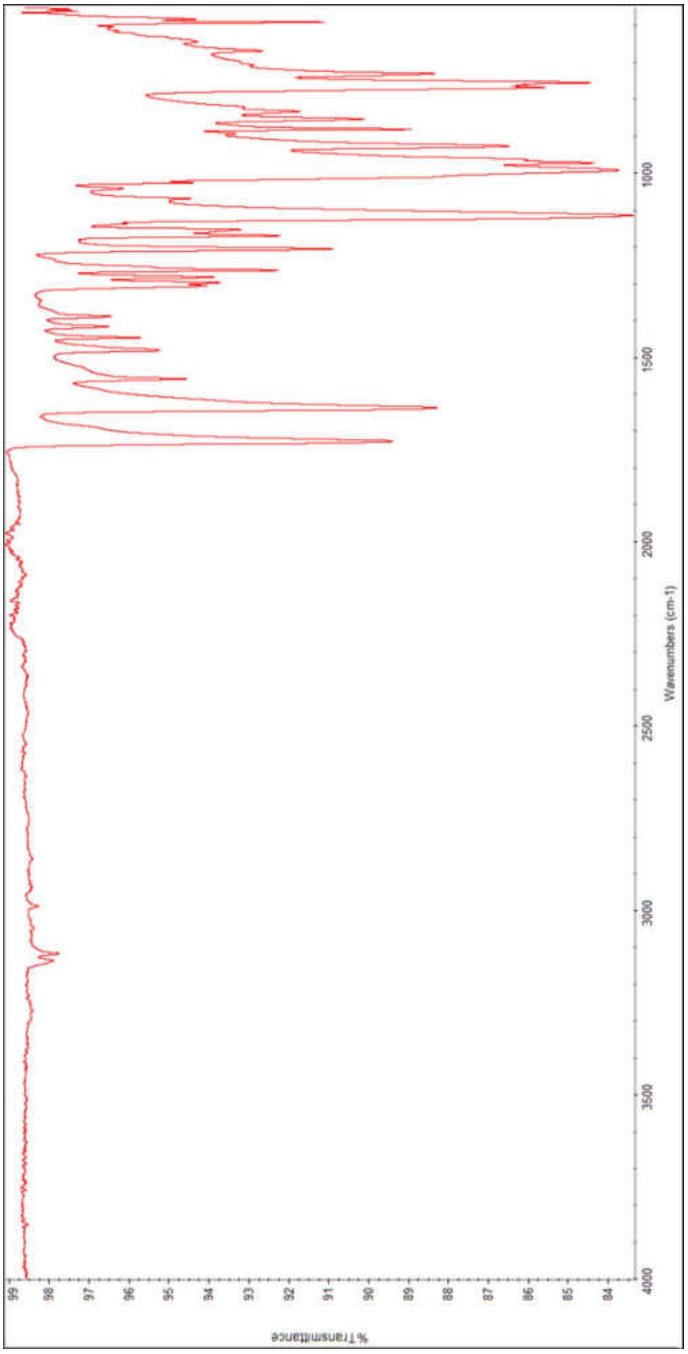

Figure 94. FT-IR spectrum of monomer **4**.

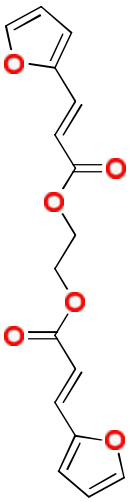

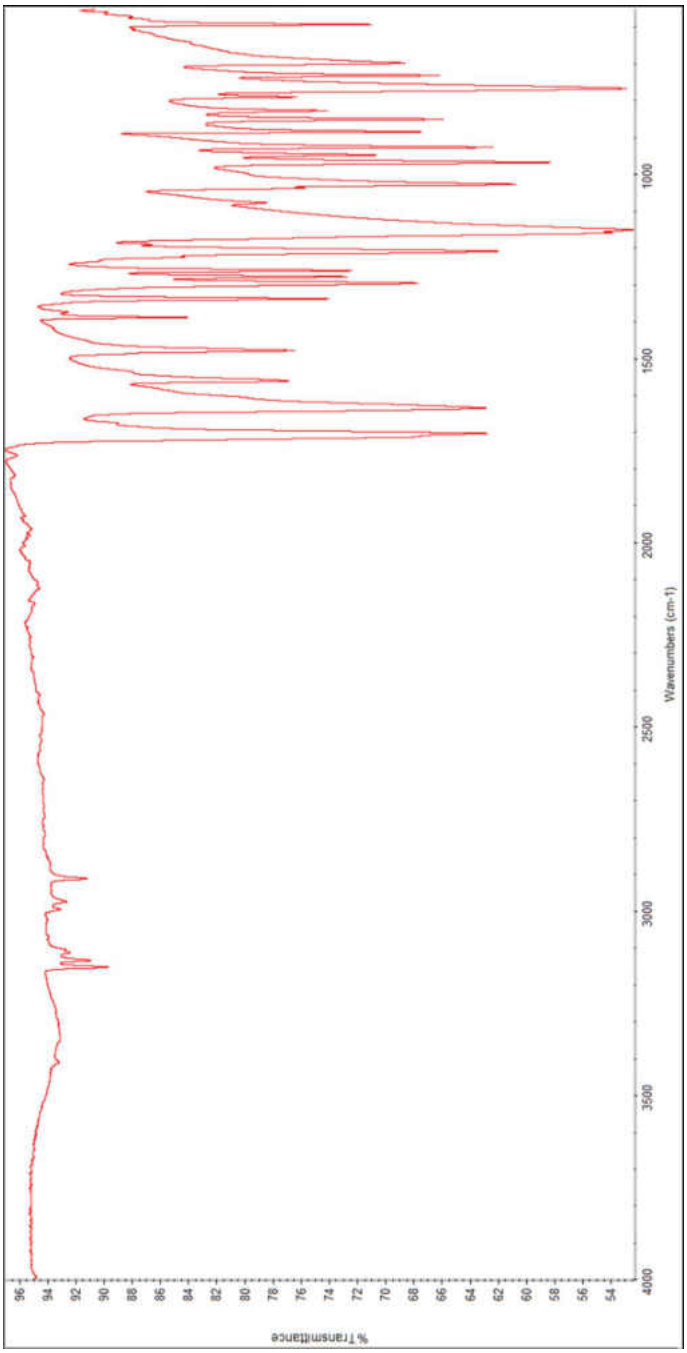

Figure 95. FT-IR spectrum of monomer **5**.

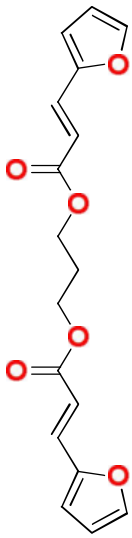

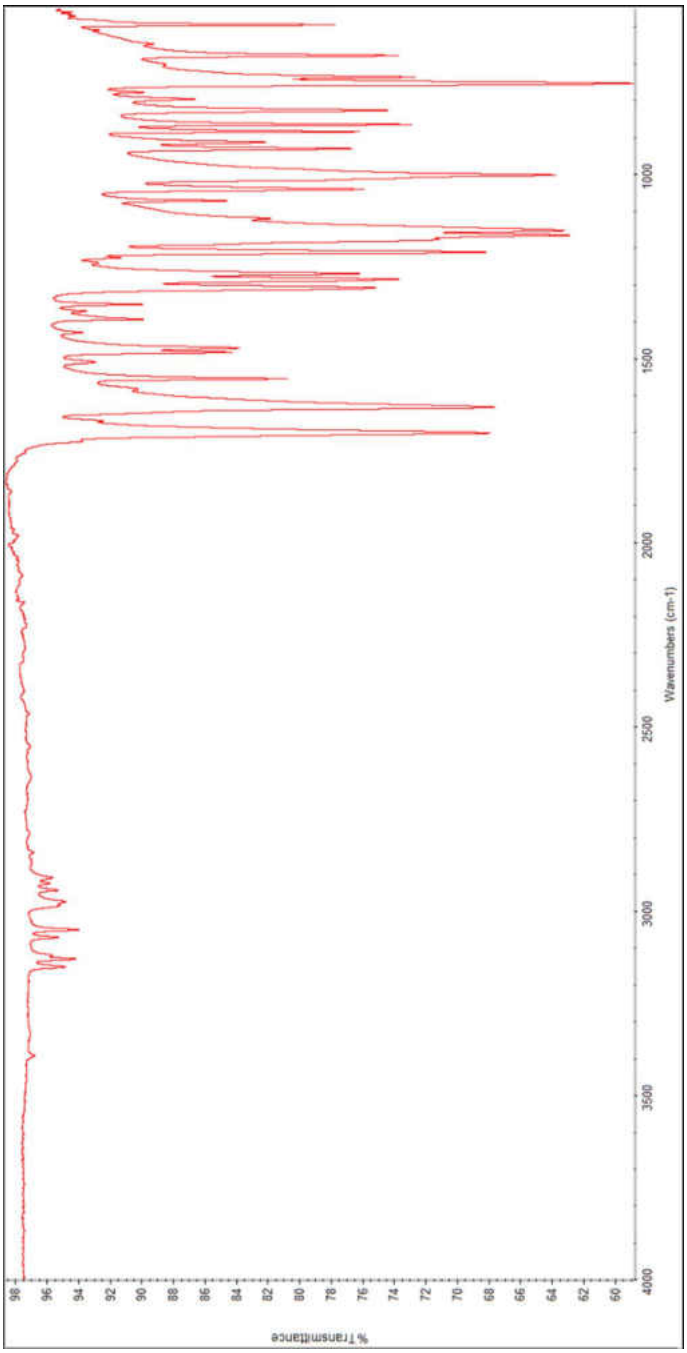

Figure 96. FT-IR spectrum of monomer **6**.

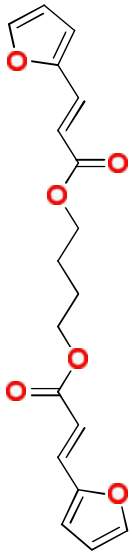

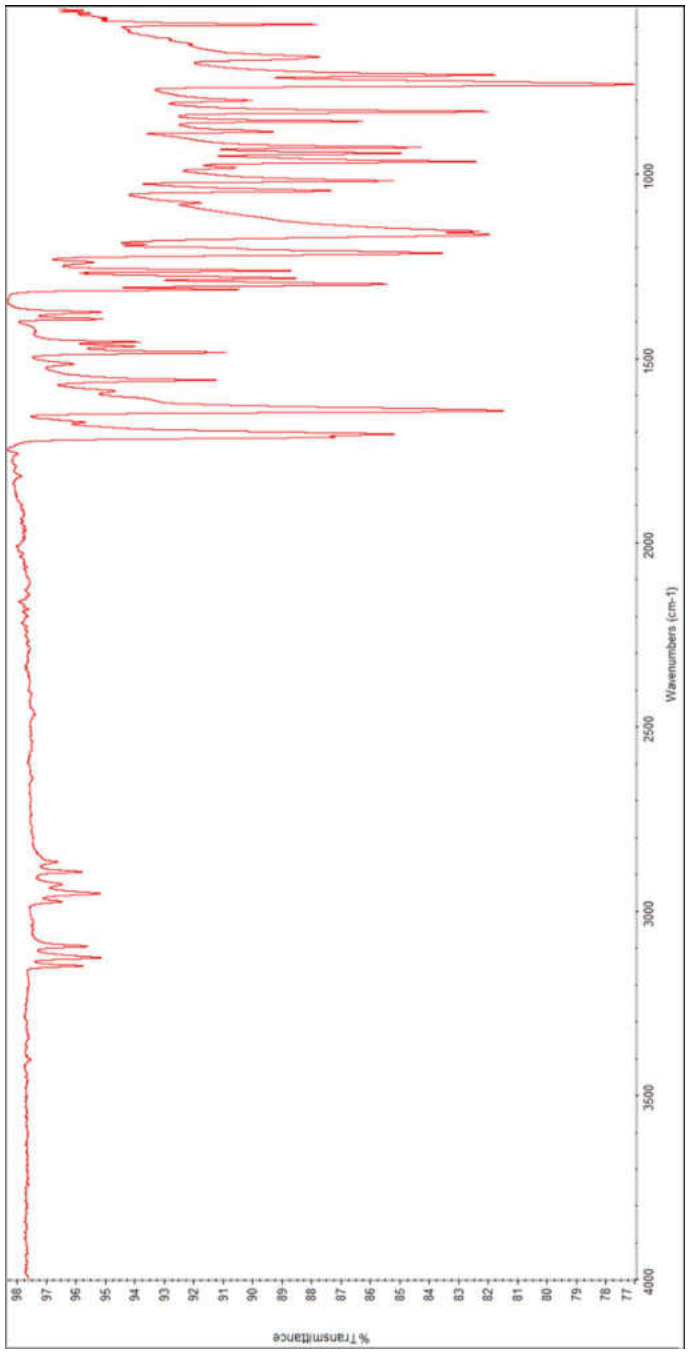

Figure 97. FT-IR spectrum of monomer **7**.

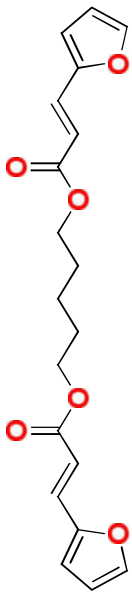

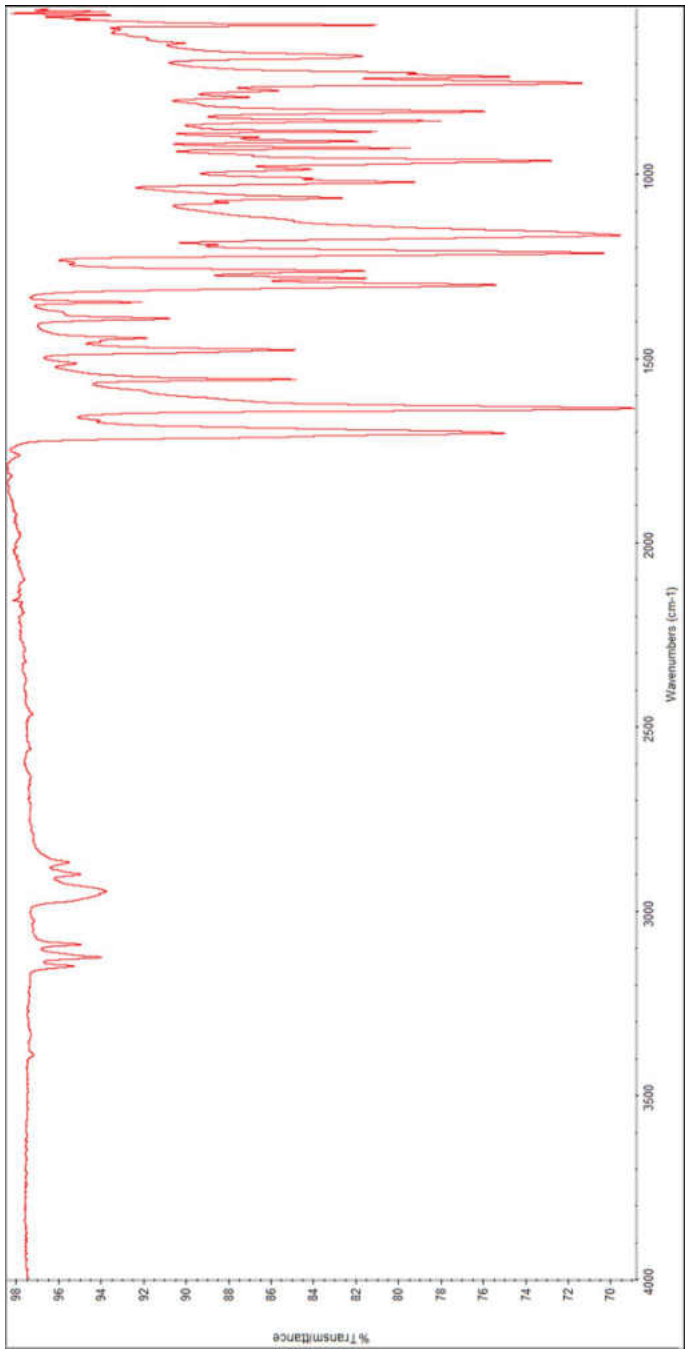

Figure 98. FT-IR spectrum of monomer **8**.

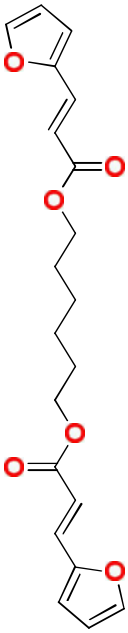

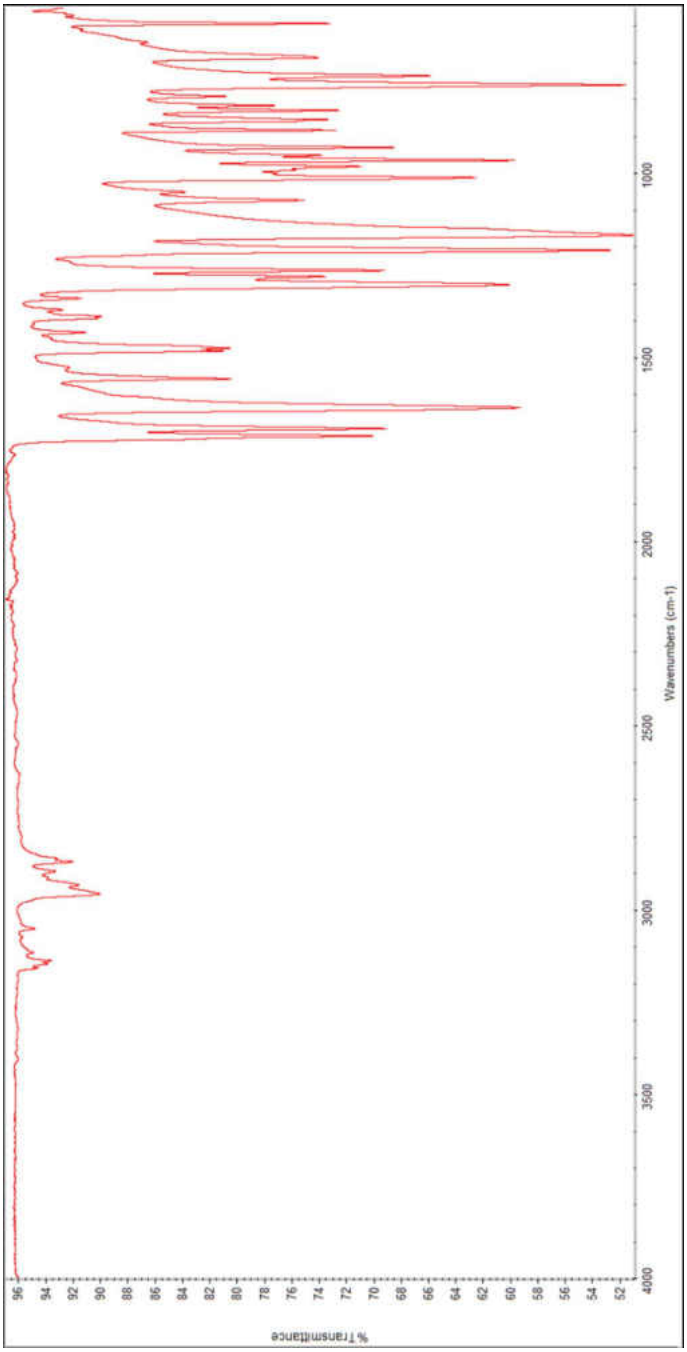

Figure 99. FT-IR spectrum of monomer **9**.

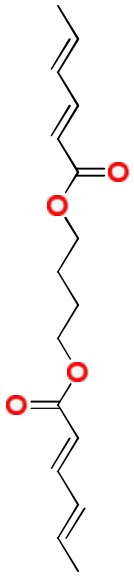

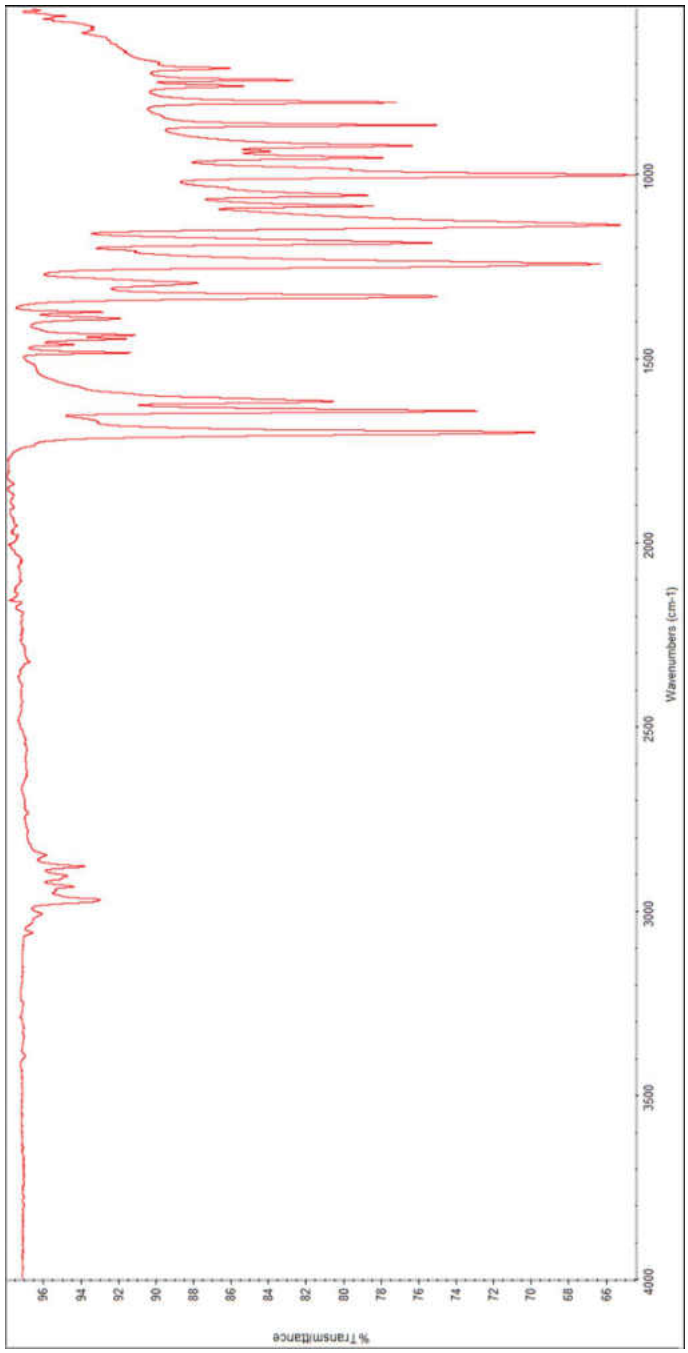

Figure 100. FT-IR spectrum of monomer **12**.

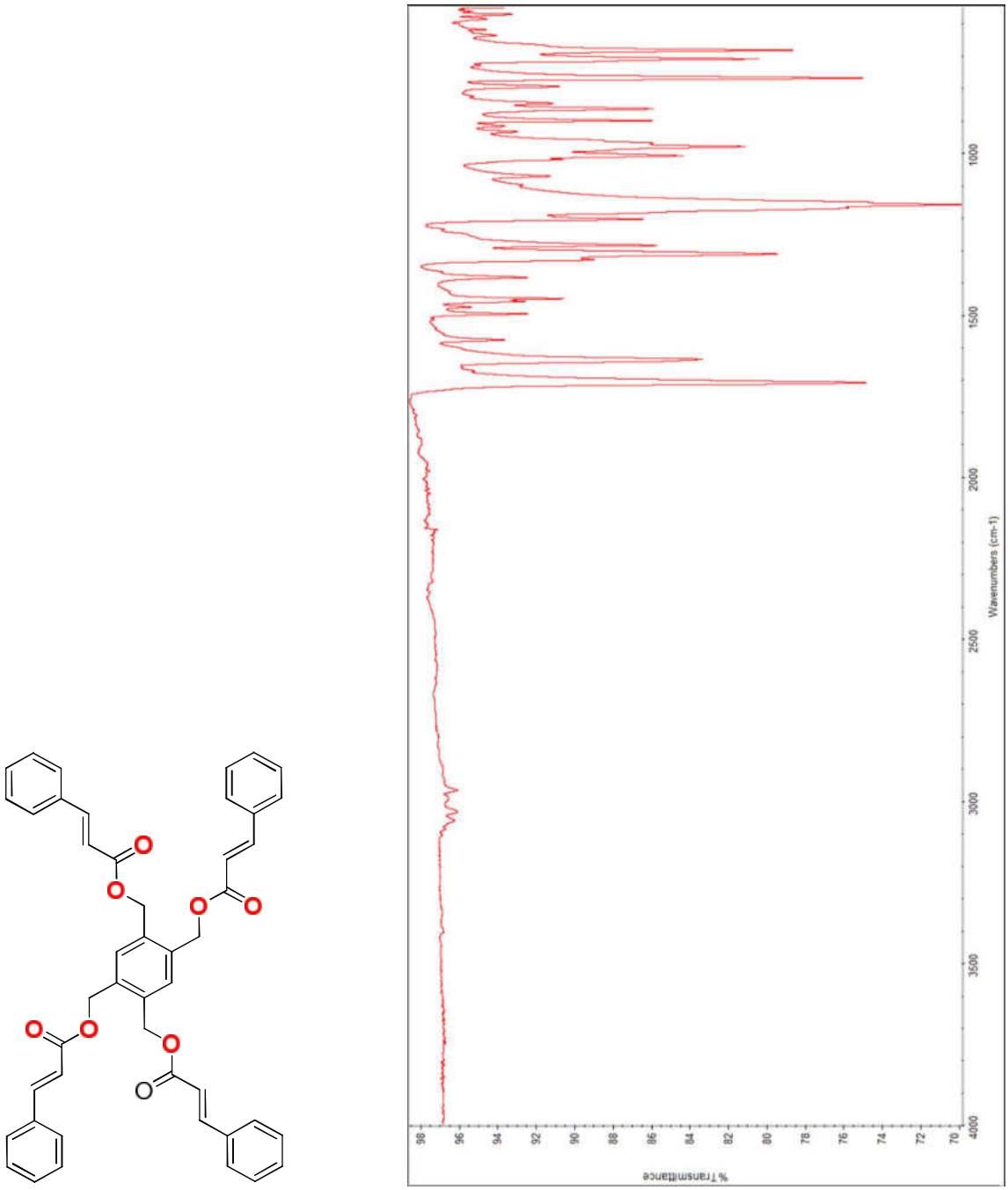

Figure 101. FT-IR spectrum of monomer **16**.

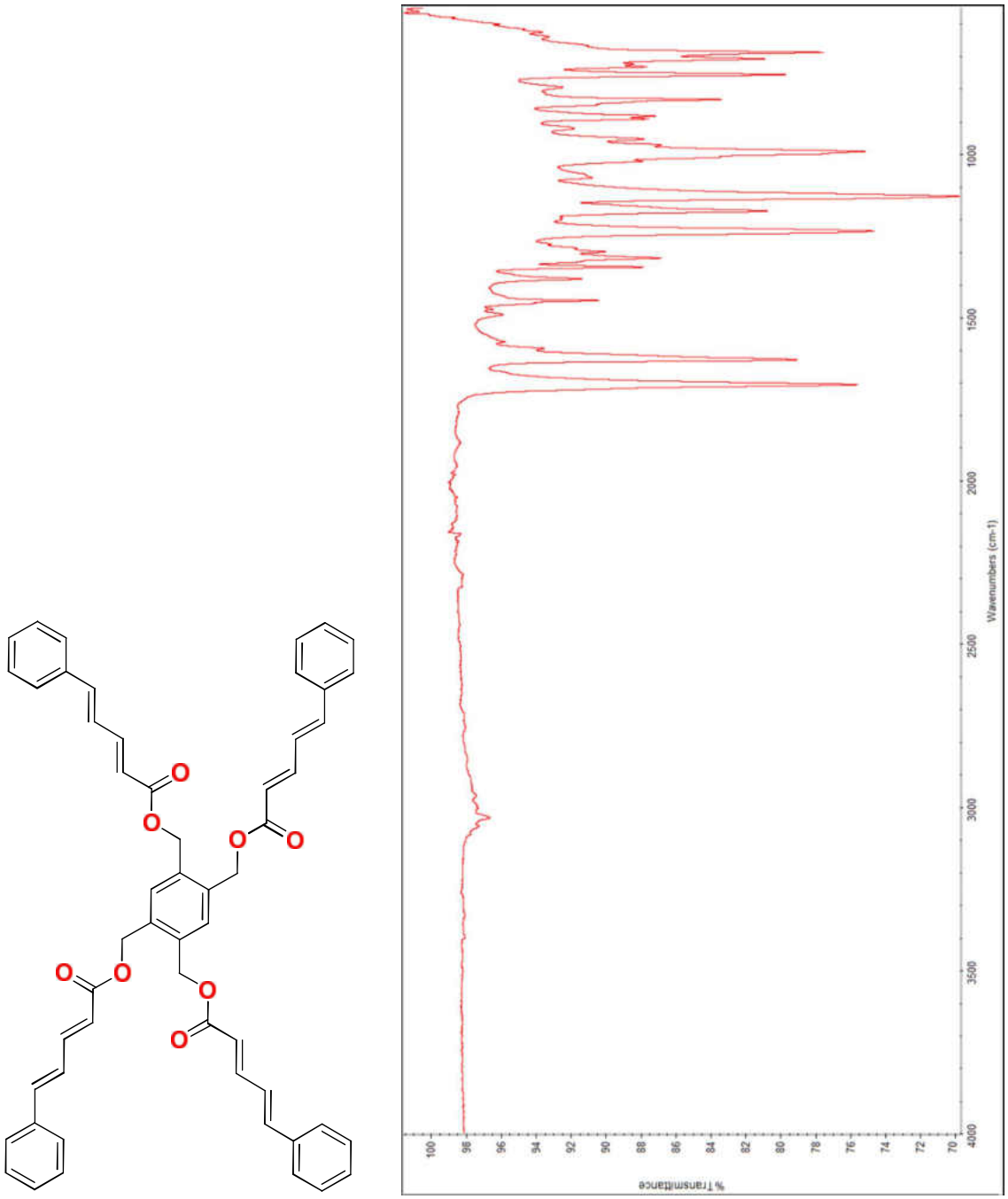

Figure 102. FT-IR spectrum of monomer **20**.

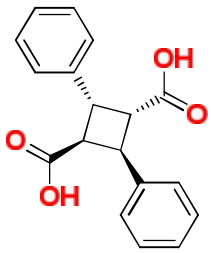

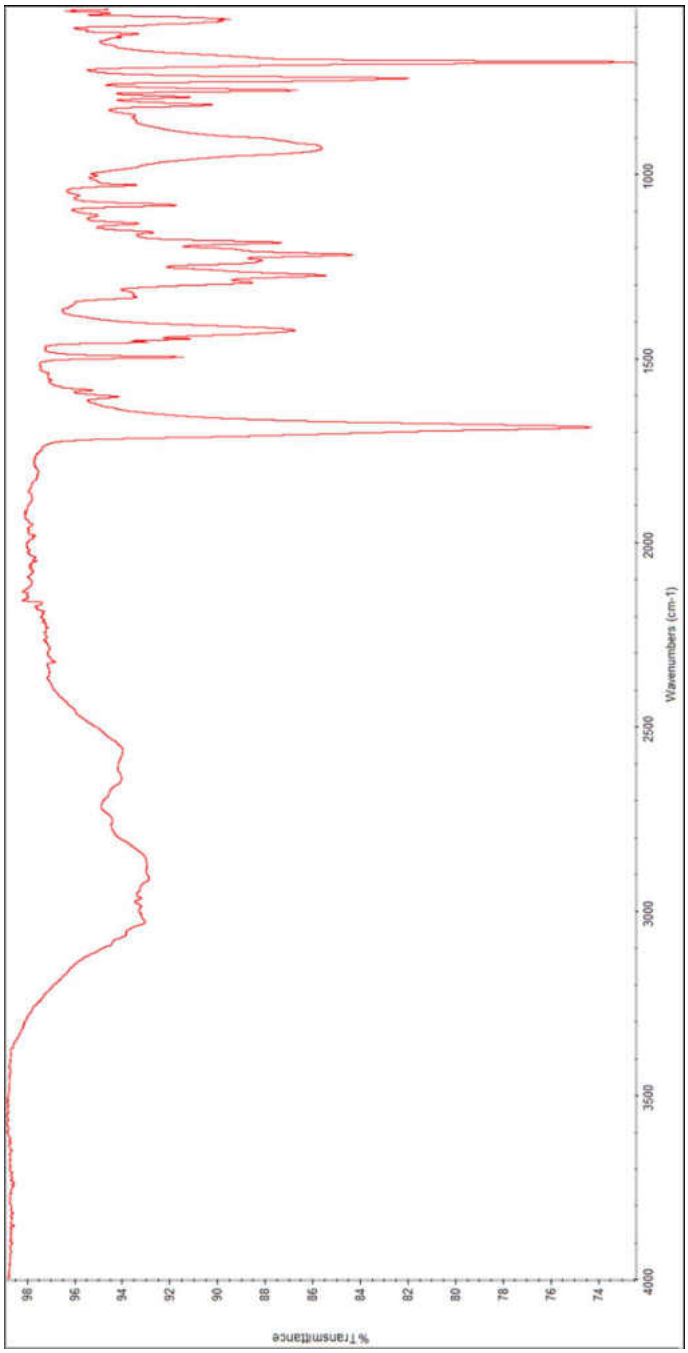

Figure 103. FT-IR spectrum of **17**.

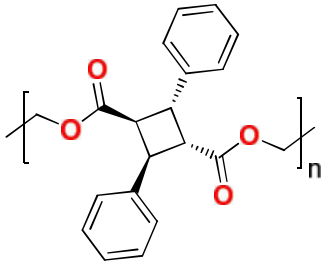

PEAT

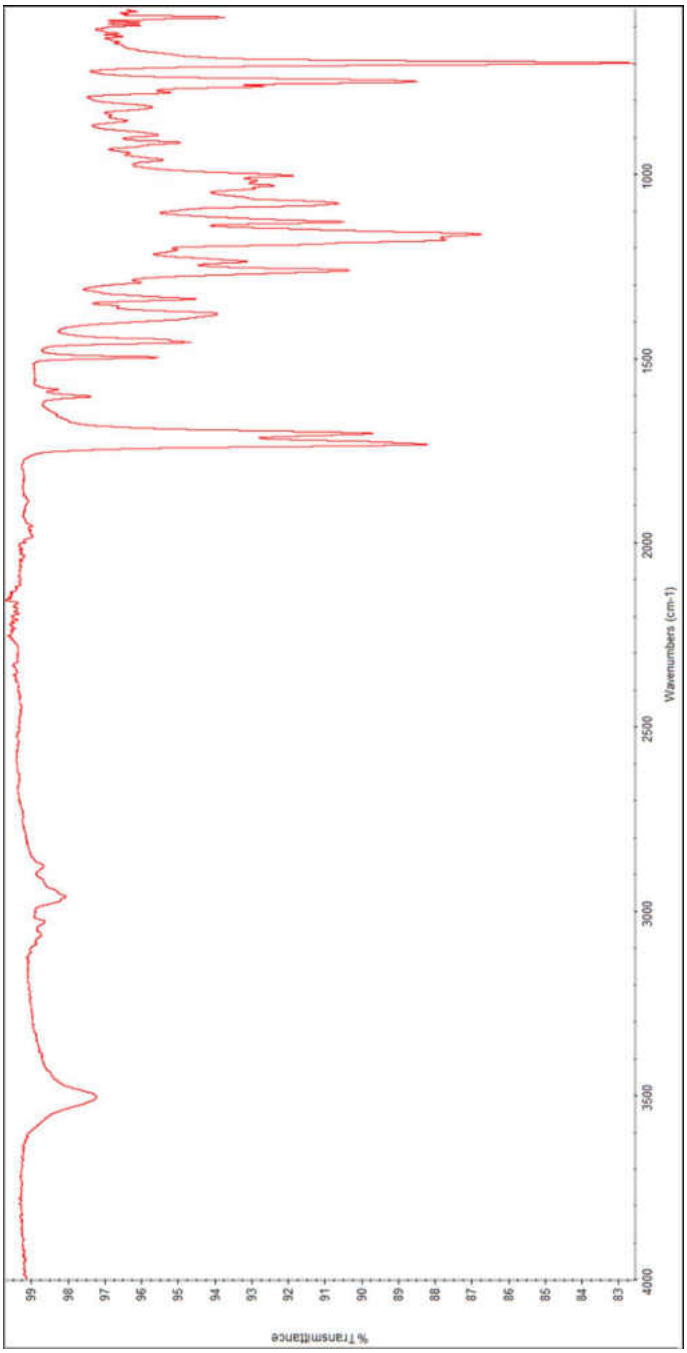

Figure 104. FT-IR spectrum of **21P**.

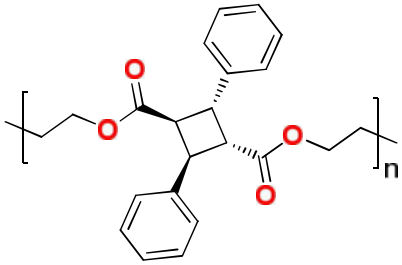

PBAT

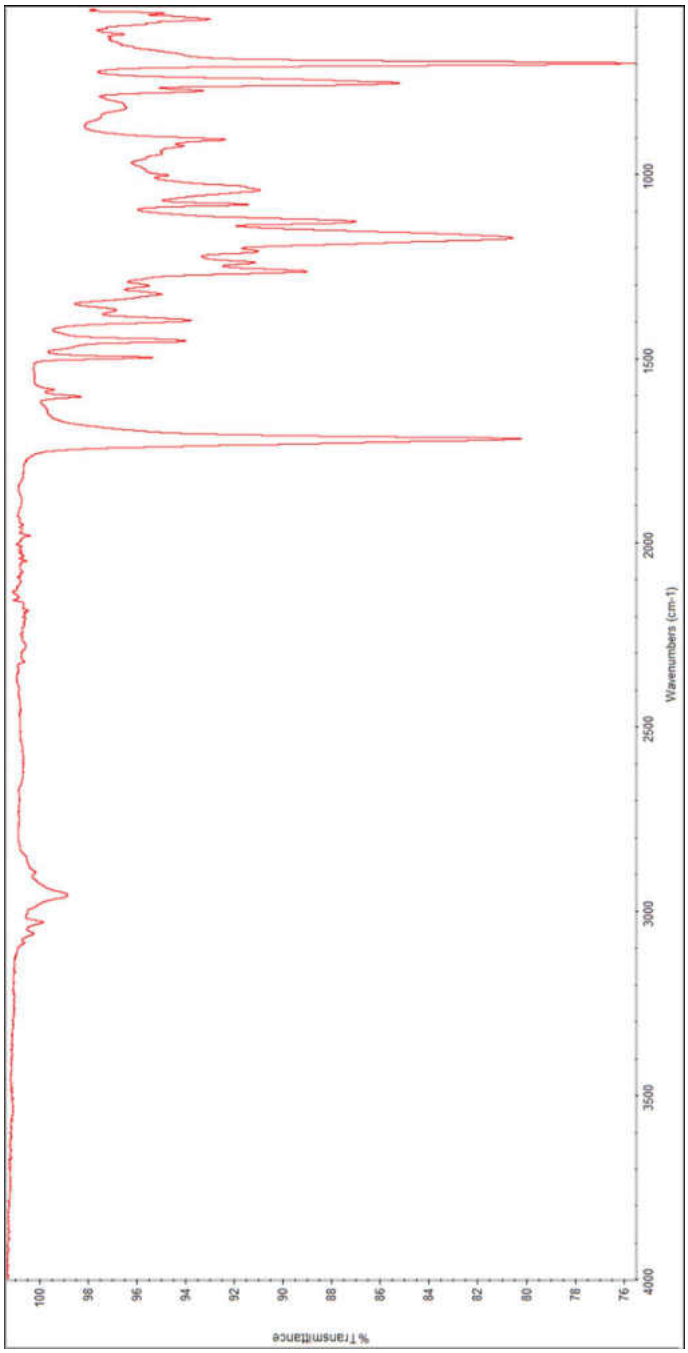

Figure 105. FT-IR spectrum of **22P**.

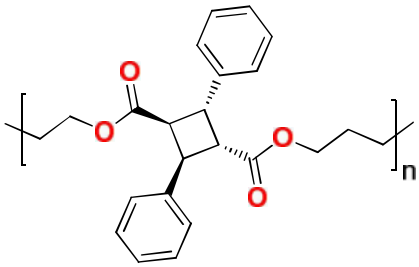

PPAT5

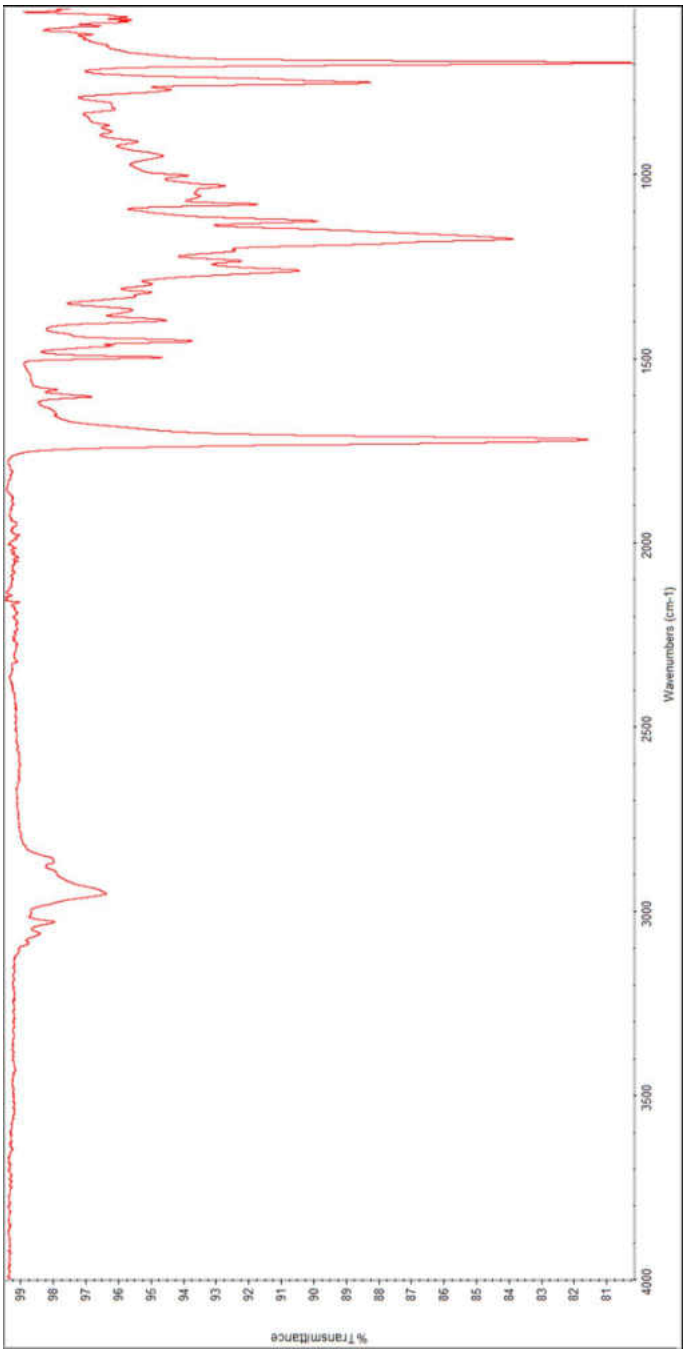

Figure 106. FT-IR spectrum of **23P**.

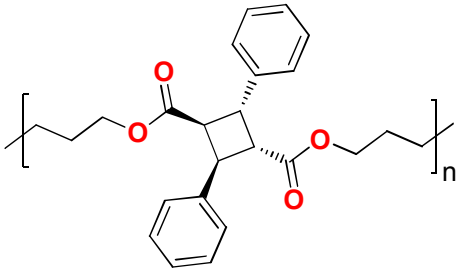

PHAT

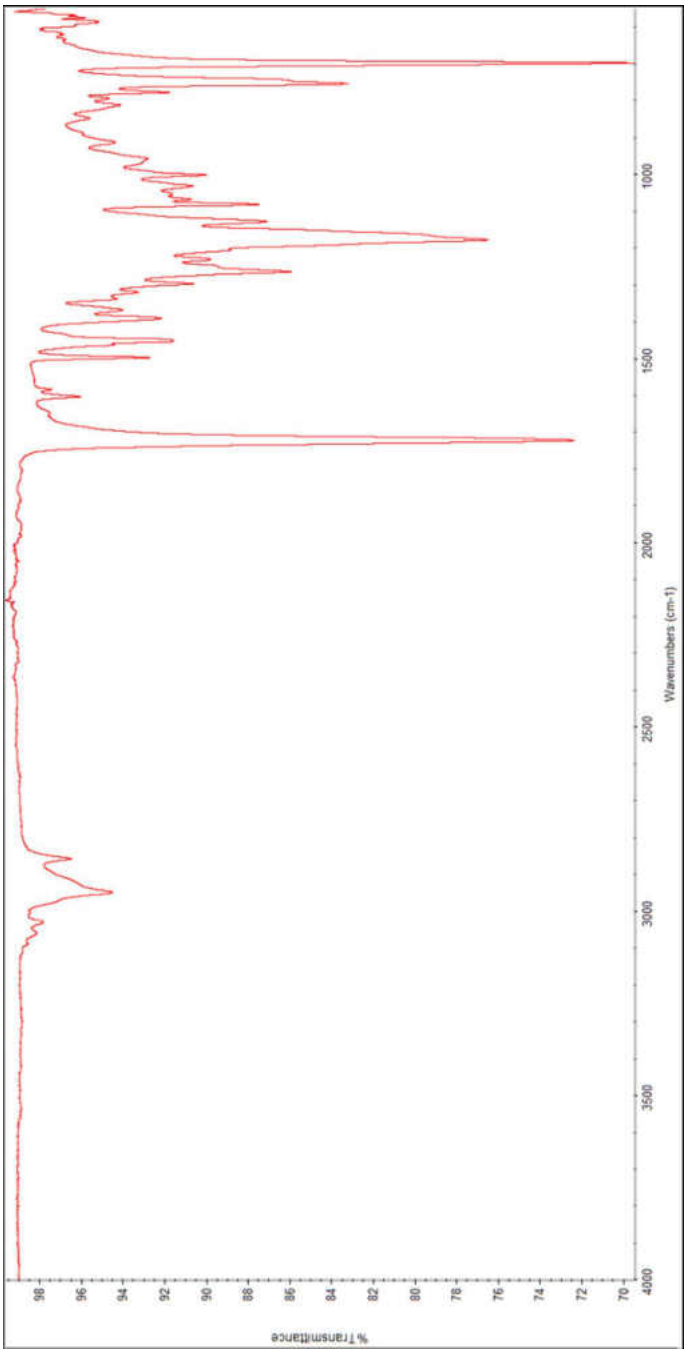

Figure 107. FT-IR spectrum of **24P**.

APPENDIX C

Selected UV-Vis Spectra

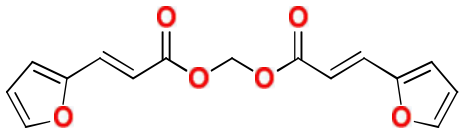

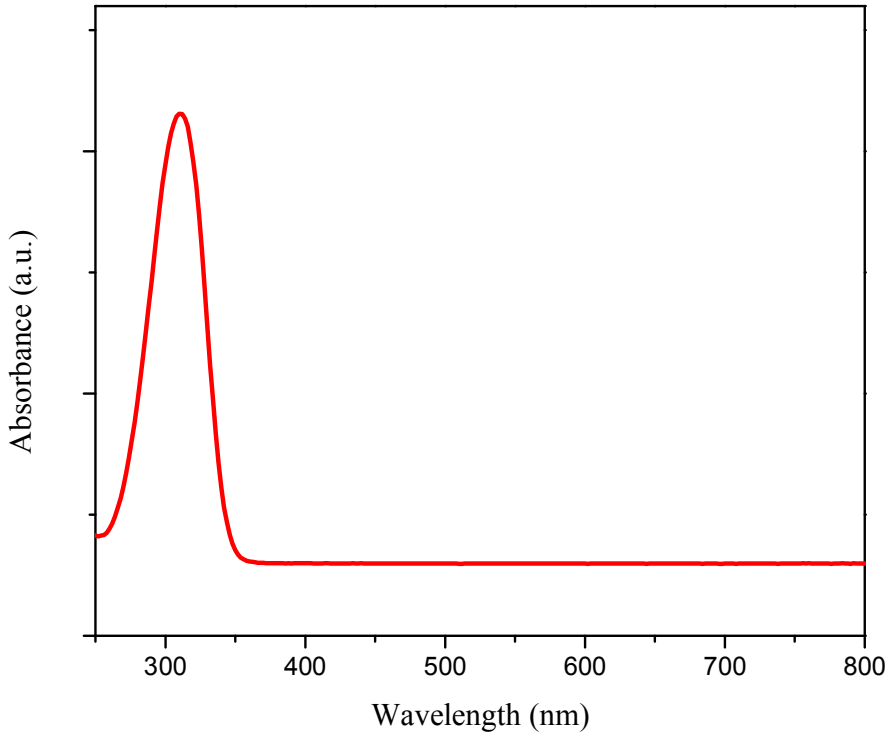

Figure 108. UV-Vis spectrum of monomer **4** in ethanol.

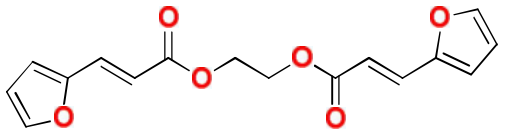

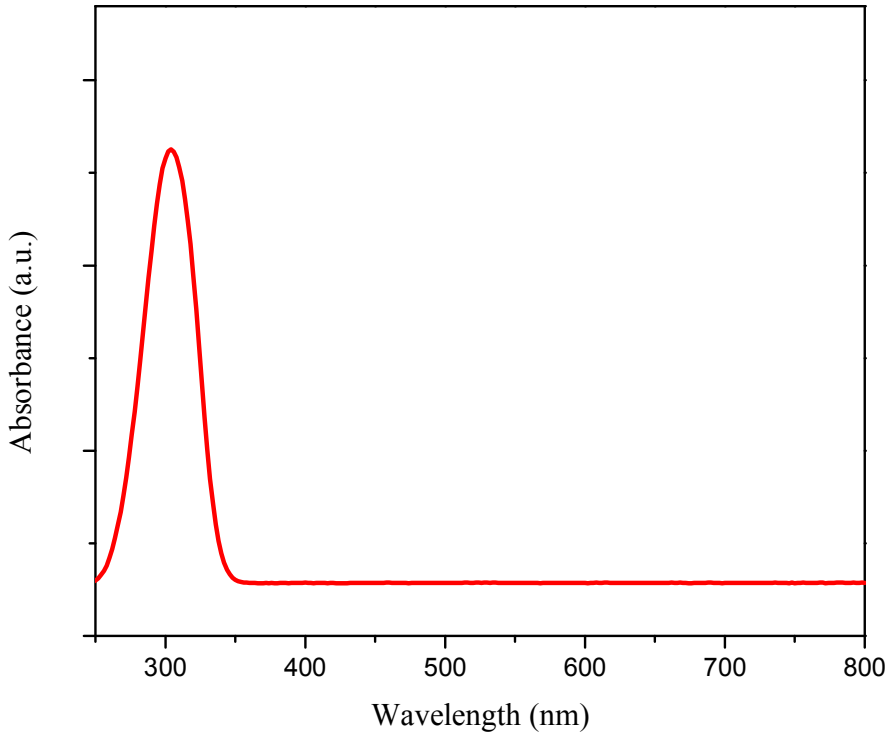

Figure 109. UV-Vis spectrum of monomer **5** in ethanol.

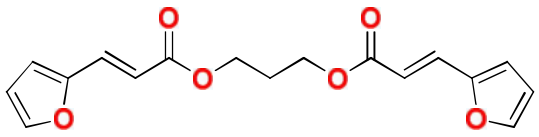

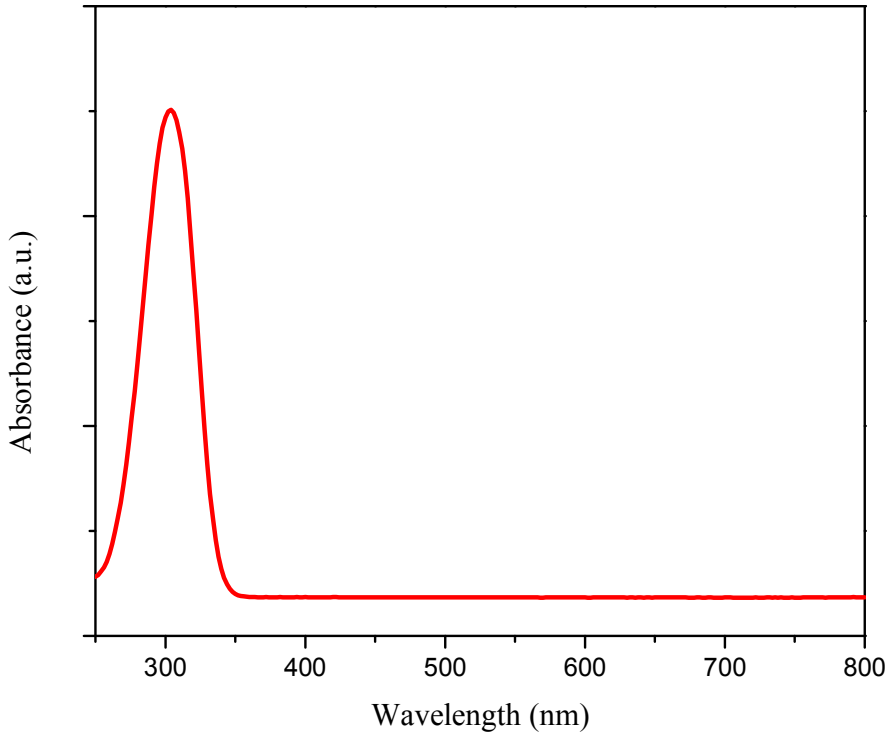

Figure 110. UV-Vis spectrum of monomer **6** in ethanol.

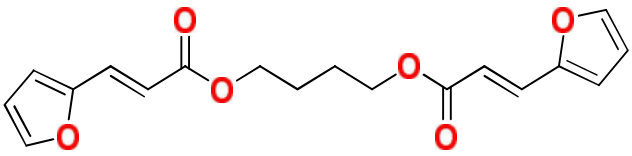

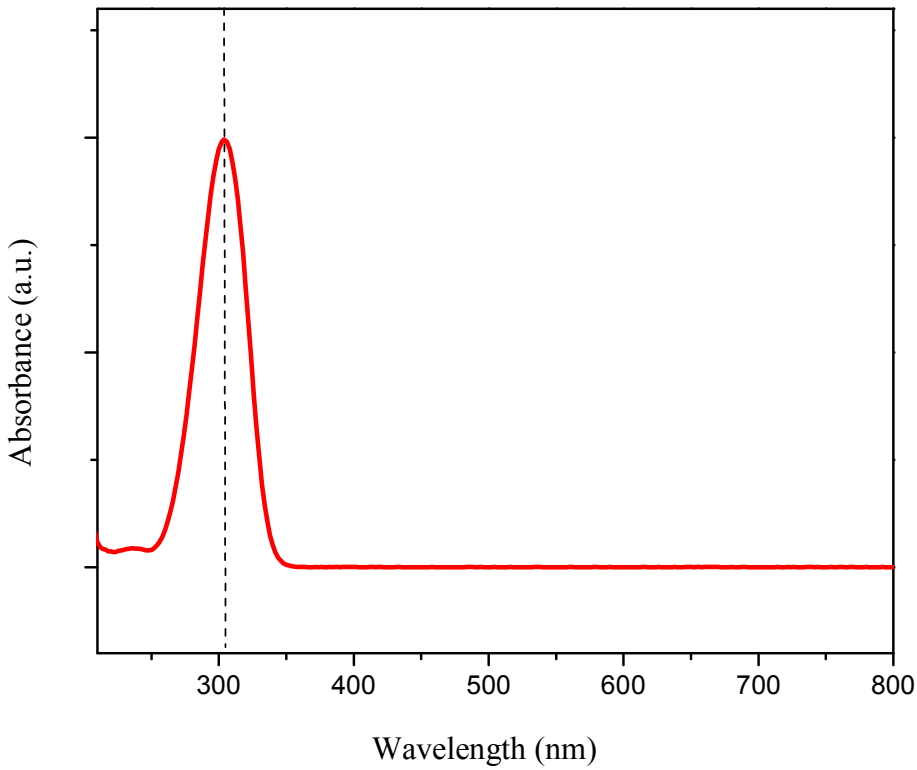

Figure 111. UV-Vis spectrum of monomer **7** in ethanol.

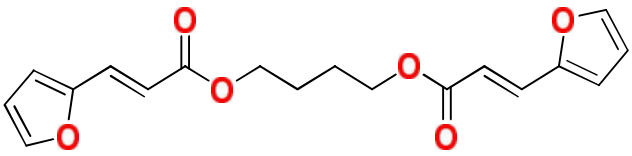

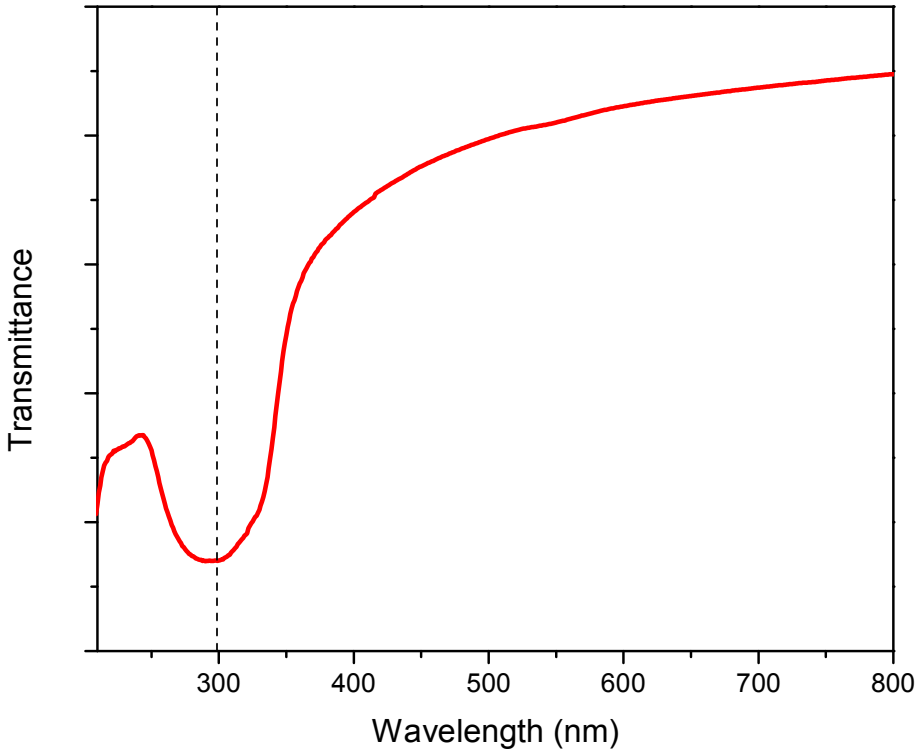

Figure 112. UV-Vis spectrum of monomer **7** in solid state.

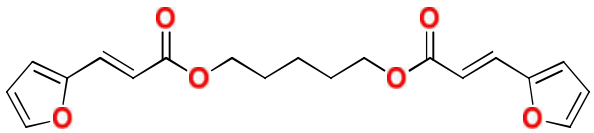

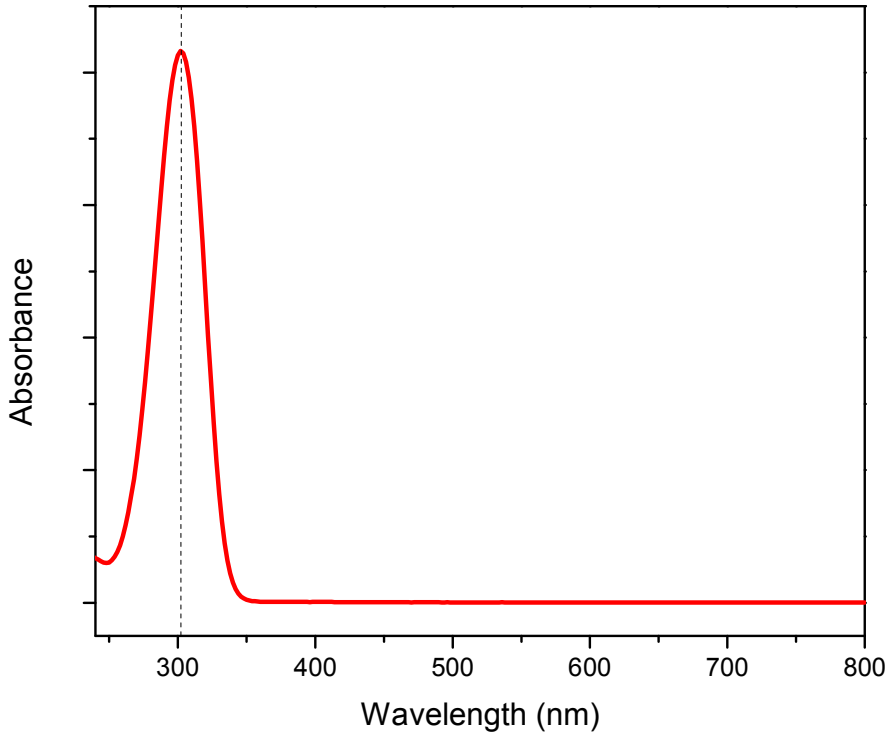

Figure 113. UV-Vis spectrum of monomer **8** in acetonitrile.

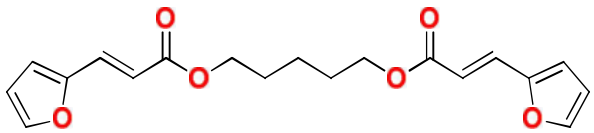

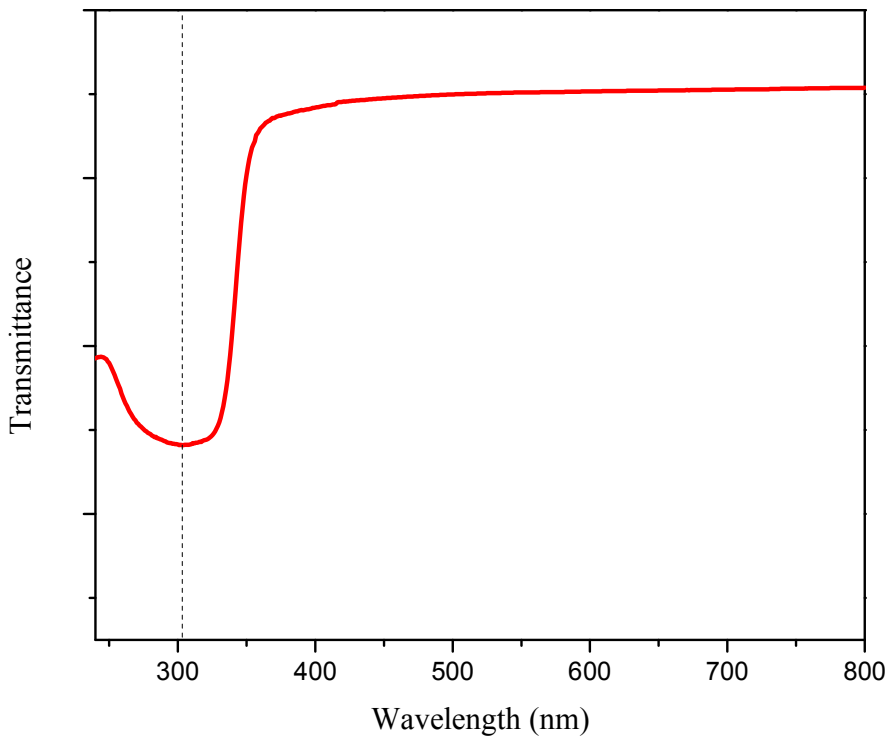

Figure 114. UV-Vis spectrum of monomer **8** in solid state.

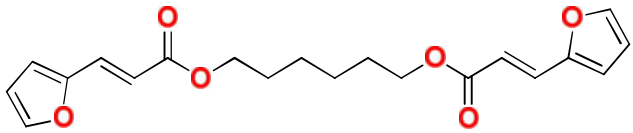

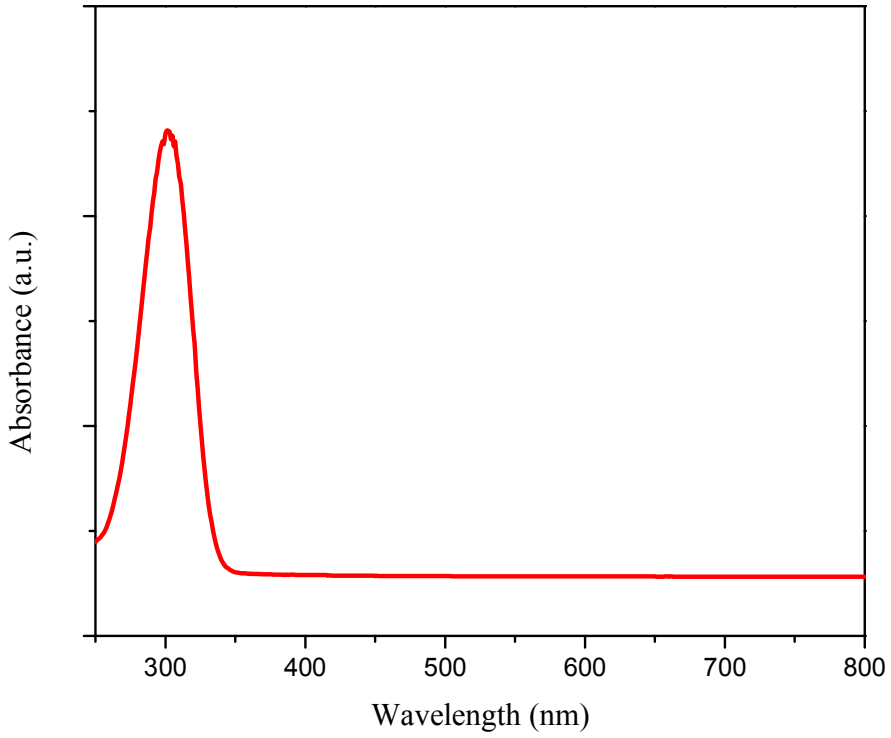

Figure 115. UV-Vis spectrum of monomer **9** in ethanol.

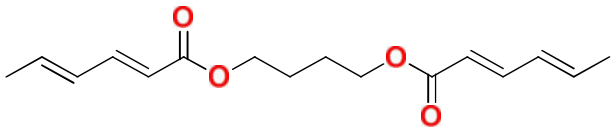

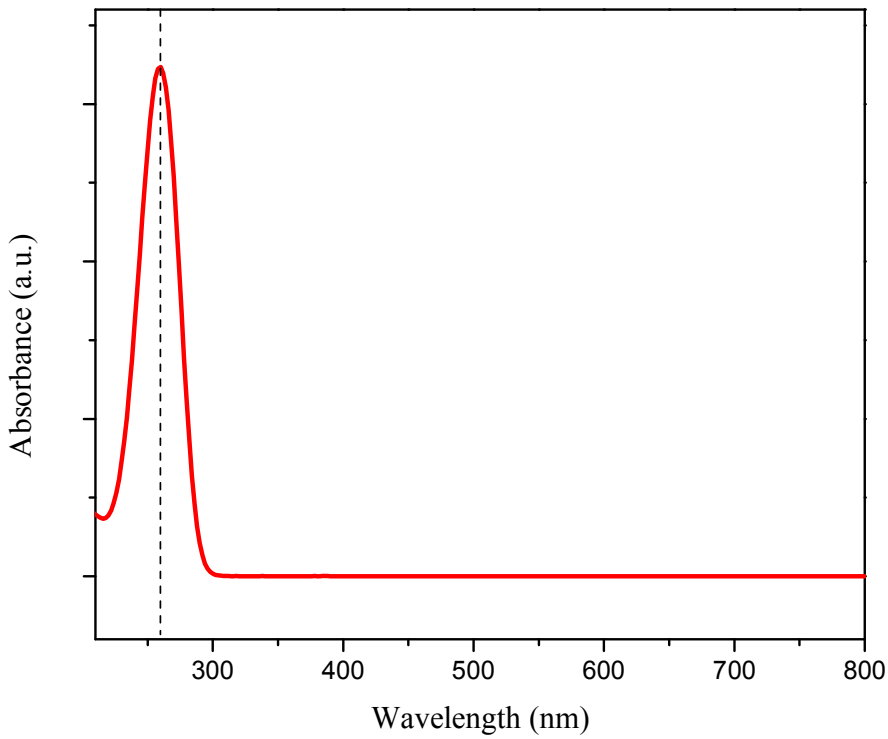

Figure 116. UV-Vis spectrum of monomer **12** in ethanol.

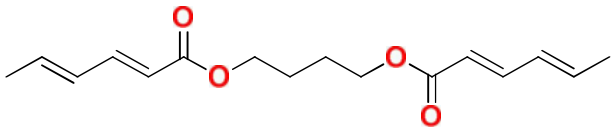

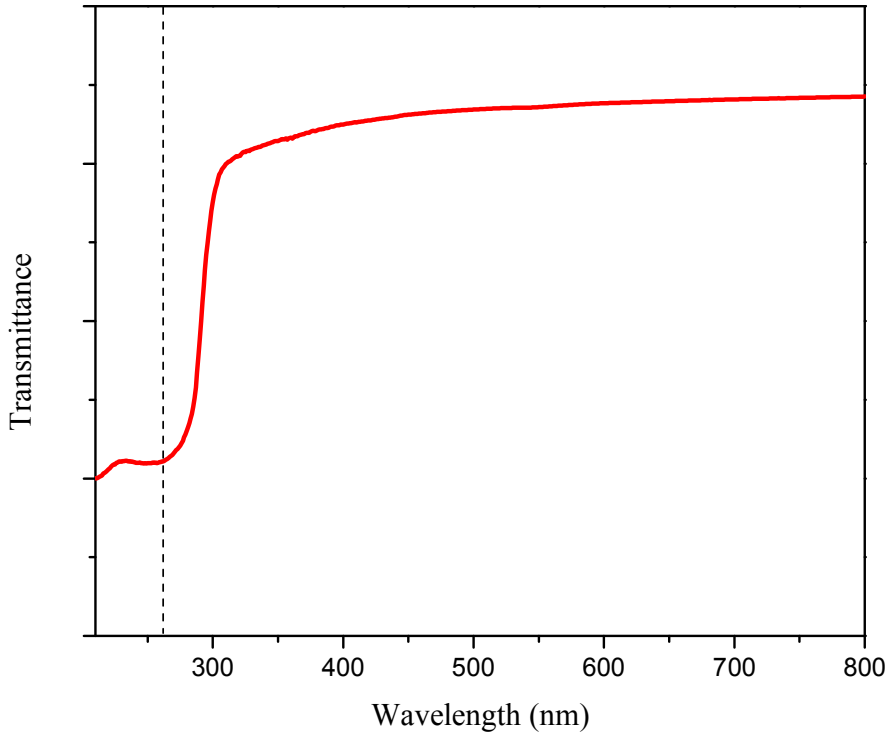

Figure 117. UV-Vis spectrum of monomer **12** in solid state.

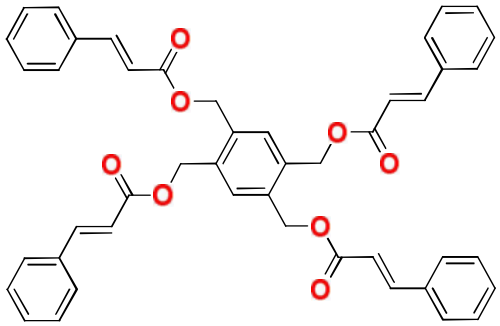

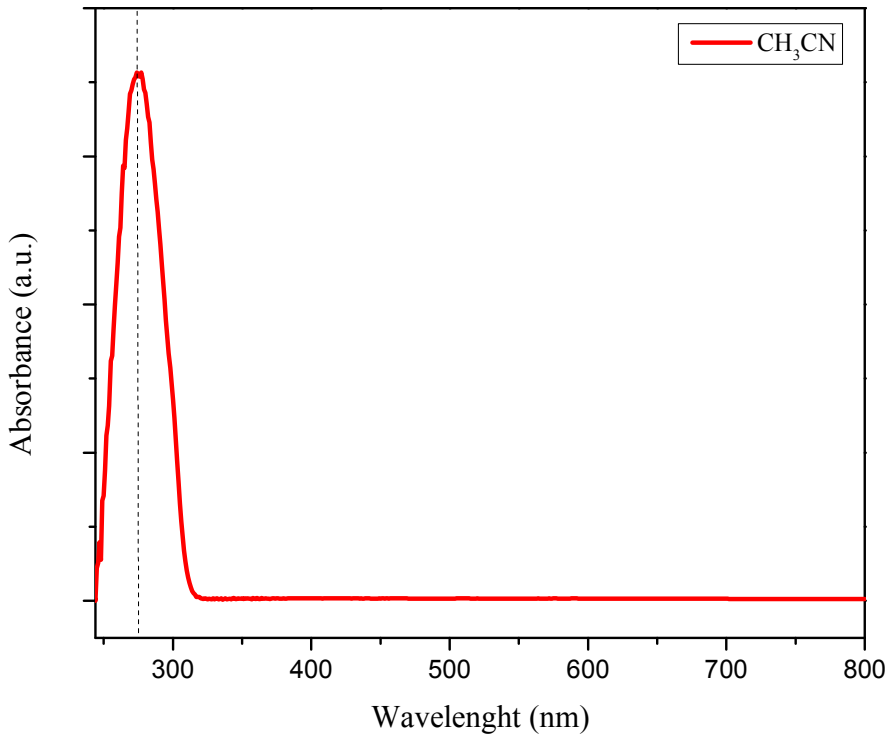

Figure 118. UV-Vis spectrum of monomer **16** in acetonitrile.

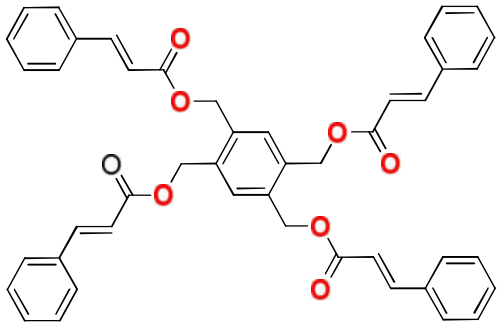

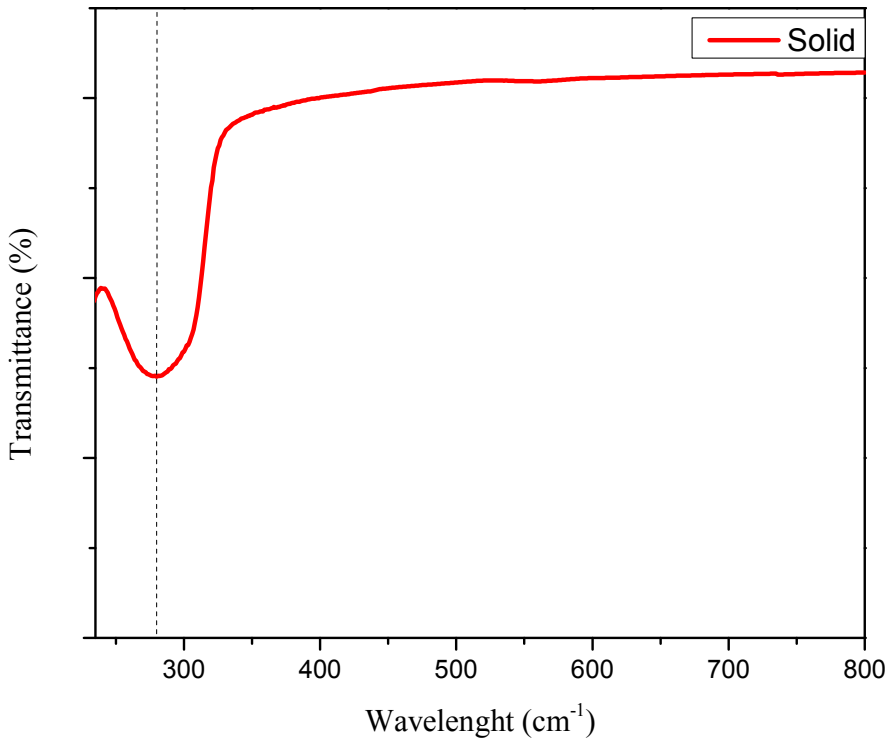

Figure 119. UV-Vis spectrum of monomer **16** in solid state.

APPENDIX D

Selected Powder-XRD Spectra

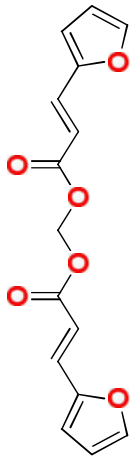

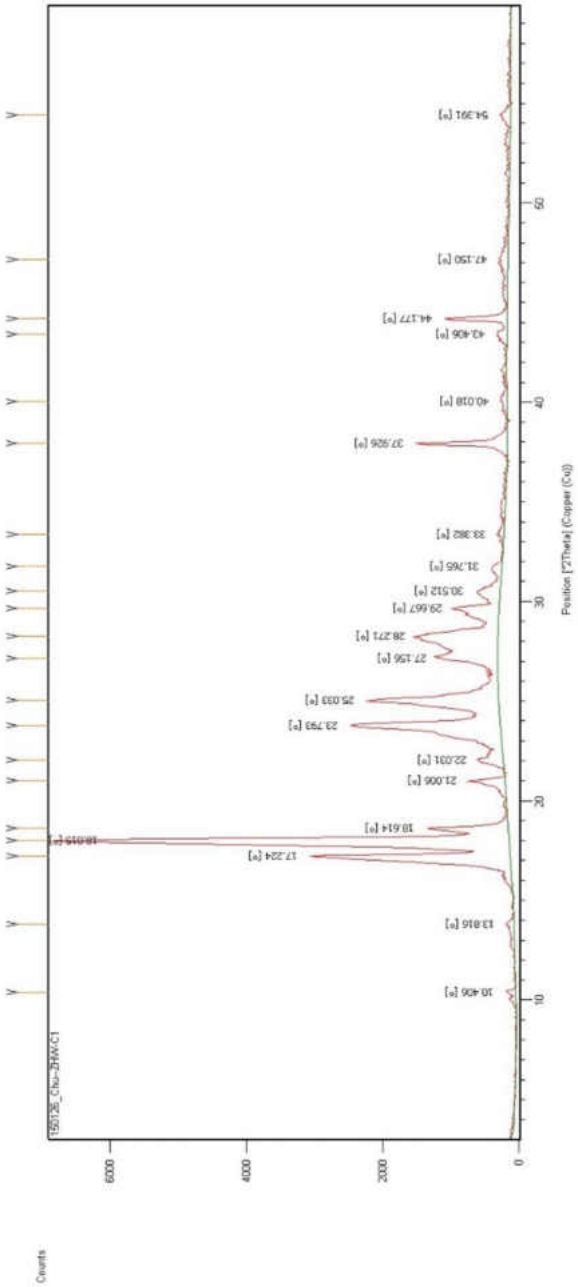

Figure 120. Powder-XRD spectrum of monomer **4**.

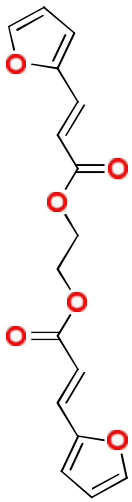

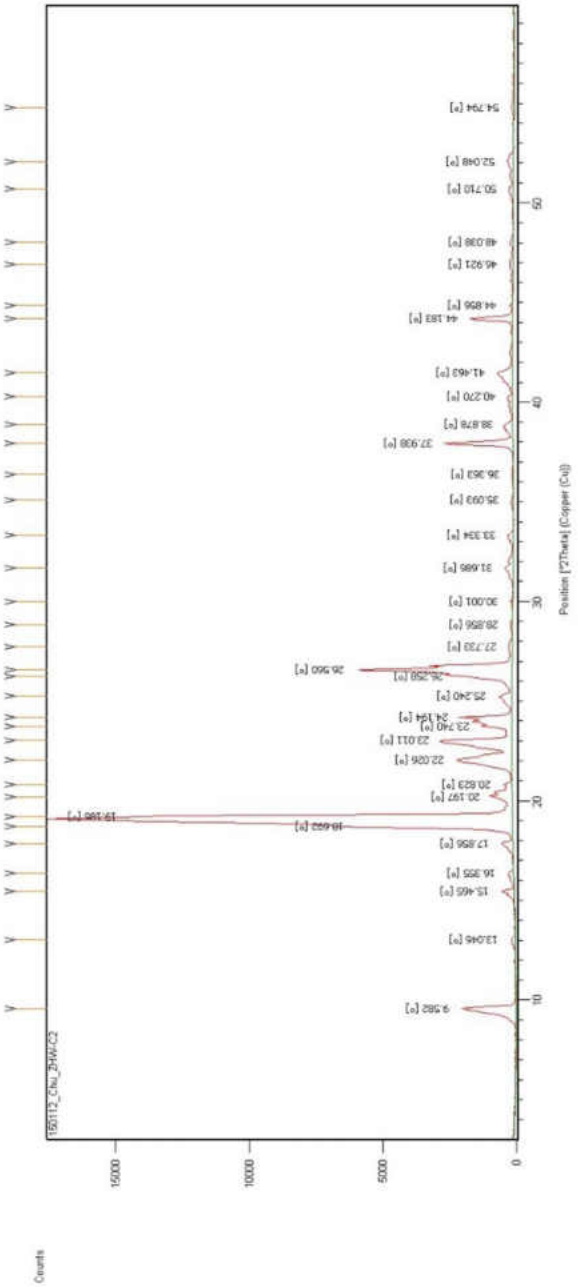

Figure 121. Powder-XRD spectrum of monomer **5**.

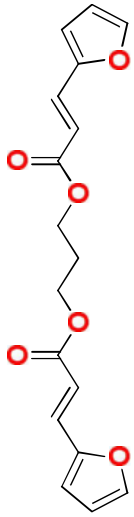

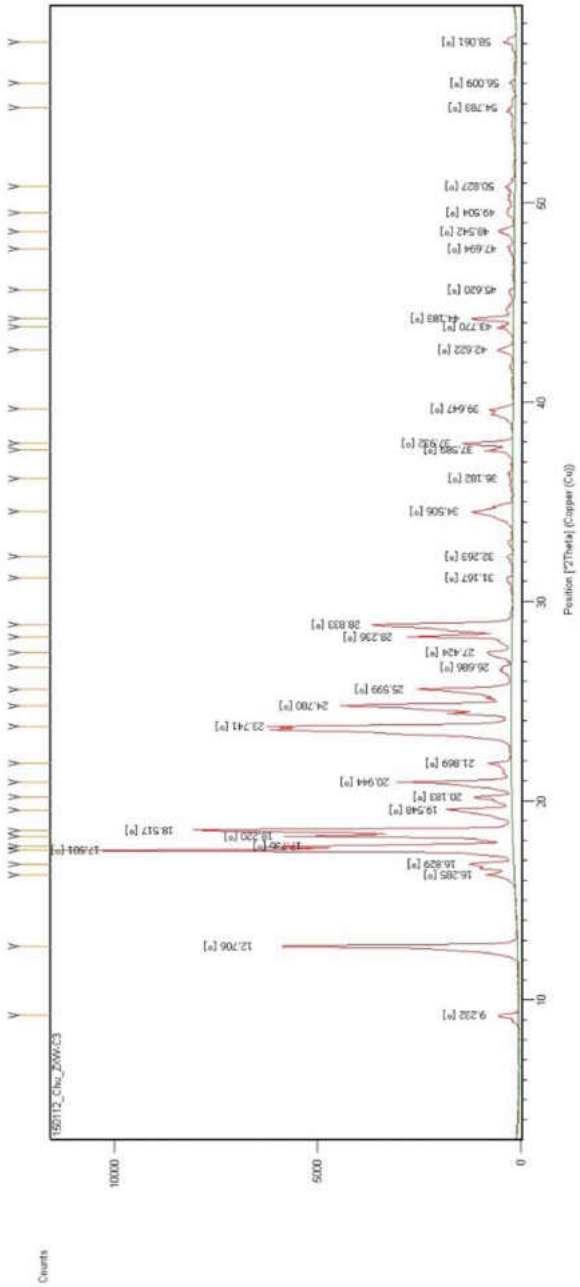

Figure 122. Powder-XRD spectrum of monomer **6**.

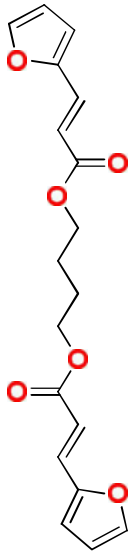

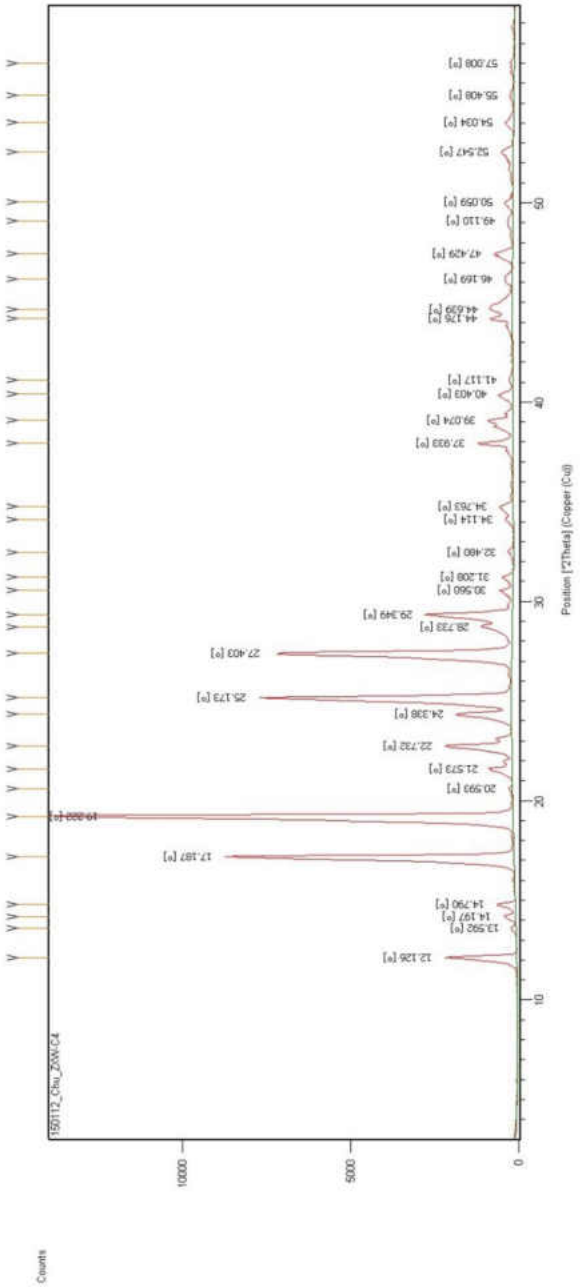

Figure 123. Powder-XRD spectrum of monomer **7**.

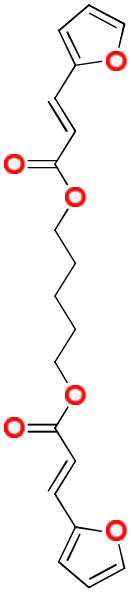

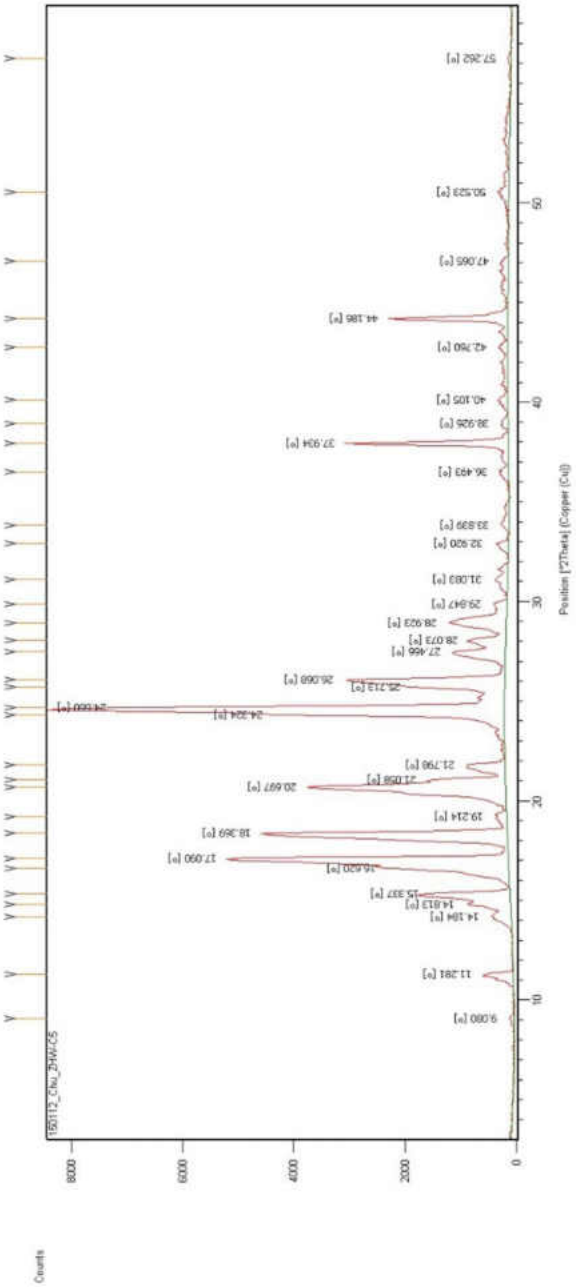

Figure 124. Powder-XRD spectrum of monomer **8**.

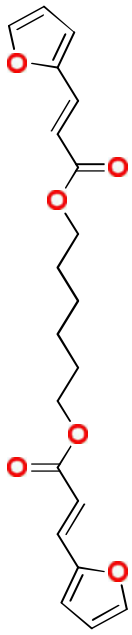

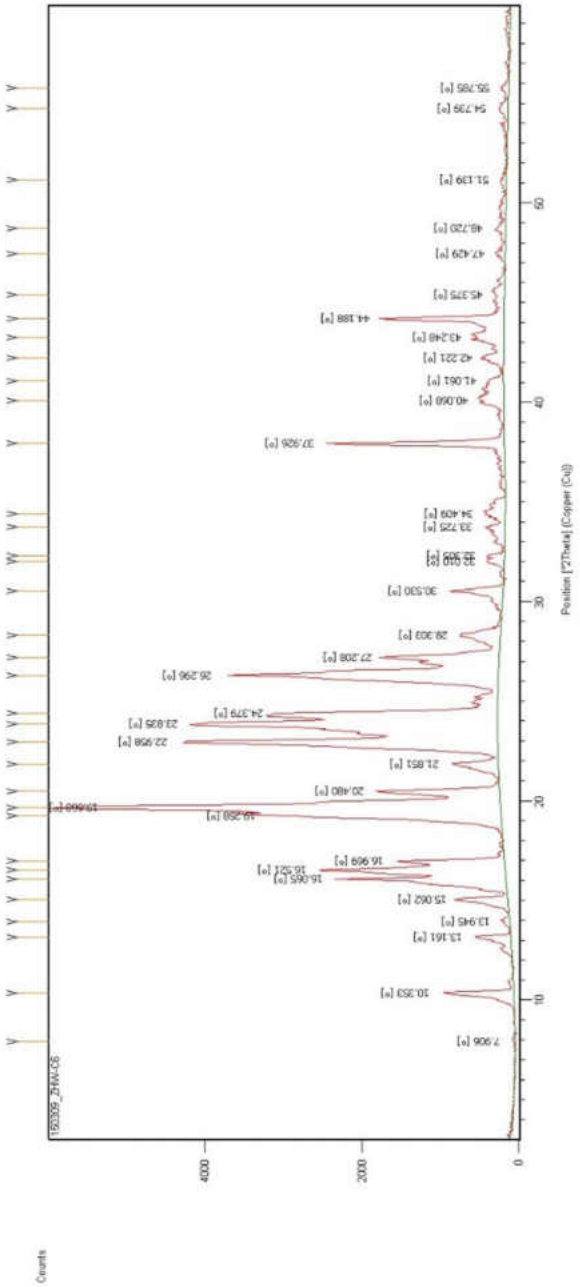

Figure 125. Powder-XRD spectrum of monomer **9**.

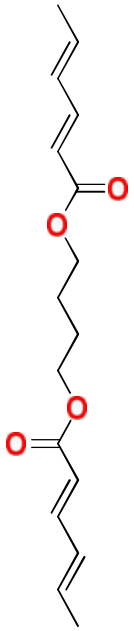

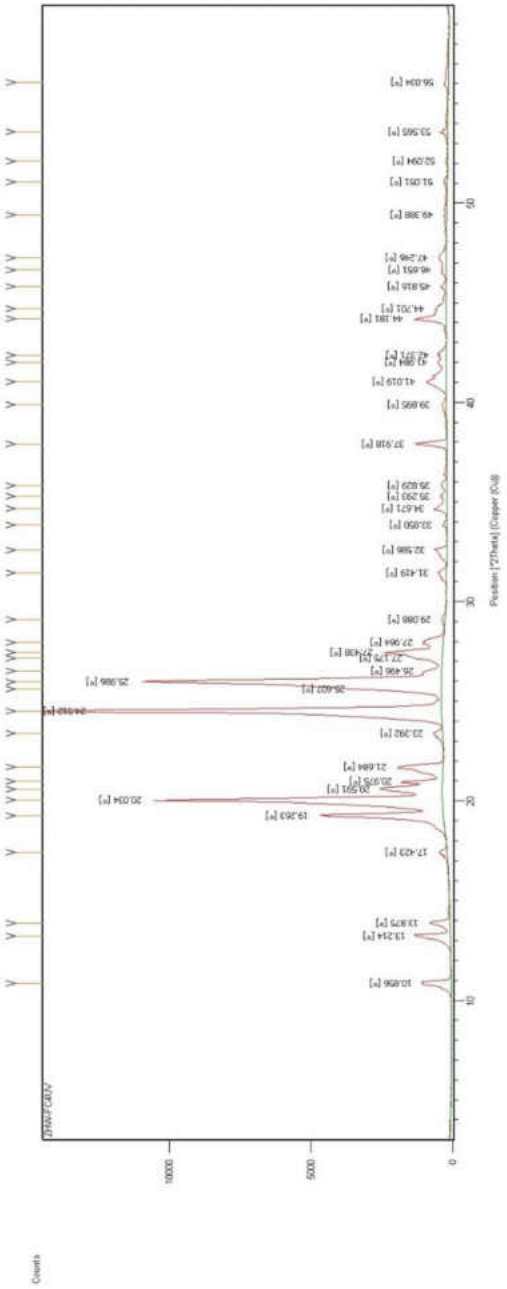

Figure 126. Powder-XRD spectrum of monomer **12**.

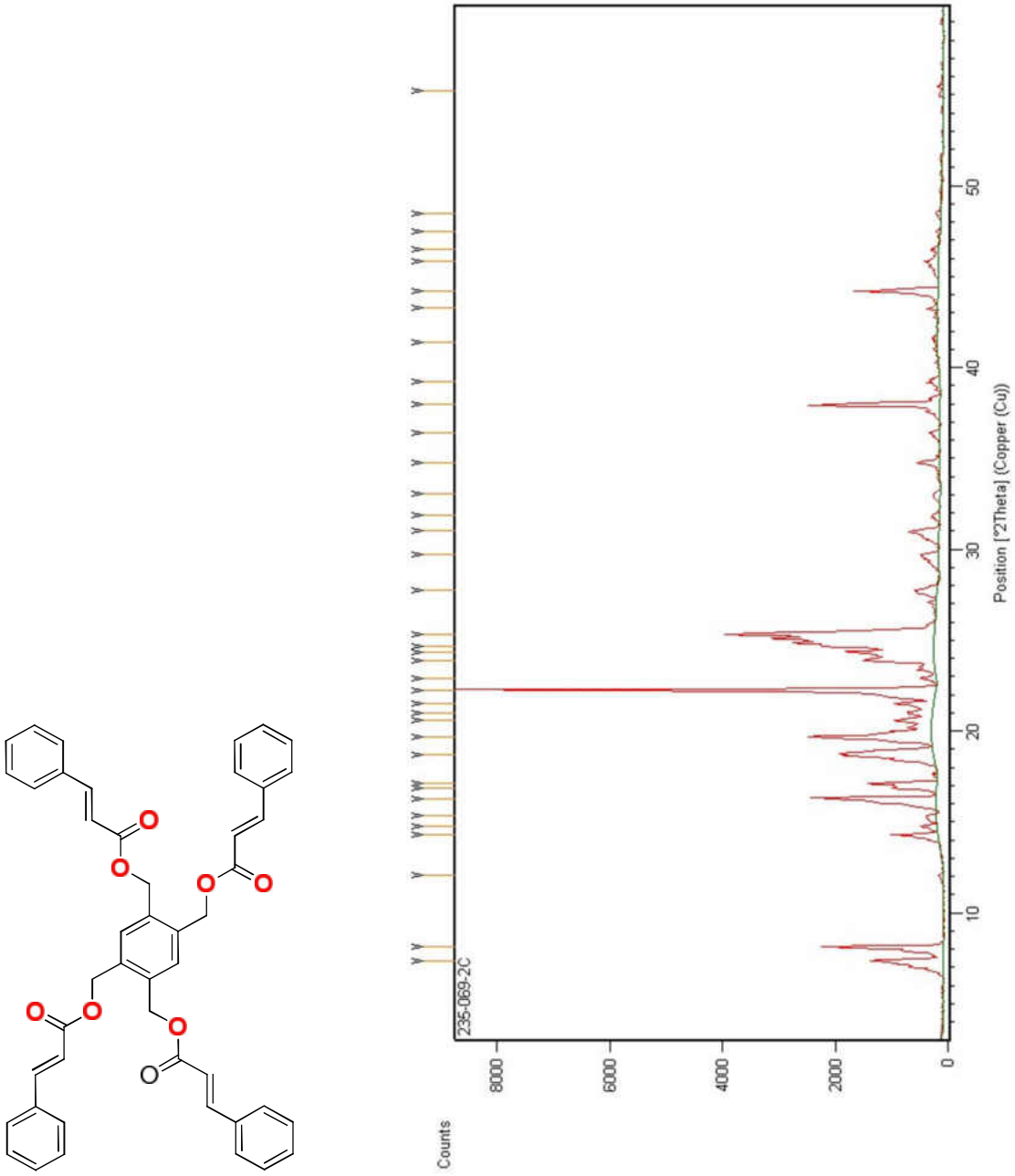

Figure 127. Powder-XRD spectrum of monomer **16**.

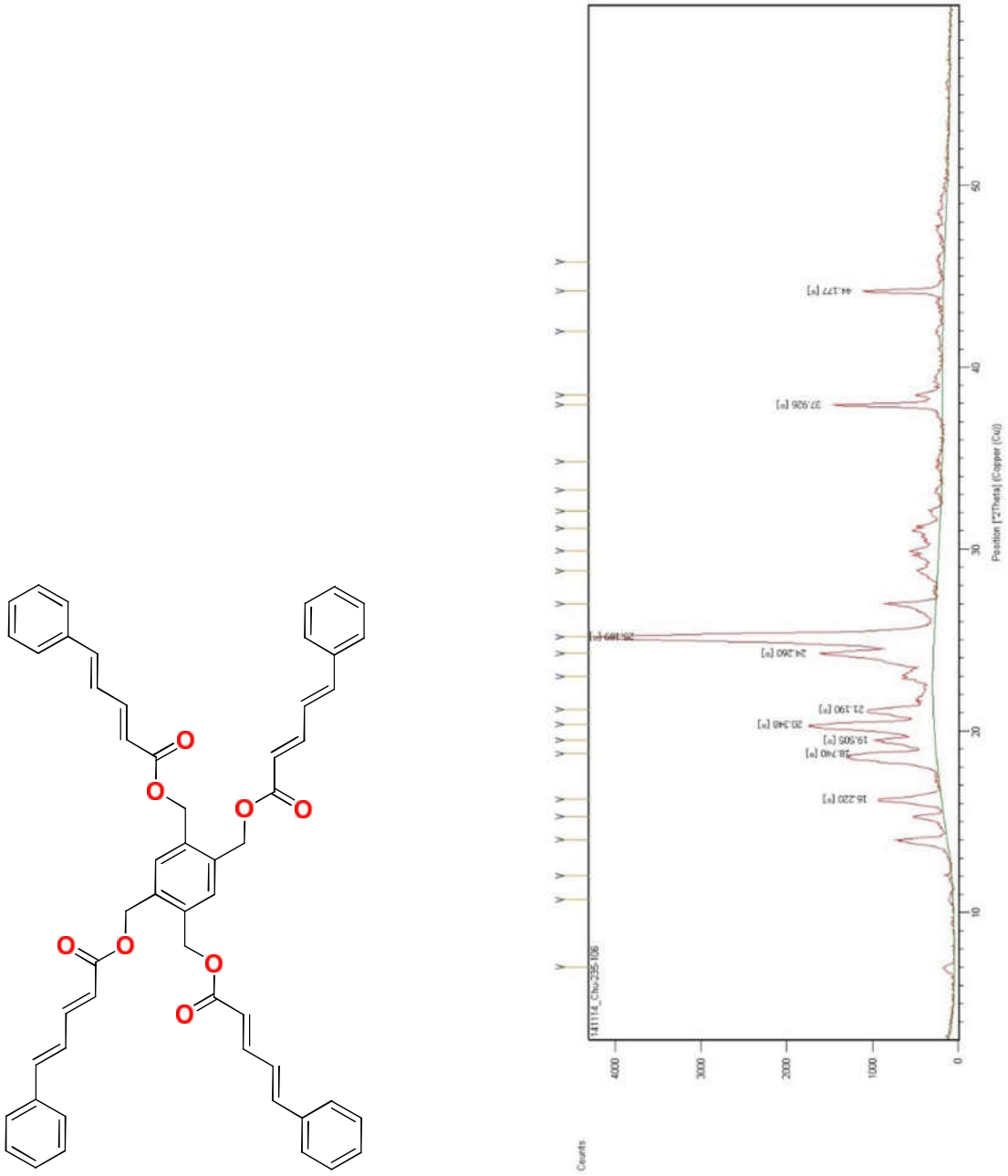

Figure 128. Powder-XRD spectrum of monomer **20**.

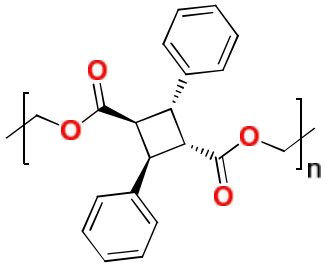

PEAT

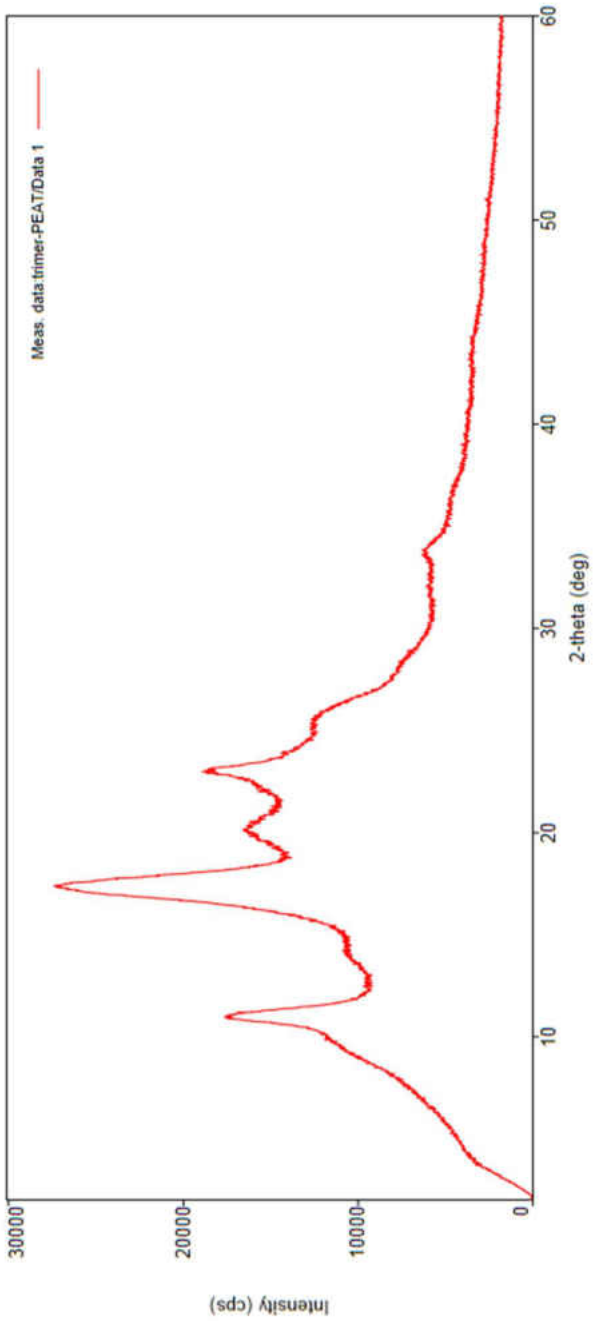

Figure 129. Powder-XRD spectrum of **21P**.

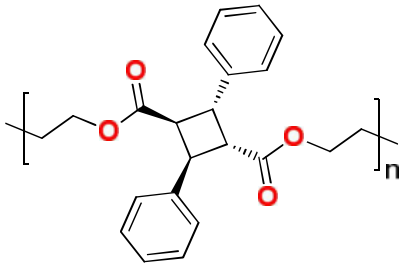

PBAT

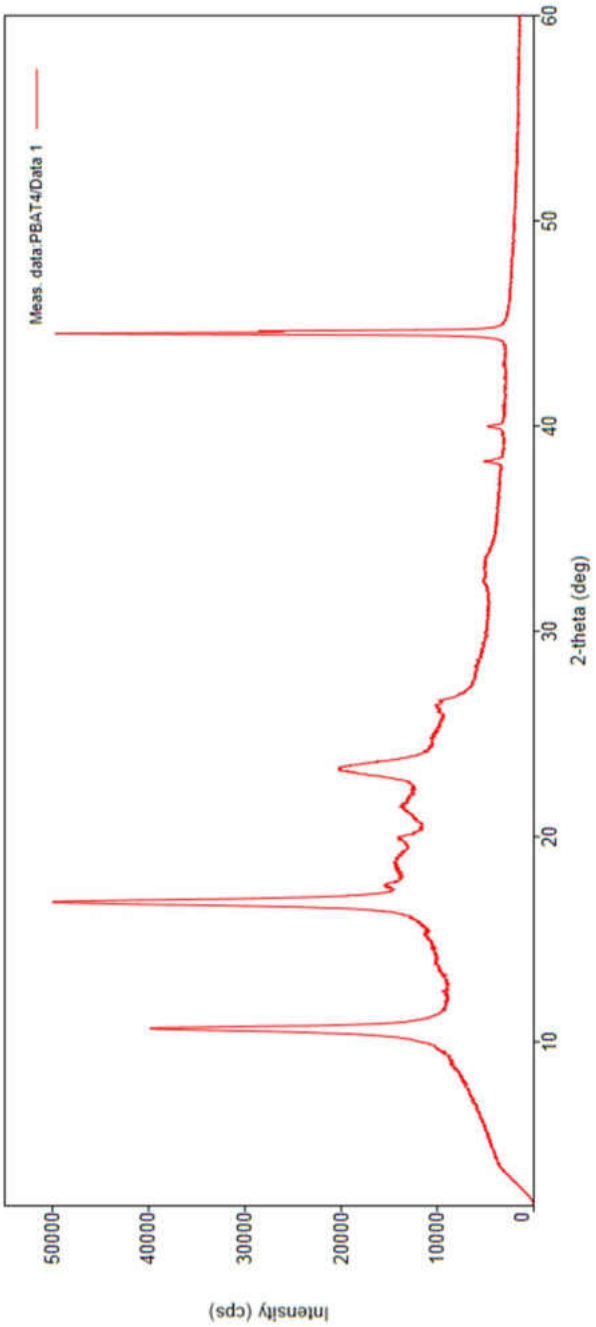

Figure 130. Powder-XRD spectrum of **22P**.

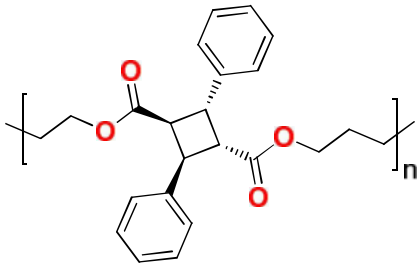

PPAT5

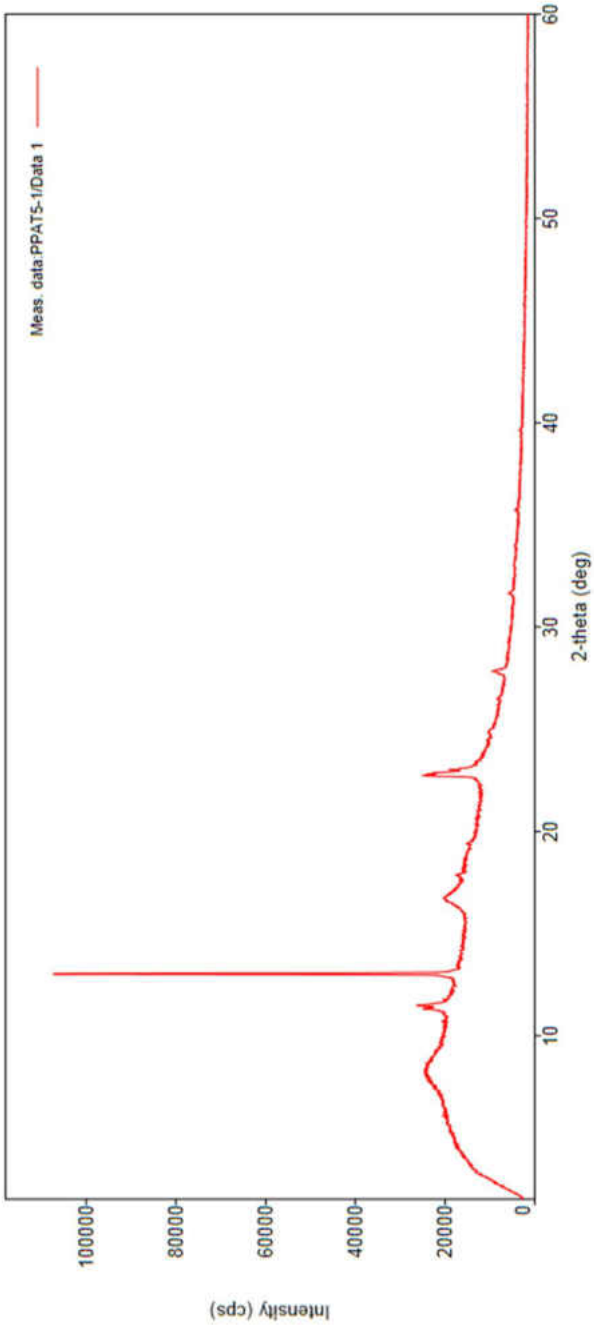

Figure 131. Powder-XRD spectrum of **23P**.

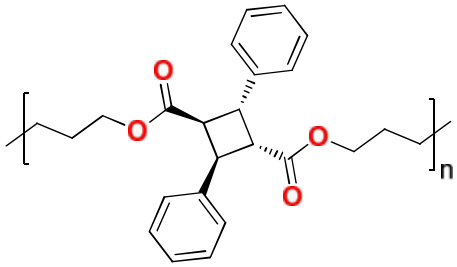

PHAT

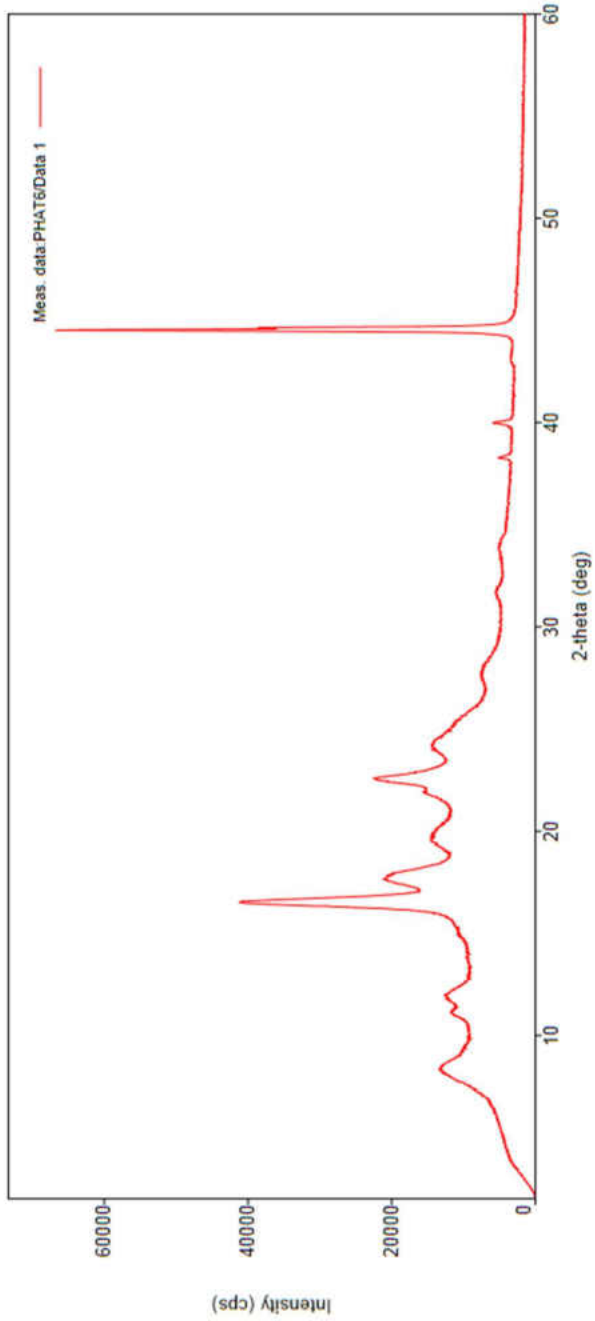

Figure 132. Powder-XRD spectrum of **24P**.

APPENDIX E

Selected DSC Data

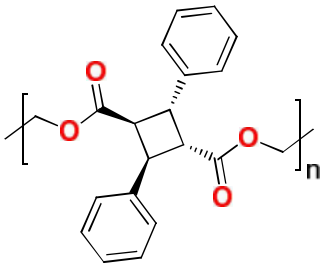

PEAT

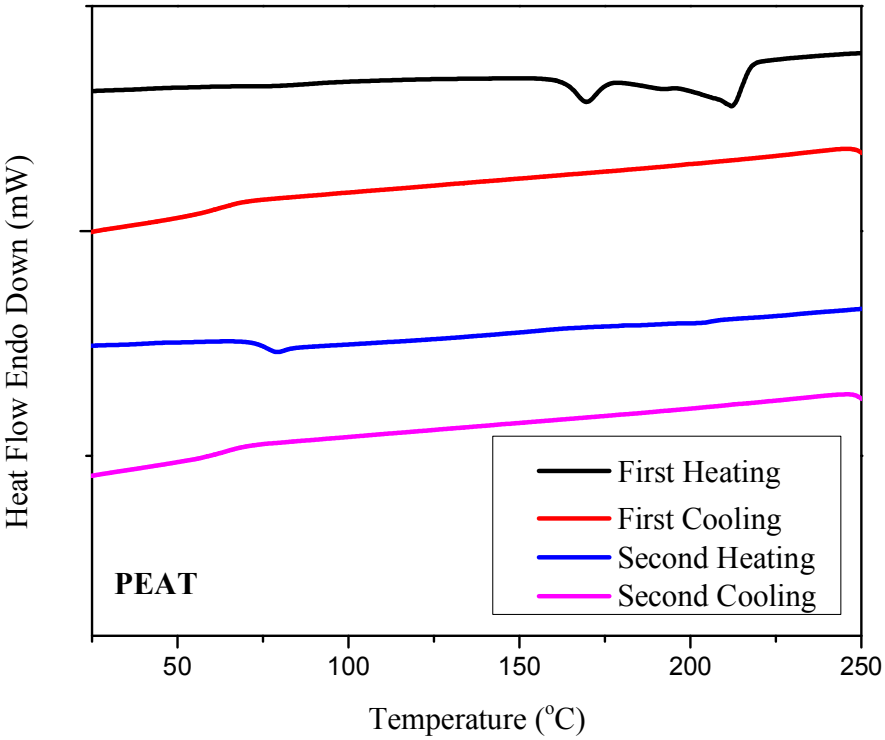

Figure 133. DSC data of **21P**.

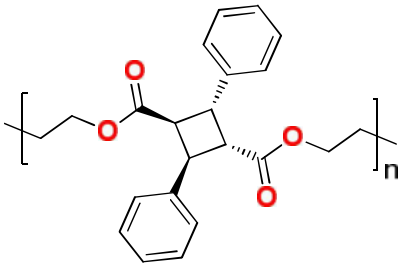

PBAT

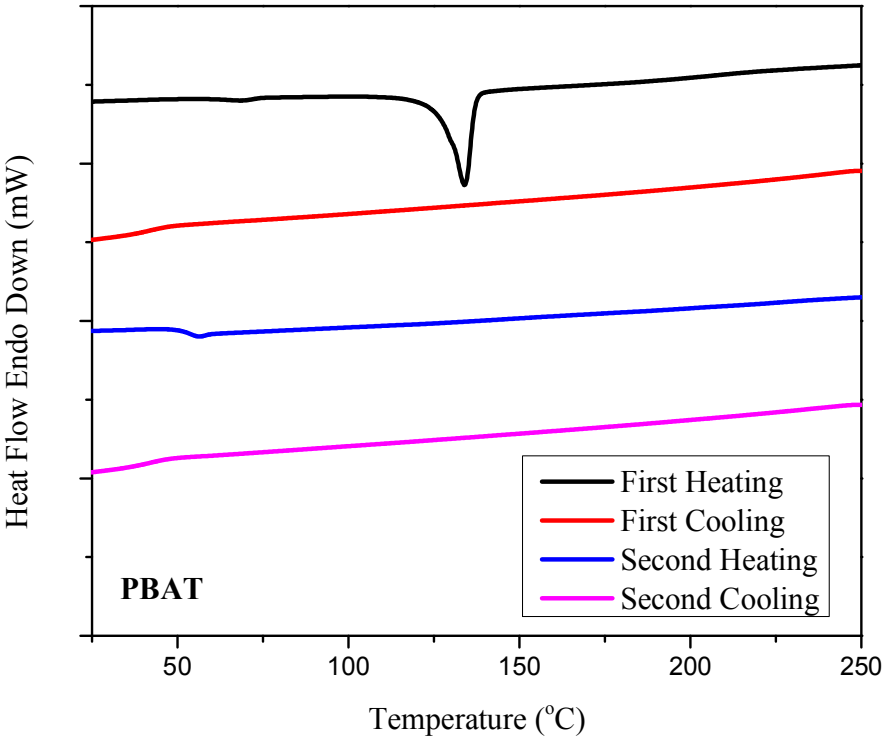

Figure 134. DSC data of **22P**.

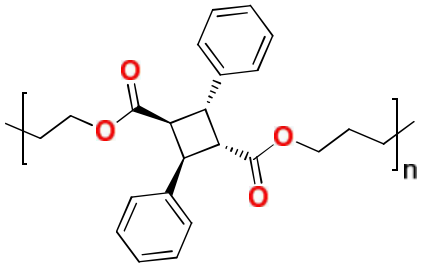

PPAT5

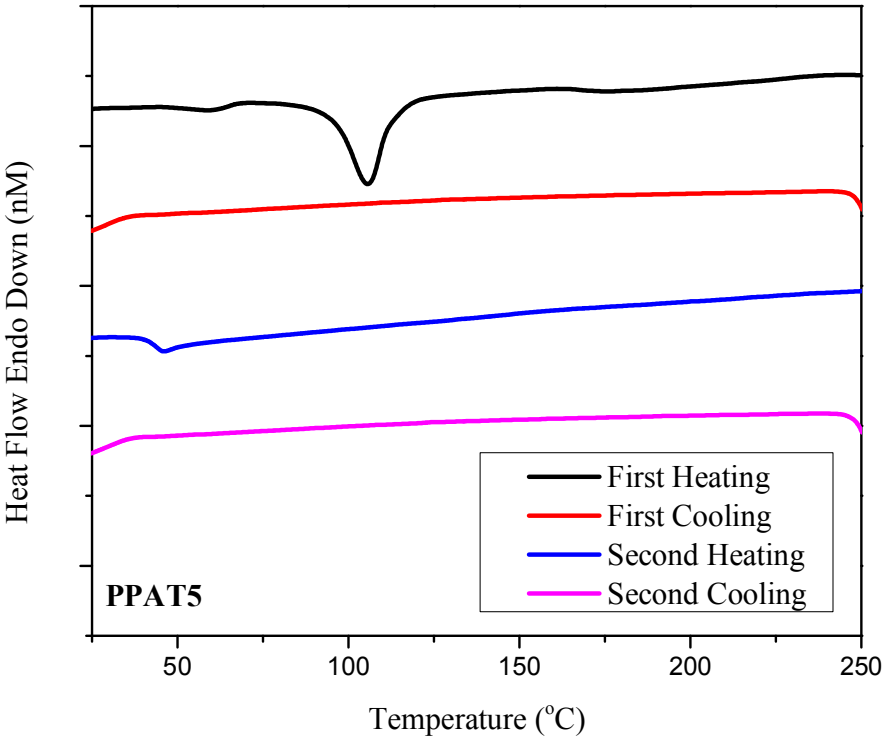

Figure 135. DSC data of **23P**.

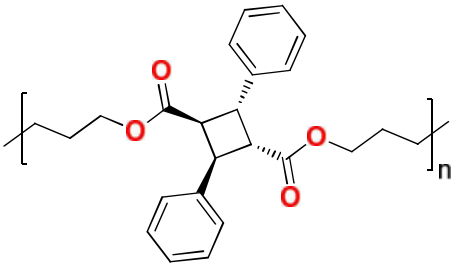

PHAT

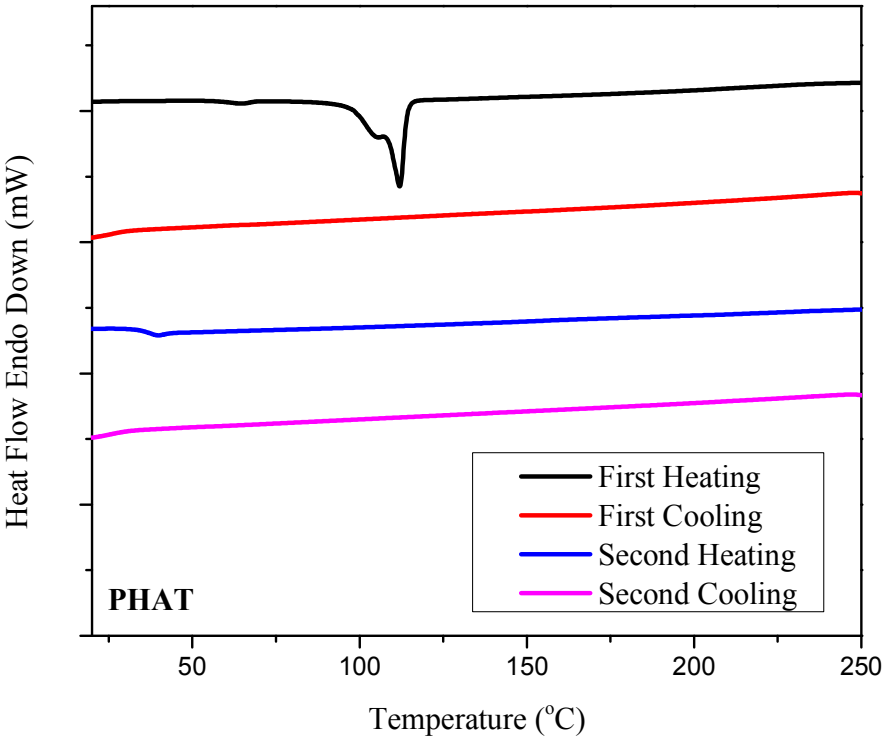

Figure 136. DSC data of **24P**.

APPENDIX F

Selected XRD Data

Table 1. Crystal data in gemini monomer synthesis

Monomer	**4**	**5**	**6**	**8b**	**9**
Formula	$C_{15}H_{12}O_6$	$C_{16}H_{14}O_6$	$C_{17}H_{16}O_6$	$C_{19}H_{20}O_6$	$C_{20}H_{22}O_6$
FW	288.25	302.27	316.30	344.35	358.38
Crystal system	Monoclinic	Monoclinic	Monoclinic	Triclinic	Triclinic
Space group	$P2_1/n$	$P2_1/c$	C2/c	P-1	P-1
Temperature (K)	100	296	100	100	296
a (Å)	7.8854(3)	7.7394(3)	20.653(3)	8.4565(16)	7.8318(3)
b (Å)	40.4674(16)	10.9097(4)	5.6096(9)	9.2121(18)	10.8235(4)
c (Å)	16.8200(6)	8.8568(3)	14.800(2)	12.338(2)	11.2825(4)
α (°)	90.00	90.00	90.00	75.225(4)	101.076(2)
β (°)	93.449(2)	108.636(2)	113.089(2)	73.326(4)	92.579(2)
γ (°)	90.00	90.00	90.00	72.042(4)	93.722(2)
Volume/Å3	5357.6(4)	708.61(5)	1577.3(4)	861.1(3)	934.98(6)
Z	15	4	8	2	2
ρcalc [g/cm^3]	1.344	1.417	1.332	1.328	1.273
μ [mm^{-1}]	0.105	0.923	0.102	0.099	
Radiation Type	MoKα (λ = 0.71073)	CuKα (λ = 1.54178)	MoKα (λ = 0.71073)	MoKα (λ = 0.71073)	MoKα (λ = 0.71073)
F(000)	2262	316	664	364	380
No. of measured refl.	75092	7068	10781	18228	12034
No. of independent refl.	18290	1250	1831	3551	5457
No. of refl. (I ≥ 2σ)	10047	1134	1501	2349	4978
R1/wR2 (I ≥ 2σ) [%]	12.21/28.86	3.22/8.67	3.35/7.92	5.70/13.76	3.88/10.61
R1/wR2 (all data) [%]	19.55/32.68	3.52/8.93	4.48/8.64	9.31/15.63	4.21/10.96

Table 2. Crystal data in polyladderane synthesis

Crystals	Monomer **12**	Monomer **7**	Intermediate **7a**
CCDC #	1497738	1497739	1497740
Formula	$C_{16}H_{22}O_4$	$C_{18}H_{18}O_6$	$C_{18}H_{18}O_6$
FW	278.34	330.33	330.33
Cryst. Size [mm]	0.30 × 0.45 × 0.60	0.42 × 0.20 × 0.14	0.20 ×0.50 ×0.60
Crystal system	Monoclinic	Monoclinic	Monoclinic
Space Group	P 2_1/c	P 2_1/n	P 2_1/n
a (Å)	8.7284(3)	7.7051(12)	7.7931(9)
b (Å)	10.1310(3)	10.1944(15)	10.1473(12)
c (Å)	9.4962(3)	10.2350(15)	10.1541(11)
α (^{o})	90	90	90
β (^{o})	113.872(2)	92.879(2)	91.361(8)
γ (^{o})	90	90	90
V (Å^3)	767.89(4)	802.9(2)	802.75(16)
Z	4	4	4
Temp. (K)	100 (2)	103.(2)	100(2)
ρcalc [g/cm^3]	1.204	1.366	1.367
μ [mm^{-1}]	0.085	0.103	0.103
Radiation Type	MoKα (λ = 0.71073)	MoKα (λ = 0.71073)	MoKα (λ = 0.71073)
F(000)	300	348	348
No of measured refl.	2783	9145	4977
No of independent refl.	881	1873	2280
No of refl. (I ≥ 2σ)	831	1502	2004
R1/wR2 (I ≥ 2σ) [%]	5.45/2.35	3.54/8.19	9.31/26.41
R1/wR2 (all data) [%]	5.61/2.37	4.97/8.93	10.28/27.61

Table 3. Crystal data in linear polyester synthesis

Crystals	Monomer **8a**	Intermediate **8c**
CCDC #	1406681	1408218
Formula	$C_{19}H_{20}O_6$	$C_{19}H_{20}O_6$
FW	344.35	344.35
Cryst. Size [mm]	0.33 × 0.16 × 0.05	0.51× 0.45 × 0.22
Crystal system	Orthorhombic	Orthorhombic
Space Group	$Pna2_1$	$Pna2_1$
a (Å)	23.0884(7)	22.9356(9)
b (Å)	10.4956(4)	10.4908(4)
c (Å)	7.3329(2)	7.3765(3)
α (°)	90	90
β (°)	90	90
γ (°)	90	90
V ($Å^3$)	1776.96(10)	1774.88(12)
Z	4	4
Temp. (K)	100(2)	100(2)
ρcalc [g/cm^3]	1.287	1.289
μ [mm^{-1}]	0.798	0.096
Radiation Type	CuKα (λ = 1.54178)	MoKα (λ = 0.71073)
F(000)	728.0	728.0
No of measured refl.	9555	10826
No of independent refl.	3093	3498
No of refl. (I ≥ 2σ)	2832	2804
R1/wR2 (I ≥ 2σ) [%]	3.15/7.91	5.35/11.51
R1/wR2 (all data) [%]	3.66/8.18	7.18/12.29

Table 4. Crystal data in two-dimensional polymer synthesis

Crystals	Monomer **16**	α-Truxillic acid **17**	α-Truxillic acid aminium salt	Monomer **20**
CCDC #	986273	986274	1005428	1033829
Formula	$C_{46}H_{38}O_8$	$C_{18}H_{14}O_4$	$C_{44}H_{68}N_8O_{10}$	$C_{54}H_{46}O_8$
FW	718.76	294.29	869.06	822.91
Cryst. Size [mm]	0.20 × 0.35× 0.50	0.22 × 0.05 ×0.02	0.37 × 0.34 × 0.11	0.20 × 0.25 × 0.60
Crystal system	Triclinic	Monoclinic	Monoclinic	Triclinic
Space Group	P-1	C2/c	$P2_1/n$	P-1
a (Å)	5.8035(6)	15.7822(6)	9.2260(3)	5.8334(2)
b (Å)	12.8761(15)	5.6013(2)	20.5019(8)	14.4688(5)
c (Å)	13.1702(13)	16.2750(5)	24.2730(9)	14.4800(5)
α (°)	66.778(4)	90	90	119.6010(10)
β (°)	82.336(5)	99.255(3)	96.132(1)	90.053(2)
γ (°)	86.696(5)	90	90	95.149(2)
V ($Å^3$)	896.34(17)	1420.00(9)	4565.0(3)	1056.90(6)
Temp. (K)	100(2)	100(2)	100(2)	100(2)
ρcalc [g/cm^3]	1.331	1.377	1.265	1.293
μ [mm^{-1}]	0.091	0.801	0.738	0.086
Radiation Type	MoKα (λ = 0.71073)	CuKα (λ = 1.54178)	CuKα (λ = 1.54178)	MoKα (λ = 0.71073)
F(000)	378	616	1872	434
No of measured refl.	8576	4256	63605	16036
No of independent refl.	3618	1231	8043	6064
No of refl. (I ≥ 2σ)	3287	1091	6544	5137
R1/wR2 (I ≥ 2σ) [%]	3.76/9.14	5.02/13.45	6.87/20.1	4.49/5.43
R1/wR2 (all data) [%]	3.42/8.88	5.57/13.82	7.73/20.4	13.05/14.83

Table 5. Crystal data in **CBDA** synthesis

Crystals	**14**	α-Truxillate-dibutylaminium
Formula	$C_9H_8O_2$	$C_{26}H_{38}N_2O_4$
FW	148.15	442.59
Cryst. Size [mm]	0.222 × 0.174 × 0.055	0.28 × 0.134 × 0.071
Crystal system	Monoclinic	Triclinic
Space Group	$P2_1/n$	P -1
a (Å)	5.5531(4)	6.1635(4)
b (Å)	17.5178(13)	9.3500(5)
c (Å)	7.7056(6)	10.8383(7)
α (°)	90	98.597(3)
β (°)	96.267(6)	91.331(5)
γ (°)	90	96.895(3)
V (Å^3)	745.11(10)	612.57(7)
Z	4	2
Temp. (K)	103	101
ρcalc [g/cm^3]	1.321	1.200
μ [mm^{-1}]	0.764	0.641
Radiation Type	CuKα (λ = 1.54178)	CuKα (λ = 1.54178)
F(000)	312.0	240.0
No of measured refl.	3308	1981
No of independent refl.	1237	1981
No of refl. (I ≥ 2σ)	1016	1621
R1/wR2 (I ≥ 2σ) [%]	4.07/11.12	6.45/16.82
R1/wR2 (all data) [%]	4.95/11.75	8.17/17.93

REFERENCES

1. *Annual Energy Outlook 2014*; U.S. Energy Information Administration: Washington, DC, 2014.

2. van Putten, R.-J.; van der Waal, J. C.; de Jong, E.; Rasrendra, C. B.; Heeres, H. J.; de Vries, J. G., Hydroxymethylfurfural, a Versatile Platform Chemical Made from Renewable Resources. *Chem. Rev.* **2013,** *113* (3), 1499-1597.

3. Lange, J.-P.; van der Heide, E.; van Buijtenen, J.; Price, R., Furfural—a Promising Platform for Lignocellulosic Biofuels. *ChemSusChem* **2012,** *5* (1), 150-166.

4. Guru, B. N.; Das, T. K.; Lenka, S., Polymers from Renewable Resources. XXVII. Studies on Synthesis, Characterization, and Thermal Properties of Resins Derived from Cardanyl Acrylate-Furfural-Organic Compounds. *Polym.-Plast. Technol. Eng.* **1999,** *38* (1), 179-187.

5. Tachibana, Y.; Yamahata, M.; Kasuya, K.-i., Synthesis and Characterization of a Renewable Polyester Containing Oxabicyclic Dicarboxylate Derived from Furfural. *Green Chem.* **2013,** *15* (5), 1318-1325.

6. Nicklaus, C. M.; Minnaard, A. J.; Feringa, B. L.; de Vries, J. G., Synthesis of Renewable Fine-Chemical Building Blocks by Reductive Coupling between Furfural Derivatives and Terpenes. *ChemSusChem* **2013,** *6* (9), 1631-1635.

7. Kukhar, V. P., Biomass-Renewable Feedstock for Organic Chemicals ("White Chemistry"). *Kem. Ind.* **2009,** *58* (2), 57-71.

8. Klass, D., *Biomass for Renewable Energy, Fuels, and Chemicals*. Elsevier Inc: 1998; p 651.

9. Tschan, M. J. L.; Brule, E.; Haquette, P.; Thomas, C. M., Synthesis of Biodegradable Polymers from Renewable Resources. *Polym. Chem.* **2012,** *3* (4), 836-851.

10. Amass, W.; Amass, A.; Tighe, B., A Review of Biodegradable Polymers: Uses, Current Developments in the Synthesis and Characterization of Biodegradable Polyesters, Blends of Biodegradable Polymers and Recent Advances in Biodegradation Studies. *Polym. Int.* **1998,** *47* (2), 89-144.

11. Bart, A. J. N.; Lidia, J.-W.; Inge van der, M.; Robbert, D.; Cor, E. K., Novel Biomass-Based Polymers: Synthesis, Characterization, and Application. In *Biobased Monomers, Polymers, and Materials*, American Chemical Society: 2012; Vol. 1105, pp 281-322.

12. Lligadas, G.; Ronda, J. C.; Galià, M.; Cádiz, V., Renewable Polymeric Materials from Vegetable Oils: A Perspective. *Mater. Today* **2013,** *16* (9), 337-343.

13. Kovash, C. S.; Pavlacky, E.; Selvakumar, S.; Sibi, M. P.; Webster, D. C., Thermoset Coatings from Epoxidized Sucrose Soyate and Blocked, Bio-Based Dicarboxylic Acids. *ChemSusChem* **2014,** *7* (8), 2289-2294.

14. Werpy, T.; Petersen, G. *Top Value Added Chemicals from Biomass: Volume 1-Results of Screening for Potential Candidates from Sugars and Synthesis Gas*; NREL/TP-510-35523; National Renewable Energy Laboratory: Golden, CO, 2004.

15. Bozell, J. J.; Petersen, G. R., Technology Development for the Production of Biobased Products from Biorefinery Carbohydrates-the Us Department of Energy's "Top 10" Revisited. *Green Chem.* **2010,** *12* (4), 539-554.

16. Pan, T.; Deng, J.; Xu, Q.; Zuo, Y.; Guo, Q.-X.; Fu, Y., Catalytic Conversion of Furfural into a 2,5-Furandicarboxylic Acid-Based Polyester with Total Carbon Utilization. *ChemSusChem* **2013,** *6* (1), 47-50.

17. Smith Patrick, B.; Gross Richard, A., *Biobased Monomers, Polymers, and Materials*. American Chemical Society: 2012; Vol. 1105.

18. Zhang, X.; Hu, C.; Bai, H.; Yan, Y.; Li, J.; Yang, H.; Lu, X.; Xi, G., Construction of Self-Supported Three-Dimensional TiO_2 Sheeted Networks with Enhanced Photocatalytic Activity. *Sci. Rep.* **2013,** *3*.

19. Gopalakrishnana, S.; Sujathaa, R., Synthesis and Thermal Properties of Polyurethanes from Cardanol-Furfural Resin. *J. Chem. Pharm. Res* **2010,** *2* (3), 193-205.

20. Belgacem, M. N.; Gandini, A., *Monomers, Polymers and Composites from Renewable Resources*. Elsevier: Oxford, UK, 2008.

21. Yoshida, N.; Kasuya, N.; Haga, N.; Fukuda, K., Brand-New Biomass-Based Vinyl Polymers from 5-Hydroxymethylfurfural. *Polym. J* **2008,** *40* (12), 1164-1169.

22. Papageorgiou, G. Z.; Tsanaktsis, V.; Bikiaris, D. N., Synthesis of Poly(Ethylene Furandicarboxylate) Polyester Using Monomers Derived from Renewable Resources: Thermal Behavior Comparison with Pet and Pen. *Phys. Chem. Chem. Phys.* **2014,** *16* (17), 7946-7958.

23. Dutta, S.; De, S.; Saha, B., A Brief Summary of the Synthesis of Polyester Building-Block Chemicals and Biofuels from 5-Hydroxymethylfurfural. *ChemPlusChem* **2012,** *77* (4), 259-272.

24. Mishra, M. K.; Varughese, S.; Ramamurty, U.; Desiraju, G. R., Odd–Even Effect in the Elastic Modulii of A,Ω-Alkanedicarboxylic Acids. *J. Am. Chem. Soc.* **2013,** *135* (22), 8121-8124.

25. Thalladi, V. R.; Nüsse, M.; Boese, R., The Melting Point Alternation in α,ω-Alkanedicarboxylic Acids. *J. Am. Chem. Soc.* **2000,** *122* (38), 9227-9236.

26. Akkerman, H. B.; Mannsfeld, S. C. B.; Kaushik, A. P.; Verploegen, E.; Burnier, L.; Zoombelt, A. P.; Saathoff, J. D.; Hong, S.; Atahan-Evrenk, S.; Liu, X.; Aspuru-Guzik, A.; Toney, M. F.; Clancy, P.; Bao, Z., Effects of Odd–Even Side Chain Length of Alkyl-Substituted Diphenylbithiophenes on First Monolayer Thin Film Packing Structure. *J. Am. Chem. Soc.* **2013,** *135* (30), 11006-11014.

27. Jacobs, H.; Day, G.; Jackson, W.; Simon, G.; Watson, K.; Zheng, S., Synthesis and Characterization of a Series of Liquid Crystal Monomers Containing a Novel Spacer Group Based on Vinylacetic Acid. *Aust. J. Chem.* **1992,** *45* (4), 695-702.

28. Zhila Vazifehasl, S. H., Mohammadreza Zamanloo, Solmaz Maleki Dizaj, New Series of Dimethacrylate-Based Monomers on Isosorbide as a Dental Material: Synthesis and Characterization. *International Journal of Composite Materials* **2013,** *3* (4), 100-107.

29. Menger, F. M.; Littau, C. A., Gemini Surfactants: A New Class of Self-Assembling Molecules. *J. Am. Chem. Soc.* **1993,** *115* (22), 10083-10090.

30. Qiu, T.; Zhang, L.; Xing, X.-D., Synthesis and Antibacterial Activities of Novel Polymerizable Gemini Quaternary Ammonium Monomers. *Des. Monomers Polym.* **2014,** *17* (8), 726-735.

31. Hait, S. K. M., S. P., Gemini Surfactants: A Distinct Class of Self-Assembling Molecules. *Curr. Sci.* **2002,** *82* (9), 1101-1111.

32. Amiri, R.; Bordbar, A.-K.; Laurents, D. V., Gemini Surfactants Affect the Structure, Stability, and Activity of Ribonuclease Sa. *J. Phys. Chem. B* **2014,** *118* (36), 10633-10642.

33. Rajendran, S.; Raghunathan, R.; Hevus, I.; Krishnan, R.; Ugrinov, A.; Sibi, M. P.; Webster, D. C.; Sivaguru, J., Programmed Photodegradation of Polymeric/Oligomeric Materials Derived from Renewable Bioresources. *Angew. Chem. Int. Ed.* **2015,** *54* (4), 1159-1163.

34. Rajendran, S.; Raghunathan, R.; Hevus, I.; Krishnan, R.; Ugrinov, A.; Sibi, M. P.; Webster, D. C.; Sivaguru, J., Inside Back Cover: Programmed Photodegradation of Polymeric/Oligomeric Materials Derived from Renewable Bioresources *Angew. Chem. Int. Ed.* **2015,** *54* (4), 1369-1369.

35. Ericson, D. P.; Zurfluh-Cunningham, Z. P.; Groeneman, R. H.; Elacqua, E.; Reinheimer, E. W.; Noll, B. C.; MacGillivray, L. R., Regiocontrol of the [2 + 2] Photodimerization in the Solid State Using Isosteric Resorcinols: Head-to-Tail

Cyclobutane Formation Via Unexpected Embraced Assemblies. *Cryst. Growth Des.* **2015,** *15* (12), 5744-5748.

36. Mubeen, S.; Singh, N.; Lee, J.; Stucky, G. D.; Moskovits, M.; McFarland, E. W., Synthesis of Chemicals Using Solar Energy with Stable Photoelectrochemically Active Heterostructures. *Nano Lett.* **2013,** *13* (5), 2110-2115.

37. Ramamurthy, V.; Venkatesan, K., Photochemical Reactions of Organic Crystals. *Chem. Rev.* **1987,** *87* (2), 433-481.

38. Cohen, M. D., The Photochemistry of Organic Solids. *Angew. Chem. Int. Ed. Engl.* **1975,** *14* (6), 386-393.

39. Rondeau-Gagné, S.; Néabo, J. R.; Desroches, M.; Larouche, J.; Brisson, J.; Morin, J.-F., Topochemical Polymerization of Phenylacetylene Macrocycles: A New Strategy for the Preparation of Organic Nanorods. *J. Am. Chem. Soc.* **2012,** *135* (1), 110-113.

40. Sonoda, Y., Solid-State [2+2] Photodimerization and Photopolymerization of A,Ω-Diarylpolyene Monomers: Effective Utilization of Noncovalent Intermolecular Interactions in Crystals. *Molecules* **2010,** *16* (1), 119.

41. Cohen, M. D.; Schmidt, G. M. J.; Sonntag, F. I., 384. Topochemistry. Part Ii. The Photochemistry of Trans-Cinnamic Acids. *J. Chem. Soc.* **1964**, 2000-2013.

42. Garai, M.; Santra, R.; Biradha, K., Tunable Plastic Films of a Crystalline Polymer by Single-Crystal-to-Single-Crystal Photopolymerization of a Diene: Self-Templating and Shock-Absorbing Two-Dimensional Hydrogen-Bonding Layers. *Angew. Chem. Int. Ed.* **2013,** *52* (21), 5548-5551.

43. Kole, G. K.; Medishetty, R.; Koh, L. L.; Vittal, J. J., Influence of C-H[Small Pi] Interactions on the Solid-State [2+2] Cycloaddition Reaction of a Ag(I) Coordination Complex in an Inorganic Co-Crystal. *Chem. Commun.* **2013,** *49* (56), 6298-6300.

44. Nishizawa, N.; Nakamura, J.; Matsumoto, A., Single-Crystal-to-Single-Crystal Transformation of Di(Isopropylammonium) (Z,Z)-Muconate into the (E,E)-Muconate During One-Way Photoisomerization in the Solid State. *Cryst. Growth Des.* **2011,** *11* (8), 3442-3447.

45. Neto, A. H. C.; Novoselov, K., Two-Dimensional Crystals: Beyond Graphene. *Materials Express* **2011,** *1* (1), 10-17.

46. Uribe-Romo, F. J.; Hunt, J. R.; Furukawa, H.; Klöck, C.; O'Keeffe, M.; Yaghi, O. M., A Crystalline Imine-Linked 3-D Porous Covalent Organic Framework. *J. Am. Chem. Soc.* **2009,** *131* (13), 4570-4571.

47. Lauher, J. W.; Fowler, F. W.; Goroff, N. S., Single-Crystal-to-Single-Crystal Topochemical Polymerizations by Design. *Acc. Chem. Res.* **2008,** *41* (9), 1215-1229.

48. Odani, T.; Matsumoto, A., Solvent-Free Synthesis of Layered Polymer Crystals. *Polym. J.* **2002,** *34* (11), 841-846.

49. Nagahama, S.; Matsumoto, A., Synchronized Propagation Mechanism for Crystalline-State Polymerization of P-Xylylenediammonium Disorbate. *J. Am. Chem. Soc.* **2001,** *123* (49), 12176-12181.

50. Lasseuguette, E.; Gandini, A.; Timpe, H.-J., Photoreactive Furan Derivatives. *J. Photochem. Photobiol., A* **2005,** *174* (3), 222-228.

51. Rajagopalan, S.; Raman., P. V. A.; Hamilton, C. S.; Alberty., R. A., Furylacrylic Acid. *Org. Synth.* **1945,** *25*, 51.

52. Wang, Z.; Randazzo, K.; Hou, X.; Simpson, J.; Struppe, J.; Ugrinov, A.; Kastern, B.; Wysocki, E.; Chu, Q. R., Stereoregular Two-Dimensional Polymers Constructed by Topochemical Polymerization. *Macromolecules* **2015,** *48* (9), 2894-2900.

53. Wang, Z.; Kastern, B.; Randazzo, K.; Ugrinov, A.; Butz, J.; Seals, D. W.; Sibi, M. P.; Chu, Q. R., Linear Polyester Synthesized from Furfural-Based Monomer by Photoreaction in Sunlight. *Green Chem.* **2015,** *17* (10), 4720-4724.

54. Hou, X.; Wang, Z.; Lee, J.; Wysocki, E.; Oian, C.; Schlak, J.; Chu, Q. R., Synthesis of Polymeric Ladders by Topochemical Polymerization. *Chem. Commun.* **2014,** *50* (10), 1218-1220.

55. Kassi, E.; Constantinou, M. S.; Patrickios, C. S., Group Transfer Polymerization of Biobased Monomers. *Eur. Polym. J.* **2013,** *49* (4), 761-767.

56. Vickery, H. B.; Palmer, J. K., The Metabolism of the Organic Acids of Tobacco Leaves: Xii. Effect of Culture of Excised Leaves in Solutions of Malonate at Ph 4 to Ph 7. *J. Biol. Chem.* **1957,** *225*, 629-640.

57. Mizugaki, T.; Yamakawa, T.; Nagatsu, Y.; Maeno, Z.; Mitsudome, T.; Jitsukawa, K.; Kaneda, K., Direct Transformation of Furfural to 1,2-Pentanediol Using a Hydrotalcite-Supported Platinum Nanoparticle Catalyst. *ACS Sustainable Chem. Eng.* **2014,** *2* (10), 2243-2247.

58. McQuarrie, D. A.; Rock, P. A.; Gallogly, E. B., *General Chemistry*. Fourth Edition ed.; University Science Books: 2010.

59. Giusti, M. M.; Wrolstad, R. E., Radish Anthocyanin Extract as a Natural Red Colorant for Maraschino Cherries. *J. Food Sci.* **1996,** *61* (4), 688-694.

60. Sajilata, M. G. S., R. S., Isolation and Stabilisation of Natural Pigments for Food Applications. *Stewart Postharvest Review* **2006,** *2* (5), 1-29.

61. Liu, S.; Amada, Y.; Tamura, M.; Nakagawa, Y.; Tomishige, K., One-Pot Selective Conversion of Furfural into 1,5-Pentanediol over a Pd-Added Ir-Reox/Sio2 Bifunctional Catalyst. *Green Chem.* **2014,** *16* (2), 617-626.

62. Kunioka, M.; Masuda, T.; Tachibana, Y.; Funabashi, M.; Oishi, A., Highly Selective Synthesis of Biomass-Based 1,4-Butanediol Monomer by Alcoholysis of 1,4-Diacetoxybutane Derived from Furan. *Polym. Degrad. Stab.* **2014,** *109*, 393-397.

63. Xiao, Z.; Jin, S.; Pang, M.; Liang, C., Conversion of Highly Concentrated Cellulose to 1,2-Propanediol and Ethylene Glycol over Highly Efficient Cucr Catalysts. *Green Chem.* **2013,** *15* (4), 891-895.

64. Nakagawa, Y.; Tomishige, K., Production of 1,5-Pentanediol from Biomass Via Furfural and Tetrahydrofurfuryl Alcohol. *Catal. Today* **2012,** *195* (1), 136-143.

65. Xu, W.; Wang, H.; Liu, X.; Ren, J.; Wang, Y.; Lu, G., Direct Catalytic Conversion of Furfural to 1,5-Pentanediol by Hydrogenolysis of the Furan Ring under Mild Conditions over Pt/Co2alo4 Catalyst. *Chem. Commun.* **2011,** *47* (13), 3924-3926.

66. Wang, A.; Zhang, T., One-Pot Conversion of Cellulose to Ethylene Glycol with Multifunctional Tungsten-Based Catalysts. *Acc. Chem. Res.* **2013,** *46* (7), 1377-1386.

67. Tai, Z.; Zhang, J.; Wang, A.; Zheng, M.; Zhang, T., Temperature-Controlled Phase-Transfer Catalysis for Ethylene Glycol Production from Cellulose. *Chem. Commun.* **2012,** *48* (56), 7052-7054.

68. Datta, B.; Pasha, M. A., Chemoselective Protection and Deprotection of Aldehydes Using Solid Supported Reagent (Silica Chloride) under Solvent-Free Conditions. *Synth. Commun.* **2011,** *41* (8), 1160-1166.

69. Nudelman, A.; Gnizi, E.; Katz, Y.; Azulai, R.; Cohen-Ohana, M.; Zhuk, R.; Sampson, S. R.; Langzam, L.; Fibach, E.; Prus, E.; Pugach, V.; Rephaeli, A., Prodrugs of Butyric Acid. Novel Derivatives Possessing Increased Aqueous Solubility and Potential for Treating Cancer and Blood Diseases. *Eur. J. Med. Chem.* **2001,** *36* (1), 63-74.

70. Songur, A.; Ozen, O.; Sarsilmaz, M., The Toxic Effects of Formaldehyde on the Nervous System. In *Reviews of Environmental Contamination and Toxicology*, Whitacre, D. M., Ed. Springer New York: 2010; Vol. 203, pp 105-118.

71. Werle, P.; Morawietz, M.; Lundmark, S.; Sörensen, K.; Karvinen, E.; Lehtonen, J., Alcohols, Polyhydric. In *Ullmann's Encyclopedia of Industrial Chemistry*, Wiley-VCH Verlag GmbH & Co. KGaA: 2000.

72. Yuya, T.; Takashi, M.; Masahiro, F.; Ken-ichi, K.; Masao, K., Synthesis of Biomass-Based Monomers from Biomass-Based Furfural for Polyesters and Evaluation of Their Biomass Carbon Ratios. In *Biobased Monomers, Polymers, and Materials*, American Chemical Society: 2012; Vol. 1105, pp 91-110.

73. Al-Sabagh, A. M.; Yehia, F. Z.; Eshaq, G.; Rabie, A. M.; ElMetwally, A. E., Greener Routes for Recycling of Polyethylene Terephthalate. *Egyptian Journal of Petroleum* **2016,** *25* (1), 53-64.

74. Cammidge, A. N., An Undergraduate Experiment in Polyester (Pet) Synthesis. *J. Chem. Educ.* **1999,** *76* (2), 236.

75. Köpnick, H.; Schmidt, M.; Brügging, W.; Rüter, J.; Kaminsky, W., Polyesters. In *Ullmann's Encyclopedia of Industrial Chemistry*, Wiley-VCH Verlag GmbH & Co. KGaA: 2000.

76. Sattler, H.; Schweizer, M., Fibers, 5. Polyester Fibers. In *Ullmann's Encyclopedia of Industrial Chemistry*, Wiley-VCH Verlag GmbH & Co. KGaA: 2000.

77. Braga, D.; Grepioni, F.; Maini, L.; Polito, M., Crystal Polymorphism and Multiple Crystal Forms. In *Molecular Networks*, Hosseini, W. M., Ed. Springer Berlin Heidelberg: Berlin, Heidelberg, 2009; pp 87-95.

78. Threlfall, T., Structural and Thermodynamic Explanations of Ostwald's Rule. *Org. Process Res. Dev.* **2003,** *7* (6), 1017-1027.

79. Carletta, A.; Meinguet, C.; Wouters, J.; Tilborg, A., Solid-State Investigation of Polymorphism and Tautomerism of Phenylthiazole-Thione: A Combined Crystallographic, Calorimetric, and Theoretical Survey. *Cryst. Growth Des.* **2015,** *15* (5), 2461-2473.

80. Nyman, J.; Day, G. M., Static and Lattice Vibrational Energy Differences between Polymorphs. *CrystEngComm* **2015,** *17* (28), 5154-5165.

81. Thallapally, P. K.; Jetti, R. K. R.; Katz, A. K.; Carrell, H. L.; Singh, K.; Lahiri, K.; Kotha, S.; Boese, R.; Desiraju, G. R., Polymorphism of 1,3,5-Trinitrobenzene Induced by a Trisindane Additive. *Angew. Chem. Int. Ed.* **2004,** *43* (9), 1149-1155.

82. Hopf, H., Step by Step—from Nonnatural to Biological Molecular Ladders. *Angew. Chem. Int. Ed.* **2003,** *42* (25), 2822-2825.

83. Martin, H.-D.; Mayer, B.; Pütter, M.; Höchstetter, H., Pterodactyladiene (Tetracyclo[4.4.0.02,5.07.10]Deca-3,8-Diene). *Angew. Chem. Int. Ed.* **1981,** *20* (8), 677-678.

84. Mehta, G.; Viswanath, M. B.; Sastry, G. N.; Jemmis, E. D.; Reddy, D. S. K.; Kunwar, A. C., Quest for Higher Ladderanes: Oligomerization of a Cyclobutadiene Derivative. *Angew. Chem. Int. Ed.* **1992,** *31* (11), 1488-1490.

85. Hopf, H.; Greiving, H.; Jones, P. G.; Bubenitschek, P., Topochemical Reaction Control in Solution. *Angew. Chem. Int. Ed.* **1995,** *34* (6), 685-687.

86. Khan, S. I.; Oliver, A. M.; Paddon-Row, M. N.; Rubin, Y., Synthesis of a Rigid "Ball-and-Chain" Donor-Acceptor System through Diels-Alder Functionalization of Buckminsterfullerene (C60). *J. Am. Chem. Soc.* **1993,** *115* (11), 4919-4920.

87. Li, W.; Fox, M. A., Syntheses, Characterization, and Photophysics Studies of Photoactive Chromophore 2-Naphthyl-Labeled [N]-Ladderanes. *J. Am. Chem. Soc.* **1996,** *118* (47), 11752-11758.

88. Sinninghe Damste, J. S.; Strous, M.; Rijpstra, W. I. C.; Hopmans, E. C.; Geenevasen, J. A. J.; van Duin, A. C. T.; van Niftrik, L. A.; Jetten, M. S. M., Linearly Concatenated Cyclobutane Lipids Form a Dense Bacterial Membrane. *Nature* **2002,** *419* (6908), 708-712.

89. Kuypers, M. M. M.; Sliekers, A. O.; Lavik, G.; Schmid, M.; Jorgensen, B. B.; Kuenen, J. G.; Sinninghe Damste, J. S.; Strous, M.; Jetten, M. S. M., Anaerobic Ammonium Oxidation by Anammox Bacteria in the Black Sea. *Nature* **2003,** *422* (6932), 608-611.

90. Byrne, N.; Strous, M.; Crepeau, V.; Kartal, B.; Birrien, J.-L.; Schmid, M.; Lesongeur, F.; Schouten, S.; Jaeschke, A.; Jetten, M.; Prieur, D.; Godfroy, A., Presence and Activity of Anaerobic Ammonium-Oxidizing Bacteria at Deep-Sea Hydrothermal Vents. *ISME J* **2008,** *3* (1), 117-123.

91. Hong, Y. J.; Tantillo, D. J., How Cyclobutanes Are Assembled in Nature - Insights from Quantum Chemistry. *Chem. Soc. Rev.* **2014,** *43* (14), 5042-5050.

92. MacGillivray, L. R.; Papaefstathiou, G. S.; Friščić, T.; Hamilton, T. D.; Bučar, D.-K.; Chu, Q.; Varshney, D. B.; Georgiev, I. G., Supramolecular Control of Reactivity in the Solid State: From Templates to Ladderanes to Metal–Organic Frameworks. *Acc. Chem. Res.* **2008,** *41* (2), 280-291.

93. Sinninghe Damsté, J. S.; Rijpstra, W. I. C.; Geenevasen, J. A. J.; Strous, M.; Jetten, M. S. M., Structural Identification of Ladderane and Other Membrane Lipids of Planctomycetes Capable of Anaerobic Ammonium Oxidation (Anammox). *FEBS J.* **2005,** *272* (16), 4270-4283.

94. Novak, I., Ring Strain in [N]Ladderanes. *J. Phys. Chem. A* **2008,** *112* (40), 10059-10063.

95. Mascitti, V.; Corey, E. J., Enantioselective Synthesis of Pentacycloanammoxic Acid. *J. Am. Chem. Soc.* **2006,** *128* (10), 3118-3119.

96. Gao, X.; Friščić, T.; MacGillivray, L. R., Supramolecular Construction of Molecular Ladders in the Solid State. *Angew. Chem. Int. Ed.* **2004,** *43* (2), 232-236.

97. Hopf, H.; Greiving, H.; Beck, C.; Dix, I.; Jones, P. G.; Desvergne, J.-P.; Bouas-Laurent, H., One-Pot Preparation of [N]Ladderanes by [2π + 2π] Photocycloaddition. *Eur. J. Org. Chem.* **2005,** *2005* (3), 567-581.

98. Santos, J. C.; Fuentealba, P., Theoretical Characterization of Linear [N]-Ladderanes and Some Isomers. *Chem. Phys. Lett.* **2003,** *377* (3–4), 449-454.

99. Nouri, D. H.; Tantillo, D. J., Attack of Radicals and Protons on Ladderane Lipids: Quantum Chemical Calculations and Biological Implications. *Org. Biomol. Chem.* **2012,** *10* (29), 5514-5517.

100. Nouri, D. H.; Tantillo, D. J., They Came from the Deep: Syntheses, Applications, and Biology of Ladderanes. *Curr. Org. Chem.* **2006,** *10* (16), 2055-2074.

101. Tantillo, D. J.; Hoffmann, R., Sigmatropic Shiftamers: Fluxionality in Broken Ladderane Polymers. *Angew. Chem. Int. Ed.* **2002,** *41* (6), 1033-1036.

102. Wagner, J. P.; Schreiner, P. R., Nature Utilizes Unusual High London Dispersion Interactions for Compact Membranes Composed of Molecular Ladders. *J. Chem. Theory Comput.* **2014,** *10* (3), 1353-1358.

103. Schmidt, G. M. J., Photodimerization in the Solid State. *Pure Appl. Chem.* **1971,** *27* (4), 647-678.

104. Sharma, C. V. K.; Panneerselvam, K.; Shimoni, L.; Katz, H.; Carrell, H. L.; Desiraju, G. R., 3-(3',5'-Dinitrophenyl)-4-(2',5'-Dimethoxyphenyl)Cyclobutane-1,2-Dicarboxylic Acid: Engineered Topochemical Synthesis and Molecular and Supramolecular Properties. *Chem. Mater.* **1994,** *6* (8), 1282-1292.

105. Coates, G. W.; Dunn, A. R.; Henling, L. M.; Ziller, J. W.; Lobkovsky, E. B.; Grubbs, R. H., Phenyl−Perfluorophenyl Stacking Interactions: Topochemical [2+2] Photodimerization and Photopolymerization of Olefinic Compounds. *J. Am. Chem. Soc.* **1998,** *120* (15), 3641-3649.

106. Vishnumurthy, K.; Guru Row, T. N.; Venkatesan, K., Fluorine in Crystal Engineering: Photodimerization of (1e,3e)-1-Phenyl-4-Pentafluorophenylbuta-1,3-Dienes in the Crystalline State. *Photochem. Photobiol. Sci.* **2002,** *1* (6), 427-430.

107. Parent, A. A.; Ess, D. H.; Katzenellenbogen, J. A., Π–Π Interaction Energies as Determinants of the Photodimerization of Mono-, Di-, and Triazastilbenes. *J. Org. Chem.* **2014,** *79* (12), 5448-5462.

108. Randazzo, K.; Wang, Z.; Wang, Z. D.; Butz, J.; Chu, Q. R., Lighting the Way to Greener Chemistry: Incandescent Floodlights as a Facile Uv Light Source for Classic and Cutting-Edge Photoreactions. *ACS Sustainable Chem. Eng.* **2016,** *4* (9), 5053-5059.

109. Yang, S.-Y.; Naumov, P.; Fukuzumi, S., Topochemical Limits for Solid-State Photoreactivity by Fine Tuning of the Π−Π Interactions. *J. Am. Chem. Soc.* **2009,** *131* (21), 7247-7249.

110. Otto G. Piringer, A. L. B., *Plastic Packaging: Interactions with Food and Pharmaceuticals, Second Edition*. Wiley-VCH: 2008.

111. Maul, J.; Frushour, B. G.; Kontoff, J. R.; Eichenauer, H.; Ott, K.-H.; Schade, C., Polystyrene and Styrene Copolymers. In *Ullmann's Encyclopedia of Industrial Chemistry*, Wiley-VCH Verlag GmbH & Co. KGaA: 2000.

112. MacDonald, W. A., Handbook of Thermoplastic Polyesters, Vols 1 and 2 S, Fakirov Weinheim, Wiley-Vch, 2002 Vol 1 pp 753, ISBN 3-527-29790-1 Vol 2 pp 624, ISBN 3-527-30113-5. *Polym. Int.* **2003,** *52* (5), 859-860.

113. Polyethylene Terephthalate (PET). http://www.plastiquarian.com/index.php?id=101 (Accessed Jun. 2016).

114. Webb, H.; Arnott, J.; Crawford, R.; Ivanova, E., Plastic Degradation and Its Environmental Implications with Special Reference to Poly(Ethylene Terephthalate). *Polymers* **2012,** *5* (1), 1-18.

115. Longo, J. M.; DiCiccio, A. M.; Coates, G. W., Poly(Propylene Succinate): A New Polymer Stereocomplex. *J. Am. Chem. Soc.* **2014,** *136* (45), 15897-15900.

116. East, A. J., Polyesters, Thermoplastic. In *Encyclopedia of Polymer Science and Technology*, John Wiley & Sons, Inc.: 2002.

117. Vilela, C.; Sousa, A. F.; Fonseca, A. C.; Serra, A. C.; Coelho, J. F. J.; Freire, C. S. R.; Silvestre, A. J. D., The Quest for Sustainable Polyesters - Insights into the Future. *Polym. Chem.* **2014,** *5* (9), 3119-3141.

118. Babu, R.; O'Connor, K.; Seeram, R., Current Progress on Bio-Based Polymers and Their Future Trends. *Prog. Biomater.* **2013,** *2* (1), 8.

119. Sudesh, K.; Iwata, T., Sustainability of Biobased and Biodegradable Plastics. *CLEAN – Soil, Air, Water* **2008,** *36* (5-6), 433-442.

120. Vilela, C.; Sousa, A. F.; Fonseca, A. C.; Serra, A. C.; Coelho, J. F. J.; Freire, C. S. R.; Silvestre, A. J. D., The Quest for Sustainable Polyesters - Insights into the Future. *Polym. Chem.* **2014,** *5* (9), 3119-3141.

121. Bomgardner, M. M., Biobased Polymers. *Chem. Eng. News* **2014,** *92* (43), 10-14.

122. Bomgardner, M. M., Biobased Polymers. *C&EN* **2014,** *92* (43), 10-14.

123. *Annual Energy Outlook 2014*. U.S. Energy Information Administration: Washington, DC, 2014; Vol. DOE/EIA-0383(2014).

124. Coates, G. W.; Hillmyer, M. A., A Virtual Issue of Macromolecules: "Polymers from Renewable Resources". *Macromolecules* **2009,** *42* (21), 7987-7989.

125. Zenner, M. D.; Madbouly, S. A.; Chen, J. S.; Kessler, M. R., Unexpected Tackifiers from Isosorbide. *ChemSusChem* **2015,** *8* (3), 448-451.

126. Samanta, S.; He, J.; Selvakumar, S.; Lattimer, J.; Ulven, C.; Sibi, M.; Bahr, J.; Chisholm, B. J., Polyamides Based on the Renewable Monomer, 1,13-Tridecane Diamine Ii: Synthesis and Characterization of Nylon 13,6. *Polymer* **2013,** *54* (3), 1141-1149.

127. Gopalakrishnana, S.; Sujathaa, R., Synthesis and Thermal Properties of Polyurethanes from Cardanol-Furfural Resin. *J. Chem. Pharm. Res.* **2010,** *2* (3), 193-205.

128. Yoshida, N.; Kasuya, N.; Haga, N.; Fukuda, K., Brand-New Biomass-Based Vinyl Polymers from 5-Hydroxymethylfurfural. *Polym. J.* **2008,** *40* (12), 1164-1169.

129. Werpy, T.; Petersen, G., *Top Value Added Chemicals from Biomass*. National Renewable Energy Laboratory: Golden, CO, 2004.

130. *Bio-Based Plastics: Materials and Applications*. 2014.

131. *Bio-Based Plastics: Materials and Applications*. John Wiley & Sons Ltd: 2013.

132. Palmer, R. J., Polyamides, Plastics. In *Encyclopedia of Polymer Science and Technology*, John Wiley & Sons, Inc.: 2002.

133. Anastas, P. T.; Warner, J. C., *Green Chemistry: Theory and Practice*. Oxford University Press: New York: 1998; p 30.

134. Loupy, A., Solvent-Free Microwave Organic Synthesis as an Efficient Procedure for Green Chemistry. *C. R. Chim.* **2004,** *7* (2), 103-112.

135. S. Varma, R., Solvent-Free Organic Syntheses . Using Supported Reagents and Microwave Irradiation. *Green Chem.* **1999,** *1* (1), 43-55.

136. Iliescu, S.; Ilia, G.; Pascariu, A.; Popa, A.; Plesu, N., Organic Solvent-Free Synthesis of Phosphorus-Containing Polymers. *Pure Appl. Chem.* **2007,** *79* (11), 1879-1884.

137. Rafael, L.; Juan Carlos, C., *An Introduction to Green Chemistry Methods*. Future Science Ltd: 2013; p 183.

138. Kumar, A.; Singh, R.; Gopinathan, S. P.; Kumar, A., Solvent Free Chemical Oxidative Polymerization as a Universal Method for the Synthesis of Ultra High Molecular Weight Conjugated Polymers Based on 3,4-Propylenedioxythiophenes. *Chem. Commun.* **2012,** *48* (40), 4905-4907.

139. Tanaka, K.; Toda, F., Solvent-Free Organic Synthesis. *Chem. Rev.* **2000,** *100* (3), 1025-1074.

140. Ouyang, X.; Fowler, F. W.; Lauher, J. W., Single-Crystal-to-Single-Crystal Topochemical Polymerizations of a Terminal Diacetylene: Two Remarkable Transformations Give the Same Conjugated Polymer. *J. Am. Chem. Soc.* **2003,** *125* (41), 12400-12401.

141. Lee, S. B.; Koepsel, R.; Stolz, D. B.; Warriner, H. E.; Russell, A. J., Self-Assembly of Biocidal Nanotubes from a Single-Chain Diacetylene Amine Salt. *J. Am. Chem. Soc.* **2004,** *126* (41), 13400-13405.

142. Curtis, S. M.; Le, N.; Fowler, F. W.; Lauher, J. W., A Rational Approach to the Preparation of Polydipyridyldiacetylenes: An Exercise in Crystal Design. *Cryst. Growth Des.* **2005,** *5* (6), 2313-2321.

143. Macgillivray, L. R.; Papaefstathiou, G. S.; Friščić, T.; Hamilton, T. D.; Bučar, D.-K.; Chu, Q.; Varshney, D. B.; Georgiev, I. G., Supramolecular Control of Reactivity in the Solid State: From Templates to Ladderanes to Metal− Organic Frameworks. *Acc. Chem. Res.* **2008,** *41* (2), 280-291.

144. Chu, Q.; Swenson, D. C.; MacGillivray, L. R., A Single-Crystal-to-Single-Crystal Transformation Mediated by Argentophilic Forces Converts a Finite Metal Complex into an Infinite Coordination Network. *Angew. Chem. Int. Ed.* **2005,** *44*, 3569-3572.

145. Vila, C.; Rueping, M., Visible-Light Mediated Heterogeneous C-H Functionalization: Oxidative Multi-Component Reactions Using a Recyclable Titanium Dioxide (TiO_2) Catalyst. *Green Chem.* **2013,** *15* (8), 2056-2059.

146. Schultz, D. M.; Yoon, T. P., Solar Synthesis: Prospects in Visible Light Photocatalysis. *Science* **2014,** *343*, 6174.

147. Song, Y. K.; Jo, Y. H.; Lim, Y. J.; Cho, S. Y.; Yu, H. C.; Ryu, B. C.; Lee, S. I.; Chung, C. M., Sunlight-Induced Self-Healing of a Microcapsule-Type Protective Coating. *ACS Appl. Mater. Interfaces* **2013,** *5* (4), 1378-1384.

148. Ciftci, M.; Tasdelen, M. A.; Yagci, Y., Sunlight Induced Atom Transfer Radical Polymerization by Using Dimanganese Decacarbonyl. *Polym. Chem.* **2014,** *5* (2), 600-606.

149. Mueller, J. O.; Guimard, N. K.; Oehlenschlaeger, K. K.; Schmidt, F. G.; Barner-Kowollik, C., Sunlight-Induced Crosslinking of 1,2-Polybutadienes: Access to Fluorescent Polymer Networks. *Polym. Chem.* **2014,** *5* (4), 1447-1456.

150. Kearsley, S. K., The Prediction of Chemical Reactivity within Organic Crystals Using Geometric Criteria. In Organic Solid State Chemistry, Desiraju, G.R., Ed. Elsevier: New York, 1987.

151. D'Auria, M.; Emanuele, L.; Esposito, V.; Racioppi, R., The Photochemical Dimerization of 3-Heteroaryl-Acrylates. *Arkivoc* **2002,** *11*, 65-78.

152. Takeuchi, D., Stereoregular Polymers. In *Stereoregular Polymers, Encyclopedia of Polymer Science and Technology*, John Wiley & Sons, Inc.: 2013.

153. Sakamoto, J.; van Heijst, J.; Lukin, O.; Schlüter, A. D., Two-Dimensional Polymers: Just a Dream of Synthetic Chemists? *Angew. Chem. Int. Ed.* **2009,** *48* (6), 1030-1069.

154. Colson, J. W.; Dichtel, W. R., Rationally Synthesized Two-Dimensional Polymers. *Nat. Chem.* **2013,** *5* (6), 453-465.

155. Kissel, P.; Murray, D. J.; Wulftange, W. J.; Catalano, V. J.; King, B. T., A Nanoporous Two-Dimensional Polymer by Single-Crystal-to-Single-Crystal Photopolymerization. *Nat. Chem.* **2014,** *6* (9), 774-778.

156. Kory, M. J.; Wörle, M.; Weber, T.; Payamyar, P.; van de PollStan, W.; Dshemuchadse, J.; Trapp, N.; Schlüter, A. D., Gram-Scale Synthesis of Two-Dimensional Polymer Crystals and Their Structure Analysis by X-Ray Diffraction. *Nat. Chem.* **2014,** *6* (9), 779-784.

157. Baek, K.; Yun, G.; Kim, Y.; Kim, D.; Hota, R.; Hwang, I.; Xu, D.; Ko, Y. H.; Gu, G. H.; Suh, J. H.; Park, C. G.; Sung, B. J.; Kim, K., Free-Standing, Single-Monomer-Thick Two-Dimensional Polymers through Covalent Self-Assembly in Solution. *J. Am. Chem. Soc.* **2013,** *135* (17), 6523-6528.

158. Lafferentz, L.; Eberhardt, V.; Dri, C.; Africh, C.; Comelli, G.; Esch, F.; Hecht, S.; Grill, L., Controlling on-Surface Polymerization by Hierarchical and Substrate-Directed Growth. *Nat. Chem.* **2012,** *4* (3), 215-220.

159. Spitler, E. L.; Dichtel, W. R., Lewis Acid-Catalysed Formation of Two-Dimensional Phthalocyanine Covalent Organic Frameworks. *Nat. Chem.* **2010,** *2* (8), 672-677.

160. Côté, A. P.; Benin, A. I.; Ockwig, N. W.; O'Keeffe, M.; Matzger, A. J.; Yaghi, O. M., Porous, Crystalline, Covalent Organic Frameworks. *Science* **2005,** *310* (5751), 1166-1170.

161. Stupp, S. I.; Son, S.; Lin, H. C.; Li, L. S., Synthesis of Two-Dimensional Polymers. *Science* **1993,** *259* (5091), 59-63.

162. Market Report: World Carbon Fiber Composite Market, Acmite Market Intelligence, 2010.

163. Hillermeier, R.; Hasson,T.; Friedrich, L.; Ball. C.; Advanced Thermosetting Resin Matrix Technology for Next Generation High Volume Manufacture of Automotive Composite Structures, http://www.speautomotive.com/SPEA_CD/SPEA2012/pdf/TS/TS1.pdfm (Accessed Nov. 2014).

164. http://www.zoltek.com/carbonfiber/how-is-it-made/ (Accessed Nov. 2014).

165. Biradha, K.; Santra, R., Crystal Engineering of Topochemical Solid State Reactions. *Chem. Soc. Rev.* **2013,** *42* (3), 950-967.

166. Grove, R. C.; Malehorn, S. H.; Breen, M. E.; Wheeler, K. A., A Photoreactive Crystalline Quasiracemate. *Chem. Commun.* **2010,** *46* (39), 7322-7324.

167. Garcia-Garibay, M. A., Engineering Carbene Rearrangements in Crystals: From Molecular Information to Solid-State Reactivity. *Acc. Chem. Res.* **2003,** *36* (7), 491-498.

168. Nakanishi, H.; Jones, W.; Thomas, J. M.; Hasegawa, M.; Rees, W. L., Topochemically Controlled Solid-State Polymerization. *Proceedings of the Royal Society of London. Series A, Mathematical and Physical Sciences* **1980,** *369* (1738), 307-325.

169. Wegner, G., Topochemical Polymerization of Monomers with Conjugated Triple Bonds. *Die Makromolekulare Chemie* **1972,** *154* (1), 35-48.

170. Antzutkin, O. N., Sideband Manipulation in Magic-Angle-Spinning Nuclear Magnetic Resonance. *Prog. Nucl. Magn. Reson. Spectrosc.* **1999,** *35* (3), 203-266.

171. Abdelmoty, I.; Buchholz, V.; Di, L.; Guo, C.; Kowitz, K.; Enkelmann, V.; Wegner, G.; Foxman, B. M., Polymorphism of Cinnamic and A-Truxillic Acids: New Additions to an Old Story. *Cryst. Growth Des.* **2005,** *5* (6), 2210-2217.

172. Chi, Y.-M.; Nakamura, M.; Yoshizawa, T.; Zhao, X.-Y.; Yan, W.-M.; Hashimoto, F.; Kinjo, J.; Nohara, T.; Sakurada, S., Anti-Inflammatory Activities of Α-Truxillic Acid Derivatives and Their Monomer Components. *Biol. Pharm. Bull.* **2005,** *28* (9), 1776-1778.

173. Chi, Y.-M.; Nakamura, M.; Zhao, X.-Y.; Yoshizawa, T.; Yan, W.-M.; Hashimoto, F.; Kinjo, J.; Nohara, T.; Sakurada, S., Antinociceptive Activities of Α-Truxillic Acid and Β-Truxinic Acid Derivatives. *Biol. Pharm. Bull.* **2006,** *29* (3), 580-584.

174. Yang, H.; Jia, L.; Wang, Z.; Di-Cicco, A. l.; Lévy, D.; Keller, P., Novel Photolabile Diblock Copolymers Bearing Truxillic Acid Derivative Junctions. *Macromolecules* **2010,** *44* (1), 159-165.

175. Berger, W. T.; Ralph, B. P.; Kaczocha, M.; Sun, J.; Balius, T. E.; Rizzo, R. C.; Haj-Dahmane, S.; Ojima, I.; Deutsch, D. G., Targeting Fatty Acid Binding Protein (Fabp) Anandamide Transporters – a Novel Strategy for Development of Anti-Inflammatory and Anti-Nociceptive Drugs. *PLoS One* **2012,** *7* (12), e50968.

176. Singh, R.; Schober, M.; Hou, X.; Seay, A.; Chu, Q., Facile and Efficient Synthesis of C3-Symmetric Benzoxazine: A Novel Tri-Arm Molecular Scaffold. *Tetrahedron Lett.* **2012,** *53* (2), 173-175.

177. Schmidt, G. M. J., Photodimerization in the Solid State. *Pure Appl. Chem.* **1971,** *27* (4), 647-678.

178. Park, I.-H.; Chanthapally, A.; Zhang, Z.; Lee, S. S.; Zaworotko, M. J.; Vittal, J. J., Addendum: Metal–Organic Organopolymeric Hybrid Framework by Reversible [2+2] Cycloaddition Reaction. *Angew. Chem. Int. Ed.* **2014,** *53* (21), 5232-5232.

179. Medishetty, R.; Husain, A.; Bai, Z.; Runčevski, T.; Dinnebier, R. E.; Naumov, P.; Vittal, J. J., Single Crystals Popping under Uv Light: A Photosalient Effect Triggered by a [2+2] Cycloaddition Reaction. *Angew. Chem. Int. Ed.* **2014,** *53* (23), 5907-5911.

180. Yang, S.-Y.; Deng, X.-L.; Jin, R.-F.; Naumov, P.; Panda, M. K.; Huang, R.-B.; Zheng, L.-S.; Teo, B. K., Crystallographic Snapshots of the Interplay between Reactive Guest and Host Molecules in a Porous Coordination Polymer: Stereochemical Coupling and Feedback Mechanism of Three Photoactive Centers Triggered by UV-Induced Isomerization, Dimerization, and Polymerization Reactions. *J. Am. Chem. Soc.* **2013,** *136* (2), 558-561.

181. Desiraju, G. R.; Vittal, J. J.; Ramanan, A., *Crystal Engineering: A Textbook* 1ed.; World Scientific Publishing Company: 2011; p 232.

182. Steed, J. W.; Atwood, J. L., *Supramolecular Chemistry*. 2 ed.; John Wiley & Sons, Ltd., Chichester: 2009; p 745.

183. Hou, X.; Wang, Z.; Overby, M.; Ugrinov, A.; Oian, C.; Singh, R.; Chu, Q. R., A Two-Dimensional Hydrogen Bonded Organic Framework Self-Assembled from a Three-Fold Symmetric Carbamate. *Chem. Commun.* **2014,** *50* (40), 5209-5211.

184. Wang, Z.; Lee, J.; Oian, C.; Hou, X.; Wang, Z.; Ugrinov, A.; Singh, R. K.; Wysocki, E.; Chu, Q. R., An Unsaturated Hydrogen Bonded Network Generated from Three-Fold Symmetric Carbamates. *CrystEngComm* **2014,** *16* (31), 7176-7179.

185. Hou, X.; Schober, M.; Chu, Q., A Chiral Nanosheet Connected by Amide Hydrogen Bonds. *Cryst. Growth Des.* **2012,** *12* (11), 5159-5163.

186. Singh, R. K.; Hou, X.; Overby, M.; Schober, M.; Chu, Q., Hydrogen Bonded Chiral Sheet Self-Assembled from a C3-Symmetric Tricarbamate. *CrystEngComm* **2012,** *14* (19), 6132-6135.

187. Prins, L. J.; Scrimin, P., Covalent Capture: Merging Covalent and Noncovalent Synthesis. *Angew. Chem. Int. Ed.* **2009,** *48* (13), 2288-2306.

188. Sada, K.; Takeuchi, M.; Fujita, N.; Numata, M.; Shinkai, S., Post-Polymerization of Preorganized Assemblies for Creating Shape-Controlled Functional Materials. *Chem. Soc. Rev.* **2007,** *36* (2), 415-435.

189. Tajima, K.; Aida, T., Controlled Polymerizations with Constrained Geometries. *Chem. Commun.* **2000,** (24), 2399-2412.

190. Khan, M.; Brunklaus, G.; Enkelmann, V.; Spiess, H.-W., Transient States in [2 + 2] Photodimerization of Cinnamic Acid: Correlation of Solid-State NMR and X-Ray Analysis. *J. Am. Chem. Soc.* **2008,** *130* (5), 1741-1748.

191. Barbour, L. J., X-Seed — a Software Tool for Supramolecular Crystallography. *J. Supramol. Chem.* **2001,** *1* (4–6), 189-191.

192. Nishikubo, T.; Takahashi, E.; Miyaji, T.; Iizawa, T., Convenient Synthesis of *B*-Truxinic Acid *Via* Photodimerization of *P*-Nitrophenyl Cinnamate in the Crystalline State. *Bull. Chem. Soc. Jpn.* **1985,** *58* (11), 3399-3400.

193. Chu, Q.; Wang, Z.; Huang, Q.; Yan, C.; Zhu, S., Fluorine-Containing Donor-Acceptor Complex: Infinite Chain Formed by Oxygen Iodine Interaction. *J. Am. Chem. Soc.* **2001,** *123* (44), 11069-11070.

194. Chu, Q.; Wang, Z.; Huang, Q.; Yan, C.; Zhu, S., Fluorine-Containing Donor-Acceptor Complexes: Crystallographic Study of the Interactions between Electronegative Atoms (N, O, S) and Halogen Atoms (I, Br). *New J. Chem.* **2003,** *27* (10), 1522-1527.

195. Neto, A. H. C.; Novoselov, K., New Directions in Science and Technology: Two-Dimensional Crystals. *Rep. Prog. Phys.* **2011,** *74* (8), 082501.

196. Gavezzotti, A., Are Crystal Structures Predictable? *Acc. Chem. Res.* **1994,** *27* (10), 309-314.

197. Brock, C. P.; Dunitz, J. D., Towards a Grammar of Crystal Packing. *Chem. Mater.* **1994,** *6* (8), 1118-1127.

198. Matsumoto, A.; Sada, K.; Tashiro, K.; Miyata, M.; Tsubouchi, T.; Tanaka, T.; Odani, T.; Nagahama, S.; Tanaka, T.; Inoue, K.; Saragai, S.; Nakamoto, S., Reaction Principles and Crystal Structure Design for the Topochemical Polymerization of 1,3-Dienes. *Angew. Chem. Int. Ed.* **2002,** *41* (14), 2502-2505.

199. Mascitti, V.; Corey, E. J., Total Synthesis of (±)-Pentacycloanammoxic Acid. *J. Am. Chem. Soc.* **2004,** *126* (48), 15664-15665.

200. Hoffmann, N., Photochemical Reactions as Key Steps in Organic Synthesis. *Chem. Rev.* **2008,** *108* (3), 1052-1103.

201. Atkinson, M. B. J.; Mariappan, S. V. S.; Bučar, D.-K.; Baltrusaitis, J.; Friščić, T.; Sinada, N. G.; MacGillivray, L. R., Crystal Engineering Rescues a Solution Organic Synthesis in a Cocrystallization That Confirms the Configuration of a Molecular Ladder. *Proc. Natl. Acad. Sci.* **2011,** *108* (27), 10974-10979.

202. Ortuno, R. M.; Moglioni, A. G.; Moltrasio, G. Y., Cyclobutane Biomolecules: Synthetic Approaches to Amino Acids, Peptides and Nucleosides. *Curr. Org. Chem.* **2005,** *9* (3), 237-259.

203. Fan, Y.-Y.; Gao, X.-H.; Yue, J.-M., Attractive Natural Products with Strained Cyclopropane and/or Cyclobutane Ring Systems. *Sci. China Chem.* **2016,** *59* (9), 1126-1141.

204. Goodman, C., Synthesis: Cyclobutanes Prove Charlatans. *Nat. Chem. Biol.* **2012,** *8* (8), 678-678.

205. Dembitsky, V. M., Naturally Occurring Bioactive Cyclobutane-Containing (Cbc) Alkaloids in Fungi, Fungal Endophytes, and Plants. *Phytomedicine* **2014,** *21* (12), 1559-1581.

206. Dembitsky, V. M., Bioactive Cyclobutane-Containing Alkaloids. *J. Nat. Med.* **2008,** *62* (1), 1-33.

207. Bucholtz, K. M.; Gareiss, P. C.; Tajc, S. G.; Miller, B. L., Synthesis and Evaluation of the First *cis*-Cyclobutane-Containing Receptor for Lipid A. *Org. Biomol. Chem.* **2006,** *4* (21), 3973-3979.

208. Sergeiko, A.; Poroikov, V. V.; Hanuš, L. O.; Dembitsky, V. M., Cyclobutane-Containing Alkaloids: Origin, Synthesis, and Biological Activities. *The Open Medicinal Chemistry Journal* **2008,** *2*, 26-37.

209. Warnecke, A.; Fichtner, I.; Garmann, D.; Jaehde, U.; Kratz, F., Synthesis and Biological Activity of Water-Soluble Maleimide Derivatives of the Anticancer Drug Carboplatin Designed as Albumin-Binding Prodrugs. *Bioconjugate Chem.* **2004,** *15* (6), 1349-1359.

210. Sproul, C. D.; Mitchell, D. L.; Rao, S.; Ibrahim, J. G.; Kaufmann, W. K.; Cordeiro-Stone, M., Cyclobutane Pyrimidine Dimer Density as a Predictive Biomarker of the Biological Effects of Ultraviolet Radiation in Normal Human Fibroblast. *Photochem. Photobiol.* **2014,** *90* (1), 145-154.

211. Sittiwong, W.; Zinniel, D. K.; Fenton, R. J.; Marshall, D. D.; Story, C. B.; Kim, B.; Lee, J.-Y.; Powers, R.; Barletta, R. G.; Dussault, P. H., Development of Cyclobutene- and Cyclobutane-Functionalized Fatty Acids with Inhibitory Activity against Mycobacterium Tuberculosis. *ChemMedChem* **2014,** *9* (8), 1838-1849.

212. Chernykh, A. V.; Radchenko, D. S.; Chernykh, A. V.; Kondratov, I. S.; Tolmachova, N. A.; Datsenko, O. P.; Kurkunov, M. A.; Zozulya, S. X.; Kheylik, Y. P.; Bartels, K.; Daniliuc, C. G.; Haufe, G., Synthesis and Physicochemical Properties of 3-Fluorocyclobutylamines. *Eur. J. Org. Chem.* **2015,** *2015* (29), 6466-6471.

213. Zheng, Y.; Tice, C. M.; Singh, S. B., The Use of Spirocyclic Scaffolds in Drug Discovery. *Bioorg. Med. Chem. Lett.* **2014,** *24* (16), 3673-3682.

214. Guchelaar, H.-J.; Uges, D. R. A.; Aulenbacher, P.; de Vries, E. G. E.; Mulder, N. H., Stability of the New Anticancer Platinum Analogue 1,2-Diaminomethyl-Cyclobutane-Platinum(Ii)-Lactate (Lobaplatin; D19466) in Intravenous Solutions. *Pharm. Res.* **1992,** *9* (6), 808-811.

215. Figueras, A.; Miralles-Llumà, R.; Flores, R.; Rustullet, A.; Busqué, F.; Figueredo, M.; Font, J.; Alibés, R.; Maréchal, J.-D., Synthesis, Anti-Hiv Activity Studies, and in Silico Rationalization of Cyclobutane-Fused Nucleosides. *ChemMedChem* **2012,** *7* (6), 1044-1056.

216. Carey, F. A.; Sundberg, R. J., *Advanced Organic Chemistry Part A: Structure and Mechanisms*. Springer US: 2007.

217. Brown, W. H.; Iverson, B. L.; Anslyn, E.; Foote, C. S., *Organic Chemistry, 7 Edt*. Cengage Learning: Belmont, CA, 2013.

218. Fu, N.-Y.; Chan, S.-H.; Wong, H. N. C., The Application of Cyclobutane Derivatives in Organic Synthesis. In *The Chemistry of Cyclobutanes*, John Wiley & Sons, Ltd: 2006; pp 357-440.

219. Rappoport, Z.; Liebman, J. F., *The Chemistry of Cyclobutanes, 2 Volume Set*. Wiley: 2015.

220. Namyslo, J. C.; Kaufmann, D. E., The Application of Cyclobutane Derivatives in Organic Synthesis. *Chem. Rev.* **2003,** *103* (4), 1485-1538.

221. White, J. D.; Li, Y.; Kim, J.; Terinek, M., Cyclobutane Synthesis and Fragmentation. A Cascade Route to the Lycopodium Alkaloid (−)-Huperzine A. *J. Org. Chem.* **2015,** *80* (23), 11806-11817.

222. Maimone, T. J.; Baran, P. S., Modern Synthetic Efforts toward Biologically Active Terpenes. *Nat. Chem. Biol.* **2007,** *3* (7), 396-407.

223. Howard, C. C.; Newton, R. F.; Reynolds, D. P.; Wadsworth, A. H.; Kelly, D. R.; Roberts, S. M., Total Synthesis of Prostaglandin-F2[Small Alpha] Involving Stereocontrolled and Photo-Induced Reactions of Bicyclo[3.2.0]Heptanones. *J. Chem. Soc., Perkin Trans. 1* **1980**, 852-857.

224. Boyer, F.-D.; Ducrot, P.-H., Syntheses of Cyclobutane Derivatives: Total Synthesis of (+) and (–) Enantiomers of the Oleander Scale Aspidiotus Nerii Sex Pheromone. *Eur. J. Org. Chem.* **1999,** *1999* (5), 1201-1211.

225. Crimmins, M. T.; Mascarella, S. W., Intramolecular Photocycloaddition-Cyclobutane Fragmentation: Total Synthesis of (.+–.)-Silphinene. *J. Am. Chem. Soc.* **1986,** *108* (12), 3435-3438.

226. Crimmins, M. T.; DeLoach, J. A., Intramolecular Photocycloadditions-Cyclobutane Fragmentation: Total Synthesis of (.+–.)-Pentalenene, (.+–.)-Pentalenic Acid, and (.+–.)-Deoxypentalenic Acid. *J. Am. Chem. Soc.* **1986,** *108* (4), 800-806.

227. Gutekunst, W. R.; Baran, P. S., Total Synthesis and Structural Revision of the Piperarborenines Via Sequential Cyclobutane C–H Arylation. *J. Am. Chem. Soc.* **2011,** *133* (47), 19076-19079.

228. Arafat, M. T.; Tronci, G.; Yin, J.; Wood, D. J.; Russell, S. J., Biomimetic Wet-Stable Fibres Via Wet Spinning and Diacid-Based Crosslinking of Collagen Triple Helices. *Polymer* **2015,** *77*, 102-112.

229. Edlund, U.; Albertsson, A. C., Polyesters Based on Diacid Monomers. *Adv. Drug Delivery Rev.* **2003,** *55* (4), 585-609.

230. Ouimet, M. A.; Faig, J. J.; Yu, W.; Uhrich, K. E., Ferulic Acid-Based Polymers with Glycol Functionality as a Versatile Platform for Topical Applications. *Biomacromolecules* **2015,** *16* (9), 2911-2919.

231. Díaz, A.; Katsarava, R.; Puiggalí, J., Synthesis, Properties and Applications of Biodegradable Polymers Derived from Diols and Dicarboxylic Acids: From Polyesters to Poly(Ester Amide)S. *Int. J. Mol. Sci.* **2014,** *15* (5), 7064-7123.

232. Zhang, Y.-R.; Yang, Y.-X.; Cai, J.-L.; Lv, W.-H.; Xie, W.-C.; Wang, Y.-Z.; Gross, R. A., Poly(Oleic Diacid-Co-Glycerol): Comparison of Polymer Structure Resulting from Chemical and Lipase Catalysis. In *Biobased Monomers, Polymers, and Materials*, American Chemical Society: 2012; Vol. 1105, pp 111-129.

233. Angelo, R. J.; Miura, H.; Gardner, K. H.; Chase, D. B.; English, A. D., Preparation and Characterization of Selectively Isotopically Labeled Nylon 66 Polymers. *Macromolecules* **1989,** *22* (1), 117-121.

234. Mathias, L. J.; Vaidya, R. A.; Canterberry, J. B., Nylon 6 - a Simple, Safe Synthesis of a Tough Commercial Polymer. *J. Chem. Educ.* **1984,** *61* (9), 805.

235. Ichikawa, Y.; Yamashita, G.; Tokashiki, M.; Yamaji, T., New Oxidation Process for Production of Terephthalic Acid from *p*-Xylene. *Ind. Eng. Chem.* **1970,** *62* (4), 38-42.

236. Harper, J. J.; Janik, P., Terephthalic Acid Solubility. *J. Chem. Eng. Data* **1970,** *15* (3), 439-440.

237. Ogata, Y.; Tsuchida, M.; Muramoto, A., The Preparation of Terephthalic Acid from Phthalic or Benzoic Acid. *J. Am. Chem. Soc.* **1957,** *79* (22), 6005-6008.

238. Smith, P. B.; Gross, R. A.; Cheng, H. N., *Green Polymer Chemistry: Biobased Materials and Biocatalysis*. American Chemical Society: 2015; Vol. 1192.

239. Smith, P. B., Bio-Based Sources for Terephthalic Acid. In *Green Polymer Chemistry: Biobased Materials and Biocatalysis*, American Chemical Society: 2015; Vol. 1192, pp 453-469.

240. Collias Dimitris I., H. A. M., Nagpal Vidhu, Cottrell Ian W., and Schultheis Mikell W., Biobased Terephthalic Acid Technologies: A Literature Review. *Ind. Biotechnol.* **2014,** *10* (2), 91-105.

241. de Jong, E.; Dam, M. A.; Sipos, L.; Gruter, G. J. M., Furandicarboxylic Acid (Fdca), a Versatile Building Block for a Very Interesting Class of Polyesters. In *Biobased Monomers, Polymers, and Materials*, American Chemical Society: 2012; Vol. 1105, pp 1-13.

242. Wilsens, C. H. R. M.; Verhoeven, J. M. G. A.; Noordover, B. A. J.; Hansen, M. R.; Auhl, D.; Rastogi, S., Thermotropic Polyesters from 2,5-Furandicarboxylic Acid and Vanillic Acid: Synthesis, Thermal Properties, Melt Behavior, and Mechanical Performance. *Macromolecules* **2014,** *47* (10), 3306-3316.

243. Beckman, E. J., Sustainable Chemistry: Putting Carbon Dioxide to Work. *Nature* **2016,** *531* (7593), 180-181.

244. Huang, Y.-T.; Wong, J.-J.; Huang, C.-J.; Li, C.-L.; Jang, G.-W. B., 2,5-Furandicarboxylic Acid Synthesis and Use. In *Chemicals and Fuels from Bio-Based Building Blocks*, Wiley-VCH Verlag GmbH & Co. KGaA: 2016; pp 191-216.

245. Thiyagarajan, S.; Vogelzang, W.; J. I. Knoop, R.; Frissen, A. E.; van Haveren, J.; van Es, D. S., Biobased Furandicarboxylic Acids (Fdcas): Effects of Isomeric Substitution on Polyester Synthesis and Properties. *Green Chem.* **2014,** *16* (4), 1957-1966.

246. Williams, I. D., Metal-Organic Frameworks: 3d Frameworks from 3d Printers. *Nat Chem* **2014,** *6* (11), 953-954.

247. Qiu, S.; Xue, M.; Zhu, G., Metal-Organic Framework Membranes: From Synthesis to Separation Application. *Chem. Soc. Rev.* **2014,** *43* (16), 6116-6140.

248. Stock, N.; Biswas, S., Synthesis of Metal-Organic Frameworks (Mofs): Routes to Various Mof Topologies, Morphologies, and Composites. *Chem. Rev.* **2012,** *112* (2), 933-969.

249. Schoedel, A.; Li, M.; Li, D.; O'Keeffe, M.; Yaghi, O. M., Structures of Metal–Organic Frameworks with Rod Secondary Building Units. *Chem. Rev.* **2016**.

250. Barman, S.; Khutia, A.; Koitz, R.; Blacque, O.; Furukawa, H.; Iannuzzi, M.; Yaghi, O. M.; Janiak, C.; Hutter, J.; Berke, H., Synthesis and Hydrogen Adsorption Properties of Internally Polarized 2,6-Azulenedicarboxylate Based Metal-Organic Frameworks. *J. Mater. Chem. A* **2014,** *2* (44), 18823-18830.

251. Rosi, N. L.; Eckert, J.; Eddaoudi, M.; Vodak, D. T.; Kim, J.; O'Keeffe, M.; Yaghi, O. M., Hydrogen Storage in Microporous Metal-Organic Frameworks. *Science* **2003,** *300* (5622), 1127-1129.

252. Tranchemontagne, D. J.; Hunt, J. R.; Yaghi, O. M., Room Temperature Synthesis of Metal-Organic Frameworks: Mof-5, Mof-74, Mof-177, Mof-199, and Irmof-0. *Tetrahedron* **2008,** *64* (36), 8553-8557.

253. Yaghi, O. M.; O'Keeffe, M.; Ockwig, N. W.; Chae, H. K.; Eddaoudi, M.; Kim, J., Reticular Synthesis and the Design of New Materials. *Nature* **2003,** *423* (6941), 705-714.

254. Wang, L. J.; Deng, H.; Furukawa, H.; Gándara, F.; Cordova, K. E.; Peri, D.; Yaghi, O. M., Synthesis and Characterization of Metal–Organic Framework-74 Containing 2, 4, 6, 8, and 10 Different Metals. *Inorg. Chem.* **2014,** *53* (12), 5881-5883.

255. Anslyn, E. V.; Dougherty, D. A., *"Chapter 2: Strain and Stability" Modern Physical Organic Chemistry*. University Science: Sausalito, CA, 2006.

256. Wade, L. G., *"Structure and Sterochemistry of Alkanes." Organic Chemistry. 6th Ed.* Pearson Prentice Hall: Upper Saddle River, NJ, 2006.

257. Abdelmoty, I.; Buchholz, V.; Di, L.; Guo, C.; Kowitz, K.; Enkelmann, V.; Wegner, G.; Foxman, B. M., Polymorphism of Cinnamic and A-Truxillic Acids: New Additions to an Old Story. *Cryst. Growth Des.* **2005,** *5* (6), 2210-2217.

258. Garbe, D., Cinnamic Acid. In *Ullmann's Encyclopedia of Industrial Chemistry*, Wiley-VCH Verlag GmbH & Co. KGaA: 2000.

259. De, P.; Baltas, M.; Bedos-Belval, F., Cinnamic Acid Derivatives as Anticancer Agents-a Review. *Curr. Med. Chem.* **2011,** *18* (11), 1672-1703.

260. Liu, L.; Hudgins, W. R.; Shack, S.; Yin, M. Q.; Samid, D., Cinnamic Acid: A Natural Product with Potential Use in Cancer Intervention. *Int. J. Cancer* **1995,** *62* (3), 345-350.

261. Park, I.-H.; Chanthapally, A.; Zhang, Z.; Lee, S. S.; Zaworotko, M. J.; Vittal, J. J., Metal–Organic Organopolymeric Hybrid Framework by Reversible [2+2] Cycloaddition Reaction. *Angew. Chem. Int. Ed.* **2014,** *126* (2), 424-429.

262. Chanthapally, A.; Oh, W. T.; Vittal, J. J., [2 + 2] Cycloaddition Reaction as a Tool to Monitor the Formation of Thermodynamically Stable Ladder Coordination Polymers. *CrystEngComm* **2013,** *15* (45), 9324-9327.

263. Conradi, M.; Junkers, T., Fast and Efficient [2 + 2] Uv Cycloaddition for Polymer Modification Via Flow Synthesis. *Macromolecules* **2014,** *47* (16), 5578-5585.

264. Lange, R. Z.; Hofer, G.; Weber, T.; Schlüter, A. D., A Two-Dimensional Polymer Synthesized through Topochemical [2 + 2]-Cycloaddition on the Multigram Scale. *J. Am. Chem. Soc.* **2017,** *139* (5), 2053-2059.

265. Takahashi, S.; Miura, H.; Kasai, H.; Okada, S.; Oikawa, H.; Nakanishi, H., Single-Crystal-to-Single-Crystal Transformation of Diolefin Derivatives in Nanocrystals. *J. Am. Chem. Soc.* **2002,** *124* (37), 10944-10945.

266. Chu, Q.; Swenson, D. C.; MacGillivray, L. R., A Single-Crystal-to-Single-Crystal Transformation Mediated by Argentophilic Forces Converts a Finite Metal Complex into an Infinite Coordination Network. *Angew. Chem. Int. Ed.* **2005,** *117* (23), 3635-3638.

267. Dutta, S.; Bucar, D.-K.; Elacqua, E.; MacGillivray, L. R., Single-Crystal-to-Single-Crystal Direct Cross-Linking and Photopolymerisation of a Discrete Ag(I) Complex to Give a 1d Polycyclobutane Coordination Polymer. *Chem. Commun.* **2013,** *49* (11), 1064-1066.

268. Celis, S.; Nolis, P.; Illa, O.; Branchadell, V.; Ortuno, R. M., Low-Molecular-Weight Gelators Consisting of Hybrid Cyclobutane-Based Peptides. *Org. Biomol. Chem.* **2013,** *11* (17), 2839-2846.

269. Aitken, D. J.; Gauzy, C.; Pereira, E., A Short Synthesis of the *cis*-Cyclobutane B-Aminoacid Skeleton Using a [2+2] Cycloaddition Strategy. *Tetrahedron Lett.* **2002,** *43* (35), 6177-6179.

270. Francesco Secci, A. F. a. P. P. P., Stereocontrolled Synthesis and Functionalization of Cyclobutanes and Cyclobutanones. *Molecules* **2013,** *18* (12), 15541-15572.

271. Papaspyrides, C. D.; Vouyiouka, S. N., Fundamentals of Solid State Polymerization. In *Solid State Polymerization*, John Wiley & Sons, Inc.: 2009; pp 1-37.

272. Tanaka, K.; Toda, F., Organic Photoreaction in the Solid State. In *Organic Solid-State Reactions*, Toda, F., Ed. Springer Netherlands: Dordrecht, 2002; pp 109-158.